

**Bioanalytical evaluation of the neuropeptide  
Substance P in human plasma using a chemometrically  
developed and validated mass spectrometric assay**

Inaugural-Dissertation

zur Erlangung des Doktorgrades  
der Mathematisch-Naturwissenschaftlichen Fakultät  
der Heinrich-Heine-Universität Düsseldorf

vorgelegt von

**Martin Feickert**  
aus Neunkirchen (Saar)

Düsseldorf, April 2021

aus dem Institut für Klinische Pharmazie und Pharmakotherapie  
der Heinrich-Heine-Universität Düsseldorf

Gedruckt mit der Genehmigung der  
Mathematisch-Naturwissenschaftlichen Fakultät der  
Heinrich-Heine-Universität Düsseldorf

Berichterstatter:

1. Prof. Dr. Stephanie Lärer
2. Prof. Dr. Eckhard Lammert

Tag der mündlichen Prüfung: 22.04.2021

*Eine Veränderung gibt immer Anlass zu weiteren.*

*Niccolò Machiavelli*

## **I. Erklärung zur Dissertation**

Hiermit versichere ich an Eides statt, dass die vorgelegte Dissertation mit dem Titel:

**Bioanalytical evaluation of the neuropeptide Substance P in human plasma using a chemometrically developed and validated mass spectrometric assay**

von mir selbstständig und ohne unzulässige fremde Hilfe unter Beachtung der Grundsätze zur Sicherung guter wissenschaftlicher Praxis an der Heinrich-Heine-Universität Düsseldorf erstellt worden ist. Die Dissertation wurde in der vorgelegten oder in ähnlicher Form noch bei keiner anderen Institution eingereicht. Ich habe bisher keinen erfolglosen Promotionsversuch unternommen.

Düsseldorf, den 29. April 2021

Martin Feickert

## II. Danksagung

Zunächst möchte ich mich bei Prof. Dr. Stephanie Lärer für die Möglichkeit bedanken, meine Promotion am Institut für Klinische Pharmazie an der Universität in Düsseldorf durchzuführen und dabei intensive Einblicke in die wissenschaftliche Arbeit des Instituts zu erhalten. Der mir gewährte wissenschaftliche Freiraum und ihr stetes Vertrauen in meine Person gaben mir die einzigartige Chance, meine eigenen forschersichen Ideen und Konzepte umzusetzen.

Ich bedanke mich herzlich bei Prof. Dr. Eckhard Lammert für die Übernahme des Zweitgutachtens dieser Arbeit und für sein aufrichtiges Interesse an meiner hier dargestellten Forschung.

Bei Dr. Björn Burckhardt bedanke ich mich für die Betreuung meiner Dissertationsarbeit und für die Einführung in das hochspannende Feld der Bioanalytik. Ohne seine Unterstützung wäre die anspruchsvolle Aufgabenstellung dieser Arbeit nicht in dieser kurzen Zeit zu bewerkstelligen gewesen. Seinen herausragenden lektorischen Fähigkeiten verdanke ich unsere gemeinsamen zahlreichen wissenschaftlichen Publikationen.

Des Weiteren danke ich allen aktuellen und ehemaligen Mitarbeitern am Institut für Klinische Pharmazie, die mich auf die eine oder andere Weise bei der Anfertigung dieser Seiten unterstützten. Besonders danke ich Ilja Burdman, ohne dessen analytischer Expertise manch praktischer Versuch nicht zustande gekommen wäre.

All meinen Freunden, aus dem Saarland, aus meinem Pharmaziestudium an der Universität in Freiburg und die ich während meiner Promotion in Düsseldorf kennenlernen durfte, danke ich für ein immer offenes Ohr und die gemeinsam verbrachte Zeit.

Ein ganz besonderer Dank geht an meine Familie, die mir stets in meinem Leben zur Seite stand und mich in allen Belangen bis zum Ende unterstützte.

### III. Zusammenfassung

Das Neuropeptid Substanz P steht seit kurzem als kardialer Entzündungsmediator im Fokus der Wissenschaft. Da die exzessive Freisetzung von Substanz P in Tiermodellen mit der Entwicklung von Kardiomyopathien und Herzinsuffizienz assoziiert ist, wäre Substanz P ein vielversprechender Biomarker. Die erhobenen humanen Substanz P-Plasmaspiegel wurden jedoch bisher ausschließlich mit Immunassays bestimmt, obwohl die Tests Kreuz-Reaktivität zu humanem Hemokinin-1 zeigten. Folglich ist der Einsatz der Massenspektrometrie eine bioanalytische gleichwohl zurzeit fehlende Alternative, um Substanz P selektiv im Blutplasma zu bestimmen. Da die Quantifizierung endogener Peptide mittels Massenspektrometrie wegen der niedrigen Konzentrationen im picomolaren Bereich eine besondere Herausforderung darstellt, war eine umfassende Methodenentwicklung gefordert, um eine sensitive massenspektrometrische Methode mit vergleichbaren Detektionslimits zu geläufigen Immunassays zu etablieren. Durch die Anwendung eines dafür eigens entwickelten statistischen Versuchskonzepts wurden systematisch kritische Methoden Aspekte wie die unspezifische Peptidadsorption, die Plasmaextraktion und die chromatographische Trennung der Analyten gezielt adressiert und optimiert. Die entwickelte Methode wurde darauf erfolgreich nach internationalen bioanalytischen Richtlinien validiert und erlaubt einen breiten Quantifizierungsbereich, der die bisher erhobenen Plasmaspiegel durch Immunassays abdeckt. Bei dem Einsatz der validierten Methode wurden jedoch unerwartet keine endogenen Level an Substanz P und humanem Hemokinin-1 in Plasmaproben detektiert, obwohl die Methode ihre Anwendbarkeit in anderen humanen Körperflüssigkeiten erfolgreich demonstrierte. Bei der Nutzung derselben Plasmaproben konnte immuno-reaktive Substanz P mittels eines kommerziellen Immunoassays quantifiziert werden. Mit Hilfe hochauflösender Massenspektrometrie wurde daraufhin an Stelle von biologisch aktiver Substanz P die biologisch inaktive freie Säure von Substanz P zum ersten Mal in Plasma identifiziert. Da die freie Säure jedoch keine Kreuz-Reaktivität zeigte, wurde zur Identifizierung von immuno-reaktiver Substanz P ein hybrides immuno-reaktives-massenspektrometrisches Verfahren entwickelt. Die darauffolgende Identifizierung der immuno-reaktiven Substanz zeigte die Anwesenheit eines Vorläufermoleküls von Substanz P als möglichen kross-reaktiven Analyten in humanem Blutplasma. Basierend auf diesen Ergebnissen ist eine Neu beurteilung der bisher von Immunassays gemessenen Substanz P-Level notwendig. Das im Plasma gefundene Propeptid von Substanz P bedarf künftiger Studien, um seine biologische Rolle und seinen möglichen Nutzen als klinischer Biomarker in entzündlichen Erkrankungen zu evaluieren.

## IV. Summary

The neuropeptide Substance P has recently received much attention as a mediator of cardiac inflammation. Since Substance P is strongly associated with the development of cardiomyopathies and heart failure in animal models, its use as a biomarker is highly promising. The limited data on Substance P levels in subjects with cardiovascular diseases demonstrate highly variable plasma concentrations and, therefore, complicates its use as a potential biomarker. Human Substance P levels have only been examined by immunoassays, although they are no longer recommended owing to their limited ability to differentiate accurately between Substance P and its relative human Hemokinin-1. The application of mass spectrometry (MS) is promising, but this bioanalytical alternative is lacking for accurate quantification of Substance P. As endogenous peptide quantification by MS is especially challenging due to the presence of Substance P in low picomolar concentrations, a comprehensive method development is required to acquire a highly sensitive MS assay with limits of detection comparable to those of existing immunoassays. By applying a newly developed multi-step Design of Experiments concept encompassing all sample preparation and assay steps, critical aspects of methodology, such as nonspecific peptide adsorption, plasma protein extraction, and chromatographic separation, were identified and optimized for reliable and sensitive quantification of Substance P and human Hemokinin-1 in human plasma. Lean development methodology was followed by successful validation according to US Food and Drug Administration bioanalytical regulatory guidelines; this resulted in a wide quantification range suitable for endogenous quantification of the neuropeptides. The implementation of the developed hyphenated technique unexpectedly revealed no detectable Substance P and human Hemokinin-1 levels in human plasma, although the assay proved its applicability in other biological fluids. Using the same plasma samples, immunoreactive Substance P plasma levels were successfully quantified by a commercially available immunoassay. Instead of biologically active Substance P, the biologically inactive carboxylic acid of Substance P was identified in human plasma by MS analysis and primarily described. As the carboxylic acid of Substance P did not show cross-reactivity in the applied immunoassay, a hybrid immunocapture MS approach was developed to identify immunoreactive Substance P. The subsequent compound discovery of the immunocaptured substance indicated the presence of a precursor of Substance P as a cross-reactor in human plasma samples. Based on these findings, the concentrations of Substance P and its function as a biomarker of cardiac inflammation described in previous studies have to be reevaluated due to the cross-reactivity issues of the immunoassays used. Accordingly, future studies have to assess the biological role of the observed propeptide of Substance P in human plasma and its potential as a clinical biomarker of inflammatory diseases.

---

## V. Table of contents

<b>I. ERKLÄRUNG ZUR DISSERTATION</b> .....	<b>1</b>
<b>II. DANKSAGUNG</b> .....	<b>2</b>
<b>III. ZUSAMMENFASSUNG</b> .....	<b>3</b>
<b>IV. SUMMARY</b> .....	<b>4</b>
<b>V. TABLE OF CONTENTS</b> .....	<b>5</b>
<b>VI. LIST OF ABBREVIATIONS</b> .....	<b>10</b>
<b>VII. LIST OF TABLES</b> .....	<b>12</b>
<b>VIII. LIST OF FIGURES</b> .....	<b>13</b>
<b>1. INTRODUCTION</b> .....	<b>16</b>
1.1 BIOCHEMISTRY OF SUBSTANCE P .....	16
1.2 PATHOPHYSIOLOGY OF SUBSTANCE P IN CARDIAC INFLAMMATION .....	21
1.3 PEDIATRIC HEART FAILURE.....	25
1.4 BIOANALYSIS OF SUBSTANCE P.....	27
1.5 DESIGN OF EXPERIMENTS AS A CHEMOMETRIC TOOL FOR METHOD DEVELOPMENT .....	32
1.6 OBJECTIVE.....	36
<b>2. SUBSTANCE P IN CARDIOVASCULAR DISEASES - A BIOANALYTICAL REVIEW</b> .....	<b>38</b>
2.1 BACKGROUND AND AIM .....	38
2.2 METHODS .....	38
2.3 RESULTS.....	38
2.3.1 <i>Quantification of Substance P blood levels in cardiovascular diseases</i> .....	38
2.3.2 <i>Quantification of pediatric Substance P blood levels</i> .....	39
2.3.3 <i>Evaluation of the reliability of Substance P quantification in blood samples</i> .....	40
2.3.4 <i>Quantification of Substance P saliva levels</i> .....	42
2.4 CONCLUSION .....	42
2.5 DISCLOSURE .....	43

---

<b>3. A DESIGN OF EXPERIMENTS CONCEPT FOR THE MINIMIZATION OF NONSPECIFIC PEPTIDE ADSORPTION IN THE MASS SPECTROMETRIC ANALYSIS OF SUBSTANCE P AND RELATED HEMOKININ-1.....</b>	<b>44</b>
3.1 BACKGROUND AND AIM .....	44
3.2 MATERIALS AND METHODS.....	45
3.2.1 <i>Chemicals and materials</i> .....	45
3.2.2 <i>Instrumentation</i> .....	46
3.2.2.1 <i>Chromatographic conditions</i> .....	46
3.2.2.2 <i>Mass spectrometry</i> .....	46
3.2.3 <i>Design of Experiments</i> .....	47
3.2.3.1 <i>D-optimal design</i> .....	47
3.2.3.2 <i>Investigated parameters and factors</i> .....	48
3.2.3.3 <i>Preparation of experimental solutions</i> .....	49
3.2.3.4 <i>Sweet-spot and setpoint analysis</i> .....	49
3.2.4 <i>Application of the experimental design</i> .....	50
3.3 RESULTS AND DISCUSSION.....	51
3.3.1 <i>Model fit and goodness of prediction</i> .....	51
3.3.2 <i>Optimization of the injection solvent composition</i> .....	52
3.3.2.1 <i>Impact of the type of organic solvent</i> .....	52
3.3.2.2 <i>Impact of dimethyl sulfoxide</i> .....	53
3.3.2.3 <i>Impact of formic acid</i> .....	54
3.3.3 <i>Impact of the container material</i> .....	55
3.3.3.1 <i>Glass vials</i> .....	56
3.3.3.2 <i>Regular polypropylene tubes</i> .....	58
3.3.3.3 <i>Protein low binding polypropylene tubes</i> .....	60
3.3.4 <i>Sweet-spot and setpoint analysis</i> .....	62
3.3.5 <i>Impact of deep-well plates</i> .....	64
3.3.6 <i>Impact of tips</i> .....	65
3.3.7 <i>Application in human plasma samples</i> .....	66
3.3.8 <i>Reliability of determined Substance P levels</i> .....	68
3.4 CONCLUSION .....	68
3.5 DISCLOSURE .....	69

---

<b>4. VALIDATED MASS SPECTROMETRIC ASSAY FOR THE QUANTIFICATION OF SUBSTANCE P AND HUMAN HEMOKININ-1 IN PLASMA SAMPLES: A DESIGN OF EXPERIMENTS CONCEPT FOR METHOD DEVELOPMENT .....</b>	<b>70</b>
4.1 BACKGROUND AND AIM .....	70
4.2 MATERIALS AND METHODS .....	71
4.2.1 <i>Chemicals and materials</i> .....	71
4.2.2 <i>Sample preparation</i> .....	72
4.2.3 <i>Preparation of peptide solutions</i> .....	72
4.2.4 <i>Instrumentation</i> .....	73
4.2.5 <i>Quality by Design</i> .....	73
4.2.5.1 <i>Design and setpoint characteristics</i> .....	76
4.2.5.1.1 <i>Micro-solid phase extraction protocol</i> .....	76
4.2.5.1.2 <i>Chromatographic phases and gradient optimization</i> .....	77
4.2.5.1.3 <i>Ion source parameters</i> .....	78
4.2.6 <i>Method validation</i> .....	79
4.2.7 <i>Application of the validated method</i> .....	80
4.3 RESULTS .....	80
4.3.1 <i>Method development using Design of Experiments</i> .....	80
4.3.1.1 <i>Development of a suitable micro-solid phase extraction protocol</i> .....	83
4.3.1.2 <i>Chromatographic phases and gradient optimization</i> .....	85
4.3.1.3 <i>Optimization of the ion source parameters</i> .....	88
4.3.2 <i>Method validation</i> .....	89
4.3.2.1 <i>Linearity, LLOQ, LOD, and carry-over</i> .....	89
4.3.2.2 <i>Accuracy and Precision</i> .....	92
4.3.2.3 <i>Recovery, selectivity and matrix effects</i> .....	92
4.3.2.4 <i>Stability</i> .....	93
4.3.3 <i>Applicability</i> .....	93
4.4 DISCUSSION .....	95
4.5 CONCLUSION .....	97
4.6 DISCLOSURE .....	97

---

<b>5. MASS SPECTROMETRIC STUDIES ON THE PEPTIDE INTEGRITY OF SUBSTANCE P AND RELATED HUMAN TACHYKININS IN HUMAN BIOFLUIDS</b>	<b>98</b>
.....	.....
5.1 BACKGROUND AND AIM .....	98
5.2 MATERIALS AND METHODS .....	100
5.2.1 Chemicals and materials .....	100
5.2.2 Preparation of peptide solutions .....	100
5.2.3 Sample processing .....	101
5.2.3.1 Biosample handling .....	101
5.2.3.2 Micro-solid phase extraction protocol .....	101
5.2.3.3 Ethics .....	102
5.2.4 Plasma extraction recovery studies .....	102
5.2.5 Sample processing studies .....	103
5.2.6 Comparative immunoassay studies .....	104
5.2.7 Cross-reactivity studies .....	105
5.2.8 Compound discovery by a hybrid immunoaffinity–LC-MS approach .....	105
5.2.9 Instrumentation .....	106
5.2.9.1 Peptide quantification by LC-MS/MS analysis .....	106
5.2.9.2 Compound elucidation by LC-HR-MS/MS analysis .....	106
5.2.9.3 Data analysis .....	107
5.3 RESULTS .....	109
5.3.1 Plasma extraction recovery studies .....	109
5.3.2 Sample processing studies .....	111
5.3.3 Protocol evaluation in human biofluids and porcine brain tissue .....	112
5.3.4 Comparative immunoassay studies .....	115
5.3.5 Cross-reactivity studies .....	116
5.3.6 Compound discovery by LC-HR-MS/MS analysis .....	117
5.3.6.1 Confirmation of the carboxylic acid of Substance P .....	117
5.3.6.2 Compound discovery of immuno-reactive Substance P in plasma .....	118
5.4 DISCUSSION .....	121
5.5 CONCLUSION .....	124
5.6 DISCLOSURE .....	125

<b>6. OVERALL CONCLUSION AND FUTURE PROSPECTS .....</b>	<b>126</b>
<b>7. FUNDING .....</b>	<b>129</b>
<b>8. REFERENCES .....</b>	<b>130</b>
<b>9. APPENDIX .....</b>	<b>144</b>
9.1 TABLE OF SUPPLEMENTARY .....	144
<b>10. LIST OF PUBLICATIONS.....</b>	<b>185</b>
10.1 PUBLICATIONS IN INTERNATIONAL PEER-REVIEWED JOURNALS.....	185
10.2 ORAL PRESENTATIONS.....	187
10.3 POSTER PRESENTATIONS.....	187

**VI. List of abbreviations**

ACE:	Angiotensin converting enzyme
ACN:	Acetonitrile
AEBSF:	4-(2-Aminoethyl)benzenesulfonyl fluoride
AUC:	Area under the curve
CAD:	Coronary arterial disease
CHF:	Chronic heart failure
CI:	Confidence interval
CINV:	Chemotherapy induced nausea and vomiting
Cps:	Counts per second
DCM:	Dilative cardiomyopathy
DPP-IV:	Dipeptidyl peptidase-IV
DoE:	Design of Experiments
DMSO:	Dimethyl sulfoxide
EDTA:	Ethylene diamine tetra acetic acid
EG:	Ethylene glycol
ELISA:	Enzyme-linked immunosorbent assay
EMA:	European Medicine Agency
FA:	Formic acid
FDA:	US Food and Drug Administration
hHK-1:	Human Hemokinin-1
HIV:	Human immunodeficient virus
HPLC:	High performance liquid chromatography
HR-MS:	High-resolution mass spectrometry
HSV:	Herpes simplex virus
IL:	Interleukin
ir-BNP:	Immunoreactive brain natriuretic peptide
LC:	Liquid chromatography
LENA:	Labeling of Enalapril from Neonates up to Adolescents
LOD:	Limit of Detection
LLOQ:	Lower limit of Quantification
MeOH:	Methanol
MMP:	Matrix metalloprotease

MS:	Mass spectrometry
MS/MS:	Tandem mass spectrometry
$\mu$ -SPE:	Micro-solid phase extraction
NEP:	Neprilysin
NK-1:	Neurokinin-1
NYHA:	New York Heart Association
OFAT:	One-factor-a-time
PhA:	Phosphoric acid
PrA:	Propionic acid
PRESS:	Predictive error sum of squares
Q:	Quadrupole filter
q:	Collision cell
RAAS:	Renin-Angiotensin-Aldosteron-system
RE:	Relative error
RIA:	Radio immunoassay
RPM:	Rounds per minute
ROS:	Reactive oxygen species
SD:	Standard deviation
SP:	Substance P
SP-LI:	Substance P-like immunoreactivity
SP(COOH):	Carboxylic acid of Substance P
TFA:	Trifluoro acetic acid
TNF $\alpha$ :	Tumor necrose factor $\alpha$
TOF:	Time-of-Flight
ULOQ:	Upper limit of Quantification
UPLC:	Ultrahigh performance liquid chromatography
USP:	US pharmacopeia

---

## VII. List of tables

TABLE 1: PHYSICOCHEMICAL CHARACTERISTICS OF SUBSTANCE P AND HEMOKININ-1.....	45
TABLE 2: MASS SPECTROMETRIC SETTINGS OF SUBSTANCE P AND HEMOKININ-1. ....	47
TABLE 3: PHYSICOCHEMICAL AND BIOLOGICAL PROPERTIES OF SUBSTANCE P, ITS CARBOXYLIC ACID, HUMAN HEMOKININ-1 AND SAR <sup>9</sup> -SUBSTANCE P (INTERNAL STANDARD). ....	71
TABLE 4: MASS SPECTROMETRIC SETTINGS OF THE ANALYTES SUBSTANCE P, HUMAN HEMOKININ-1 AND THE CARBOXYLIC ACID OF SUBSTANCE P AND THE INTERNAL STANDARD ((SAR <sup>9</sup> )-SUBSTANCE P) .....	73
TABLE 5: OUTLINE OF THE INVESTIGATED METHOD ASPECTS, CHARACTERISTICS AND INVESTIGATED FACTORS OF THE UTILIZED DESIGN OF EXPERIMENTS MODELS. ....	74
TABLE 6: FOUND ROBUST SETPOINTS OF THE INVESTIGATED METHOD ASPECTS WITH THEIR OBTAINED PROCESS CAPABILITY INDICES FOR EACH RESPONSE. ....	81
TABLE 7: COMPARATIVE STUDIES BETWEEN THE ENZYME-LINKED IMMUNOSORBENT ASSAY AND THE MASS SPECTROMETRIC ASSAY USING VARIOUS SAMPLE PROCESSING PROTOCOLS. ...	116

---

## VIII. List of figures

FIGURE 1: ENZYMATICAL ACTIVATION OF SUBSTANCE P. ....	16
FIGURE 2: METABOLIC DEGRADATION OF SUBSTANCE P IN BLOOD. ....	17
FIGURE 3: SCHEMATIC ACTIVATION OF THE NEUROKININ-1 RECEPTOR BY SUBSTANCE P AND ITS CELLULAR EFFECTS. ....	18
FIGURE 4: INFLAMMATORY DISEASES, WHICH ARE ASSOCIATED WITH REPORTED ELEVATED PLASMA LEVELS OF SUBSTANCE P. ....	20
FIGURE 5: MOLECULAR SCHEME OF THE IMPACT OF SUBSTANCE P IN THE PATHOPHYSIOLOGY OF CARDIOVASCULAR DISEASES. ....	22
FIGURE 6: SCHEMATIC NON-COMPETITIVE IMMUNOASSAY TO QUANTIFY SUBSTANCE P IN BIOANALYTICAL SAMPLES. ....	27
FIGURE 7: CHEMICAL STRUCTURES OF SUBSTANCE P AND HUMAN HEMOKININ-1. ....	28
FIGURE 8: SCHEMATIC COMPOSITION OF A LIQUID CHROMATOGRAPHY COUPLED TO A TANDEM MASS SPECTROMETER. ....	29
FIGURE 9: REPRESENTATIVE HIGH-RESOLUTION MS/MS SPECTRUM OF SUBSTANCE P AND ITS TYPICAL FRAGMENTATION PATTERN IN THE ONE-LETTER AMINO ACID CODE. ....	30
FIGURE 10: SCHEMATIC PRESENTATION OF THE ONE-FACTOR-A-TIME APPROACH AND THE CHEMOMETRIC APPROACH USING VARIOUS DESIGN OF EXPERIMENTS MODELS. ....	34
FIGURE 11: REPORTED BLOOD LEVELS OF SUBSTANCE P OF HEALTHY CHILDREN PLOTTED AGAINST THEIR AGE. ....	41
FIGURE 12: GOODNESS OF FIT PLOT FOR THE STATISTICAL EVALUATION OF THE DESIGN OF EXPERIMENTS MODEL. ....	52
FIGURE 13: POLAR PLOT OF THE OVERALL INDIVIDUAL EFFECTS OF THE INVESTIGATED FACTORS ON THE PREDICTED PEAK AREA OF SUBSTANCE P AND HUMAN HEMOKININ-1. ....	54
FIGURE 14: CONTOUR PLOTS OF THE IMPACT OF THE INJECTION SOLVENT COMPOSITION ON THE PREDICTED PEAK AREAS OF SUBSTANCE P AND HUMAN HEMOKININ-1 IN GLASS VIALS. ...	57
FIGURE 15: CONTOUR PLOTS OF THE IMPACT OF THE INJECTION SOLVENT COMPOSITION ON THE PREDICTED PEAK AREAS OF SUBSTANCE P AND HUMAN HEMOKININ-1 IN REGULAR POLYPROPYLENE TUBES. ....	59
FIGURE 16: CONTOUR PLOTS OF THE IMPACT OF THE INJECTION SOLVENT COMPOSITION ON THE PREDICTED PEAK AREAS OF SUBSTANCE P AND HUMAN HEMOKININ-1 IN PROTEIN LOW BINDING POLYPROPYLENE TUBES. ....	61

---

FIGURE 17: IMPACT ON THE INVESTIGATED TUBES AND VIALS ON THE OBSERVED PEAK AREA OF SUBSTANCE P AND HUMAN HEMOKININ-1. ....	62
FIGURE 18: CONTOUR PLOTS OF THE MINIMAL-RISK ANALYSIS IN REGULAR AND PROTEIN LOW BINDING POLYPROPYLENE TUBES. ....	63
FIGURE 19: IMPACT OF THE INVESTIGATED DEEP WELL PLATES ON THE OBSERVED PEAK AREA OF SUBSTANCE P AND HUMAN HEMOKININ-1. ....	65
FIGURE 20: IMPACT OF THE INVESTIGATED TIPS ON THE PREDICTED PEAK AREAS OF SUBSTANCE P AND HUMAN HEMOKININ-1. ....	66
FIGURE 21: REPRESENTATIVE STACKED CHROMATOGRAM OF SPIKED SUBSTANCE P AND HUMAN HEMOKININ-1 UNDER OPTIMIZED CONDITIONS IN HUMAN PLASMA. ....	67
FIGURE 22: EXEMPLARY GOODNESS OF FIT PLOT FOR THE STATISTICAL EVALUATION FOR THE OPTIMIZATION OF THE COMPOSITION OF THE MOBILE PHASES.....	82
FIGURE 23: PROCESS-CONTROL CHART OF THE OBSERVED PEAK AREAS AT THE CENTER POINT FOR EACH RESPONSE IN CONSECUTIVE RUN ORDER.....	82
FIGURE 24: COEFFICIENT PLOTS OF THE IMPACT OF THE INVESTIGATED FACTORS DURING THE SOLID-PHASE PROTOCOL.....	83
FIGURE 25: ROBUST SETPOINTS OF THE WASH STEP AND THE ELUTION STEP IN THE SOLID-PHASE EXTRACTION PROTOCOL CALCULATED BY THE MONTE-CARLO SIMULATION. ....	84
FIGURE 26: COEFFICIENT PLOT OF THE MAIN AND INTERACTIVE EFFECTS OF THE COMPOSITION OF THE MOBILE PHASES ON THE ANALYTES.....	86
FIGURE 27: COEFFICIENT PLOT OF THE IMPACT OF CHROMATOGRAPHIC SETTINGS ON THE ANALYTES. ....	86
FIGURE 28: POLAR PLOTS FOR THE EVALUATION OF THE MOST SUITABLE C-18 COLUMN.....	87
FIGURE 29: COEFFICIENT PLOT OF THE IMPACT OF THE INVESTIGATED ION SOURCE PARAMETERS ON SUBSTANCE P AND HUMAN HEMOKININ-1.....	89
FIGURE 30: FINAL LC-MS/MS METHOD BASED ON THE DESIGN OF EXPERIMENTS CONCEPT....	90
FIGURE 31: REPRESENTATIVE CHROMATOGRAMS OF THE BLANK, THE LOQ AND THE ULOQ SAMPLE OF THE VALIDATED METHOD. ....	91
FIGURE 32: REPRESENTATIVE CHROMATOGRAMS OF SPIKED AND NON-SPIKED PLASMA SAMPLES FROM FIVE INDIVIDUALS.....	94
FIGURE 33: CUSTOMIZED BLOOD DRAW IN PROTEIN LOW BINDING TUBES USING A MICRONEEDLE TO AVOID UNSPECIFIC PEPTIDE ADSORPTION TO THE SAMPLING MATERIAL. ....	104

FIGURE 34: WORKFLOW OF THE USED MASS SPECTROMETRY METHODS FOR PEPTIDE QUANTIFICATION APPLYING TRIPLE QUADRUPOLE MASS SPECTROMETRY AND FOR COMPOUND ELUCIDATION BY UTILIZING HIGH RESOLUTION MASS SPECTROMETRY. .... 108

FIGURE 35: POLAR CHARTS INDICATING THE MEAN PLASMA EXTRACTION RECOVERY RATES OF SPIKED SUBSTANCE P AND HUMAN HEMOKININ-1..... 110

FIGURE 36: IMPACT OF DIFFERENT PROTEASE INHIBITOR CLASSES AND SAMPLING DEVICES ON THE MEAN RECOVERY RATES OF SUBSTANCE P AND HUMAN HEMOKININ-1..... 112

FIGURE 37: REPRESENTATIVE CHROMATOGRAMS AND MEASURED LEVELS OF THE NEUROPEPTIDES IN DIFFERENT BIOFLUIDS AND TISSUES. .... 114

FIGURE 38: HIGH-RESOLUTION MS/MS SPECTRA OF SPIKED SUBSTANCE P IN HUMAN PLASMA AND THE INTERFERING SUBSTANCE. .... 119

FIGURE 39: WORKFLOW AND RESULTS OF THE PROTEIN CHARACTERIZATION BY IMMUNOCAPTURE-LC-HR-MS/MS APPROACH..... 120

# 1. Introduction

## 1.1 Biochemistry of Substance P

Substance P was firstly identified in 1931 as extract from equine brain and gut [1]. It was isolated as white powder (which was leading to its name Substance P(owder)) and demonstrated hemodynamic effects on smooth muscle cells. Substance P belongs to the peptide family of the tachykinins, which are phylogenetically one of the most ancient neurotransmitters in mammals [2]. Firstly described as a neurotransmitter in the central nervous system, Substance P recently gained focus as an immune and inflammatory modulator, was subsequently described ubiquitously in the human body and was found in brain tissues, spinal cord, blood, breast milk, saliva, semen and cerumen [3–7].

As a neuropeptide, Substance P is released from primary afferent neurons and derives from its precursor preprotachykinin-A [8]. An essential step for the biological activity of Substance P is the amidating of the C-terminal part, which made it more hydrophobic and finally allows to bind to the binding pocket of the neurokinin receptor. Substance P shares this property with many neuropeptides including neuropeptide Y, thyrotropin, oxytocin, vasopressin, gastrin or calcitonin [9]. This conversions to their biologically active forms is mediated by the peptidyl-Gly- $\alpha$ -amidating monooxygenase [10]. Utilizing copper as cofactor the prolonged form of Substance P (Glycine is added to the C-terminal part) will be metabolized to the biological active form under releasing glyoxylate (Figure 1). Beside its more hydrophobic C-terminal part, the amidated form of Substance P possesses thereby a beta-sheet structure, which is also needed for the biological activity [11].

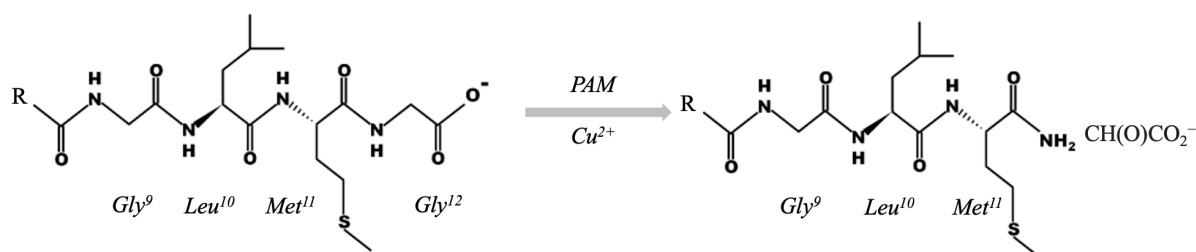
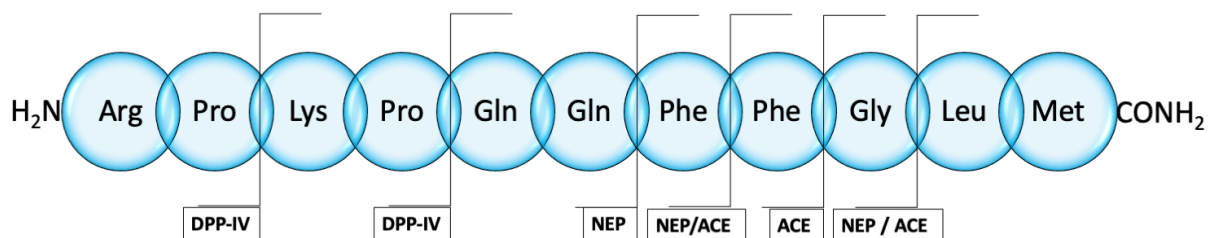


Figure 1: Enzymatical activation of Substance P.

Substance P is biologically activated by the peptidyl-Gly- $\alpha$ -amidating monooxygenase (PAM) utilizing copper as co-factor, leading to its C-terminal amidated form.

The half-life of Substance P and its precursor are very short in biological tissues (5.8 min for its precursor; 3.5 min for Substance P). As moderately hydrophilic undecapeptide, Substance P is rapidly metabolized by various degrading peptidases [12]. Different to the metabolism of Substance P in the central nervous system, Substance P is dominantly metabolized by three enzymes in blood [13]: the serine protease dipeptidyl peptidase-4 (DPP-IV) [14] and the metalloenzymes angiotensin converting enzyme (ACE) [15] and neprilysin [16]. These enzymes do not solely inactivate Substance P but also cleave it in several active metabolites, whereby C-terminal metabolites showed a high affinity to the neurokinin-1 receptor [17]. Both the degradation by ACE and neprilysin led to the inactivation of Substance P, whereas the metabolic degradation of Substance P by DPP-IV led to biological active C-terminal fragments [18,19] (Figure 2).



*Figure 2: Metabolic degradation of Substance P in blood.*

*The amino acid sequence of Substance P is shown in the three-letter-code and is degraded by Dipeptidyl-peptidase-IV (DPP-IV), Angiotensin converting enzyme (ACE) and Neprilysin (NEP) in blood.*

The biological effects of the tachykinins are mediated by the neurokinin receptors [20]. These receptors belong to the rhodopsin-like membrane structures, consisting of seven hydrophobic transmembrane domains, connected by extra and intracellular loops and are coupled to G-proteins. Receptor activation leads to the intracellular inositol 1,4,5-triphosphate conversion with following increase of intracellular calcium (Figure 3). Neurokinin receptors are rapidly desensitized leading to the internalization of the receptors [21]. The hydrophobic C-terminal part of the tachykinins is necessary for the binding into the hydrophobic ligand binding pocket of the receptor [19]. Regarding Substance P, the neurokinin-1 receptor is its preferred receptor. Substance P is also able to bind and activate the other neurokinin receptors, but with lower affinity. Within the tachykinin family, Substance P demonstrated the highest association rate constant of  $0.24 \pm 0.046 \text{ nM}^{-1} \cdot \text{min}^{-1}$  to the neurokinin-1 receptor, which was correlated with the highest potency and the maximal response for receptor activation [22].

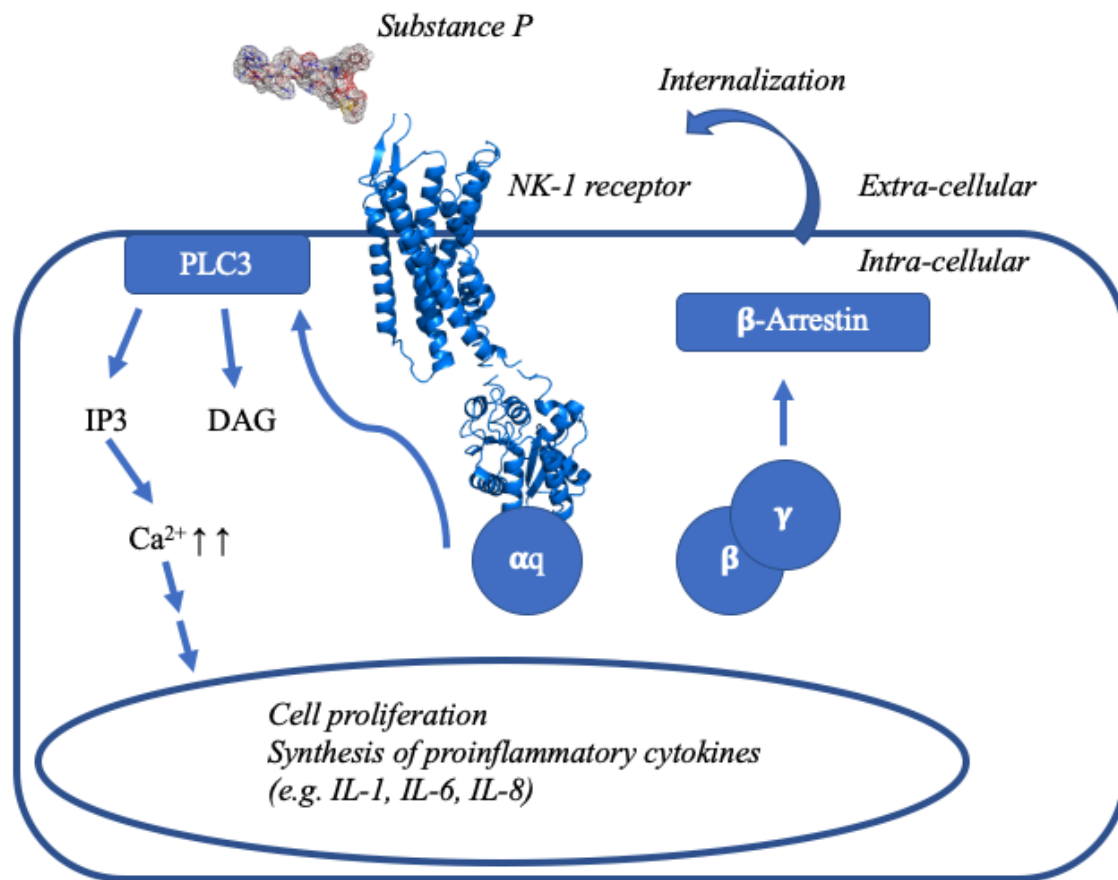
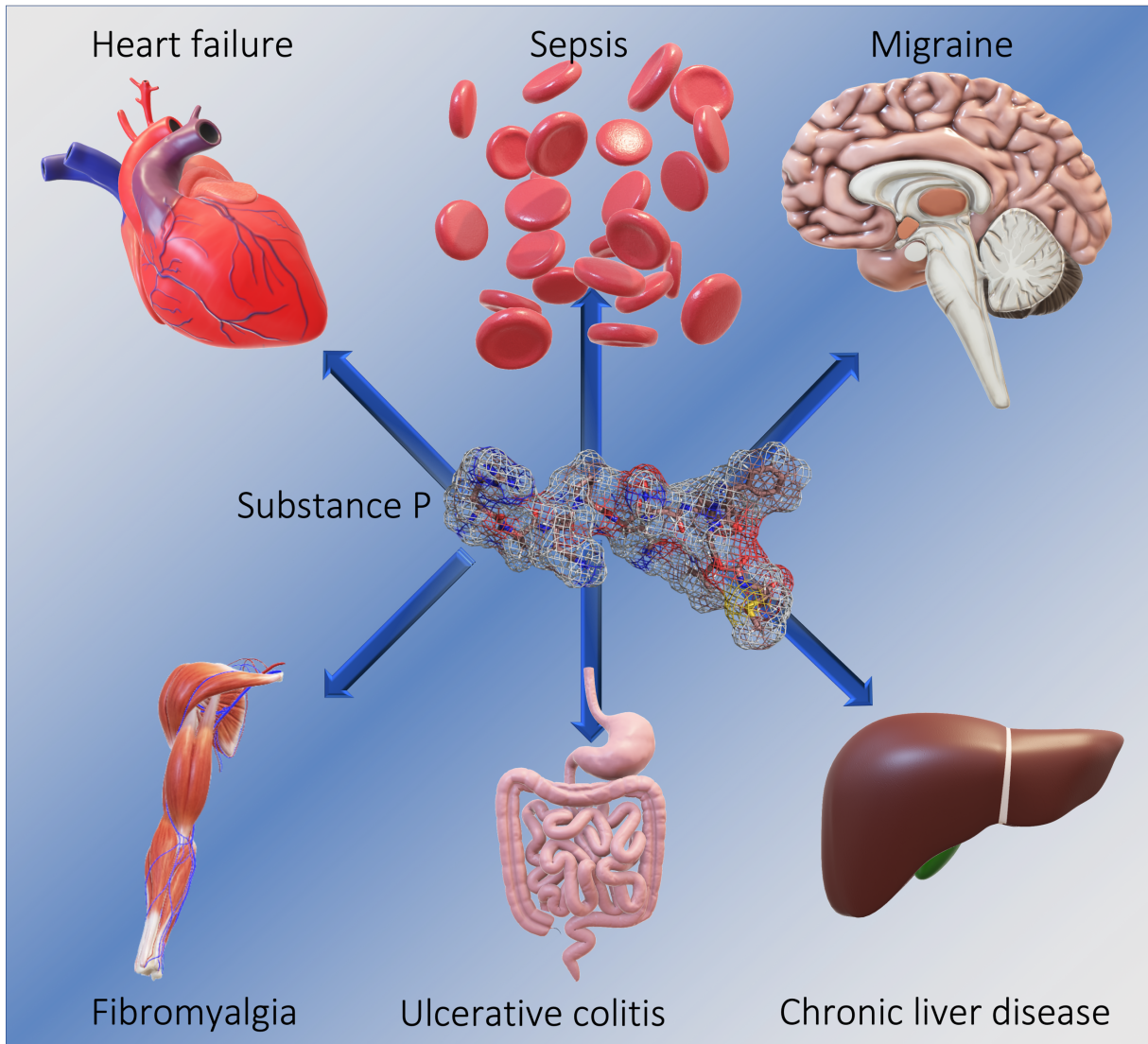


Figure 3: Schematic activation of the neurokinin-1 receptor by Substance P and its cellular effects.

(DAG: diacylglycerol; IL: interleukin; IP3: inositol-triphosphate; NK-1: neurokinin-1; PLC3: phospholipase C3)

The interaction of Substance P to the neurokinin-1 receptor was identified as a potential target for pharmaceutical intervention. Aprepitant - a selective antagonist of the neurokinin-1 receptor - is licensed as an antiemetic agent in the supportive therapy of chemotherapy induced nausea and vomiting (CINV) in 2003 [23,24]. Its safety was broadly investigated in adults and children, demonstrating a good tolerability without severe adverse effects [25–27]. In clinical phase III studies, a higher incidence of hiccough, elevated liver enzymes and obstipation were observed as typical side effects by the application of aprepitant to children and adolescents [28]. This acceptable adverse effect profile subsequently led to the registration of aprepitant for CINV diseased children over 6 months in 2015 [29].

As a neuropeptide Substance P is a transmitter of neuroinflammation and mediator within the immune system [1]. Thereof, Substance P is critically involved in a fast immune response by upregulating proinflammatory cytokines and by inducing the differentiation of lymphocytes [30–33]. As elevated blood levels of Substance P were found in a wide range of preclinical studies of inflammatory diseases, the inhibition of its receptor seemed to be a promising pharmaceutical target [34–38]. The profound knowledge of the proinflammatory pathomechanism of Substance P in cell and animal models consequently led to an interest in developing pharmaceutical agents antagonizing the tachykinin-system in current clinical research. The inhibition of the neurokinin-1 receptor is the pivot of actual clinical investigations because its endogenous agonist Substance P is the most involved tachykinin in various pathological processes and inflammatory diseases (Figure 4) [1]. Due to its involvement within the immune system, the potential application of aprepitant was especially investigated in infectious diseases as e.g. human immunodeficient virus (HIV) infection [39]. Subsequently, the anti-inflammatory potential use of aprepitant was investigated in HIV-infected subjects, resulting as a well-tolerated adjuvant therapy for comorbidities in HIV infection [40,41]. Furthermore, in rodent models, the application of aprepitant was highly effective against cardiac inflammation due to viral or toxic cardiomyopathy [42,43]. The emerging role of Substance P in cardiac inflammation and adverse heart remodeling should therefore further illustrated in the next chapter.



*Figure 4: Inflammatory diseases, which are associated with reported elevated plasma levels of Substance P.*

## 1.2 Pathophysiology of Substance P in cardiac inflammation

Recently, the role of Substance P emerged to its wide influence within peripheral tissues as the heart. Current reviews describe the role of the tachykinins as strong influencers of cardiac function and coronary tone [44].

In detail, Substance P plays both a beneficial and a noxious role in the heart pathology [32,33]. The release of Substance P from nerve fibers between cardiomyocytes and coronary artery endothelial cells during cardiac ischemia/reperfusion triggered an acute protective effect by preventing hypoxic cardiac damage and cardiac cell death by activation of neurokinin-1 receptors on cardiomyocytes [47]. Additionally, cardiac hypoxia led to an upregulation of neurokinin-1 receptors on cardiomyocytes, suggesting an acute survival strategy of the heart [48]. Moreover, Substance P was an indirect potent vasodilator by releasing nitric oxide from endothelial cells, resulting in increased myocardial perfusion and restored contractile function of the left ventricle [49].

For the long-term, the adverse impact overweighed the acute positive effects of Substance P on the heart [45], which is illustrated in Figure 5. Adverse cardiac remodeling and cardiac inflammation were mainly driven by Substance P through activation of cardiac mast cells, which were associated with end-stage cardiomyopathy and myocardial infarction [50]. Neurokinin-1 receptor activation on cardiac mast cells led to the release of various proinflammatory cytokines like tumor-necrosis-factor- $\alpha$  (TNF $\alpha$ ), interleukins, and matrix metalloproteases (e.g. MMP-2, MMP-9) [51,52]. Matrix metalloproteases were associated with changes in myocardial collagen fibers and a fibrillary collagen degradation leading to adverse cardiac remodeling. Subsequently, increased matrix metalloproteases levels were found in dilated ventricles in human heart failure patients and in animal myocarditis [53]. In addition, Substance P induced the release of renin from cardiac mast cells, a protease cleaving angiotensinogen to angiotensin-I [54]. Consequently, Substance P promoted the production of biologically active angiotensin-II, which was amongst others associated as a mediator of myocardial necrosis [55]. Moreover, Substance P activated the production of vascular endothelial growth factor in cardiac mast cells, a strong mediator of angiogenesis and releaser of inflammatory cytokines [56]. Coherently, by antagonizing the neurokinin-1 receptor, the degranulation of mast cells and subsequently the release of renin, matrix metalloproteases, and

TNF $\alpha$  were inhibited [51]. Furthermore, neurokinin-1 receptor antagonism of cardiac mast cells prevented adverse cardiac remodeling of the left ventricle [52].

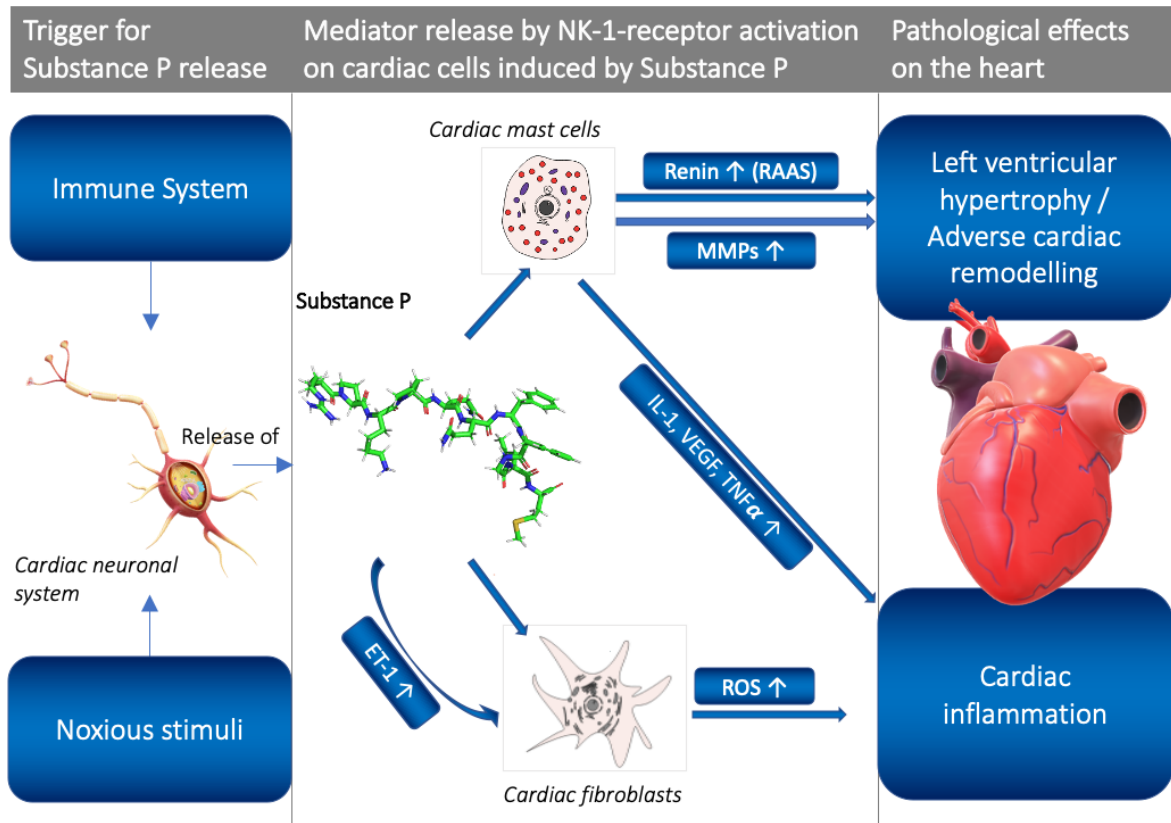


Figure 5: Molecular scheme of the impact of Substance P in the pathophysiology of cardiovascular diseases.

(ET-1: endothelin-1, IL-1: interleukin-1, MMP: matrix metalloproteases, NK-1: Neurokinin-1, RAAS: Renin-Angiotensin-Aldosterone-system, ROS: reactive oxygen, TNF $\alpha$ : tumor necrosis factor  $\alpha$ , VEGF: vascular endothelial growth factor)

Apart from the activation of cardiac mast cells, by upregulating endothelin-1, Substance P led to cardiac fibrosis and activation of fetal genes, which were associated with pathological cardiac hypertrophy [57]. By activation of the neurokinin-1-receptor on cardiac fibroblasts, Substance P caused cardiac inflammation through the release of reactive oxygen species [58]. In a parasite-infected murine model, Substance P was moreover associated with compensatory cardiomyocyte hypertrophy resulting in dilated cardiomyopathy.

In encephalomyocarditis virus (EMCV) infected mice, more than 60-fold higher levels of Substance P were detected in heart tissue [59]. The virus infection led to high mortality (51%)

and significant cardiac hypertrophy in two weeks. On the contrary, Substance P precursor-knockout mice were completely protected from cardiac inflammation, necrosis, and hypertrophy and all survived the EMCV-infection. Furthermore, the pre-treatment with a neurokinin-1 receptor antagonist significantly reduced mortality and cardiac hypertrophy in EMCV infected mice [43]. Wang et al. underlined the association of Substance P with viral myocarditis in EMCV infected mice [60]. The reasons for the intense Substance P release in viral myocarditis is not elucidated and invites to speculations. Besides an initial immune response due to viral infection [61] or the aforementioned cardiac survival strategy to prevent myocardial cell damage, there could be also the possibility of molecular mimicry by various viruses [62].

Moreover, Substance P seems to play a role in the cardiovascular adverse effects of the cytostatic doxorubicin. In (pediatric) cytostatic therapies, doxorubicin is known by its induction of toxic cardiomyopathy, leading to heart failure in young children [63]. In a rat cardiomyocyte cell line (H9C2), the use of aprepitant (licensed neurokinin-1 receptor antagonist) led to a decrease of doxorubicin-induced reduction of cell variability, to a decrease of apoptotic cell death (7-fold) and to a decrease of reactive oxygen species production (4.3-fold). Additionally, it was shown that doxorubicin led to a 2.2-fold increase in Substance P levels [42]. Consequently, in 8-week-old Sprague-Dawley rats, a doxorubicin oncological treatment was mimicked by applying 1.5 mg/kg/week doxorubicin over six cycles in eight weeks (cumulative dose of 9 mg/kg). The application of L732138 (neurokinin-1 receptor antagonist) (5 mg/kg/d) was started a week earlier and was applied over nine weeks in total. The application of the neurokinin-1 receptor antagonist inhibited the reduction of the left ventricular mass, ameliorated the collagen deposition induced by doxorubicin treatment and reduced the apoptosis (3-fold) [64]. There did not seem to be a direct doxorubicin-Substance P axis since aprepitant (2 mg/kg/day) also diminished systolic and diastolic dysfunction and oxidative stress caused by erlotinib, another cytostatic known by its cardiac adverse effects in pediatric cytostatic therapy. In this model of male Sprague-Dawley rats, the neurokinin-1 receptor blockade resulted in the reduction of cardiac remodeling and fibrosis [65]. As young children (especially under 4 years) are more susceptible to the cardiac adverse effects of doxorubicin and erlotinib and are a special risk group to develop cardiac toxicity [66], the underlying mechanism of toxic cardiomyopathy is of special interest.

In summary, there is evidence that Substance P is involved in adverse heart remodeling and the pathogenesis of myocarditis [59], consequentially leading to cardiomyopathy and heart failure. Consequently, the neuropeptide Substance P may be critically involved in the pathogenesis of both viral and toxic cardiomyopathy, two principal cardiomyopathies leading to pediatric heart failure.

### 1.3 Pediatric heart failure

Heart failure is defined by the European heart society as a clinical syndrome caused by a structural or functional cardiac abnormality resulting in a reduced cardiac output and intracardiac elevated pressures [67]. In adults, the prevalence of heart failure is approximately 1-2% of the adult population, showing the highest prevalence (>10%) in the eldest population (>70 age) [68,69]. In this population, the presence of hypertension and ischemic heart diseases are principal reasons to develop heart failure. Following their diagnosis, there exist a wide range of evidence-based pharmacological treatment options for heart failure involving angiotensin converting enzyme (ACE) inhibitors, angiotensin-1 receptor antagonists, beta-receptor antagonists and diuretics as first-line therapy [67].

In contrary, pediatric heart failure is a very rare disorder. In childhood, heart failure is considerably lower than in adults but the prime reason for cardiovascular mortality and heart transplantation [70]. Besides congenital heart diseases, cardiomyopathy is the main reason for the development of heart failure in children [71,72]. Whereas, congenital heart diseases can be diagnosed prenatally by fetal echocardiography and their surgical intervention is the favorable therapy option in industrial nations, cardiomyopathy is often not detected until the first symptoms of developing heart failure occurs [71–73]. Pediatric cardiomyopathy is a rare but severe disorder with an incidence of 1.1 - 1.5 per 100,000 children [73]. In the pediatric population, the highest incidence of cardiomyopathies is present under one year of age. Dilated cardiomyopathy (DCM) (incidence of 0.57 per 100,000 children) is the most common form of cardiomyopathy in children and is characterized by a typically dilated thin-walled left heart ventricle and a resulting depressed ventricular function. Concerning a 2-years prediction of DCM in children, 40 % of the children require heart transplantation or die [73]. As a consequence, survivors suffer under heart failure receiving long-life heart medication or immunosuppression after transplantation. One of the major causes for the development of pediatric DCM are inflammatory cardiomyopathies due to viral infection [74]. 35 - 48% of DCM diseased children have evidence of viral myocarditis. Especially in children, infection of Enteroviruses and Adenovirus are the most common causes provoking viral cardiomyopathy [74]. Besides Influenza, Eppstein-Barr, HIV and Herpes simplex viruses (HSV) were also found in endomyocardial biopsies of DCM diseased children. The pathophysiology of viral myocarditis is not yet fully elucidated. Both direct viral myocardial damage and an extensive immune response seem to be involved in the pathogenesis of viral cardiomyopathy [75].

Moreover, the current pharmacotherapy from adults is not strongly evident due to the other etiology and pathogenesis of heart failure in children [76–78]. Enalapril (ACE-inhibitor) therapy, for example, the gold standard for heart failure therapy in adults, showed no long-term benefits in a retrospective study of children with toxic cardiomyopathy and resulted for all children in cardiac transplantation or death [63]. Furthermore, there is still a lack of effective treatment options for pediatric heart failure since the current therapies are often unable to restore the contractile function [71]. Pediatric evidence-based medicine is difficult to achieve as clinical trials were rarely performed due to e.g. the tough recruitment of patients, the conduct of pediatric studies and the bioanalytical challenges concerning pediatric study samples [79,80].

Concerning this lack of meaningful clinical trials the European Union supports the research of pediatric and orphan diseases, resulting amongst others in the LENA (Labeling of Enalapril from Neonates up to Adolescents) project, which was an investigator-driven clinical investigation funded by the European Commission (Seventh Framework Program [FP7/2007-2013] under grant agreement n°602295 [LENA]) [81]. The LENA project had the aim to introduce a child-friendly therapy option (orally disintegrating mini-tablets containing enalapril) to the European market by generating (pharmacokinetic) data to apply for market authorization. The pharmacokinetic data of enalapril in serum samples of children suffering from heart failure were determined and aligned as primary outcome. As secondary study outcome it aimed to obtain exploratory pharmacodynamic data to understand the distinct pathogenesis and etiology of pediatric heart failure by investigating various biomarkers of the renin-angiotensin-aldosterone system [82–85].

Within the renin-angiotensin-aldosterone system, enalapril inhibits the ACE, which metabolize angiotensin 1 to angiotensin 2, a strong mediator of cardiac remodeling. Besides of this well-known and widely investigated conversion of angiotensin 1 to angiotensin 2, ACE is also responsible for the metabolic degradation of several other peptides including Substance P [13]. As the inhibition of ACE is associated with higher Substance P plasma levels [86], the monitoring of Substance P plasma levels may be also of special interest, as Substance P is involved in the development and progress of cardiac inflammation. Thus, the bioanalysis of Substance P plasma levels in cardiovascular-diseased children may provide valuable additional information for the etiology of pediatric heart failure.

## 1.4 Bioanalysis of Substance P

Up to now, the bioanalysis of Substance P in blood samples was generally implemented by radioimmunoassays (RIA) and enzyme-linked immunosorbent assays (ELISA) [87]. The function of immunoassays bases on the principle of an antigen-antibody interaction, which needs a specific antibody raised against the analyte of interest. Most of the immunoassays manufactured for Substance P are non-competitive (sandwich) assays, which consist of an immobilized primary antibody and a secondary antibody with a detectable label (Figure 6). The analyte of interest in the bioanalytical matrix e.g. blood plasma firstly binds to specific raised immobilized antibodies. In the next step, the secondary antibody binds to the remained free primary antibodies, which finally leads to a radioactive detection (RIA) or an enzyme-based luminescence (ELISA) of the bound label to the secondary antibody.

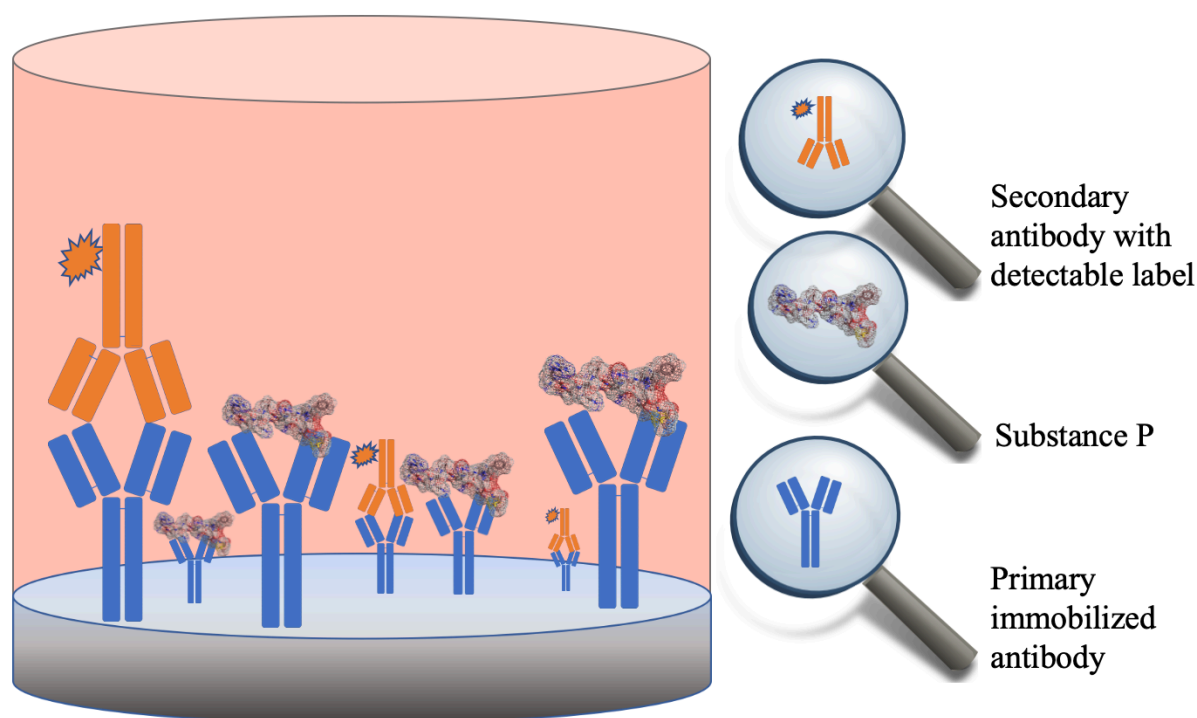


*Figure 6: Schematic non-competitive immunoassay to quantify Substance P in bioanalytical samples.*

In clinical trials and bioanalytical investigations, the use of immunoassays is common due to their commercial availability, advantages in automatization of work procedures and the non-requirement of specialized trained personnel. Nevertheless, immunoassays show several limitations concerning the determination of Substance P [88]. The selectivity of immunoassays,

especially cross-reactivity to bioactive metabolites of Substance P, still remains a challenge and depends on the used antibody. Furthermore, with the discovery of human Hemokinin-1 in 2002 [89], a tachykinin showing more than 70% primary amino acid analogy to Substance P [90] and possessing the same pharmacological active binding site [91] (Figure 7), immunoassays face the limits of meaningful results. C-terminal targeting antibodies used in immunoassays are not only blind to differentiate between Substance P and its bioactive C-terminal metabolites but also between Substance P and human Hemokinin-1, leading to biased values. As human Hemokinin-1 is also involved in heart physiology [92,93], a selective determination of Substance P is mandatory to evaluate the specific role of Substance P in the cardiovascular system, particularly since reported human Hemokinin-1 blood levels were substantially higher (more than 10 fold) than Substance P blood levels [34]. Furthermore, most of the suppliers of these immunoassays did not recommend their use to quantify Substance P in plasma anymore due to the cross-reactivity to human Hemokinin-1. Reported plasma levels of Substance P were merely measured by immunoassays, leading to the question of their reliability.

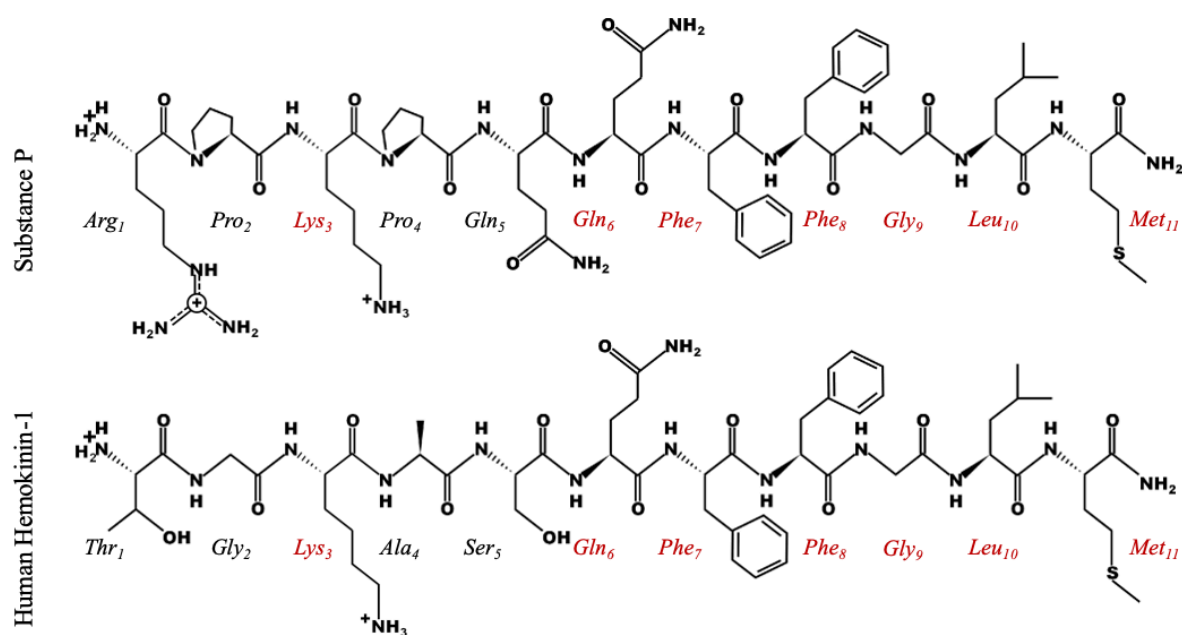
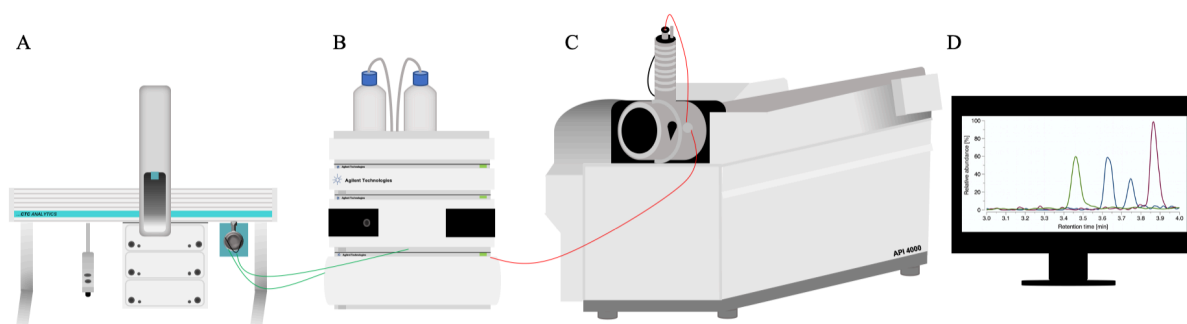


Figure 7: Chemical structures of Substance P and human Hemokinin-1.

Similar amino acids between both peptides are marked red.

Hence, due to the described cross-reactivity of the immunoassays, an alternative analytical method is mandatory for the reliable bioanalysis of Substance P. Compared to the widely used and established immunoassays, the use of liquid chromatography coupled to mass spectrometry

(LC-MS) is a bioanalytical technique, which would overcome the selectivity and cross-reactivity issues of immunoassays (Figure 8) [94]. Its wide use is limited for bigger diagnostic laboratories as it is very cost-expensive and needs highly trained personnel. Based on the principle of measuring the mass to charge ratio of gas phase ions ( $m/z$ ), Substance P can be easily distinguished from human Hemokinin-1 due to its distinct mass. Furthermore, using LC-MS/MS the simultaneous quantification of both neuropeptides would be achievable using a single bioanalytical sample [95].



*Figure 8: Schematic composition of a liquid chromatography coupled to a tandem mass spectrometer.*

*(A) Autosampler, which stores the (extracted) bioanalytical samples and injects them to the valve port, (B) High performance liquid chromatographic system to separate the analytes from interfering matrix on an analytical column; (C) Analytes were ionized in the electrospray source, the precursor ion of the analytes were analyzed in the first quadrupole, were fragmented in the collision cell by a collision gas (nitrogen, helium or argon) and the fragments (product ions) were analyzed by the second quadrupole; (D) the detected ions were converted to electronic signal finally resulting in an evaluable chromatogram.*

As MS techniques principally base on the determination of  $m/z$  ratios of the gas phase ions produced by the electrospray ionization, mass analyzers as e.g. a quadrupole filter (Q) or a time of flight (TOF) analyzer are used for the measurement of the analytes of interest. In the proteomic research, MS techniques are used for two principal purposes, the quantification or identification of peptides and proteins [96,97]. Therefore, two mass analyzers are combined, resulting in a tandem mass spectrometer (MS/MS) such as a triple quadrupole MS (QqQ) (two combined quadrupole filters) or a QqTOF MS (quadrupole combined to a time of flight analyzer) [98]. In MS/MS systems both mass analyzers are linked by a collision cell (q), which uses an inert collision gas (e.g. nitrogen, helium or argon) to fragment the precursor ions of the

analyte to its product ions. The detection of the precursor ion in the first mass analyzer and the subsequent detection of the product ions in the second mass analyzer can be used for the identification of the proteomic analyte as peptides and proteins demonstrate typical fragment patterns, resulting in b and y fragments, specific for their amino acid sequence. Using the transition of a precursor ion to its product ion, peptides can be selectively and sensitively quantified (Figure 9).

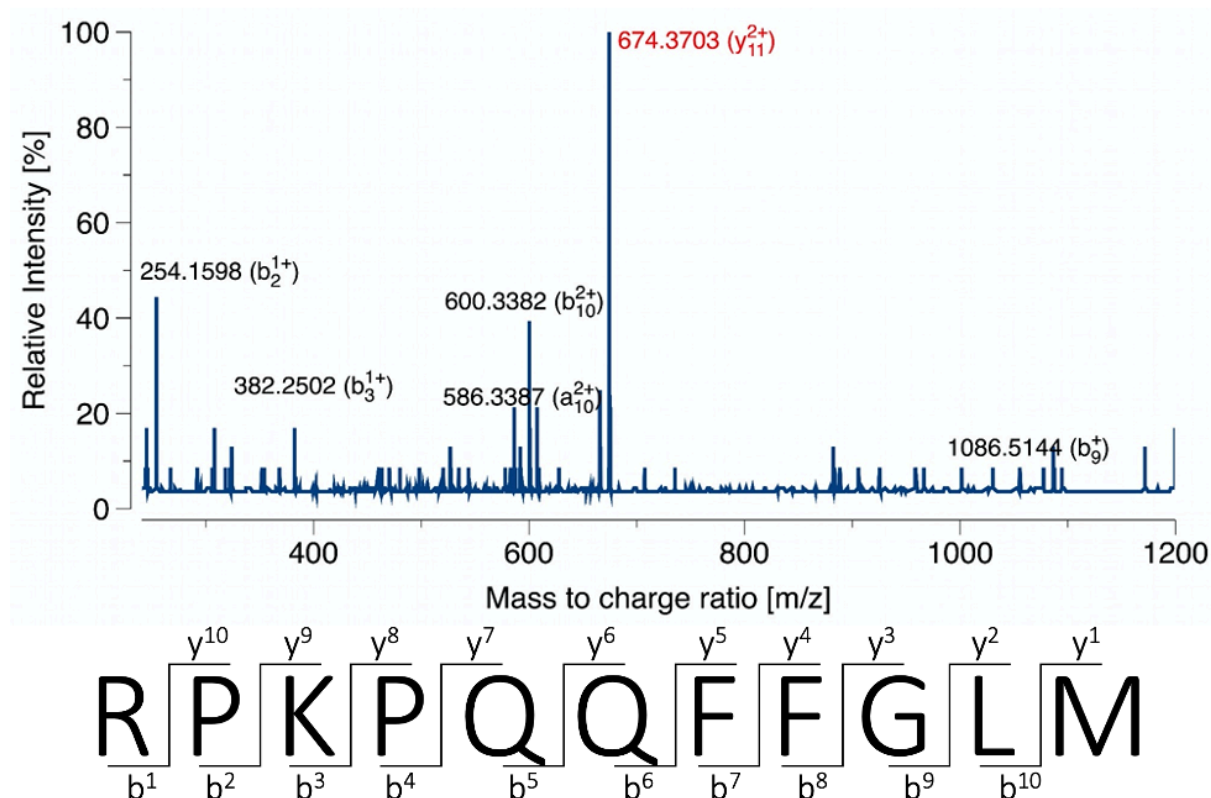


Figure 9: Representative high-resolution MS/MS spectrum of Substance P and its typical fragmentation pattern in the one-letter amino acid code.

The precursor ion of Substance P is twofold charged and marked in red ( $y_{11}^{2+}$ ). Due to its specific fragmentation pattern owed to its unique amino acid sequence, the product ions can be used for its identification or their transition (e.g. 674.3703 m/z  $\rightarrow$  600.3382 m/z) can be used for the quantification of Substance P.

The described advantages using LC-MS/MS analysis led to their wide application for small molecules as pharmaceutical agents and exogenous toxins. Despite its superiority concerning selectivity, MS analysis often lacks the sensitivity to measure levels of endogenous analytes as e.g. biomarkers, peptides and proteins due to their presence in low concentrations in biological

fluids. Moreover, due to the properties of peptides to be multiply charged, the sensitivity of measuring peptides is strongly reduced in distinction to small molecules.

Especially for Substance P which is present in low picomolar concentrations in blood ( $21.94 \pm 18$  pg/mL ; healthy volunteers,  $n = 7$ ) [99,100], this lack of sensitivity is the principal reason, that no Substance P plasma levels measured by LC-MS analysis were reported until yet. Existing assays lacked the sensitivity to measure endogenous Substance P blood levels [101]. However, MS techniques were successfully applied for the quantification of Substance P in biological matrices, in which Substance P is present in higher concentrations as e.g. in tears fluid, brain tissue or spinal cord [102–104]. So far, several working groups quantified Substance P by LC-MS, but merely Substance P levels in various central nervous system tissues in animals [102,105–107], whereby Substance P is present in higher concentrations (ng/mL) than in blood (concentrations about fg/mL – pg/mL). Thus, for the development of a LC-MS/MS method to quantify low abundant peptides as Substance P, much effort and workload have to be done to increase the sensitivity of the method to determine endogenous levels in peripheral tissues as blood. This is often associated with time consuming efforts and a high waste of chemicals and materials, which may be repeated if the developed method is not robust and not qualified for regulatory guidelines. For this purpose, chemometric tools as a Design of Experiments concept may be useful as it led to a lean method development by concordantly evaluate the robustness of the method using statistical tools and the comprehensive optimization of critical method aspects for improving the sensitivity of the assay.

## 1.5 Design of Experiments as a chemometric tool for method development

In the bioanalytical field, method development might be a time-consuming effort, due to many critical steps such as e.g. the biosamples preparation, adequate analyte separation or the method robustness. These critical steps were typically addressed by the traditional one-factor-a-time (OFAT) approach during method development, which is characterized by the separate and subsequent investigation of each factor, a high workload for the experimenter and unidentified interaction and synergism potentials between the investigated factors (Figure 10-A). Consequently, (unknown) interactions and synergisms between investigated method factors might lead to a non-optimized, unprecise or non-robust bioanalytical assay, resulting in the complete redevelopment of the method in the worst case. To address these potential issues, chemometric tools might be used, which are already applied in other disciplines as e.g. in the pharmaceutical industry [108].

The concept of Design of Experiments as a chemometric tool was firstly introduced by Fisher in 1926 to solve fundamental experimental problems. In the recent years, the Design of Experiments concept was embedded in Quality by Design approaches, which were predominantly applied in the pharmaceutical industry to improve the quality and robustness of industrial processes. The application of statistical designs leads to the identification of vulnerable, critical processes and the reduction of variability. The identification of critical components as well as the reduction of day-to-day variations are also recommended and valuable for the method development within the (bio-)analytical chemistry [108].

The consequent new-born discipline of chemometry combines the use of statistical tools as Design of Experiments in the analytical chemistry, which can be applied for the design and conduct of analytical experiments [109]. Since the development and validation of a bioanalytical assay might be a time-consuming effort due to lack of method inter-run robustness and variable outcomes, the implementation of chemometric approaches are recommended for a lean and robust method development. In contrast to the traditional OFAT approach, a Design of Experiments approach enables the investigation and optimization of various factors conjointly, revealing possible interactions or synergism between single factors. Combining all factors conjointly results in a full factorial design, which lead to a better understanding of the interactions of the various factors compared to the OFAT approach, but the number of experiments is still extensive and not material and time saving (Figure 10-B). Thus, classical models as full-factorial designs are thereof delimited to D-optimal designs, which are computer-

based designs. Utilizing D-optimal designs, the most outcome is achieved by a limited number of experiments, whereas the missed (not performed) experiments are statistically calculated. For the purpose of a lean method development, D-optimal designs seems favorable as the aim is the maximization of the **D**eterminants (the response outcome) by simultaneously minimizing the number of experiments for a sufficient reliable statement (Figure 10-C). Moreover, D-optimal designs enable the investigation of constraints, combinations of factor settings unfeasible to conduct in practical experiments as e.g. restriction of chemical concentrations to avoid instrumental damage or interactions with the analytes (Figure 10-D). In consequence, applying a Design of Experiments concept lead to a better understanding of the fundamental underlying mechanism of the investigated settings by revealing their interactions and synergisms.

For a robust statistical model leading to a reliable bioanalysis, several statistical aspects have to be addressed. First, as day-to-day variations may affect the conducted experiments and may lead to a weak inter-day robustness, experiments should be blocked to evaluate the day-to-day deviation, which is a principal issue in the conduction of bioanalytical methods. Secondly, experiments should be randomized when suitable to monitor uncontrollable errors. Third, a replication of experiments is needed to calculate the pure error of the analytical setting. Various chemometric tools as the regression evaluation ( $R^2$ ), process capability indices ( $C_{pK}$ ) and control charts can be further used to monitor the goodness, reliability and the robustness of the model [110].

Due to the described advantages in method development, a recent draft of the US Pharmacopeia (USP) Validation and Verification expert panel (USP 1220) proposed the implementation of a Quality by Design approach using Design of Experiments during method development for a better method understanding and improved risk control management [111,112]. The USP draft highlights the improvement of analytical knowledge and the intelligent method design by applying a Design of Experiments concept.

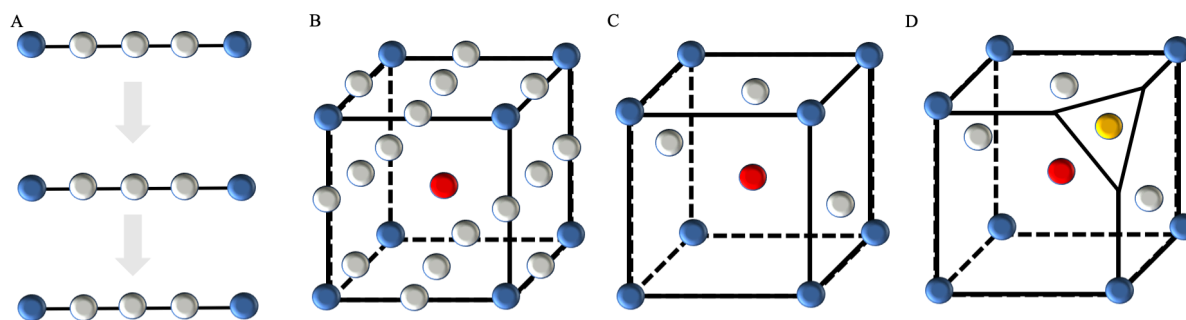


Figure 10: Schematic presentation of the one-factor-a-time approach and the chemometric approach using various Design of Experiments models.

(A) Usually used one-factor-a-time approach, whereby each factor (represented by the black lines) is separately investigated by a certain number of experiments (represented by the circles); the blue ones indicate the limits chosen by the experimenter, (B) Using a chemometric approach, a full factorial design enables the investigation of all factors conjointly, consequently shows interactions between factors, but is associated with a high number of experiments; a center point experiment (red circle) is co-analyzed to determine the reproducibility of the chemometric model, (C) Utilizing a D-optimal design, whereby a limited number of experiments were measured and the missed ones were computed by the model encompasses both the analysis of interactions between the factors and a reduced number of practical experiments, (D) Moreover, a D-optimal design enables the investigation of models with constraints (represented by the yellow circle), which are combinations of factor settings unfeasible to conduct in practical experiments (e.g. restriction of chemical concentrations to avoid instrumental damage or interactions with the analytes).

Following the USP recommendations, several workgroups has implemented Design of Experiments within their method development as e.g. to optimize the sample preparation [113] or the analyte separation [114]. Although these recent publications demonstrated a successful optimization of single bioanalytical aspects, no comprehensive concept was presented for a complete assay development starting from sample preparation to final analysis, ensuring a highly optimized bioanalytical method. Due to the low abundance of endogenous Substance P plasma levels, a comprehensive investigation and optimization of each method component was absolutely mandatory using the given analytical instruments.

Thus, by applying a chemometric approach and using Design of Experiments, critical method aspects such as plasma sample preparation, analyte selectivity, and method sensitivity could be systematically and comprehensively investigated and optimized, finally resulting in a robust method for analyzing the neuropeptides. By operating D-optimal designs, a limited number of experiments was necessary resulting in a time-saving and eco-friendly approach by reducing chemical and material waste. In consequence, a lean method development for the LC-MS/MS quantification of Substance P and human Hemokinin-1 would be achievable and would result in a robust, highly sensitive, reliable and comprehensively optimized LC-MS/MS assay.

## 1.6 Objective

Owing to its pathological role in the cardiovascular system, Substance P may be a potentially useful biomarker to monitor the development and progress of inflammatory cardiovascular diseases such as cardiomyopathy and heart failure. As it has been described as present in human plasma, determination of the plasma levels of Substance P would have clinical utility. However, the currently available bioanalytical assays for quantification of Substance P in human plasma are limited to immunoassays which are no longer recommended due to cross-reactivity issues of the antibodies used. Therefore, a selective and reliable bioanalytical assay, which facilitates the critical reevaluation of the role of Substance P in inflammatory as well as cardiovascular diseases, is required. Thus, the objective of this thesis is divided into four parts:

- (i) First, the current assessment of Substance P in cardiovascular diseases, in combination with the bioanalytical methods for measurement of Substance P in human blood, has to be reviewed by summarizing the recent bioanalysis of Substance P in the blood of adults and children with cardiovascular disease. A comprehensive investigation of bioanalytical methods and blood sample processing used in the literature should reveal reported critical aspects to address them in the development of the LC-MS/MS assay.
- (ii) Second, the thesis describes the lean development of a highly sensitive LC-MS/MS for bioanalysis of Substance P and its close relative human Hemokinin-1 in human plasma. As existing LC-MS/MS assays lack the sensitivity to measure endogenous plasma levels, which are present in low picomolar concentrations, development of a comprehensive method is required to realize maximal sensitivity and robustness. This will be addressed by a specifically developed Quality by Design concept. Based on these innovative chemometric tools, various aspects of critical methodology, such as the injection solvent composition, analytical material used, plasma extraction, and chromatographic separation, as well as the sensitivity of the method will be investigated for a better understanding of critical aspects of method failure. These critical aspects will be tackled and optimized by newly introducing and customizing a comprehensive Design of Experiments concept for bioanalysis of peptide quantification via LC-MS/MS.

- (iii) Third, validation according to international bioanalytical guidelines should follow method development to guarantee reliable and robust results for the measured concentrations of the peptides. Therefore, international bioanalytical guidelines will be used to demonstrate the accuracy, precision, sensitivity, selectivity, plasma recovery and matrix effects, and stability of the developed assay.
  
- (iv) Fourth, by applying the validated assay, the presence of endogenous concentrations of Substance P and human Hemokinin-1 will be investigated in human plasma samples. The results obtained will be compared to immunoreactive Substance P concentrations measured by a commercially available immunoassay. By using HR-MS analysis, analogs of Substance P will be identified, and possible cross-reactors with the immunoassay will be revealed.

In summary, by establishing and applying a validated LC-MS/MS assay, this study should make a decisive contribution to the assessment of the exposure of previously described Substance P levels in humans. If previously reported results cannot be confirmed, the assay will contribute to the critical rethinking of Substance P as a marker in other studies and allow a new assessment of its clinical utility.

## **2. Substance P in cardiovascular diseases - A bioanalytical review**

### **2.1 Background and Aim**

Detailed molecular mechanisms of Substance P in the cardiovascular system are broadly reviewed [3,44,115–117] (see also section 1.2) and therefore should not be the principal subject of the present review. However, there exists a crucial lack of information about the bioanalytical determination of Substance P blood levels in cardiovascular diseases, especially in children. Therefore, this review will (1) investigate the determination of Substance P blood levels in cardiovascular diseases in humans focusing on bioanalytical aspects; (2) briefly summarize the actual measurement of Substance P levels in children; and (3) discuss influencing factors, may lead to biased Substance P levels in blood samples.

### **2.2 Methods**

For the review of the bioanalysis of Substance P in cardiovascular-diseased subjects and healthy children, a literature research was conducted using PubMed as a search tool. Following Mesh-terms were applied: (Substance P AND bioanalysis OR immunoassay OR ELISA OR RIA OR mass spectrometry OR levels OR concentrations OR blood OR saliva). Studies without cardiovascular-diseased or pediatric subjects were excluded. Original publications and reviews in English were included until December 2018.

### **2.3 Results**

#### **2.3.1 Quantification of Substance P blood levels in cardiovascular diseases**

The existing data of Substance P blood levels in cardiovascular diseases in adults are limited and summarized in Supplementary Table 1. Data of cardiovascular-diseased children are lacking until now. First, Valdemarsson et al. (1991) investigated the Substance P plasma levels in patients with chronic heart failure (CHF), either receiving an Angiotensin converting enzyme (ACE)-inhibitor or not [86]. In their study, mild (NYHA I-II) and severe (NYHA III-IV) CHF were associated with higher Substance P levels compared to healthy controls (mean  $\pm$  standard deviation (SD):  $4.1 \pm 0.4$  pg/mL [n = 10; NYHA I-II],  $3.1 \pm 0.4$  pg/mL [n = 17; NYHA III-IV], respectively, vs.  $1.7 \pm 0.2$  pg/mL [n = 31; healthy]), which correlates with the findings in the cell and animal model. As expected, due to the inhibited metabolic degradation of Substance P,

patients under ACE-inhibitor treatment had significantly higher levels of Substance P (mean  $\pm$  SD:  $5.5 \pm 1.1$  pg/mL [n = 15]) than untreated diseased subjects (mean  $\pm$  SD:  $3.1 \pm 0.4$  pg/mL [n = 15]). In 2012, Wang et al. studied the Substance P serum levels in patients with coronary artery disease (CAD) and diabetes [118]. The presence of CAD led to decreased Substance P levels (mean  $\pm$  SD:  $35 \pm 5$  pg/mL [n = 44]) compared to healthy subjects (mean  $\pm$  SD:  $65 \pm 15$  pg/mL [n = 44]). In 2014, Han et al. measured the Substance P serum levels in patients with cardiac infarction (mean  $\pm$  SD:  $191 \pm 141$  pg/mL [n = 30]), unstable angina (mean  $\pm$  SD:  $103 \pm 111$  pg/mL [n = 21]), stable angina pectoris (mean  $\pm$  SD:  $31 \pm 80$  pg/mL [n = 30]) and control subjects (mean  $\pm$  SD:  $70 \pm 132$  pg/mL [n = 29]) [119]. They demonstrated higher Substance P levels in patients with acute cardiac infarction and suggested the potential role of Substance P as an early diagnostic biomarker. Due to the metabolic degradation of Substance P by neprilysine, Vodovar et al. (2015) demonstrated the negative correlation of Substance P and neprilysine in plasma levels of 684 subjects with acute decompensated heart failure and CHF [16]. Furthermore, the Substance P levels could be significantly stratified regarding immunoreactive B-Type natriuretic peptide (ir-BNP) as a marker for the severity of heart failure (median [interquartile range (IQR)]:  $43 [37 - 49]$  pg/mL [ir-BNP < 916 pg/mL] vs.  $59 [57 - 64]$  pg/mL [ir-BNP > 916 pg/mL]). In 2018, Noug   et al. investigated the Substance P plasma levels of CHF patients under sacubitril treatment, a selective neprilysine-inhibitor, basically showing higher Substance P levels under treatment than at baseline (median [IQR]:  $75 [25 - 275]$  pg/mL vs.  $36 [27 - 44]$  pg/mL) [120], as expected due to the inhibited degradation by neprilysine.

### 2.3.2 Quantification of pediatric Substance P blood levels

Generally focusing on the measurement of blood markers in children, low blood volumes are required, hence, the children should not be overly stressed. Blood volumes in children of 80 – 85 mL/kg restrict “blood-expensive” methods to evaluate Substance P levels, especially in neonates and infants. For ethic reasons, several international ethical pediatric guidelines allow maximum blood volumes of 0.8 - 4.0 mL/kg for a single blood draw [121]. Thus far, lower blood volumes (25  $\mu$ L) required elaborated purification methods as antibody magnetic beads used in the immunoassay of Butler et al. [122].

Consequently, data of Substance P blood levels are limited in children and predominantly exist from healthy children, which are summarized in Supplementary Table 2. Regarding the

development process of children, O'Dorisio et al. (2002) studied Substance P plasma levels in healthy children and adolescents [n = 41] between one month and 21 years [123]. Substance P levels varied, predominantly in preadolescent children. Therefore, they did not show any significant alterations in different pediatric and juvenile ages. As transmitter in various emotional behaviour processes, the variation of Substance P plasma levels might base on psychological influences. Therefore, Herberth et al. (2008) investigated the heparinized plasma samples from 6 years old children [n = 234] to identify the influence of stressful life events on neuropeptides levels [124]. Their results suggested that the impact of psychological factors is limited on the variation of Substance P levels. In 2010, Wong et al. investigated the alteration of Substance P plasma levels in healthy neonates during their first two life weeks [n = 142], resulting in a variation of Substance P levels which was not age-dependent [125]. Besides of the impact of Substance P levels on the pediatric development process, El-Raziky et al. (2005) measured the Substance P blood levels of healthy children with a mean age of 6.3 ( $\pm$  SD: 2.5) years [126]. Theirs determined Substance P levels (mean  $\pm$  SD: 16.2  $\pm$  4.6 pg/mL [n = 10]) were similar to the values of Butler et al. (2015) and Brandow et al. (2016), who studied the Substance P plasma levels of children with 5 – 11 years [n = 18], respectively with 7-19 years [n = 21] as healthy control cohorts (35  $\pm$  20 pg/mL, respectively 21  $\pm$  7.1 pg/mL) [122,127]. So, the variability of Substance P blood levels seemed not to be affected by the age moreover by other factors (Figure 11).

### 2.3.3 Evaluation of the reliability of Substance P quantification in blood samples

A profound understanding of the metabolism of Substance P in blood is mandatory to determine accurate Substance P blood levels (see section 1.1). Investigations of Substance P metabolites were predominantly executed in tissues from the central nervous system, whereby the metabolomics play an essential role in the modulation of neuronal functions. In peripheral tissues, Substance P metabolites seem to play a minor role due to the hundred-fold lower Substance P levels in the blood [107]. Not to be neglectable is the metabolic degradation of Substance P during blood sampling and analysis may lead to falsified Substance P levels.

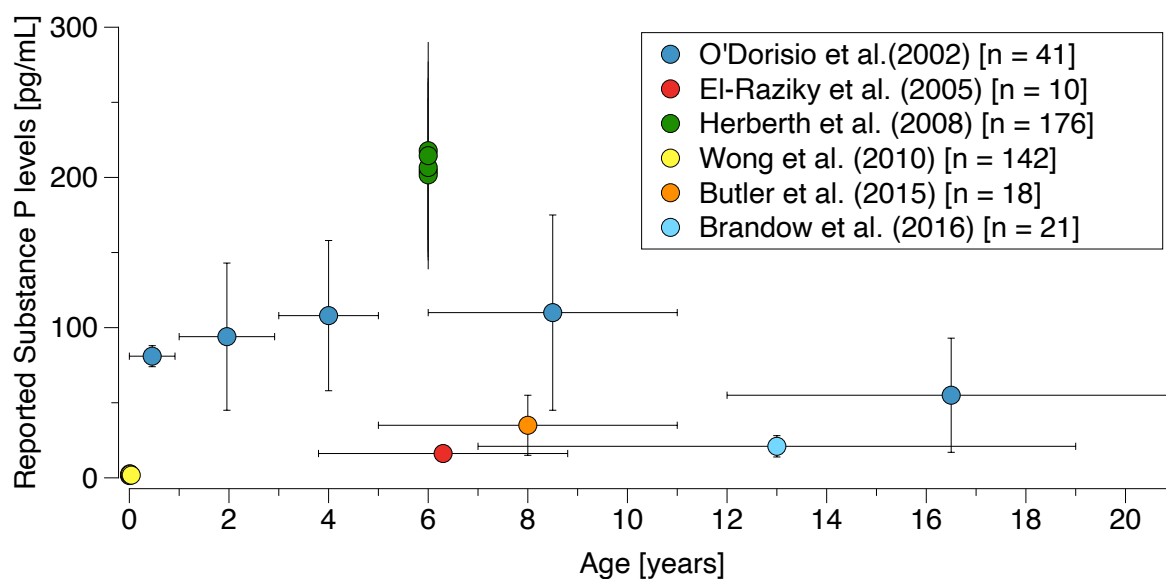


Figure 11: Reported blood levels of Substance P of healthy children plotted against their age. The points represent the mean blood concentration and their mean age. The standard deviation of the age (x-axis) and of the blood concentration (y-axis) are shown as error bars [122–127].

Due to the short metabolic half-life of Substance P, a mixture of different enzyme inhibitors to the sampling equipment is required for effective inhibition of Substance P degradation. In this context, Mosher et al. investigated the degradation of Substance P using different enzyme inhibitors in the sampling equipment and processing the samples at distinct temperature levels [128]. Aprotinin, a serine protease inhibitor, and ethylene diamine tetra acetic acid (EDTA), a cation chelator inhibiting metalloproteases, are similarly effective to prevent the degradation of Substance P than commercial broad-spectrum protease inhibitors, which reflect the major degrading enzymes of Substance P in the blood. Besides, they concluded that not only the enzyme inhibitor mix is critical, but also the rapid sample procedure after sample collecting. With longer holding of the blood samples by ambient temperatures, a substantial loss of Substance P was observed compared to holding them on ice (approximately 50% in one hour).

Most of the workgroups measuring Substance P were adding either aprotinin or EDTA to the sampling equipment (Supplementary Table 1). So, it is remarkable that different workgroups generated distinct Substance P plasma levels regarding similar collectives. Valdemarsson et al. [86] and Noug e et al. [16] both investigated CHF patients publishing significant different Substance P plasma levels (mean  $\pm$  SD:  $3.1 \pm 0.4$  pg/mL vs. median [IR]: 36 [27 - 44] pg/mL), measured by a radioimmunoassay. Besides of differences in sample preparation (10 min centrifugation vs. 15 min centrifugation at 4°C) and sample storage (-20°C vs. -80°C),

metabolites of Substance P or structure related tachykinins may lead to unprecise Substance P levels. Furthermore, the comparison of same assay technology (immunoassay) by using identical samples resulted in distinct Substance P plasma levels for adults with cardiac infarction (median: 367 pg/mL vs. 215 pg/mL) due to the use of distinct antibodies [129]. The variability of Substance P blood levels seems to base mainly on the cross-reactivity and selectivity of the used antibodies.

### 2.3.4 Quantification of Substance P saliva levels

Focusing on the necessary sensitivity of an analytical assay and the limited access to blood, an interesting clinical approach to quantify Substance P in a minimal-invasive way would be the determination of Substance P saliva levels. Through the variability of Substance P levels in saliva, Jang et al. demonstrated the significant correlation of Substance P in saliva (mean  $\pm$  SD: 236.1  $\pm$  114.1 pg/mL vs. 177.5  $\pm$  106.2 pg/mL) and plasma (mean  $\pm$  SD: 168.8  $\pm$  89.5 pg/mL vs. 105.0  $\pm$  67.1 pg/mL) samples of adult chronic migraine patients and control subjects [38]. Besides Sato et al. also showed the correlation of Substance P in human saliva (mean area under the curve (AUC)  $\pm$  SD: 2394  $\pm$  864.4 ng\*min/mL) and plasma (mean AUC  $\pm$  SD: 5060  $\pm$  1271.3 ng\*min/mL) samples [130]. Regarding these promising preliminary results, the correlation between Substance P saliva and plasma levels needs further investigations potentially providing a minimal-invasive, painless sampling method to evaluate Substance P levels, especially in severely cardiovascular-diseased patients.

## 2.4 Conclusion

Current research into the pathophysiology of cardiomyopathy suggests that Substance P plays an influent role in adverse cardiac remodeling and cardiac inflammation. The scarcity of effective treatment of cardiomyopathies leads to the interest to evaluate the role of Substance P in cardiomyopathy diseased subjects. Existing data of Substance P blood levels in cardiovascular-diseased humans show high variability, owed by differences in sampling and analytical methods. Strict standardization of blood sampling and selective determination of Substance P levels (by e.g. LC-MS) would facilitate the collection of meaningful and reliable data sets.

## **2.5 Disclosure**

*Parts of this chapter were previously published as a review in Clinica Chimica Acta (doi:10.1016/j.cca.2019.05.014). The author of this thesis was responsible for the conceptualization, the methodology, the formal analysis, the investigation, the data curation and visualization and the writing of the original draft of this publication.*

### **3. A Design of Experiments concept for the minimization of nonspecific peptide adsorption in the mass spectrometric analysis of Substance P and related Hemokinin-1**

#### **3.1 Background and Aim**

The quantification of Substance P blood levels are predominantly executed by immunoassays, which often lack the required selectivity to differentiate between Substance P and its related human Hemokinin-1 due to cross-reactivity [90,131]. Furthermore, the high variability of Substance P blood levels might be caused by distinct analytical techniques and sample preparation methods [87,128,132]. Consequently, the measurement of Substance P and human Hemokinin-1 by LC-MS/MS is a promising, highly selective alternative. However, LC-MS/MS applications were not described for the determination of human Hemokinin-1 or lacked the sensitivity to determine endogenous blood levels of Substance P [101]. One of the principal reasons for the lack of sensitivity and a bad reproducibility by measuring biomolecules in LC-MS/MS applications are adsorption processes to the container material and components of the analytical system [133,134]. As Substance P and human Hemokinin-1 are positively charged and moderately hydrophobic peptides (Table 1), they unify the potential to adsorb to glass as well as plastic surfaces [135–137]. Due to their low concentrations in picomolar ranges in plasma samples [132], adsorption processes are highly critical and play an essential role during accurate sample preparation and measurement. Moreover, the phenomenon of adsorption may lead to an underestimation of peptide levels in the case of biomarker assays and subsequently results in incorrect conclusions of biomarker levels and poor comparability between different studies [138,139].

Therefore, the objective of this study was the minimization of nonspecific peptide adsorption of Substance P and human Hemokinin-1 by modifying (1) the injection solvent composition (2) in distinct container materials as the most critical influencing parameters in preliminary experiments and the literature [113,140]. This was accomplished by a Design of Experiments concept to optimize the composition of the injection solvent and conjointly identifying the most suitable container material. The study aimed to increase the signal intensities of both peptides,

which allowed for detection of clinically relevant endogenous levels in blood by minimizing nonspecific peptide adsorption.

*Table 1: Physicochemical characteristics of Substance P and Hemokinin-1.*

	<b>Substance P</b>	<b>Human Hemokinin-1</b>
Molecular weight [g/mol]	1347.63	1185.43
GRAVY Index (Hydrophobicity)	- 0.70	0.31
Isoelectric Point (GenScript©)	11.66	8.86

## 3.2 Materials and Methods

### 3.2.1 Chemicals and materials

Substance P and human Hemokinin-1 were purchased from Sigma-Aldrich (Darmstadt, Germany) as lyophilized acetic salts in HPLC grade with a purity of 98% for Substance P and 99% for human Hemokinin-1. As recommended by the supplier, stock solutions of 1 mg/mL Substance P and 0.5 mg/mL human Hemokinin-1 were prepared in water fortified with 0.1% formic acid (FA) and stored in 100  $\mu$ L polypropylene aliquots at -80°C until analysis. Water (MS grade) was supplied by Honeywell (Erkrath, Germany); acetonitrile (ACN), methanol (MeOH), dimethyl sulfoxide (DMSO), FA (all HPLC grade) were acquired from VWR chemicals (Langenfeld, Germany); polypropylene tubes (1.5 mL) were obtained from Eppendorf (Hamburg, Germany) and Sarstedt (Nuembrecht, Germany) in regular and protein low binding quality; glass vials (1 mL) were supplied by Waters (Eschborn, Germany) in regular and deactivated glass quality; deep well plates were obtained from Eppendorf, Sarstedt, Waters, Brandt (Wertheim, Germany) and Corning (Corning, NY, USA) made of polypropylene and polystyrene in Protein low binding (Eppendorf) and regular quality (others); low retention tips were supplied from Eppendorf and Sarstedt, regular pipetting tips were additionally acquired from Sarstedt.

### 3.2.2 Instrumentation

LC-MS/MS was performed on an Agilent 1200 series binary pump system (Waldbronn, Germany) coupled to an AB SCIEX API 4000 triple quadrupole mass spectrometer (Darmstadt, Germany). Sample handling was executed by a CTC Analytics HTS PAL system (Zwingen, Switzerland).

#### 3.2.2.1 Chromatographic conditions

Samples were injected in full loop mode (20- $\mu$ L injection volume). Substance P and human Hemokinin-1 were separated onto a Waters XSelect CSH<sup>TM</sup> C18 column (3.5  $\mu$ m, 3.0x150 mm) at an oven temperature of 60°C using a gradient of mobile phase A (water:DMSO:FA, 98.9:1:0.1, v/v/v) and mobile phase B (MeOH:DMSO:FA, 98.9:1:0.1, v/v/v). The gradient started with 5% of mobile phase B for 3 minutes and was linearly changed to 25% mobile phase B from 3 to 5.5 minutes. It was followed by a further change to 98% mobile phase B in 0.5 min. The gradient was kept at 98% mobile phase B until another 4 minutes elapsed before being reduced to 5% of mobile phase B again. The total runtime from injection to injection was 13 min. The flow rate was set to 400  $\mu$ L/min.

#### 3.2.2.2 Mass spectrometry

The detection of both peptides was performed in positive mode, utilizing electrospray ionization (ESI). Nitrogen was used as collision and curtain gas. Collision gas was set to 10 psi, curtain gas to 25 psi, nebulizer gas to 55 psi, heater gas to 75 psi, and ion spray voltage to 5500 V. The temperature in the SCIEX Turbo V<sup>TM</sup> ion source was held at 550°C. The dwell times for both peptides were set to 125 ms. Detection was executed in multiple reaction monitoring (MRM) mode using ion transitions at 674.6 m/z to 600.5 m/z for Substance P and 1185.7 m/z to 1037.7 m/z for human Hemokinin-1 (Supplementary Table 3). The MRM transitions and ion source parameters were optimized during the LC-MS/MS method development by flow injection analysis (Table 2). Data acquisition was performed using Analyst<sup>©</sup> (SCIEX, version 1.6.2) and MultiQuant<sup>©</sup> (SCIEX, version 3.0.2).

Table 2: Mass spectrometric settings of Substance P and Hemokinin-1.

	Substance P		Human Hemokinin-1	
Declustering Potential [V]	86		107	
Entrance Potential [V]	7		10	
MRM transitions [m/z]	674.6→ 600.5 (quantifier)	674.6 → 254.2 (qualifier)	1185.7 → 1037.7 (quantifier)	1185.7 → 287.1 (qualifier)
Collision Energy [V]	33	37	57	77
Collision Exit Potential [V]	16	20	32	22

(V: volt; m/z: mass to charge ratio; MRM: multiple reaction monitoring)

### 3.2.3 Design of Experiments

In preliminary experiments, the composition of the injection solvent and the used container material had a critical impact on the MS intensity of Substance P and human Hemokinin-1, leading to inappropriate limits of detection. Therefore, both critical parameters were jointly investigated in the Design of Experiments concept. MODDE Pro© (MKS Instruments AB, Malmoe, Sweden, version 12.0) was used for planning and analyzing the Design of Experiments. Partial least squares regression was applied to generate the model.

#### 3.2.3.1 D-optimal design

A D-optimal design as a quadratic model was selected to find the optimal composition of the injection solvent and the most suitable container material. The purpose of the D-optimal design is the minimizing of the generalized variance of the parameter estimates (here: composition of the injection solvent and most suitable container material) [141]. The D-optimal design is a computer-aided design, which is – in contrast to factorial or fractional designs - able to handle constraints in the factor settings of the here-presented model (see therefore the restrictions in factor settings in section 3.2.3.2.). Different to a full factorial design, whereby each combination has to be investigated, a D-optimal design needs only a limited number of experiments, and the results for the omitted experiments were statistically calculated as predicted peak areas. Thus, the D-optimal design allowed for the investigation of a larger selection of process and mixture factors in a limited number of experiments [here: n = 42] (Supplementary Table 4). Since the

simple addition of an internal standard, which would have masked any increase of mass signal as the internal standard would also be affected by nonspecific peptide adsorption, appeared not reasonable, the possible variability due to electrospray ionization or MS detection was addressed by two aspects: First, each experiment was independently prepared in triplicate and all experiments ran in random order spread over multiple days to calculate the repeatability of each peptide. Second, the center point of the D-optimal design, measured in nonreplicate - ran also in random order - was included to ensure the inter-day repeatability. Substance P and human Hemokinin-1 were separately investigated to avoid possible adsorption interactions of the two peptides, resulting in a total of 270 runs for both peptides. The responses were set to the peak areas of Substance P and human Hemokinin-1, as the aim of this investigation was the maximization of the MS intensity.

A cross-validation of the obtained model was performed based on the predictive error sum of squares (PRESS) value. The PRESS value was expressed as  $Q^2$ , which was reserved as a parameter for the goodness of prediction. The predefined requirement was a value of at least 0.5 for  $Q^2$  to generate an appropriate model with a good predictive power [142]. Furthermore, the difference between  $R^2$  (coefficient of regression) and  $Q^2$  should be less than 0.3 for a reliable model.

### 3.2.3.2 Investigated parameters and factors

Four quantitative parameters (MeOH, ACN, DMSO, FA) considered as additives to the injection solvent were investigated in the Design of Experiments concept, based on their ability to improve the solubility (organic solvents, DMSO) [143] and to reduce ionic interactions (FA) [113]. The investigated ranges started from the absence of each component (0%) and were limited to 10% of FA, 75% of DMSO, and 50% of either MeOH or ACN. The resulting injection solvent consisted of a composition of a maximum of three additives to water, whereby the water fraction in the injection solvent was set to a minimum of 25% to guarantee sufficient solubility of Substance P. The organic fraction was restricted to 50% to avoid breakthroughs and peak distortions in the reversed phase chromatography, while the FA fraction was limited to 10% to evade corrosive damages in the sensible parts of the HPLC system. The addition of TFA to the injection solvent was abandoned, as TFA led to strong ion suppression in preliminary experiments.

Furthermore, the variable composition of the injection solvent was conjointly examined in different container materials. Polypropylene tubes from two suppliers, each in distinct quality (regular and protein low binding) and regular glass vials were included in the Design of Experiments to investigate the adsorption affinity of Substance P and human Hemokinin-1 to the material surfaces. Additionally, the benefit of using deactivated glass vials was examined and compared to the best performing container material of the Design of Experiments approach.

In a next step, various deep well plates were tested utilizing an aqueous injection solvent (water fortified with 10% FA) and the optimized injection solvent composition to evaluate the usefulness of the Design of Experiments approach and to find the most suitable deep well plate. As polystyrene is not resistant to DMSO or organic solvents, these plates were merely investigated using the aqueous injection solvent (Supplementary Table 5). The tips in different qualities were analogically tested both using the aqueous injection solvent and the optimized injection solvent composition (Supplementary Table 6).

### 3.2.3.3 Preparation of experimental solutions

For analysis, freshly thawed stock solutions were consequently diluted in a generic mixture of 2% FA added to equal parts of ACN and water (50:50 [v/v]) as recommended to avoid nonspecific peptide adsorption [133]. 10  $\mu\text{L}$  of either 0.1  $\mu\text{g/mL}$  Substance P solution or 1  $\mu\text{g/mL}$  human Hemokinin-1 solution was evaporated to dryness in the investigated test containers for 10 min at 40°C and 300 rpm under a gentle steam of nitrogen. The residual was reconstituted in 1 mL of the experimental solution to obtain a final concentration of 1 ng/mL Substance P and 10 ng/mL human Hemokinin-1 and was stored on ice until same-day measurement by LC-MS/MS.

### 3.2.3.4 Sweet-spot and setpoint analysis

A sweet-spot was created to find the optimal composition of the injection solvent, which depends on the best performing container material for Substance P and human Hemokinin-1, when measuring both peptides simultaneously. Especially in simultaneous determination of compounds with opposite physicochemical properties, the sweet-spot analysis allows to identify the intersecting set for optimal quantification in bioanalysis. The focus in the sweet-spot analysis lied on the predicted peak area of Substance P, as reported endogenous blood

levels were much lower than blood levels of human Hemokinin-1 [34]. The sweet spot was defined as injection solvent composition, in which a maximally accepted deviation to the maximal predicted peak area of both Substance P and human Hemokinin-1 must not exceed the predefined limits (conjoint optimal conditions for both peptides). Therefore, the predefined acceptable limits to the maximal predicted peak area were set to -5% for Substance P and -15% for human Hemokinin-1.

To confirm the accuracy of the sweet-spot as conjoint optimal injection solvent composition, a minimal-risk analysis was performed. The minimal-risk analysis bases on the Monte-Carlo simulation and indicates the probability of failing the desired peak area, which is predicted by the model. By taking into account the response specifications, the standard error of the model and the factor precision, the predicted peak areas were simulated one million times and the probability of failure was determined. In the here-presented model, failure was defined as a loss of more than 15% of the maximal predicted peak area for both peptides. This requirement was derived from regulatory bioanalytical recommendations [144]. The area with a probability of failure of less than 0.5% (5,000 defects per million simulations) was defined as the design space, involving the robust setpoint.

### 3.2.4 Application of the experimental design

As one of the objectives of this study was the determination of endogenous plasma levels of both peptides, the chromatographic method was also optimized to facilitate the reduction of the lower limit of detection of both peptides and to enable the determination of endogenous peptide levels. First, 5% instead of 1% DMSO were added as supercharger to both mobile phases to improve the electrospray ionization. Second, 50- $\mu$ L instead of 20- $\mu$ L injection volume was used to increase the signal intensity during the applicability experiments. Under these conditions, the benefit of using the optimized injection solvent composition in the most suitable container material was further evaluated in human plasma samples, as the presence of endogenous plasma matrix components could also affect adsorption processes. The degradation of the endogenous peptides was induced at ambient temperatures to generate blank plasma (donated by one male volunteer) [128]. Afterwards, 300  $\mu$ L of fresh blank plasma was spiked with 1 ng/mL Substance P and human Hemokinin-1. As endogenous Substance P plasma levels, determined by immunoassays, were found in the picomolar range (median: 217.8 pg/mL in healthy children (n = 80) [124]; mean  $\pm$  SD: 116.5  $\pm$  20.5 pg/mL in healthy adults (n = 110) [145]), blank plasma

samples were further spiked with 100 pg/mL Substance P and human Hemokinin-1, as low-concentrated samples are more critically affected by adsorption processes.

Spiked plasma samples were purified with a customized solid-phase extraction protocol using a mix-mode weak anion exchanger (Oasis WAX  $\mu$ elution, Waters). Substance P and human Hemokinin-1 were eluted by 125  $\mu$ L of MeOH fortified with 10% FA evaporated to dryness at 35°C and 300 RPM under nitrogen and were reconstituted in both (A) the optimized solvent composition in the most suitable container and (B) the start gradient as injection solvent (93.9% water, 5% MeOH, 1% DMSO, 0.1% FA) in regular tubes. The mean observed peak areas of Substance P and human Hemokinin-1 in settings A and B [ $n = 3$ ] at different concentration levels (1 ng/mL and 100 pg/mL) were compared to evaluate the benefit of the experimental design in human plasma samples.

### 3.3 Results and discussion

#### 3.3.1 Model fit and goodness of prediction

The goodness of fit ( $R^2$ ) was determined by an observed-versus-predicted peak area plot, resulting in an  $R^2$  of 0.92 for Substance P and 0.88 for human Hemokinin-1 (Figure 12). The goodness of prediction is expressed by the  $Q^2$  value and amounted to 0.68 for Substance P and 0.73 for human Hemokinin-1, fulfilling the predefined requirements for a predictive model.

As the addition of an internal standard was not reasonable, each replicate of an experiment ran in a random order spread over five days to ensure the robustness of the analytical setting. The calculated repeatability—based on the variance of the replicates over the whole study period—amounted to 92.0% and 91.9% for Substance P and human Hemokinin-1, respectively. Moreover, the evaluation of the center point demonstrated robust mass signals (mean  $\pm$  standard deviation (SD): 2545.6  $\pm$  518.5 counts per second (cps) for Substance P and 2317.9  $\pm$  310.4 cps for human Hemokinin-1 [each peptide;  $n = 9$ ]), indicating stable and repeatable analytical conditions during the experimental conduct.

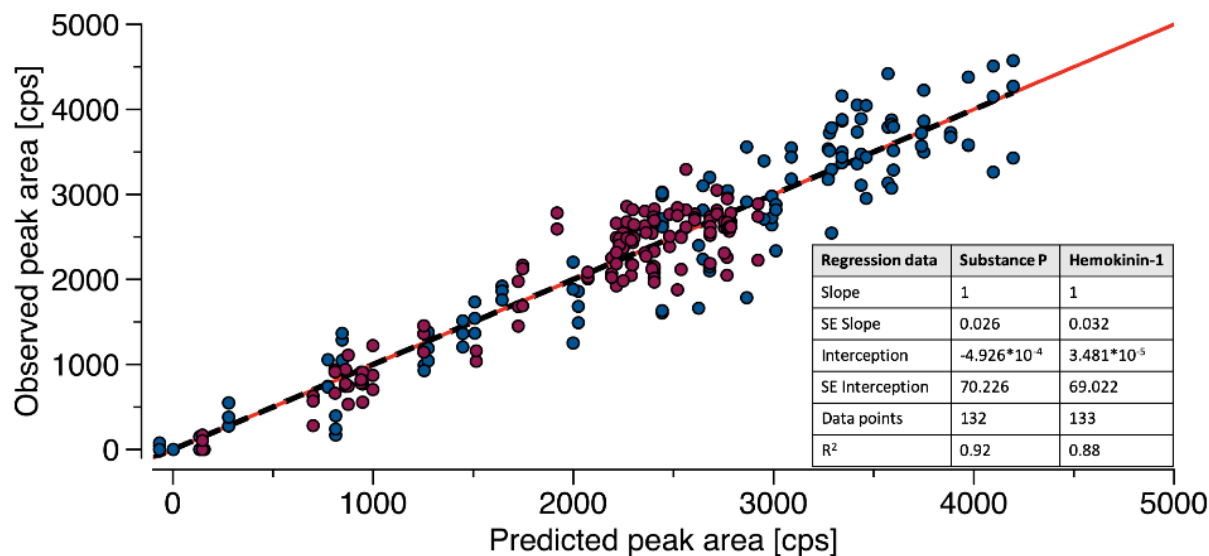


Figure 12: Goodness of fit plot for the statistical evaluation of the Design of Experiments model. The plot shows the observed versus predicted peak areas of Substance P (blue) and human Hemokinin-1 (red) with the identity line (solid red line) and the regression lines (dashed black lines). (cps: counts per second; SE: standard error)

### 3.3.2 Optimization of the injection solvent composition

#### 3.3.2.1 Impact of the type of organic solvent

The gain of intensity did not only depend on the percentage but, moreover, on the type of organic solvent. Regardless of the container material, the predicted peak areas for Substance P and human Hemokinin-1 generally profited from adding organic solvents to the injection solvent, whereby predominantly adding 25% MeOH led to substantial increases of predicted peak areas (+69.1% for Substance P and +69.4% for human Hemokinin-1) compared to the absence of organic solvent. With a higher fraction of 50% MeOH, the increase of intensity was not as pronounced compared to adding 25% MeOH (+5.7% for Substance P and +0.1% for human Hemokinin-1). Contrarily, by adding 25% ACN to the injection solvent, the predicted peak areas were increased by 27.8% for Substance P and by 63.2% for human Hemokinin-1 compared to the absence of organic solvent. Furthermore, by adding 50% ACN to the injection solvent, the predicted peak areas were decreased by 20.3% for Substance P and 17.4% for human Hemokinin-1 compared to the addition of 25% ACN. Therefore, ACN was classified as inferior in this setting for both compounds of interest. Substance P, as a hydrophilic peptide,

seems to be more soluble in MeOH as a polar protic solvent, leading to less nonspecific adsorption. For human Hemokinin-1, as a hydrophobic peptide, the benefit of adding MeOH or ACN to the injection solvent was almost equivalent.

### 3.3.2.2 Impact of dimethyl sulfoxide

The predicted peak areas of the tachykinins benefited from distinct maximal fractions of DMSO (45% for Substance P, 60% for human Hemokinin-1). The conjoint investigation of the impact of DMSO and the used container material led to substantial differences in benefit of adding DMSO to the injection solvent composition. In regular polypropylene tubes an increase of 91.8% for the predicted peak area of Substance P and 63.9% for the predicted peak area of human Hemokinin-1 was achieved. In contrast, the predicted peak areas of Substance P and human Hemokinin-1 were increased by 34.8% and 36.9% respectively, using protein low binding polypropylene tubes. In glass vials the benefit of adding DMSO was pronounced for the predicted peak area of Substance P (+209.6%), whereby the benefit for the predicted peak area of human Hemokinin-1 was limited (+26.0%).

As a strong solubilizer in the injection solvent, DMSO plays a critical role of minimizing nonspecific adsorption of the tachykinins to the container material (Figure 13). The substantial differences between the investigated container materials led to the assumption that the principal function of DMSO in the injection solvent was the reduction of nonspecific peptide adsorption by improving the peptide solubility. Coherently, the reduction of nonspecific peptide adsorption by DMSO was previously shown for digested peptides, which underline the here presented results [143]. On the other hand, the possible impact of DMSO on the electrospray ionization cannot be ruled out but seems to be inferior with regard to the identified high variability in distinct container materials (+209.6% in glass vials compared to +34.8% in protein low binding polypropylene for the predicted peak area of Substance P). If DMSO primarily acted as a super charger for electrospray ionization, less extent of variability between the different materials would had been expected. Due to the potential of DMSO to oxidize methionine residuals of both peptides, the use of DMSO as injection solvent composition requires critical evaluation. However, no degradation during short-term investigations over 12 hours was observed under the here presented experiments.

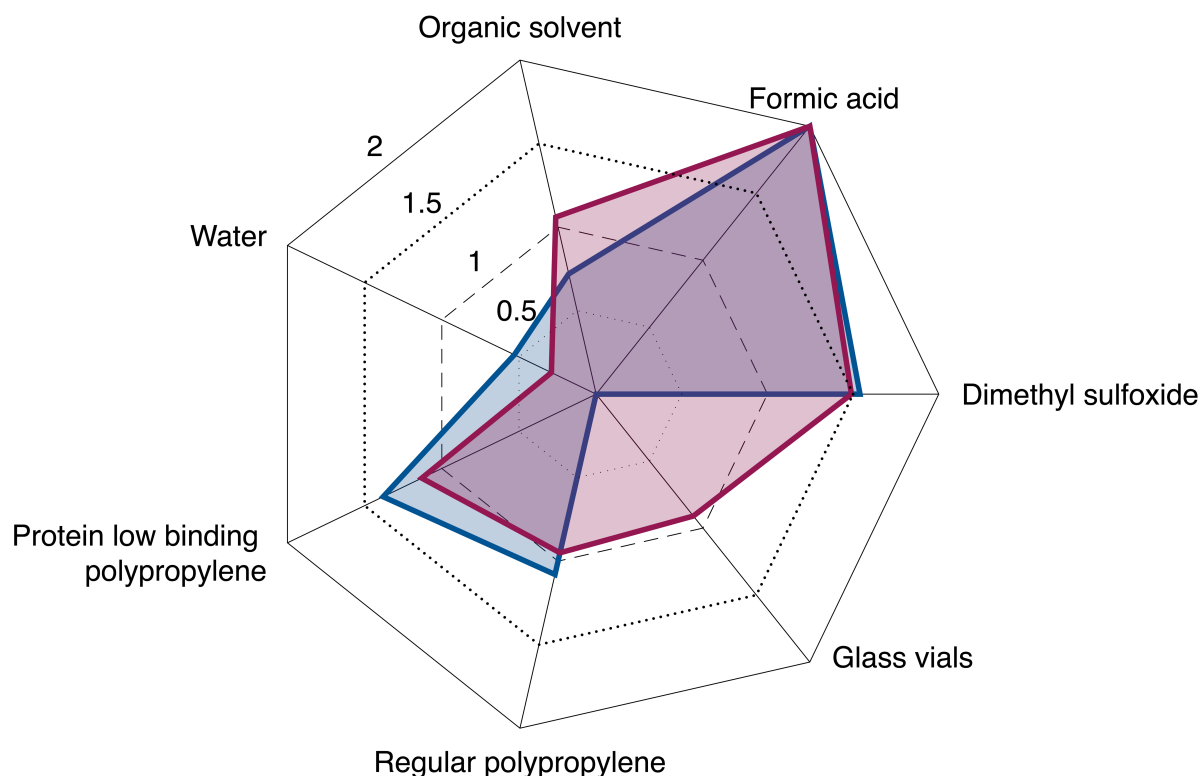


Figure 13: Polar plot of the overall individual effects of the investigated factors on the predicted peak area of Substance P and human Hemokinin-1.

The coefficient effects of the investigated factors on the predicted peak area of Substance P (blue) and human Hemokinin-1 (red) were normalized to the coefficient effect of formic acid (set to 2) which is indicated by the outer black solid line as maximal response. The inner black dashed line indicates the reference injection solvent composition (5% methanol, 1% dimethyl sulfoxide, 0.1% formic acid and 93.9% water) (set to 1).

### 3.3.2.3 Impact of formic acid

The addition of FA to the injection solvent was one of the essential ways to optimize the signal intensity of both peptides (Figure 13). Regardless of the container material, the addition of 10% FA to the injection solvent resulted in a maximum gain of the predicted peak area of Substance P (+85.8%). The maximum of the predicted peak area of human Hemokinin-1 was achieved by the addition of 8.5% FA (+58.0%). Contrary to Substance P, a higher FA fraction showed no further benefit for the gain of the MS intensity of human Hemokinin-1.

The observed peak areas in regular polypropylene and glass containers were reduced by more than 97% for Substance P in the absence of FA (mean  $\pm$  SD:  $16.8 \pm 29.0$  cps in pure aqueous

injection solvent versus  $634.3 \pm 140.1$  cps in pure aqueous solvents fortified with 10% FA [ $n = 9$ ]) and by more than 80% for human Hemokinin-1 in absence of FA (mean  $\pm$  SD:  $203.8 \pm 106.4$  cps in pure aqueous injection solvent versus  $1088.9 \pm 206.0$  cps in pure aqueous solvents fortified with 10% FA [ $n = 9$ ]). In contrast, the comparison in protein low binding polypropylene led to an increase of 48.2% of observed peak area of Substance P (mean  $\pm$  SD:  $2612.3 \pm 577.3$  cps in pure aqueous solvents fortified with 10% FA versus  $1763.2 \pm 144.4$  cps in pure aqueous injection solvent [ $n=6$ ]) and 76.8% of observed peak area of human Hemokinin-1 (mean  $\pm$  SD:  $1991 \pm 274.8$  cps in pure aqueous solvents fortified with 10% FA versus  $1126.4 \pm 263.2$  cps in pure aqueous injection solvent [ $n=6$ ]), indicating fewer nonspecific peptide adsorption of Substance P and human Hemokinin-1 in aqueous solvents using protein low binding polypropylene tubes.

Under acid conditions, the affinity of the positively charged tachykinins to negatively charged glassware was lower than in neutral solutions probably due to the saturation of the free silanol groups by protons. Moreover, the building of a more soluble FA cluster with Substance P and human Hemokinin-1 seemed to avoid further adsorption processes. As an acid building a cluster with positively charged molecules, FA has a high potential to reduce nonspecific adsorption. The results of the experimental design suggested that more hydrophilic peptides like Substance P profit from a higher fraction of FA to adsorb less to the material surfaces.

Although trifluoroacetic acid (TFA) is often used in chromatographic separations due to the strong cluster building, it also leads to strong ion suppression in MS applications [146]. In preliminary experiments, the addition of 0.25% TFA to the injection solvent led to a substantial decrease of peak area of Substance P (-72.2%). Moreover, the ion suppression was not only observed in runs with TFA added to the injection solvent, but also in consecutive runs without TFA added to the injection solvent. Since a gain of intensity was the principal objective of the experimental design, the use of TFA was abolished in the experimental design to avoid extensive chromatographic wash procedures between each run.

### 3.3.3 Impact of the container material

Besides the selection of modifiers as well as the optimal composition of the injection solvent, the container material used played an essential role in the accurate measurement of Substance P and human Hemokinin-1 (Figure 14 - 16).

### 3.3.3.1 Glass vials

As expected from the literature [137], regular glass vials were unsuitable for measuring Substance P sensitively. It is most likely that the two positive charges of arginine and lysine in the amino acid sequence of Substance P showed high affinity to the untreated negatively charged silanol groups of glassware, resulting in a substantial loss of predicted peak area (-71.6% compared to regular polypropylene tubes). Human Hemokinin-1, as a more hydrophobic and single-charged peptide, tolerated regular glassware better, which was principally suitable for the determination of human Hemokinin-1 (+10.8% compared to regular polypropylene tubes) (Figure 14).

Deactivated glass vials promised less adsorption of positively charged peptides compared to regular glassware by capping the free negatively charged silanol groups of glass. Therefore, the use of deactivated glass vials was independently investigated by comparing to untreated glass vials and regular polypropylene tubes both in the optimized injection solvent in triplicates. The peak areas of Substance P substantially benefited from the use of deactivated glass vials compared to untreated glass vials (+66.0%). Nevertheless, the mean observed peak area in deactivated glass vials were lower with a higher standard deviation than in regular polypropylene tubes (mean  $\pm$  SD: 4358.7  $\pm$  797.3 cps versus 5174.7  $\pm$  234.8 cps [n = 3]). On the other side, the observed peak areas of human Hemokinin-1 showed bare differences in deactivated glass vials compared to regular polypropylene tubes (mean  $\pm$  SD: 3410.0  $\pm$  462.0 cps versus 3519.3  $\pm$  136.3 cps [n = 3]). In contrast to regular and deactivated glass vials, regular polypropylene tubes were the most suitable material to measure Substance P accurately and sensitively.

3. A Design of Experiments concept for the minimization of nonspecific peptide adsorption in the mass spectrometric analysis of Substance P and related Hemokinin-1

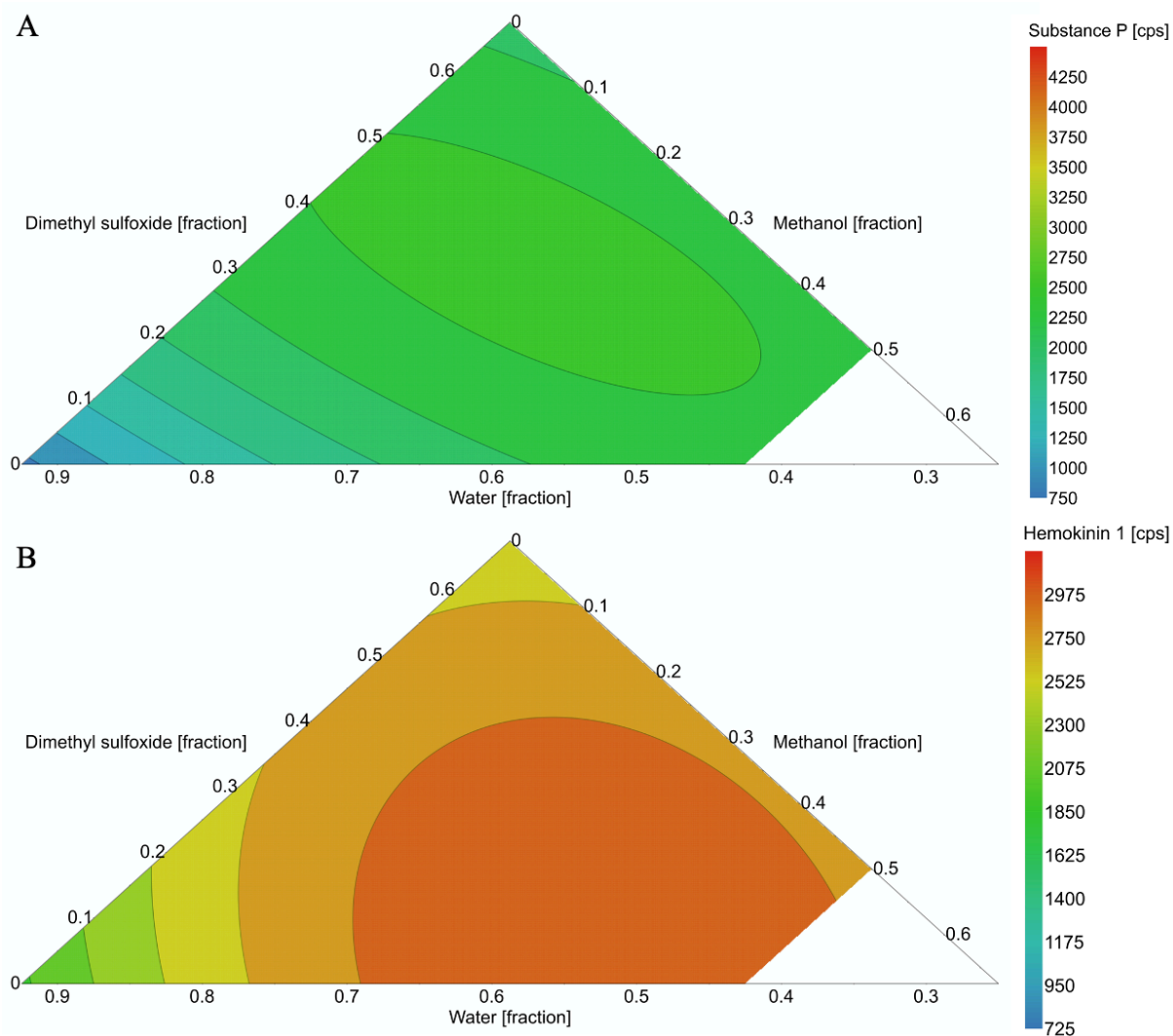


Figure 14: Contour plots of the impact of the injection solvent composition on the predicted peak areas of Substance P and human Hemokinin-1 in glass vials.

The red area indicates the highest, whereby the blue area the lowest predicted peak area of (A) Substance P and (B) human Hemokinin-1. Due to the limitation of the organic solvent to 50%, a Monte-Carlo simulation was not possible for the white area. (cps: counts per second)

### 3.3.3.2 Regular polypropylene tubes

Regarding regular polypropylene tubes, the composition of the injection solvent played a critical role to reduce nonspecific adsorption of Substance P and human Hemokinin-1. For both peptides, regular polypropylene tubes were predominantly unsuitable in pure aqueous solutions due to the substantial loss of intensity. Without the addition of DMSO, organic solvents, or acid to the injection solvent, no quantifiable peak signals of 1 ng/mL Substance P or 10 ng/mL human Hemokinin-1 (mean  $\pm$  SD:  $25.2 \pm 61.6$  cps and  $59.3 \pm 71.0$  cps, respectively, [n = 6]) were observed in regular polypropylene tubes. Each investigated modifier added to the injection solvent continuously increased the predicted peak areas in regular polypropylene tubes. For Substance P, the benefit of adding MeOH was more pronounced than for human Hemokinin-1 (up to 177.0% versus up to 90.6%) (Figure 15). A composition of the highest MeOH fraction and 10% FA was necessary to achieve the maximum desired peak areas in regular polypropylene tubes. As a minimal fraction of 25% water was required to guarantee the solubility, the addition of DMSO had to be limited to 15%.

3. A Design of Experiments concept for the minimization of nonspecific peptide adsorption in the mass spectrometric analysis of Substance P and related Hemokinin-1

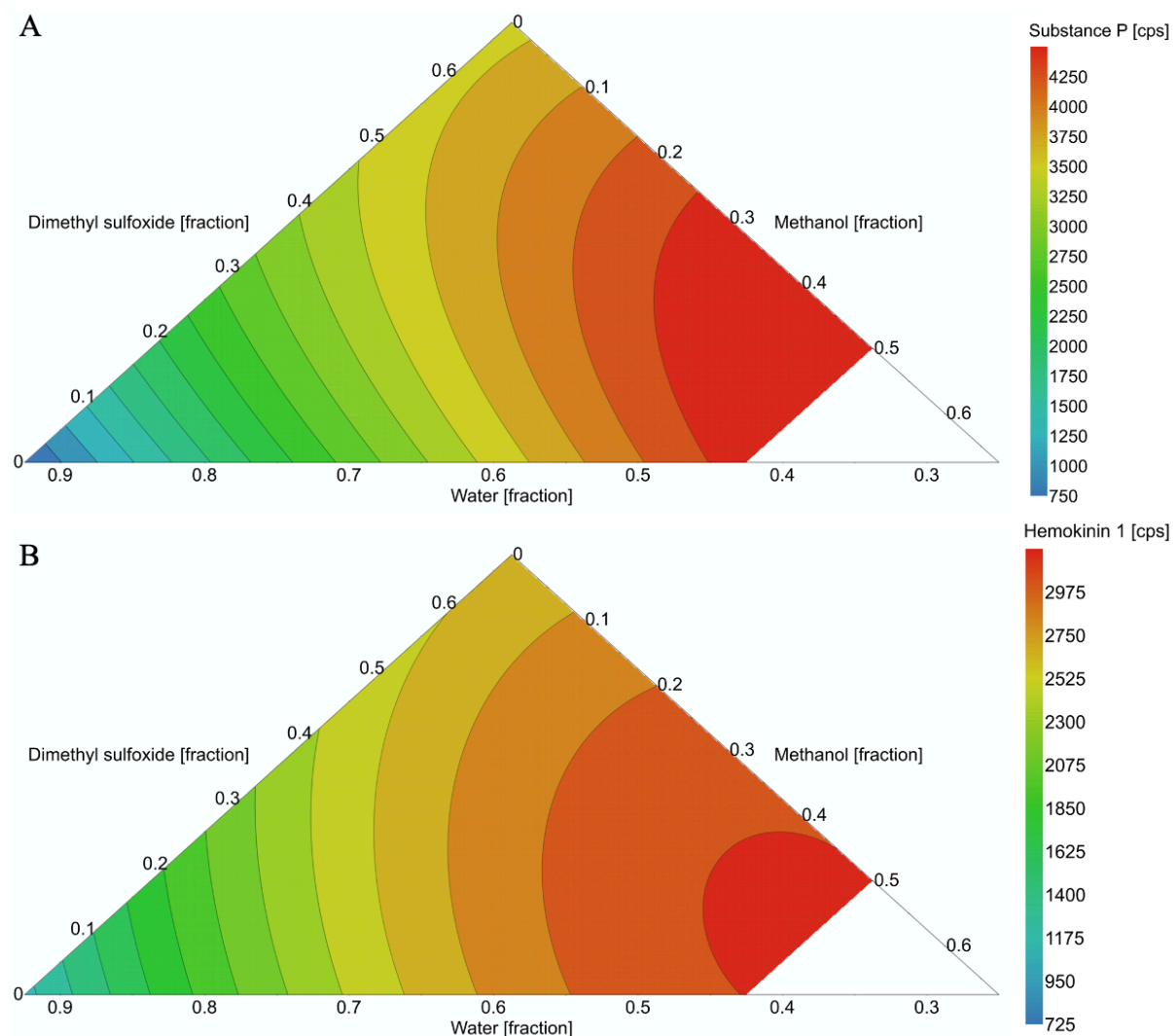


Figure 15: Contour plots of the impact of the injection solvent composition on the predicted peak areas of Substance P and human Hemokinin-1 in regular polypropylene tubes.

The red area indicates the highest, whereby the blue area the lowest predicted peak area of (A) Substance P and (B) human Hemokinin-1. Due to the limitation of the organic solvent to 50%, a Monte-Carlo simulation was not possible for the white area. (cps: counts per second)

### 3.3.3.3 Protein low binding polypropylene tubes

Protein low binding polypropylene tubes promise fewer adsorption of peptides and proteins based on a distinct manufacturing method resulting in high-density, fine-pored polypropylene with a minimized hydrophobic interaction potential. Protein low binding polypropylene tubes from both suppliers showed the most considerable advantage in pure aqueous solutions compared to regular polypropylene tubes (+329.7% and +115.1% for Substance P and human Hemokinin-1, respectively) (Figure 17). As nonspecific peptide adsorption was minimized in protein low binding tubes, there was no further profit in the addition of MeOH to the injection solvent (Figure 16). The predicted peak areas of human Hemokinin-1 profited from a maximum of 30% MeOH using protein low binding tubes, whereby the advantage was not as substantial as that in regular polypropylene tubes (+35.2% in protein low binding polypropylene versus +81.3% in regular polypropylene). The predicted peak areas of both peptides in protein low binding polypropylene tubes were not much affected by the composition of the injection solvent as compared to regular polypropylene tubes and were constant over a considerable range of variable compositions of injection solvent (Figure 16). Contrary to regular polypropylene tubes, in protein low binding tubes, a maximum of the predicted peak area of Substance P was predominantly achieved in an injection solvent composition of equal parts of DMSO and water fortified with 10% FA. For human Hemokinin-1, differences in predicted peak areas were not distinctive in protein low binding compared to regular polypropylene tubes.

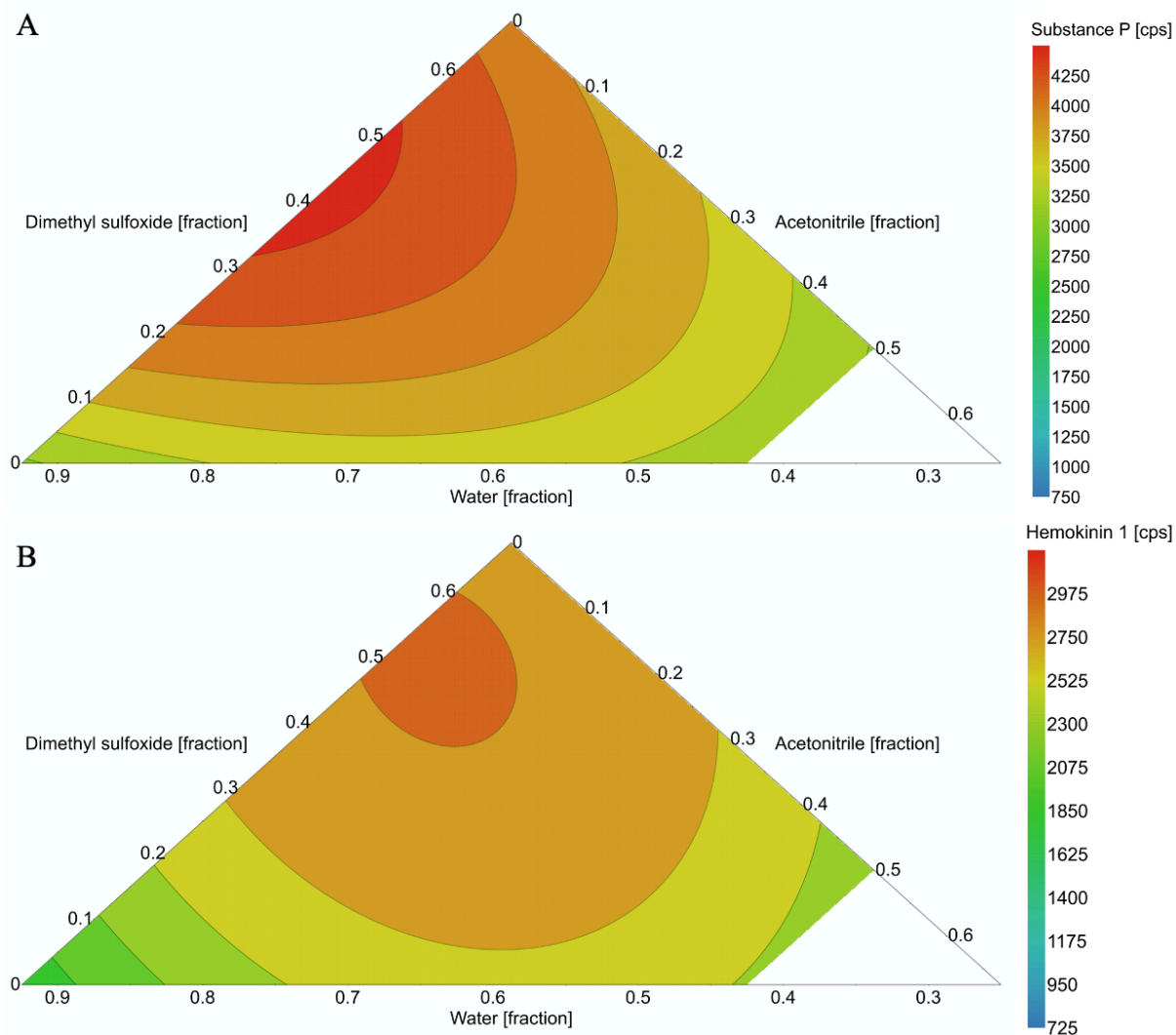


Figure 16: Contour plots of the impact of the injection solvent composition on the predicted peak areas of Substance P and human Hemokinin-1 in protein low binding polypropylene tubes. The red area indicates the highest, whereby the blue area the lowest predicted peak area of (A) Substance P and (B) human Hemokinin-1. Due to the limitation of the organic solvent to 50%, a Monte-Carlo simulation was not possible for the white area. (cps: counts per second)

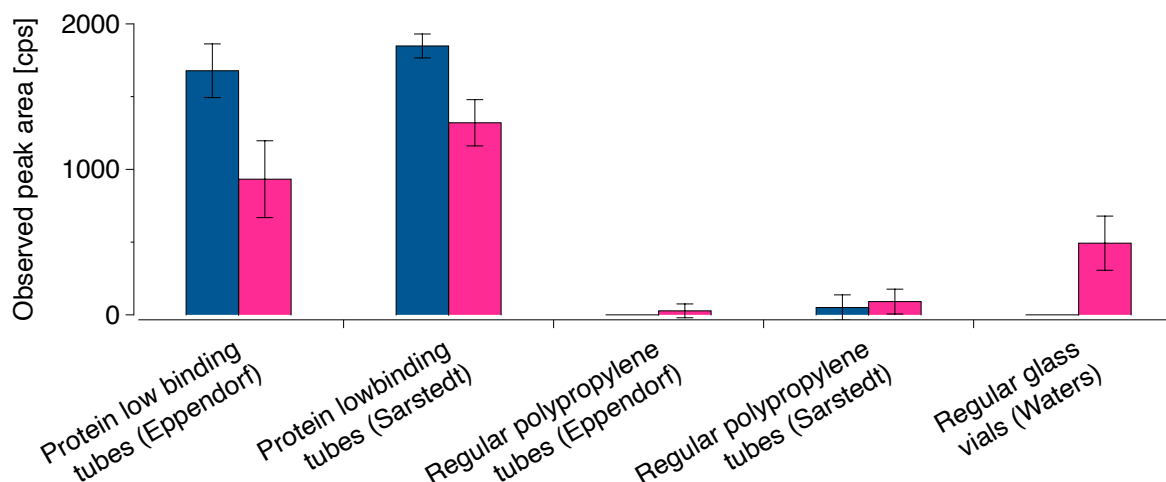


Figure 17: Impact on the investigated tubes and vials on the observed peak area of Substance P and human Hemokinin-1.

When using pure aqueous injection solvents, the observed peak area of Substance P (blue) and human Hemokinin-1 (red) substantially depended on the used container material. (cps: counts per second [mean  $\pm$  standard deviation,  $n = 3$ ])

### 3.3.4 Sweet-spot and setpoint analysis

Focusing on the maximum gain of intensity for Substance P and human Hemokinin-1, the sweet-spot analysis was performed to evaluate the optimal composition of the injection solvent when measuring both peptides simultaneously. The minimal-risk analysis was executed to confirm the sweet-spot, resulting in the first design space including a robust setpoint of injection solvent composition of 50% MeOH, 15% DMSO, 25% water, and 10% FA in regular polypropylene tubes (Figure 18-A).

As protein low binding tubes were substantially advantageous in non-organic compositions of injection solvents, an alternative robust setpoint was included to evaluate their benefit compared to regular polypropylene tubes. On the basis of the alternative setpoint, a separate minimal-risk analysis was executed resulting in the second design space with an injection solvent composition consisting of 45% DMSO, 45% water, and 10% FA in protein low binding polypropylene tubes (Figure 18-B).

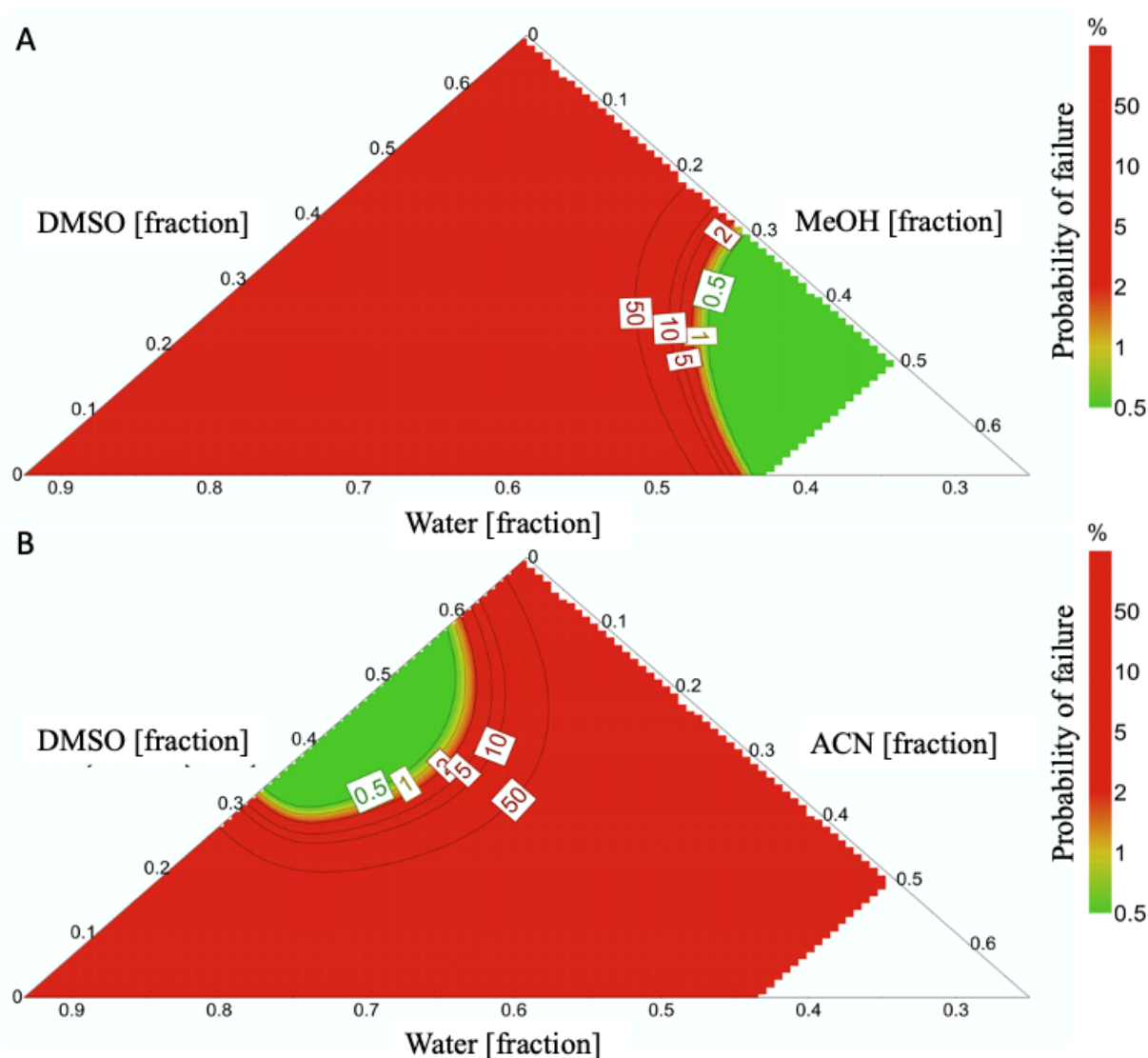


Figure 18: Contour plots of the minimal-risk analysis in regular and protein low binding polypropylene tubes.

The optimized injection solvent composition depended on the use of (A) regular or (B) protein low binding polypropylene tubes. The colors represent the probability of failing the maximal accepted deviation (-15%) to the maximal predicted peak areas of Substance P and human Hemokinin-1, whereby the design spaces (probability of failure < 0.5%) are colored in green. Due to the limitation of the organic solvent to 50%, a Monte-Carlo simulation was not possible for the white area. (ACN: acetonitrile, DMSO: dimethyl sulfoxide; MeOH: methanol)

The mean values of the observed peak areas of the investigated tachykinins in triplicates dissolved in (A) the start gradient (93.9% water, 5% MeOH, 1% DMSO, 0.1% FA), (B) the optimized solvent in regular polypropylene tubes, and (C) the optimized solvent in protein low

binding polypropylene tubes were compared to evaluate the benefit of the Design of Experiments. Predominantly, the observed peak areas of Substance P profited from the optimization and resulted in an approximately 135% higher intensity and lower standard deviation in both optimized injection solvents (mean  $\pm$  SD: (A)  $2,203.5 \pm 748.4$  cps versus (B)  $5,174.7 \pm 234.7$  cps and (C)  $4,926.7 \pm 426.0$  cps [ $n = 3$ ]). For human Hemokinin-1, a gain of intensity of 33% was achieved (mean  $\pm$  SD: (A)  $2,628.0 \pm 216.4$  cps versus (B)  $3,519.3 \pm 136.3$  cps and (C)  $3,456.0 \pm 72.3$  cps [ $n = 3$ ]). The differences in the hydrophobicity and charge state seemed to be crucial for the effect of optimization. Substance P, as a more hydrophilic peptide, was affected by higher adsorption processes in unmodified injection solvents due to stronger ionic interactions to the material surfaces than human Hemokinin-1. There were no substantial differences in performance identified by comparing both optimized injection solvents in protein low binding and regular polypropylene tubes.

As both robust setpoints were equivalent regarding the observed peak areas, the use of the optimized solvent in regular polypropylene tubes (50% MeOH, 15% DMSO, 25% water, 10% FA) was abandoned in further experiments to avoid breakthroughs using a 50- $\mu$ L injection volume due to high organic fraction.

The sensitivity of the method was investigated under the optimized conditions, which were obtained by the Design of Experiments. Thus, a dilution series of Substance P and human Hemokinin-1 was prepared in the optimized solvent composition (45% DMSO, 45% water, 10% FA) in protein low binding polypropylene tubes and was measured in triplicate. Limits of quantification of 20 pg/mL for Substance P and of 40 pg/mL for human Hemokinin-1 in compliance with regulatory guidelines [144] were achieved by using 50- $\mu$ L injection volume.

### 3.3.5 Impact of deep-well plates

As the selection of the used material had a substantial impact on the predicted peak area of Substance P and human Hemokinin-1, furthermore, various deep well plates made of plastic (polypropylene and polystyrene) were investigated from different suppliers. Utilizing an aqueous peptide solution (fortified with 10% FA), the observed peak areas of Substance P and human Hemokinin-1 strongly varied in polypropylene plates from Brand to polystyrene plates from the same supplier, indicating the favorite use of deep well plates made of polypropylene. In contrast, using the optimized injection solvent composition, the observed peak areas of both

peptides were in similar ranges in each polypropylene dee-well plate from five suppliers (Figure 19). These results confirmed the successful minimization of unspecific peptide adsorption to different plates by using the optimized injection solvent composition.

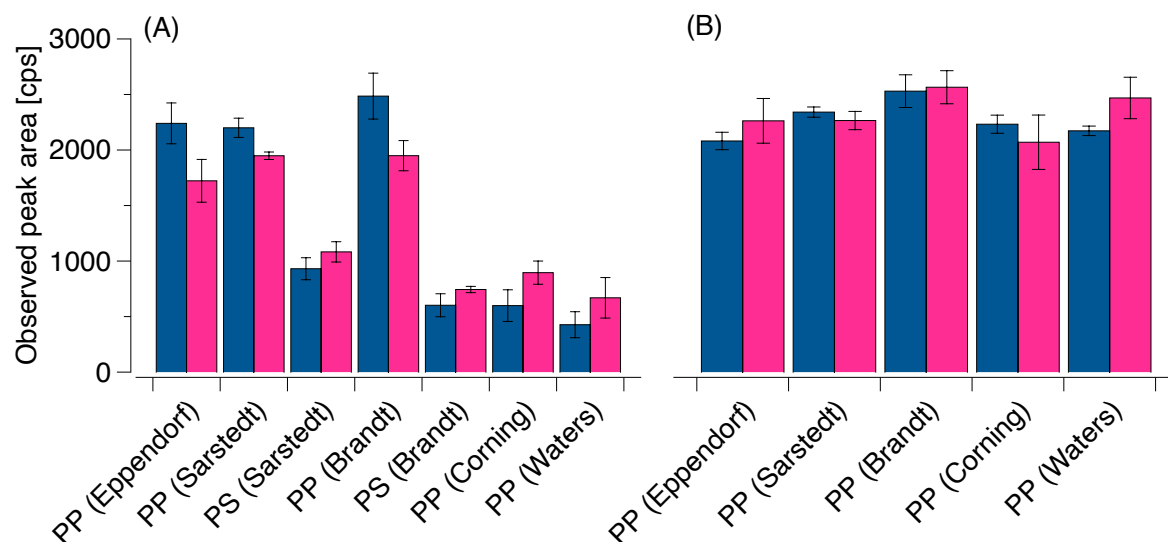


Figure 19: Impact of the investigated deep well plates on the observed peak area of Substance P and human Hemokinin-1.

(A) When using an aqueous injection solvent composition (water fortified with 10% formic acid), the observed peak area of Substance P (blue) and human Hemokinin-1 (red) were substantially affected by the choice of the material (polypropylene (PP), polystyrene (PS)) and the supplier. (B) In the optimized injection solvent composition, the differences between the suppliers were neglectable. (cps: counts per second; [mean  $\pm$  standard deviation;  $n = 3$ ])

### 3.3.6 Impact of tips

Besides the selection of the most appropriate container material and deep well plates, the choice of the tips may also affect by unspecific peptide adsorption. By comparing the use of low retention and regular polypropylene tips, the use of low retention polypropylene tips was favorable, when dissolving the peptides in an aqueous solution fortified with 10% FA. These effects were not significant, when using the optimized injection solvent composition, resulting in the equivalent use of regular and low retention polypropylene tips (Figure 20).

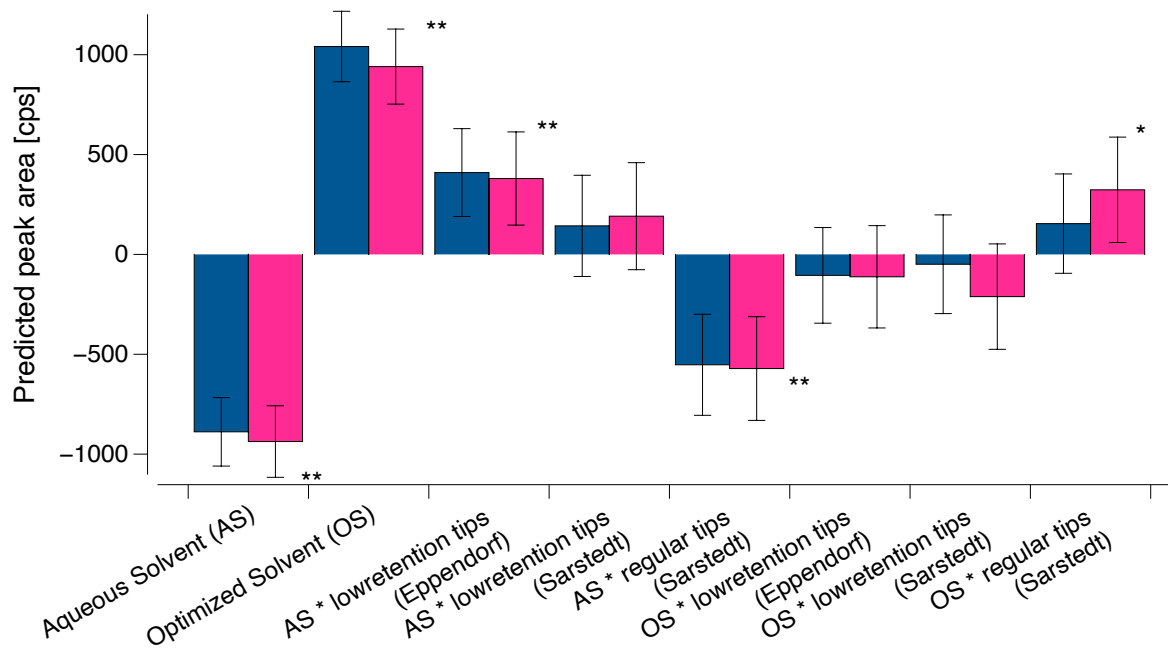


Figure 20: Impact of the investigated tips on the predicted peak areas of Substance P and human Hemokinin-1.

The effect on the predicted peak area of Substance P (blue) and human Hemokinin-1 (red) depended on the use of an aqueous solvent (AS: water fortified with 10% formic acid) or the optimized injection solvent composition (OS). (T: 95% confidence interval; cps: counts per second, \*significant: ( $p < 0.05$ ), \*\* highly significant ( $p < 0.01$ ), based on the students t-test)

### 3.3.7 Application in human plasma samples

Analogically to the neat solution, the observed peak areas of 1 ng/mL Substance P —spiked in human plasma samples—predominantly benefited from (A) the optimized solvent in protein low binding (45% DMSO, 45% water, 10% FA) resulting in an increase of intensity of 74% compared to (B) the start gradient as the injection solvent in regular tubes (93.9% water, 5% MeOH, 1% DMSO, 0.1% FA) (mean  $\pm$  SD: (A)  $20,943.3 \pm 2,630.9$  cps versus (B)  $11,983.0 \pm 1,835.3$  cps [ $n = 3$ ]). The substantial increase of signal intensity between neat solution and spiked plasma (2,203.5 cps versus 11,983.0 cps) based on the combined effects of all identified optimization potentials during the here presented investigations (50- $\mu$ L injection volume and optimized chromatographic conditions (e.g. 5% DMSO)). The comparison of the observed peak areas of 1 ng/mL human Hemokinin-1, spiked in human plasma samples, resulted in an increased intensity of 15% (mean  $\pm$  SD: (A)  $3,510.4 \pm 775.4$  cps versus (B)  $3,051.3 \pm 216.9$  cps [ $n = 3$ ]). Plasma matrix components may also reduce adsorption processes by likely concurring

with the investigated tachykinins, resulting in a lower benefit of observed peak areas compared to the results in the neat solution (section 3.4). No substantial matrix effect was observed in the here presented experiments.

In physiological relevant endogenous levels (100 pg/mL) [124,145], the comparison of the setpoint composition to the start gradient as an injection solvent resulted in an increase of intensity of 107.5% for Substance P (mean  $\pm$  SD: (A)  $2,433.8 \pm 616.1$  cps versus (B)  $1,172.8 \pm 162.0$  cps [ $n = 3$ ]) and enabled the determination of 100 pg/mL human Hemokinin-1 (mean  $\pm$  SD: (A)  $378.4 \pm 100.4$  cps versus (B)  $177.4 \pm 94.0$  cps (signal to noise < 10:1) [ $n = 3$ ]) in human plasma samples (Figure 21). As expected, due to the more pronounced adsorption effects in low-concentrated samples, the setpoint composition was essential for the sensitive determination of endogenous tachykinin concentrations.

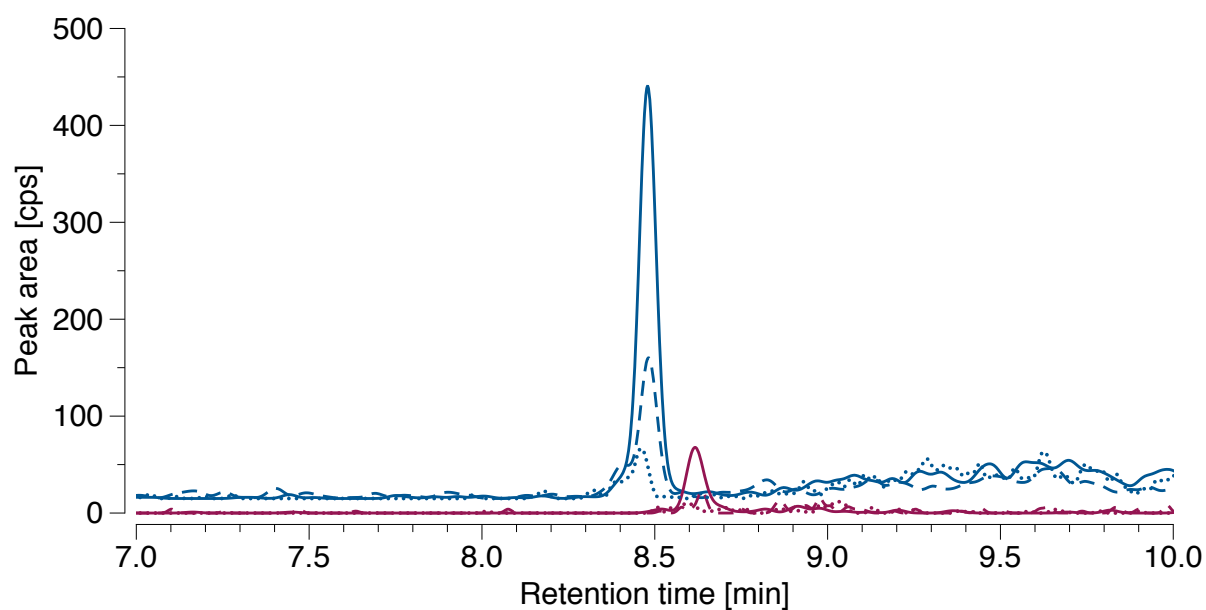


*Figure 21: Representative stacked chromatogram of spiked Substance P and human Hemokinin-1 under optimized conditions in human plasma.*

*Plasma was spiked with 100 pg/mL of Substance P (blue) and human Hemokinin-1 (red) (solid lines). For comparison, the start gradient composition in standard containers is presented in dashed lines and non-spiked plasma in dotted lines. (cps: counts per second)*

### 3.3.8 Reliability of determined Substance P levels

Substance P plasma levels were significantly distinct between diseased and healthy subjects, and therefore could be a potential biomarker to support a diagnostic or monitor the progress of pathological events. However, measured Substance P plasma levels showed high variability between clinical studies [132]. Variability was known to be caused by distinct analytical methods and different sampling procedures. The results of the Design of Experiments further indicated that adsorption processes account for another reason for the high variability of Substance P plasma levels. The used container materials possessed a high impact on the adsorption extent of Substance P and were rarely mentioned in investigated Substance P plasma levels. Predominantly, the use of regular glassware in sampling and measuring may result in significantly lower reported Substance P levels. Therefore, for accurate determination of Substance P, the pronounced adsorption behavior has to be concerned.

Furthermore, with the discovery of human Hemokinin-1 in 2003, a tachykinin with a similar amino acid sequence targeting the same receptor as Substance P, more specific analytical methods than immunoassays are required to differentiate accurately between Substance P and human Hemokinin-1 levels. The role of both peptides has to be re-evaluated, and therefore the selective and simultaneous determination is a crucial step to obtain non-biased concentrations of Substance P and human Hemokinin-1 for a better insight into the complex tachykinin system.

## 3.4 Conclusion

Nonspecific peptide adsorption as a major reason for a lack of MS intensity of Substance P and human Hemokinin-1 was successfully addressed by the presented Design of Experiments concept. The results of the concept should encourage other scientists working with peptides to implement concepts to investigate and minimize unspecific peptide adsorption for the sensitive determination of low abundant peptides by LC-MS. For the here investigated peptides, a high extent of DMSO and FA substantially reduced adsorption processes, resulting in an injection solvent composition of 45% DMSO, 45% water and 10% FA. By combining the aforementioned solvent composition with the most suitable container material (protein low binding polypropylene), low picomolar concentrations of Substance P (20 pg/mL) and of human Hemokinin-1 (40 pg/mL) were detectable. Thus, the experimental design facilitated the

simultaneous and sensitive determination of both peptides in human plasma samples by LC-MS/MS to overcome the current limitations by immunoassay determination.

### **3.5 Disclosure**

*Parts of this chapter were previously published as an original publication in the Journal of Separation Science (doi: 10.1002/jssc.201901038). The author of this thesis was responsible for the conceptualization, the methodology, the formal analysis, the investigation, the data curation and visualization and the writing of the original draft of this publication. Due to the Journal's style, the results and discussion sections are combined in this chapter.*

## **4. Validated Mass Spectrometric Assay for the Quantification of Substance P and human Hemokinin-1 in Plasma Samples: A Design of Experiments concept for Method Development**

### **4.1 Background and Aim**

Besides the described effects of peptide adsorption of Substance P [10], one principal reason for the high variance of reported tachykinin levels might be caused by the fact that Substance P plasma levels were measured by immunoassays with limitations in differentiating properly between Substance P and the related human Hemokinin-1, which may lead to falsified levels. Recently, most of the manufacturers have begun recommending against the use of these immunoassays for measuring Substance P plasma levels due to their cross-reactivity with human Hemokinin-1. Thus, LC-MS/MS could be a promising, selective alternative to measure the endogenous neuropeptides Substance P and human Hemokinin-1 in plasma. However, existing LC-MS/MS assays lack the required sensitivity for appropriate limits of detection (LOD) and have unsatisfactory lower limits of quantification (LLOQ) that cannot allow for the quantification of endogenous plasma levels in low picomolar ranges [11,12].

Consequently, the development of a sensitive, selective, and robust LC-MS assay is essential for reliable quantification of Substance P and human Hemokinin-1 in human plasma samples. In respect to the reliability of a bioanalytical assay, the European Medicine Agency (EMA) and the US Food and Drug Association (FDA) regulatory guidelines state strict recommendations for the method validation of compounds of interest in biological matrices [13,14]. In this context, method development can be a time-consuming effort and may lead to redevelopment if the method fails the guideline criteria due to a lack of sensitivity and inter-run robustness. A recent draft of the US Pharmacopeia (USP) Validation and Verification expert panel (USP 1220) proposed the implementation of a Quality by Design approach during method development for a better method understanding and improved risk control management [15,16]. By applying a chemometric approach and using Design of Experiments, critical method aspects such as plasma sample preparation, analyte selectivity, and method sensitivity could be systematically and comprehensively investigated and optimized [17,18], finally resulting in a robust method for analyzing the neuropeptides.

Thus, the aims of this study were (1) to develop a comprehensive LC-MS/MS assay using Designs of Experiments to enhance the sensitivity in order to measure endogenous plasma neuropeptide levels; (2) to validate this assay utilizing the robust setpoints found in the Designs of Experiments; and (3) to quantify Substance P, its biologically inactive analog - the carboxylic acid of Substance P - and human Hemokinin-1 (Table 3) in plasma samples by applying the validated assay.

*Table 3: Physicochemical and biological properties of Substance P, its carboxylic acid, human Hemokinin-1 and Sar<sup>9</sup>-Substance P (internal standard).*

Analyte	SP	SP(COOH)	hHK-1	(Sar <sup>9</sup> )-SP
Molecular mass [g/mol]	1347.63	1348.66	1185.43	1361.65
Isoelectric point (GeneScript Peptide Calculator©)	11.66	11.00	8.86	11.66
GRAVY Index (ExPaSy ProtParam tool©)	- 0.70	- 0.70	0.31	- 0.50
Neurokinin-1 receptor activation	yes	no	yes	yes

*(hHK-1: human Hemokinin-1; SP: Substance P; SP(COOH): Carboxylic acid of Substance P)*

## 4.2 Materials and Methods

### 4.2.1 Chemicals and materials

Substance P, human Hemokinin-1, and (Sar<sup>9</sup>)-Substance P, as internal standard, were purchased from Sigma-Aldrich (Darmstadt, Germany) as lyophilized acetic salts in HPLC grade with a purity of 96% for Substance P, 99% for human Hemokinin-1 and 96% for (Sar<sup>9</sup>)-Substance P, respectively. The carboxylic acid of Substance P was supplied by VWR chemicals in HPLC grade as trifluoroacetic salt with a purity of >95%. Water (MS grade) was obtained from Honeywell (Offenbach, Germany); acetonitrile (ACN) (HPLC grade), dimethyl sulfoxide

(DMSO) (analytical reagent grade), ethylene glycol (EG) (analytical reagent grade), methanol (MeOH) (MS grade) and propionic acid (PrA) (analytical reagent grade) were acquired from Fisher chemicals (Langenfeld, Germany); 4-(2-Aminoethyl)benzenesulfonyl fluoride (AEBSF), ethylene diamine tetraamine (EDTA), formic acid (FA) and phenanthroline were purchased from Sigma-Aldrich; polypropylene tubes in protein low binding quality (1.5 mL) and 1.6 mg/mL EDTA monovettes were obtained from Sarstedt (Nuembrecht, Germany); a Substance P enzyme-linked immunosorbent assay (ELISA) (EIA 3120) was bought from DRG (Marburg, Germany).

#### 4.2.2 Sample preparation

For the quantification of endogenous peptide levels, monovettes were pre-spiked with 140  $\mu$ M AEBSF (serine protease inhibitor) to stabilize the integrity of the endogenous peptides in blood, as recommended for Substance P [19]. 75 mM EDTA and 10 mM phenanthroline (both metalloprotease inhibitors) were additionally pre-spiked to control the metabolism of the carboxylic acid of Substance P. Blood was drawn on ice by aspiration, immediately centrifuged for 15 min at 0 °C and 1500  $\times$  g, and plasma was stored at -20 °C, when not directly processed. 120  $\mu$ L thawed or fresh plasma was acidified with 120  $\mu$ L water fortified with 10% FA and vortexed for 5 min at 1000 rpm to disrupt the plasma-protein binding of the peptides. The samples were stored on ice in protein low binding tubes until further purification by micro-solid phase extraction ( $\mu$ -SPE) using a hydrophilic-lipophilic balance (HLB) exchanger (Oasis Prime HLB  $\mu$ Elution plate, Waters, Eschborn, Germany).

#### 4.2.3 Preparation of peptide solutions

Stock solutions of 1 mg/mL Substance P, 1 mg/mL (Sar9)-Substance P, 4 mg/mL of the carboxylic acid of Substance P and 0.5 mg/mL human Hemokinin-1 were prepared in water fortified with 0.1% FA and stored in 100  $\mu$ L aliquots in protein low binding polypropylene tubes at -80 °C. For analysis, freshly thawed stock solutions were diluted in a mixture of 10% FA added to equal parts of DMSO and water (50:50 [v/v]) in protein low binding tubes to avoid nonspecific peptide adsorption as elsewhere published [10]. Within the Design of Experiments concept, blank plasma samples were spiked on the bench with the peptide mix to obtain final concentrations of 1 ng/mL.

#### 4.2.4 Instrumentation

Peptide separation and detection were achieved on a UHPLC-MS/MS system (Agilent 1200 series SL binary pump system [Waldbronn, Germany] coupled to a SCIEX API 4000 triple quadrupole mass spectrometer [Darmstadt, Germany]). Sample handling and injection were executed by a CTC Analytics HTC PAL system (Zwingen, Switzerland) using a 45  $\mu$ L injection volume. Peptide detection was performed in positive mode, utilizing electrospray ionization and multiple reaction monitoring (MRM). The MRM transitions and potentials are summarized in Table 4. Data acquisition and evaluation were performed using Analyst<sup>©</sup> (SCIEX, version 1.6.2) and Multiquant<sup>©</sup> (SCIEX, version 3.0.2).

Table 4: Mass spectrometric settings of the analytes Substance P, human Hemokinin-1 and the carboxylic acid of Substance P and the internal standard ((Sar<sup>9</sup>)-Substance P)

	SP		hHK-1		SP(COOH)		(Sar <sup>9</sup> )-SP
<b>Declustering Potential [V]</b>	86		95		100		99
<b>Entrance Potential [V]</b>	7		8.5		8		8.5
<b>MRM transitions [m/z]</b>	674.6 → 600.5	674.6 → 254.3	593.4 → 519.3	593.4 → 505.2	674.6 → 254.3	674.6 → 600.5	681.6 → 607.3
<b>Collision Energy [V]</b>	33	37	23	27	37	33	31
<b>Collision Exit Potential [V]</b>	16	6	14	14	6	16	18

(hHK-1: human Hemokinin-1; MRM: multiple reaction monitoring; m/z: mass to charge ratio; SP: Substance P; SP(COOH): Carboxylic acid of Substance P)

#### 4.2.5 Quality by Design

The method development was embedded in a chemometric approach operating Designs of Experiments for optimizing plasma extraction, peptide separation, and method sensitivity (Supplementary Table 7 - 9). The method components investigated, the Design of Experiments characteristics used, and the selected ranges and limitations of the examined factors are

presented in Table 5. For planning, analyzing, and calculating the risk of the Design of Experiments, MODDE Pro© (MKS Instruments AB, Malmoe, Sweden, version 12.0) was used.

*Table 5: Outline of the investigated method aspects, characteristics and investigated factors of the utilized Design of Experiments models.*

<b>Method aspect</b>	<b>SPE protocol</b>	<b>Mobile phase composition</b>
DoE model	D-optimal design	D-optimal design
Number of experiments	26	26
Center points	6	3
Replicates	3	5
Investigated factors [ranges] <i>*Limit selection</i>	Wash volume [150 µL – 450 µL*] <i>*limited by cartridge volume</i> Organic wash fraction [0% - 40%* MeOH] <i>*limited by analyte breakthrough</i> Elution volume [50 µL – 400 µL*] <i>*limited by deep well plate volume</i> Organic elution fraction [50%* - 99% MeOH] <i>*limited by analyte properties</i> Acid elution fraction [1% - 10%* FA] <i>*limited by cartridge material</i>	Supercharger type [DMSO, EG, PrA] Supercharger fraction [0% - 5%*] <i>*limited by HPLC system</i> Mobile phase B type [ACN, MeOH] FA fraction [0.1% - 1%*] <i>*limited by column material</i>

4. Validated Mass Spectrometric Assay for the Quantification of Substance P and human Hemokinin-1 in Plasma Samples: A Design of Experiments concept for Method Development

<b>Method aspects</b>	<b>Chromatographic conditions</b>	<b>Ion source parameters</b>
DoE model	D-optimal design	Onion D-optimal design
Number of experiments	33	31
Center points	3	3
Replicates	3	3
Investigated factors [ranges] <i>*Limit selection</i>	Time of accumulation phase [0 min – 5 min] Time of separation phase [0.1 min – 3 min] Time of elution phase [0.1 min – 3 min] Elution fraction [50%* - 100%] <i>*limited by analyte properties</i> Column temperature [45 °C – 80 °C*] <i>*limited by column material</i>	Curtain gas [25 psi – 50 psi*] Nebulizer gas [40 psi – 80 psi*] Heater gas [40 psi – 80 psi*] Ion spray voltage [3500 eV - 5500 eV*] Ion source temperature [350 °C – 650 °C*] <i>*limited by hardware</i>

(ACN: Acetonitrile, DMSO: Dimethyl sulfoxide, DoE: Design of Experiments; EG: Ethylene glycol, FA: Formic acid, MeOH: Methanol, PrA: Propionic acid; SPE: solid phase extraction)

#### 4.2.5.1 Design and setpoint characteristics

Within the Design of Experiments concept, D-optimal designs were selected for the optimization of the investigated method components. Distinct D-optimal designs as quadratic models were selected to optimize (1) the SPE protocol, (2) the mobile chromatographic phases, (3) the chromatographic gradient, and (4) the ion source parameters.

Each experiment was independently prepared in at least triplicate and all experiments were run in random order (if technically appropriate) during multiple days. The experimental runs were accompanied by a minimum of three center point runs, measured in triplicate, to determine the repeatability of each model. In each design, a robust setpoint was calculated by performing a Monte-Carlo simulation (50.000 runs), indicating the probability of failing the preset limits of specifications. In the case of non-existing guideline criteria, limits of specifications were principally chosen in order to maximize the predicted peak area, as the improvement of the method sensitivity was a principal aim of the Design of Experiments concept. Subsequently, a robust setpoint was expressed as process capability indices ( $C_{pK}$ ) for each investigated response. Based on the USP chapter 1080 Appendix II, a minimum  $C_{pK}$  of 1 was required ( $C_{pK} > 1$  indicates that less than 0.3% [ $3 \times$  standard deviation] of the simulated predicted results do not meet the predefined limits of specification), and a minimum  $C_{pK}$  of 1.3 ( $4 \times$  standard deviation) was desired for a robust setpoint [20].

##### 4.2.5.1.1 Micro-solid phase extraction protocol

For the micro-solid phase extraction protocol, the aim was to use the maximum organic wash fraction and wash volume possible along with the minimum organic elution fraction and elution volume possible to obtain sufficient recovery rates while also reducing co-elution of other compounds, e.g., phospholipids, which may lead to interfering matrix effects. Thus, various steps in the micro-solid phase extraction protocol were investigated to maximize the recovery of the peptides and minimize possible plasma matrix effects. First, the HLB sorbent material was conditioned with 300  $\mu$ L MeOH and equilibrated with 300  $\mu$ L water fortified with 0.1% FA as recommended by the manufacturer. For each experiment, 240  $\mu$ L acidified plasma samples were loaded onto the sorbent material. The first wash step used 300  $\mu$ L water fortified with 0.1% FA and was held constant in each experiment, as no peptide elution was detected using aqueous solutions in preliminary experiments. The second wash step consisted of a

variable washing volume (150–450  $\mu\text{L}$  [maximal cartridge volume]) of a water/MeOH mixture containing 0–40% MeOH (v/v). As higher concentrations of MeOH likely lead to losses of the hydrophilic peptides, its proportion in the wash fraction was limited to 40%. Subsequently, the elution fraction was composed of a water/MeOH/FA mixture containing between 50% MeOH (minimum expected elution fraction for the lipophilic peptide human Hemokinin-1) and 99% MeOH (v/v/v). A minimum of 1% FA was added both to acidify the eluate and to increase the ionic strength of the elution fraction and was limited to 10% FA to avoid the co-elution of sorbent material. The peptides were eluted in two steps utilizing a minimum elution volume of 50  $\mu\text{L}$  (minimum volume according to the manufacturer) and a maximum of 400  $\mu\text{L}$  (maximum volume allowed by the applied deep well plates). The eluate was evaporated to dryness at 60  $^{\circ}\text{C}$  and 650 rpm under nitrogen and was reconstituted in the optimized injection solvent composition to minimize peptide adsorption during the evaporation process [10]. The process efficiency of each peptide, calculated as the quotient of pre-spiked extracted plasma samples and the corresponding peptide concentration in the neat solution, was defined as the model response.

#### 4.2.5.1.2 Chromatographic phases and gradient optimization

The evaluation was subdivided into three groups. First, the optimal mobile phase composition was investigated using a standard column. Second, the best performing C18 column was assessed using the optimal mobile phase composition. Lastly, the gradient was optimized using the optimal mobile phase and the best-performing column.

The compositions of the mobile phases were optimized for the maximum peak intensities of the peptides by utilizing a C18 column (Waters XSelect CSH, 130 A, 3.5  $\mu\text{m}$ , 3.0 x 150 mm). Water was considered as mobile phase A, and ACN or MeOH was mobile phase B. FA was added to both mobile phases for a better ionization of the peptides in a range of 0.1–1% (v/v), which was limited by the column material. As potential superchargers, DMSO, EG, and PrA were added to both mobile phases in a range of 0–5% (v/v), which was limited to avoid instrumental corrosion damages to MS optics.

Next, different C18 solid phases were investigated to determine which was most suitable using the optimized mobile phase compositions. Six C18 columns (XSelect CSH 130 A, 3.5  $\mu\text{m}$ , 3.0 x 150 mm; XSelect Peptide CSH 130 A, 3.5  $\mu\text{m}$ , 2.1 x 150 mm; Xbridge BEH 130 A, 3.5  $\mu\text{m}$ ,

3.0 x 150 mm, Xbridge XP 130 A, 2.5  $\mu\text{m}$ , 2.1 x 150 mm; Cortecs C18+ 90 A, 1.6  $\mu\text{m}$ , 2.1 x 100 mm [all from Waters]; and Kinetex 100 A, 1.7  $\mu\text{m}$ , 2.1 x 100 mm [from Phenomenex, Aschaffenburg, Germany]) were pre-screened for sufficient peak resolution ( $>2$  as recommended by the FDA [21]) between Substance P and its carboxylic acid, since both peptides had similar MRM transitions, and adequate peak tailing factor ( $<1.5$ ), as suggested by the USP [22].

Utilizing the best-performing column, the gradient was optimized for the peak intensities of the peptides, the peak resolution between Substance P and its carboxylic acid, and the gradient time. The gradient consisted of three consecutive phases encompassing (1) the accumulation phase, in which the peptides were concentrated onto the HPLC column; (2) the separation phase, in which Substance P and its carboxylic acid were separated; and (3) the elution phase, in which the most lipophilic peptide (human Hemokinin-1) was eluted. The time varied between 0–5 min in the peptide accumulation phase (5% to 25% mobile phase B, no peptide elution expected), 0.1–3 min in the separation phase (25% to 45% mobile phase B), and 0.1–3 min in the elution phase (from 45% up to 50% - 100% mobile phase B, lipophilic peptide elution expected). The oven temperature was changed from a minimum of 45  $^{\circ}\text{C}$  up to the highest temperature tolerance of the column (80  $^{\circ}\text{C}$ ). The flow rate was fixed to the maximum possible velocity limited by the backpressure of the LC system (450  $\mu\text{L}/\text{min}$ ) to obtain sharp peak forms. As recommended by the FDA, a resolution of  $>2$  between Substance P and its carboxylic acid was set as the limit of specification. Furthermore, a maximum gradient time of 5 min was set as a further limit of specification for the development of a fast assay.

#### 4.2.5.1.3 Ion source parameters

Since no gradient-elution–flow-injection analysis was supported by the MS software (only analysis for isocratic elution), the ion source parameters were optimized by Design of Experiments to maximize the predicted peak areas of the peptides. The parameters were ranged and limited based on the operator's guide for the ion source. Therefore, curtain gas pressure was changed from a minimum of 25 psi to the maximum (50 psi), nebulizer and heater gas pressure from 40 psi to 80 psi, ion spray voltage from 3500 eV to the maximum (5500 eV), and ion source temperature from 350  $^{\circ}\text{C}$  to the maximum tolerable temperature (650  $^{\circ}\text{C}$ ).

#### 4.2.6 Method validation

Using the robust setpoints found in the Designs of Experiments during method development, the method was validated regarding its accuracy, precision, linearity, sensitivity, and carry-over according to the FDA and EMA bioanalytical guidelines. Nine non-zero calibration standards were prepared using blank human plasma samples (see section 2.2 for its generation) encompassing a concentration range from 7.8 pg/mL (LLOQ) to 2000 pg/mL (Upper limit of quantification: ULOQ). Therefore, 5  $\mu$ L of a working solution containing Substance P, its carboxylic acid and human Hemokinin-1 (each 100 ng/mL) was spiked to 245  $\mu$ L blank plasma to obtain the ULOQ sample. For the subsequent calibrators, the ULOQ sample was serially diluted by 1:2 with blank human plasma in protein low binding tubes. Four quality control (QC) levels (7.8 pg/mL, 15.6 pg/mL, 1000 pg/mL, 2000 pg/mL) were independently prepared analogically to the calibrators and measured in quintuplicate in three runs over two days to determine the intra- and inter-run accuracy and precision. The calibrators and QC samples were freshly prepared for each validation run and were stored on ice until plasma extraction. In line with the guidelines, the acceptance criteria for relative error (accuracy) and coefficient of variation (precision) were  $\pm 15\%$  for all levels, except for the lowest QC (7.8 pg/mL), for which they were  $\pm 20\%$ . A one-way ANOVA was applied to evaluate repeatability and inter-day precision. The LOD was calculated as 3.3 times the quotient of the standard deviation of the y-intercept and the mean slope of the regression line, utilizing three calibration curves consisting of ten calibrators from 3.9 pg/mL to 2000 pg/mL. Additionally, blank and zero samples were measured following the ULOQ sample to determine carry-over effects. A signal-to-noise ratio of the LLOQ compared to the blank sample higher than 5 was required.

As internal standard, 5  $\mu$ L of a (Sar<sup>9</sup>)-Substance P working solution (10 ng/mL) were spiked on the benchtop to 245  $\mu$ L of each acidified calibrator, QC, zero sample and analytical sample before the extraction to obtain a final concentration of 200 pg/mL of (Sar<sup>9</sup>)-Substance P in all experiments.

The recovery was calculated as the quotient of an aqueous peptide solution, which was extracted by  $\mu$ -SPE and an analog unextracted peptide solution. Absolute matrix effects were determined using blank plasma samples from one human source. Thus, blank human plasma was extracted by  $\mu$ -SPE and the reconstituted residual was post-spiked with the peptide working solution. The matrix effect was calculated as the ratio of spiked plasma sample after plasma extraction and

peptide neat solution. For the stability experiments the peptides were pre-spiked to the plasma and processed as follows. The benchtop stability of the spiked plasma samples was examined at two temperature levels (4°C, 20 °C) for 90 min, the autosampler stability (<15°C) for 24 h and three freeze-thaw cycles (-80°C) were investigated for both plasma samples and the stock solution. Each experiment for recovery, matrix effects and stability was measured in triplicate utilizing three levels (20 pg/mL, 1000 pg/mL, 2000 pg/mL, each peptide).

#### 4.2.7 Application of the validated method

Non-spiked fresh plasma samples from five volunteers were measured in triplicate to determine endogenous plasma concentrations of Substance P, its carboxylic acid and human Hemokinin-1. Blood draws from male (n = 3) and female (n = 2) volunteers was done by aspiration in monovettes utilizing a butterfly device. The monovettes were pre-spiked with 140 µM AEBSF and the freshly collected plasma of the volunteers was immediately processed on ice as described in section 2.2 to avoid metabolic degradation of the peptides within one hour from blood collection to sample extraction by µ-SPE. EDTA and phenanthroline were not spiked to allow for the generation of the carboxylic acid of SP. A maximum of one hour elapsed between taking blood and preparing samples using µ-SPE. Additionally, blood draw from one male volunteer was done utilizing monovettes spiked with the protease inhibitor mix to obtain blank plasma samples (AEBSF, EDTA and phenanthroline). The obtained whole blank blood samples were spiked with 100 pg/mL of each analyte to investigate peptide integrity during sampling and plasma preparation. Furthermore, plasma samples from one male volunteer were parallelly measured in triplicate by ELISA following the manufacturer's protocol. The blood sampling was conducted following the tenets of the Helsinki Declaration and has been approved by the authors' institutional review committee (ethics commission of the medical faculty, Heinrich Heine University, study number: 2019-705).

### 4.3 Results

#### 4.3.1 Method development using Design of Experiments

Utilizing the Design of Experiments concept, robust setpoints were determined with the aim of developing a final LC-MS method. The identified robust setpoints, including their  $C_{pK}$  values, are summarized in Table 6. After a total of 106 experiments using four different Designs of

Experiments, the method sensitivity was profoundly improved to enable the determination of endogenous low picomolar concentrations of the neuropeptides. Goodness of fit and prediction was monitored for each Design of Experiments (Figure 22). When a random order of the experiments was not technically possible, control charts of the center points were used to detect possible outliers during the experiments (Figure 23).

*Table 6: Found robust setpoints of the investigated method aspects with their obtained process capability indices for each response.*

<b>Investigated method aspects</b>	<b>Found robust setpoints</b>	<b>Relative error</b>	<b>C<sub>pk</sub> values</b>
Solid phase extraction protocol	190 $\mu$ L Wash volume (11% MeOH)	+9.8% (SP)	1.75
	2 x 60 $\mu$ L Elution volume (83% MeOH, 7% FA)	+7.4% (hHK-1)	1.09
		-9.0% (SP(COOH))	1.90
Composition of mobile phases	Mobile phase A: water + 5% DMSO + 0.1% FA	-2.8% (SP)	2.34
	Mobile phase B: MeOH + 5% DMSO + 0.1% FA	-11.7% (hHK-1)	2.67
Column pre-screening	Waters XSelect Peptide CSH 130 A, 3 $\mu$ m, 2.1 x 150 mm	-	-
Chromatographic gradient	Accumulation phase: 2 min	-10.8% (SP)	1.64
	Separation phase: 1.5 min	+13.0% (hHK-1)	1.91
	Elution phase: 0.5 min	+11.3% (SP(COOH))	2.05
	Organic elution fraction: 50%	-6.3% (T)	2.46
	Oven temperature: 80°C	-0.9% (R)	1.18
Ion source parameters	Curtain gas: 40 psi	-4.3% (SP)	2.01
	Nebulizer gas: 40 psi	-0.6% (hHK-1)	1.66
	Heater gas: 80 psi		
	Ion spray voltage: 5000 eV		
	Ion source temperature: 425°C		

*The relative error at the robust setpoint was calculated as quotient of predicted vs observed response. (C<sub>pk</sub>: Process capability index; DMSO: dimethyl sulfoxide, FA: formic acid, hHK-1: human Hemokinin-1, MeOH: methanol, R: Resolution; SP: Substance P (SP), SP(COOH): Carboxylic acid of Substance P; T: Gradient time)*

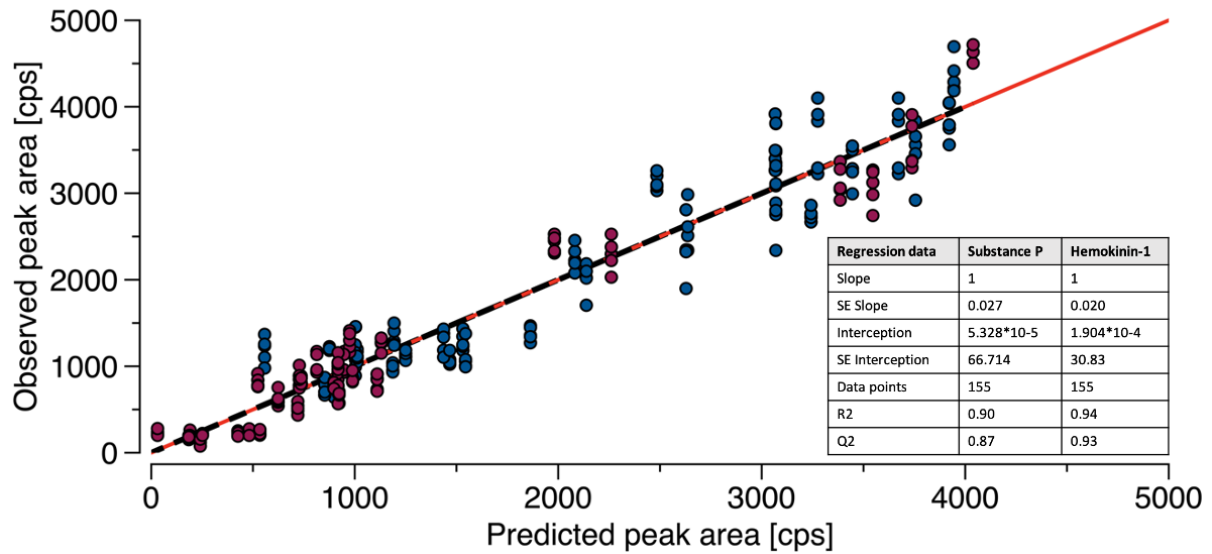


Figure 22: Exemplary goodness of fit plot for the statistical evaluation for the optimization of the composition of the mobile phases.

The plot shows the observed versus predicted peak areas of Substance P (blue) and human Hemokinin-1 (red) with the identity line (solid red line) and the regression lines (dashed black lines). (cps: counts per second; SE: standard error)

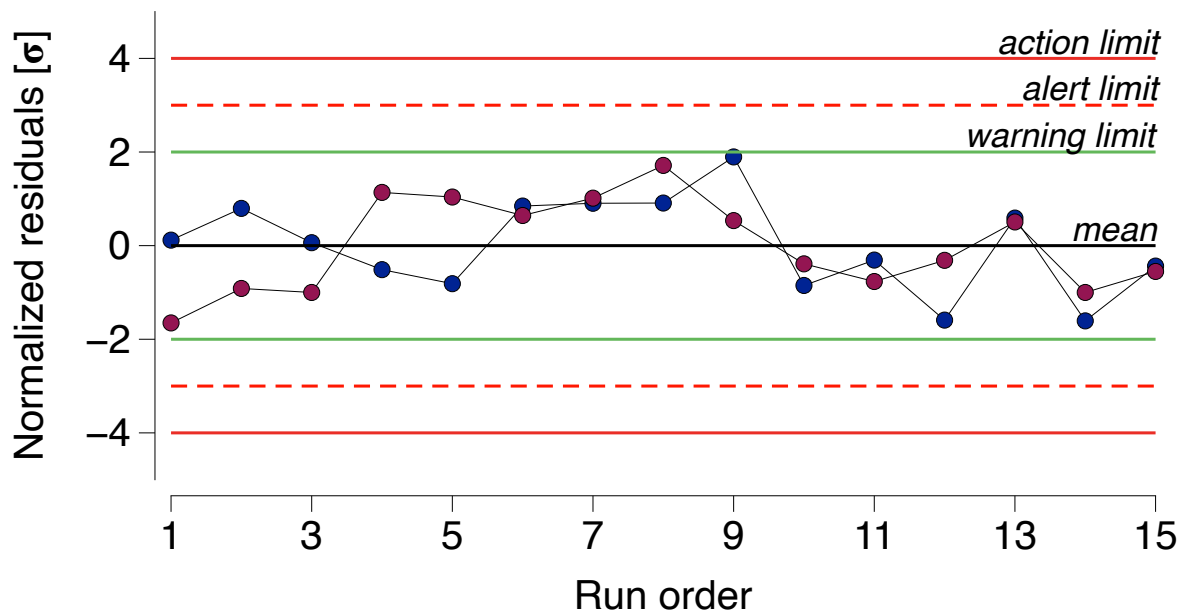


Figure 23: Process-control chart of the observed peak areas at the center point for each response in consecutive run order for the optimization of the mobile phases.

The green lines indicate  $2\sigma$ , red dashed lines  $3\sigma$  and red solid lines  $4\sigma$  the standard deviation ( $\sigma$ ) of the process mean peak area at the center point per response ((Substance P (blue), human Hemokinin-1 (red) [ $n = 15$ ])

#### 4.3.1.1 Development of a suitable micro-solid phase extraction protocol

Within the limits of specifications, a maximum organic wash fraction of 12% MeOH was feasible using up to 220  $\mu\text{L}$  wash volume (Figure 25-A, design space). As expected, due to the hydrophilicity of Substance P and its analog, a substantial loss of peptides was observed utilizing higher organic wash fractions (up to -50.5% predicted recovery for the carboxylic acid of Substance P when comparing 10% to 40% MeOH fractions) and higher organic wash volumes (up to -13.0% predicted recovery for Substance P when comparing 200  $\mu\text{L}$  to 450  $\mu\text{L}$  wash volume). The variance of the elution volume and the addition of a higher FA fraction did not have a statistically significant effect on the recovery of the peptides (Figure 24). A minimum of 80% organic elution fraction was necessary to enable sufficient elution of the peptides (Figure 25-B, design space). Consequently, a robust setpoint ( $C_{pK} \geq 1.09$ ) was found using 190  $\mu\text{L}$  wash volume (11% MeOH) and two 60  $\mu\text{L}$  elution volumes (83% MeOH, 7% FA, 10% water). Thus, the final protocol was as follows: 300  $\mu\text{L}$  MeOH for conditioning, 300  $\mu\text{L}$  water fortified with 0.1% FA for equilibration, loading of 240  $\mu\text{L}$  acidified plasma samples onto the sorbent material, 300  $\mu\text{L}$  water fortified with 0.1% FA for the first wash, 190  $\mu\text{L}$  water/MeOH (89/11 [v/v]) for the second wash, and two rounds of 60  $\mu\text{L}$  MeOH/FA/water (83/7/10 [v/v/v]) for elution.

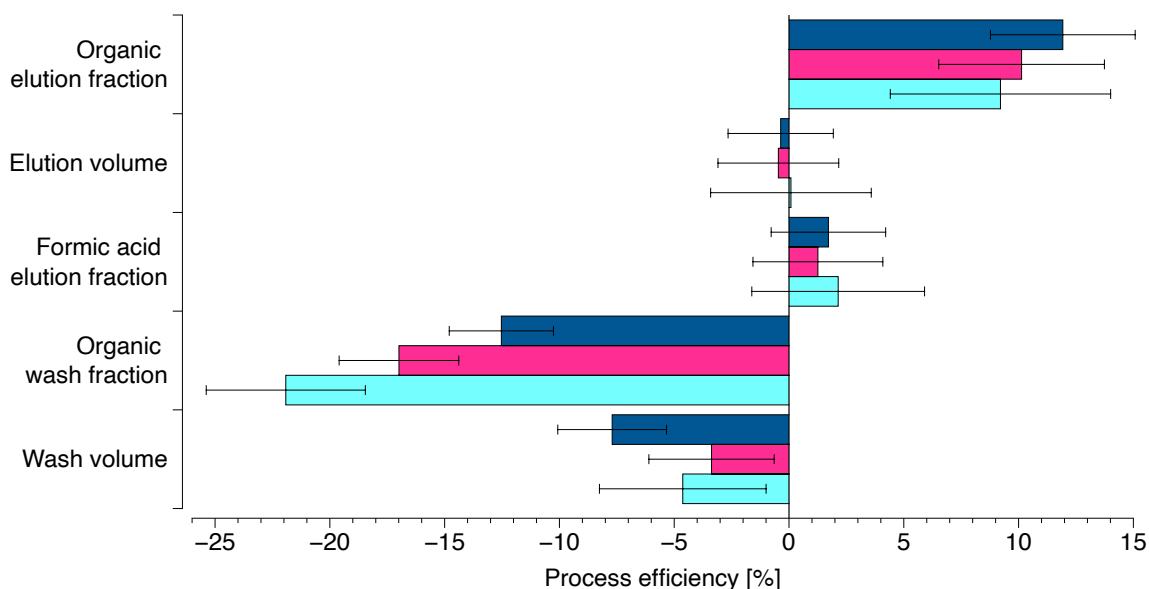


Figure 24: Coefficient plots of the impact of the investigated factors during the solid-phase protocol.

(Substance P (dark blue); human Hemokinin-1 (red); Carboxylic acid of Substance P (light blue); T: 95% confidence interval)

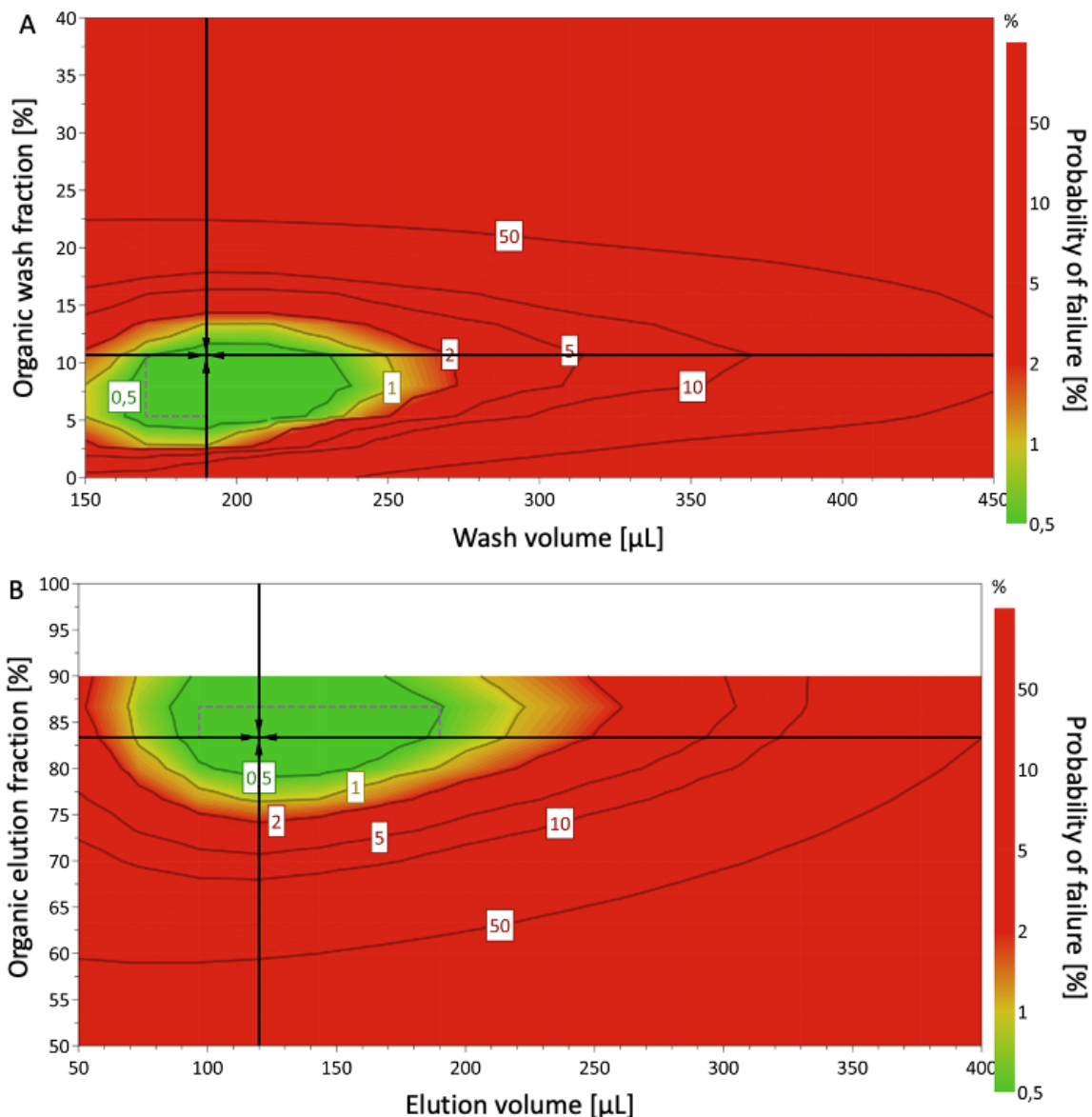


Figure 25: Robust setpoints of the wash step and the elution step in the solid-phase extraction protocol calculated by the Monte-Carlo simulation.

The colors and numbers indicate the probability to fail the robust setpoints during (A) the wash step and (B) the elution step. The design space (green area) denotes a probability of failure <0.5% and includes the robust setpoint (hair-cross). In graphic B, the white area illustrates the fixed proportion of formic acid in the elution fraction at the robust setpoint. Thus, a calculation of the organic elution fraction using Monte Carlo simulation was not possible in this area and is therefore shown in white.

#### 4.3.1.2 Chromatographic phases and gradient optimization

The compositions of the mobile phases were optimized for maximum method sensitivity. The results indicate that the use of a supercharger was mandatory to measure Substance P and human Hemokinin-1 sensitively (Figure 26; main effects). The addition of 5% DMSO and PrA both significantly enhanced the predicted peak area of Substance P, whereas the effect of EG addition was not as pronounced (+138.1% (DMSO); +209.0% (PrA); +68.6% (EG)). In the case of human Hemokinin-1, its predicted peak area was substantially increased by the addition of 5% DMSO compared to the other superchargers (+426.1% (DMSO); +79.7% (PrA); +22.3% (EG)). By the addition of a high FA fraction, the predicted peak areas of both peptides were also improved, but the magnitude was less compared to the effects of the superchargers (+18.2% for Substance P; +18.8% for human Hemokinin-1). The most advantageous type of mobile phase B was dependent on the peptide: the predicted peak area of Substance P was significantly increased by the use of MeOH, while the predicted peak area of human Hemokinin-1 was enhanced with ACN. Since the combination of MeOH and DMSO significantly improved the predicted peak areas of both peptides, MeOH was selected as mobile phase B (Figure 26; interactive effects). Thus, a conjoint sensitive optimum for both peptides was found resulting in a robust setpoint ( $C_{pK} \geq 2.34$ ) utilizing water and MeOH as the mobile phases, with 5% DMSO and 0.1% FA added to both.

Using the optimized mobile phase compositions, the investigated C18 columns were pre-screened for peak resolution between Substance P and its carboxylic acid and peak tailing expressed by the USP tailing factor. Three columns demonstrated a peak resolution  $<2$  between Substance P and its carboxylic acid, which were unsatisfactory according to the FDA recommendations (Figure 28-A). Two of the remaining columns displayed a tailing factor of  $<1.5$ , as recommended by the USP (Figure 28-B). Owing to the mass resolution of the mass filter if the triple quadrupole is used in MRM mode (0.7 amu), the mass-to-charge ratio of Substance P [674.6 m/z] and its carboxylic acid [674.8 m/z] impedes their precise quantification if they are not sufficiently separated by liquid chromatography. Therefore, the XSelect Peptide CSH column was finally chosen due to its superior separation power and was further used for the systematic investigation of the gradient.

4. Validated Mass Spectrometric Assay for the Quantification of Substance P and human Hemokinin-1 in Plasma Samples: A Design of Experiments concept for Method Development

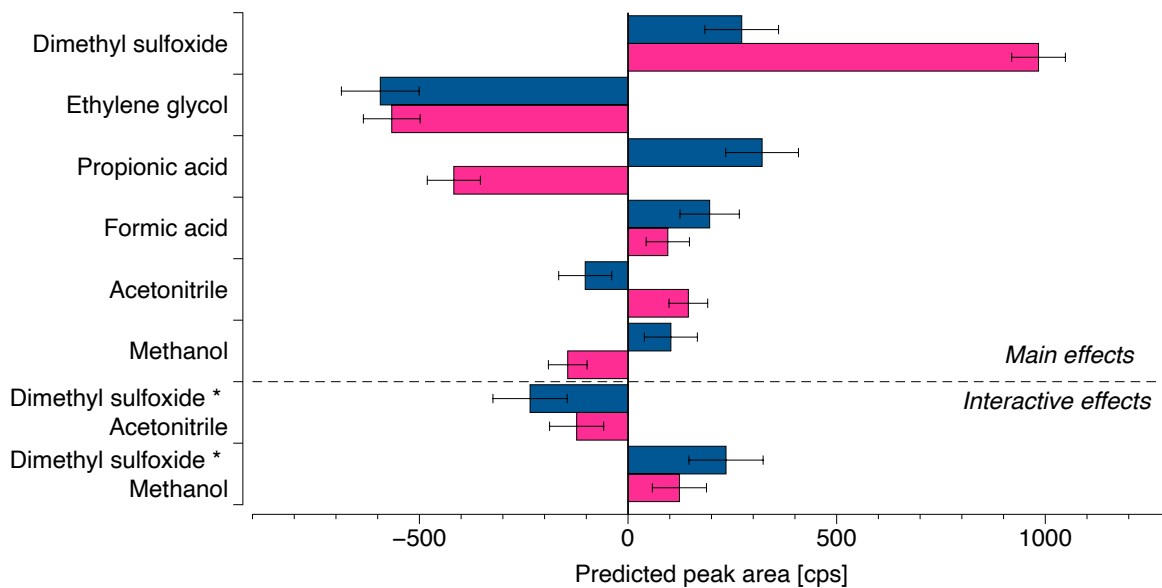


Figure 26: Coefficient plot of the main and interactive effects of the composition of the mobile phases on the analytes.

(Substance P (blue); human Hemokinin-1 (red); T: 95% confidence interval; cps: counts per second)

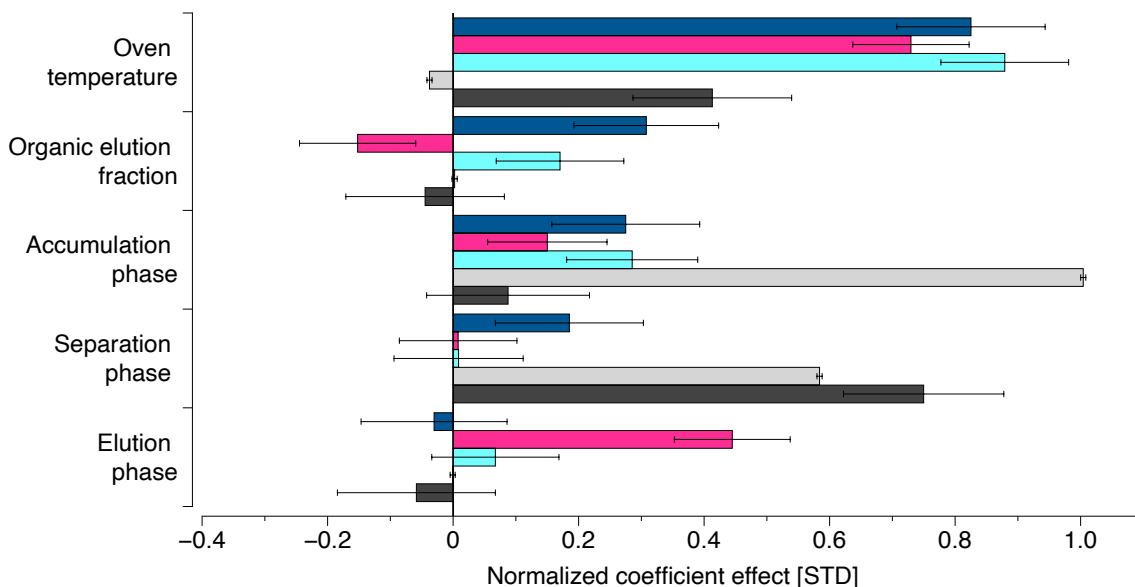


Figure 27: Coefficient plot of the impact of chromatographic settings on the analytes.

(Substance P (dark blue); human Hemokinin-1 (red); Carboxylic acid of Substance P (slight blue); gradient time (slight grey); resolution (dark grey); T: 95% confidence interval; cps: counts per second; STD: normalized to the responses' standard deviations)

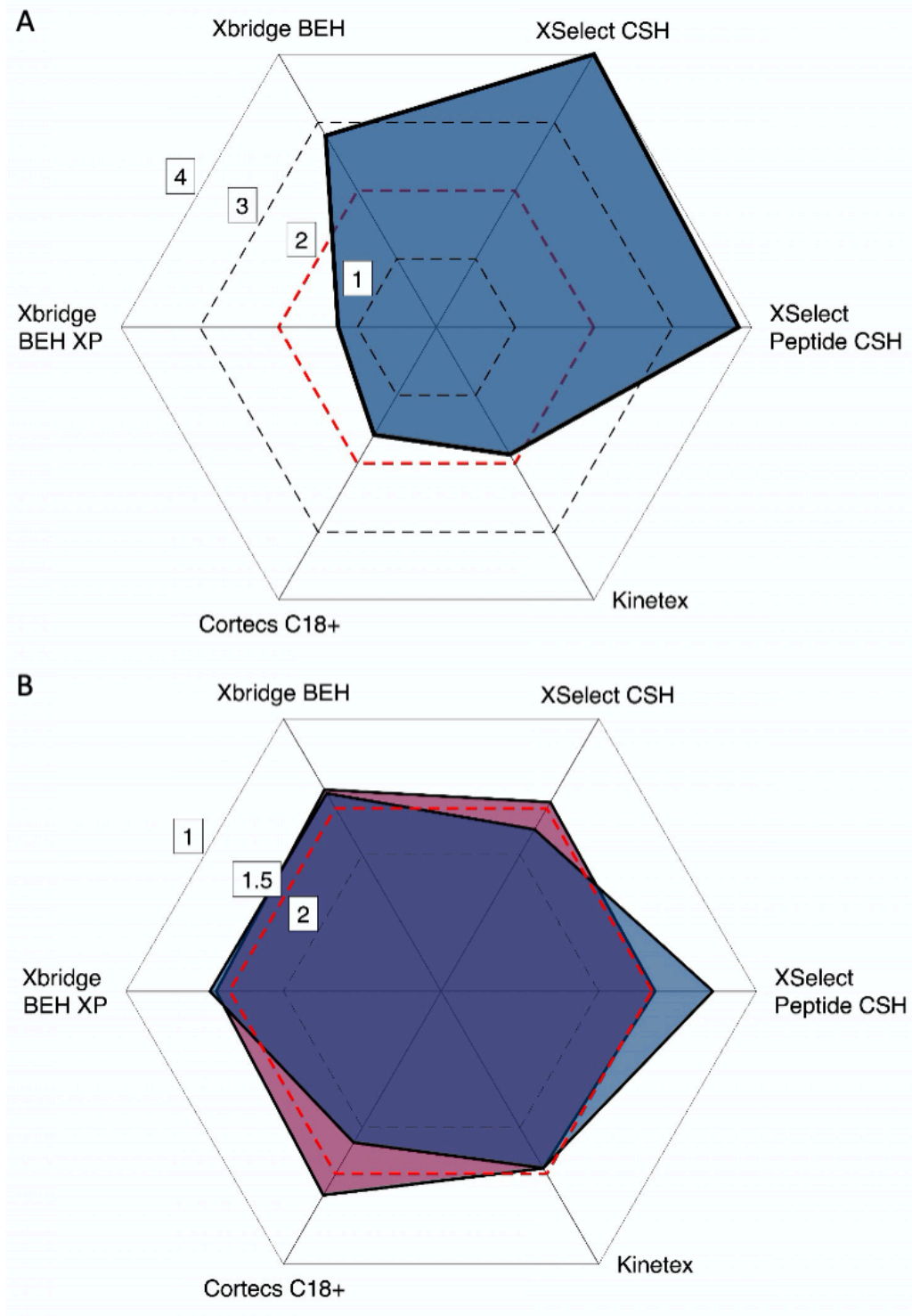


Figure 28: Polar plots for the evaluation of the most suitable C-18 column.

(A) Peak resolution between Substance P and its carboxylic acid (the red line indicates the minimal peak resolution recommended by the FDA guidelines); (B) USP peak tailing factor of Substance P (blue) and human Hemokinin-1 (red) (the red line indicates the minimal peak tailing factor recommended by the USP); each experiment  $n = 3$ .

The gradient was investigated and optimized for predicted peak areas, peak resolution, and gradient time. The most major impact on the investigated responses was due to variance of the oven temperature (Figure 27). An increased temperature (80 °C) was the principal factor that significantly increased the predicted peak areas (up to +43.9% for Substance P). Higher organic elution fractions led to higher predicted peak areas of the more hydrophilic peptides (+15.1% for Substance P; +6.9% for its carboxylic acid), but to lower predicted peak areas of the more hydrophobic peptide human Hemokinin-1 (-7.0%) and had no impact on the resolution and gradient time. A longer accumulation phase led to significantly higher predicted peak areas of the peptides (up to +12.2% for Substance P). A longer separation phase was necessary for a sufficient predicted resolution (+0.6), while the impact on the predicted peak areas was not substantial for Substance P (+8.9%) and not significant for its carboxylic acid) and human Hemokinin-1. The length of the elution phase had no significant impact on the predicted peak areas of Substance P or its carboxylic acid, the resolution, or the gradient time, but it did increase the predicted peak area of human Hemokinin-1 (+26.0%). Within the specification limits, a robust setpoint ( $C_{pK} \geq 1.18$ ) was found utilizing a 4 min gradient (0–2 min: 5% → 25% mobile phase B; 2–3.5 min: 25% → 45% mobile phase B; 3.5–4 min: 45% → 50% mobile phase B) and an 80 °C oven temperature.

#### 4.3.1.3 Optimization of the ion source parameters

Maximum responses were found by setting the curtain gas pressure to 40 psi, resulting in higher predicted peak areas (up to +7.8% for human Hemokinin-1). A higher nebulizer gas pressure led to significantly lower predicted peak areas (up to -14.5% for Substance P); whereas a higher heater gas pressure had no significant impact on the predicted peak areas. Maximum peak areas were predicted when setting the ion spray voltage to 5000 V, leading to significantly increased predicted peak areas (up to 23.9% for human Hemokinin-1). Lower ion source temperatures had major impacts on the predicted peak areas (Figure 29). For the hydrophilic peptide Substance P and the hydrophobic peptide human Hemokinin-1, the maximum peak areas were predicted at ion source temperatures of 470 °C and 350 °C, respectively. For simultaneously determining concentrations of both peptides with high sensitivity, a conjoint robust setpoint ( $C_{pK} \geq 1.66$ ) was found using 40 psi curtain gas, 40 psi nebulizer gas, 80 psi heater gas, 5000 V ion spray voltage, and a 425 °C ion source temperature.

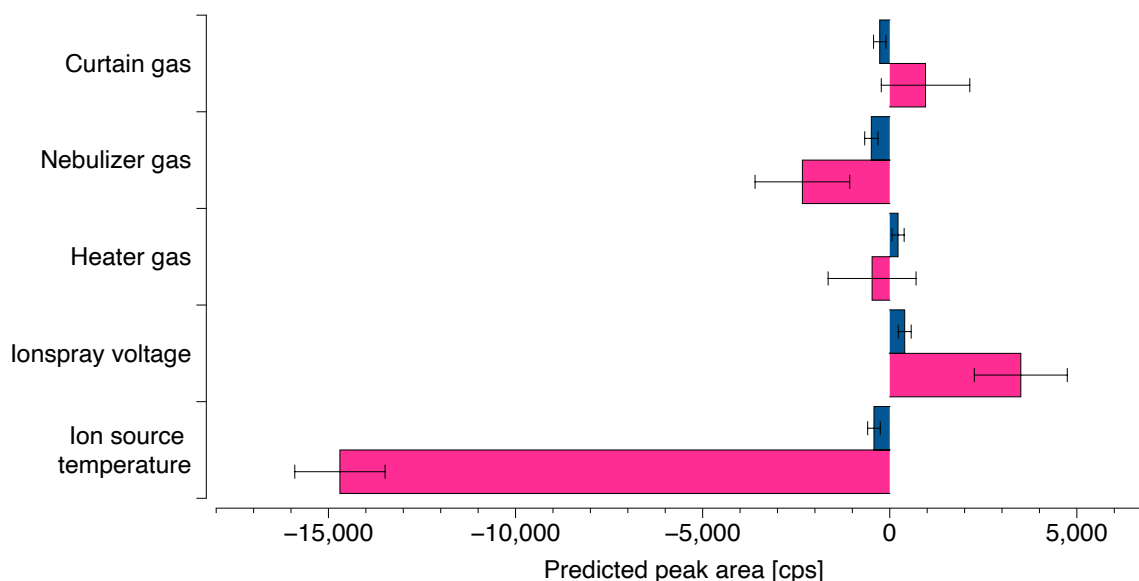


Figure 29: Coefficient plot of the impact of the investigated ion source parameters on Substance P and human Hemokinin-1.

(Substance P (blue); human Hemokinin-1 (red); T: 95% confidence interval; cps: counts per second)

### 4.3.2 Method validation

The final LC-MS/MS method based on the 106 experiments within the Design of Experiments concept is summarized in Figure 30 and was used for the validation and applicability experiments.

#### 4.3.2.1 Linearity, LLOQ, LOD, and carry-over

The fit was achieved by linear regression with a  $1/x^2$  weighting for all three analytes ( $r \geq 0.995$ ). Linearity was demonstrated from the LLOQ (7.8 pg/mL) to the ULOQ (2000 pg/mL) in three independent runs on two days (Supplementary Table 13). In these runs, a minimum of seven non-zero calibration levels including the LLOQ were within the recommended  $\pm 15\%$  nominal concentration for all analytes, fulfilling FDA bioanalytical guidelines. Signal to noise ratios of maximal 5.1 for Substance P, 5.2 for human Hemokinin-1, and 5.3 for the carboxylic acid of Substance P were achieved, indicating no pronounced carry-over, satisfying FDA bioanalytical guidelines regarding the LLOQ (Figure 31). Based on the conducted calculations using the obtained regression, LODs of 5.8 pg/mL for Substance P, 5.3 pg/mL for human Hemokinin-1, and 6.2 pg/mL for the carboxylic acid of Substance P were determined.

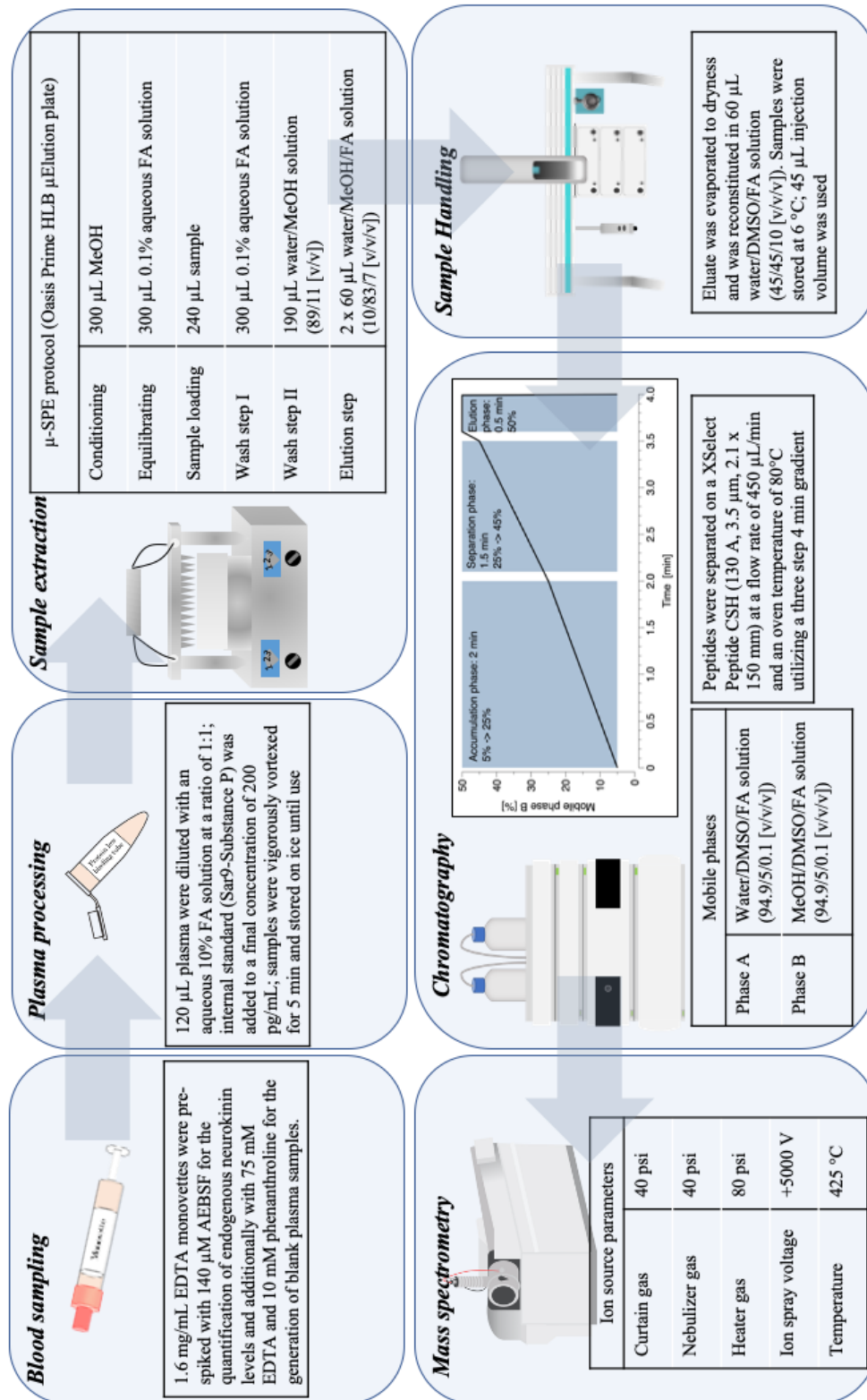


Figure 30: Final LC-MS/MS method based on the Design of Experiments concept [AEBSF: 4-(2-Aminoethyl)benzenesulfonyl fluoride, DMSO: Dimethylsulfoxide, EDTA: Ethylene diamine tetra acetic acid, FA: Formic acid, MeOH: Methanol]

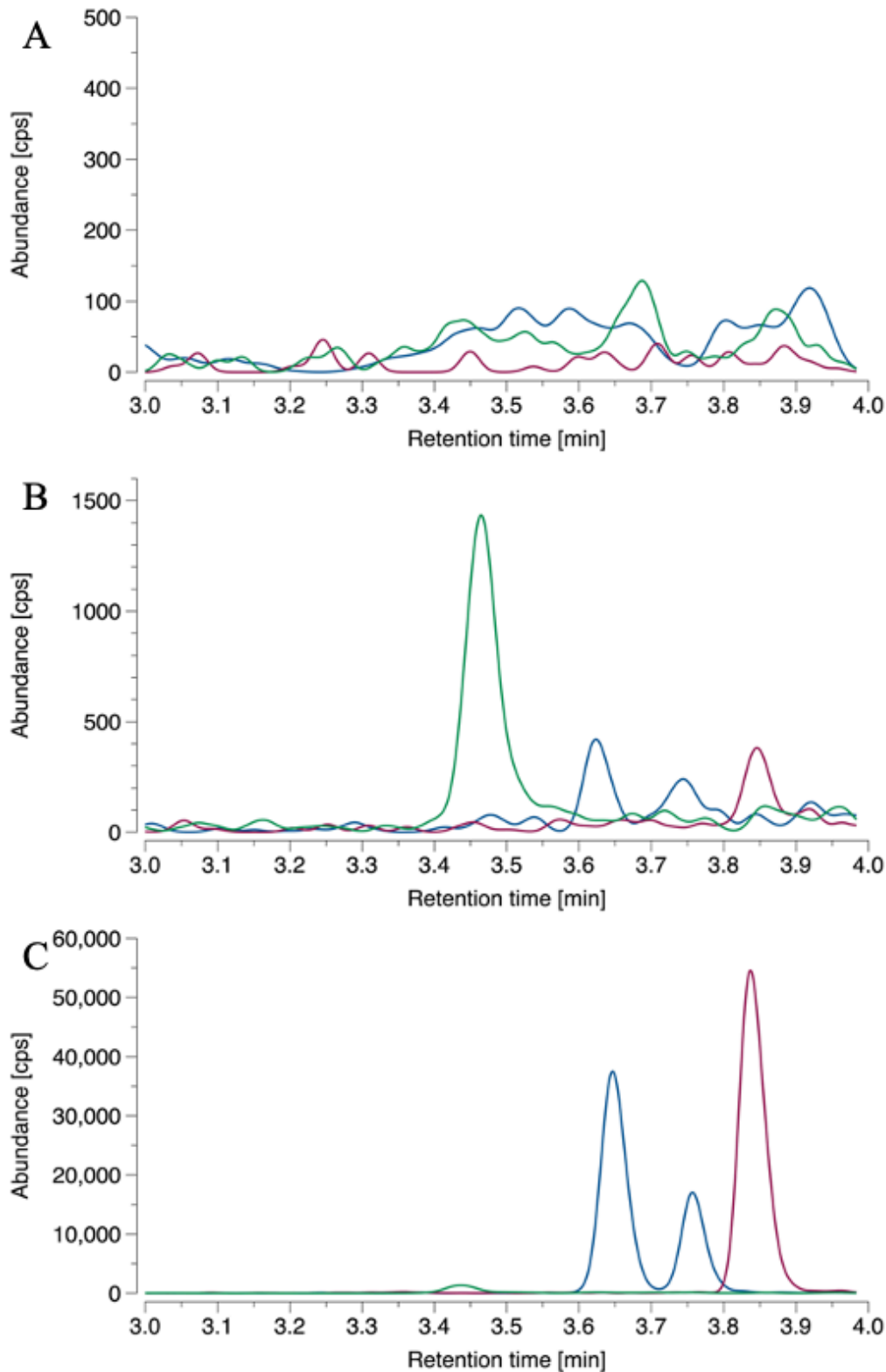


Figure 31: Representative chromatograms of the blank, the lower and upper limit of quantification of the validated method.

(A) Blank sample, (B) LLOQ (lower limit of Quantification) sample, (C) ULOQ (upper limit of Quantification sample) for Substance P, its carboxylic acid (both blue), human Hemokinin-1 (red) and (Sar9)-Substance P (green) (cps: counts per second).

#### 4.3.2.2 Accuracy and Precision

In three independent runs, the accuracy and precision of four QC levels were determined (Supplementary Table 10 - 12). Each validation run fulfilled the guideline criteria concerning intra- and inter-run accuracy (Supplementary Table 14). For the four concentration levels, mean intra-run accuracy was 93.0–113.8% for Substance P, 89.6–107.6% for human Hemokinin-1, and 92.2–111.1% for the carboxylic acid. Mean inter-run accuracy was 97.9–109.5% for Substance P, 98.6–102.2% for human Hemokinin-1, and 101.3–104.7% for the carboxylic acid. Repeatability (intra-run precision) was calculated as  $\leq 8.5\%$  for Substance P,  $\leq 10.2\%$  for human Hemokinin-1 and  $\leq 8.4\%$  for the carboxylic acid, respectively. The inter-day precision was determined as  $\leq 9.9\%$  for Substance P,  $\leq 10.2\%$  for human Hemokinin-1 and  $\leq 11.2\%$  for the carboxylic acid (Supplementary Table 15). All results for intra-run and inter-run precision did not exceed the guideline limits of 15%.

#### 4.3.2.3 Recovery, selectivity and matrix effects

Obtained recoveries and absolute matrix effects for the three analytes at three QC levels (20 pg/mL, 1000 pg/mL, 2000 pg/mL) are shown in Supplementary Table 16. Mean recoveries were  $90.4\% \pm 9.8\%$  for Substance P,  $110.8\% \pm 13.3\%$  for human Hemokinin-1, and  $103.9\% \pm 6.0\%$  for the carboxylic acid ( $\pm$  standard deviation; each  $n = 3$ ) at the lowest QC level (20 pg/mL). At the middle QC level (1000 pg/mL), the mean recoveries were  $106.2\% \pm 2.8\%$  for Substance P,  $97.5\% \pm 4.3\%$  for human Hemokinin-1, and  $95.1\% \pm 0.1\%$  for the carboxylic acid. At the highest QC level (2000 pg/mL), the mean recoveries were  $103.3\% \pm 1.1\%$  for Substance P,  $95.0\% \pm 1.5\%$  for human Hemokinin-1, and  $95.4\% \pm 2.1\%$  for the carboxylic acid. The absolute matrix effects were calculated for each QC level, and they resulted in acceptable ion suppressions through the whole calibration range. The effect was highest at 20 pg/mL for Substance P (-15.6%), at 20 pg/mL for human Hemokinin-1 (-9.8%), and at 1000 pg/mL for the carboxylic acid (-19.7%). The mean resolution between Substance P and its carboxylic acid, which was an indicator of selectivity, was higher than 2.3 in each validation run.

#### 4.3.2.4 Stability

Benchtop stability of the peptides depended on the storage temperatures (Supplementary Table 16). Whereas the spiked analytes in plasma were stable on ice (4°C) (>96.0% ± 10.3% (Substance P), >93.8% ± 9.7% (human Hemokinin-1), >95.1% ± 0.1% (carboxylic acid), substantial analyte losses were observed when storing them at room temperature (20°C) (>59.2% ± 2.4% (Substance P), >49.7% ± 3.2% (human Hemokinin-1), >44.5% ± 7.4% (SP(COOH) [mean ± SD; each n = 3]). The autosampler stability of the peptides pre-spiked in plasma was tested over 24 h (<15 °C). The samples were stable when using the optimized injection solvent composition (>94.0% ± 10.6% (Substance P), >91.5% ± 4.9% (human Hemokinin-1), >88.2% ± 5.0% (SP(COOH) [mean ± SD; each n = 3]). The investigation of the freeze-thaw stability of the spiked peptides in plasma over three cycles (-80°C) demonstrated the labile nature of the three analytes, resulting in recoveries of >70.5% ± 2.3% for Substance P, >67.4% ± 2.9% for human Hemokinin-1 and >67.5% ± 0.8% for SP(COOH) in the first cycle and >54.9% ± 4.2% for Substance P, 39.0% ± 3.3% for human Hemokinin-1 and >44.6% ± 8.5% for SP(COOH) in the third cycle [mean ± SD; each n = 3]. A minor degradation was observed in three freeze-thaw cycles of the stock solution (>82.1% ± 0.9% (Substance P), >79.9% ± 2.7% (human Hemokinin-1), >81.6% ± 1.4% (SP(COOH)) (Supplementary Table 17).

#### 4.3.3 Applicability

The peptide integrity of exogen spiked neurokinins during sampling was demonstrated by their mass spectrometric detection (Substance P, its carboxylic acid and human Hemokinin-1, each 100 pg/mL) (Figure 32-A). Neurokinin plasma concentrations from non-spiked samples of five volunteers (aged 26–38 years) were determined using the developed LC-MS/MS assay. In each non-spiked sample, Substance P and human Hemokinin-1 plasma levels were lower than the LOD (Figure 32-B–F). Plasma levels of the carboxylic acid of Substance P varied from 202.5 pg/mL to 1024.1 pg/mL between the individuals. Additionally, plasma samples from one volunteer were parallelly measured by immunoassay, resulting in Substance P plasma concentrations of 51.2 ± 10.5 pg/mL (n = 3), although Substance P levels were not quantifiable by the mass spectrometric assay.

4. Validated Mass Spectrometric Assay for the Quantification of Substance P and human Hemokinin-1 in Plasma Samples: A Design of Experiments concept for Method Development

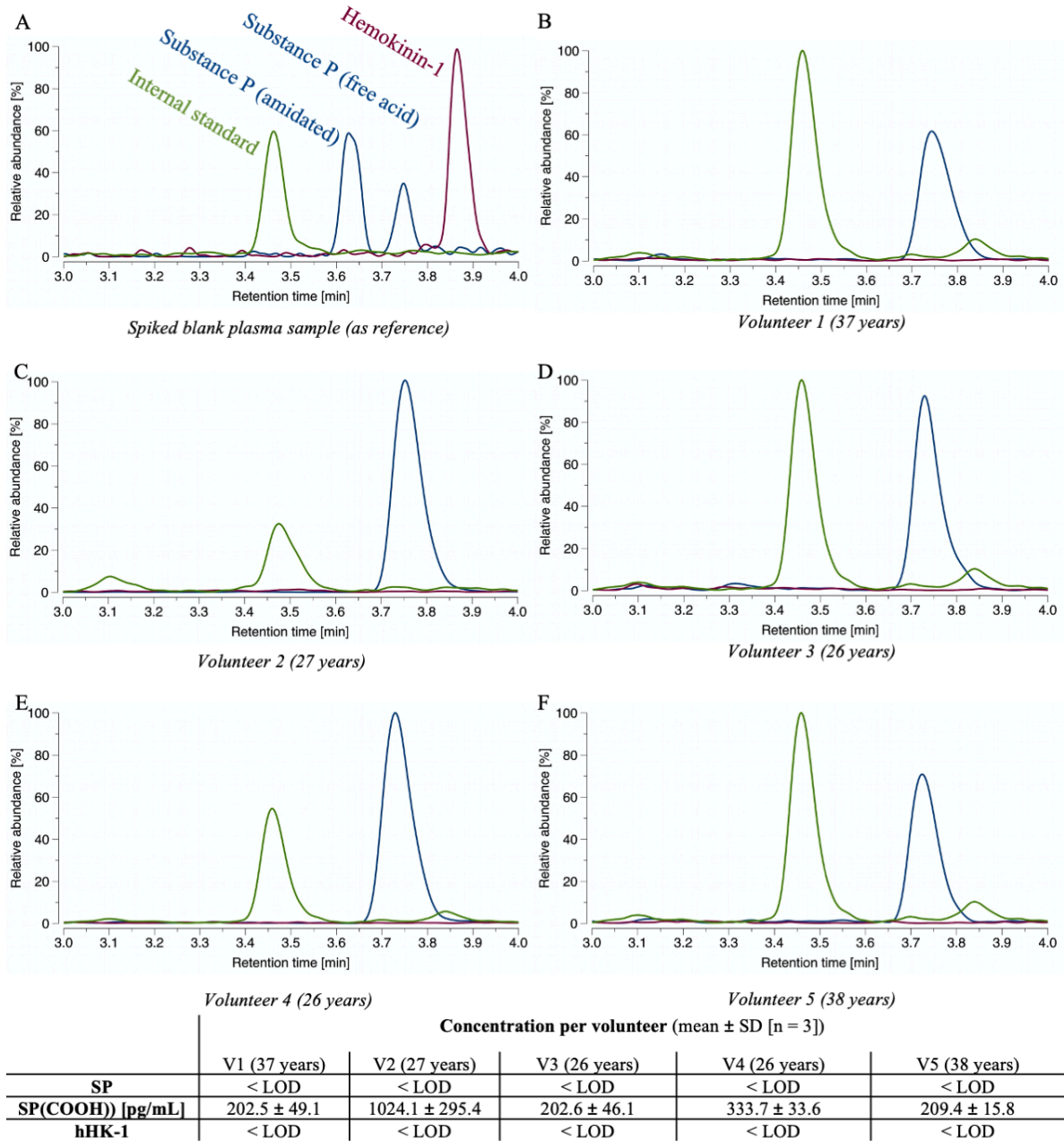


Figure 32: Representative chromatograms of spiked and non-spiked plasma samples from five individuals.

(A): 100 pg/mL of each peptide were spiked to plasma and analyzed. (B-F): Neither Substance P (blue; retention time: 3.65 min) nor human Hemokinin-1 (red) were found in the non-spiked samples. The carboxylic acid of Substance P (blue; retention time: 3.75 min) was observed in each individual. The chromatograms of the internal standard (Sar9)-Substance P are marked in green. (LOD: limit of detection; SD: standard deviation)

## 4.4 Discussion

An accurate and precise LC-MS/MS method for the simultaneous determination of Substance P, human Hemokinin-1, and the biologically inactive carboxylic Substance P analog was successfully established using 120  $\mu$ L human plasma. By utilizing the here-presented Design of Experiments concept, critical aspects of method development were tackled within 106 experiments. This meticulous approach allowed for the gain of sensitivity, which was lacking in former LC-MS assays and therefore hindered the determination of Substance P in plasma. Additionally, to the best of our knowledge, a LC-MS/MS assay for the quantification of human Hemokinin-1 has not yet been reported.

In peptidomics, enabling a low LLOQ is essential for the determination of endogenous plasma concentrations. For achieving these low limits of quantification, much time and effort must usually be invested during method development. In the recent years, chemometric approaches were successfully applied to optimize the chromatographic separation of diverse analytes in line with a lean and robust development of LC-UV/VIS methods [17,23]. Additionally, the Design of Experiments approach has proven its usefulness as a lean tool for method development of multifactor-dependent settings and contributes to signal increase in LC-MS/MS. The applied Design of Experiments concept ensured comprehensive evaluation and optimization of the method using a lean and cost-efficient approach and a manageable number of experiments. The method is characterized by an appropriate LLOQ (7.8 pg/mL for Substance P and human Hemokinin-1) that facilitates the reliable detection of described low picomolar concentrations (12.5–32.9 pg/mL) [9]. The addition of a supercharger to the mobile phases predominantly contributed to the gain of method sensitivity, which was systematically evaluated within the applied Design of Experiments concept. In the here presented experiments, the additives were principally selected based on their ability to enhance the protonation state towards one specific charge state within multiple-charged peptides (DMSO, EG) or to reduce ion-suppression effects of co-eluting compounds due to e.g. ion pairing (PrA) [24,25]. In line with the proteomics recommendations of Hahne et al. [26], the addition of 5% DMSO superiorly enhanced the signal intensity of both peptides ( $\sim$ 3x for Substance P;  $\sim$ 8x for human Hemokinin-1). The addition of the superchargers was limited to 5% to avoid corrosive damage to the sensible parts of the LC and the column although the Design of Experiments results and data in literature suggest that higher fractions would even lead to higher peak intensities, which may be applicable by post column infusion [24]. However, the usefulness

also in post column approaches needs careful consideration as ion source and optics might be negatively affected.

Moreover, during the Design of Experiments, Substance P and human Hemokinin-1 demonstrated distinct setpoint optima due to their different physicochemical characteristics. As reported [10,18], the statistical experimental design allowed for the determination of a conjoint optimum, enabling the sensitive quantification of both peptides simultaneously.

The method was successfully validated according to FDA bioanalytical guidelines concerning linearity, sensitivity, accuracy, precision, and carry-over to obtain reliable results of the neurokinin levels. Special attention was given to peptide separation, as Substance P (674.3 m/z) and its carboxylic acid (674.8 m/z) are not distinguishable by tandem MS (mass resolution 0.7 amu) due to their similar fraction patterns. Thus, a peak resolution by liquid chromatography above 2 was prioritized and achieved to reliably differentiate between these peptides. Additionally, emphasis was placed on achieving a sufficient LOD to measure endogenous levels over a wide linear range (7.8–2000 pg/mL) covering most of the neurokinin levels reported elsewhere from immunoassays (12.3–397.0 pg/mL in healthy adults) [9]. The ability to reliably quantify and distinguish between the three similar peptides was proven by pre-spiked plasma samples with typical concentrations ranges of Substance P in healthy volunteers [27].

However, contrary to expectations, Substance P and human Hemokinin-1 levels could not be detected in any of the five investigated subjects, despite LODs of 5.8 pg/mL for Substance P and 5.3 pg/mL for human Hemokinin-1. In each plasma sample, the carboxylic acid of Substance P was detected instead, which has not yet been described in plasma. As the stability experiments showed the labile nature of Substance P and human Hemokinin-1 during freeze and thaw cycles, the volunteers' plasma samples were freshly drawn and immediately processed to prevent the peptide integrity. Since a short half-life of Substance P was described (3-10 min), a highly concentrated protease inhibitor cocktail containing AEBSF, EDTA, and phenanthroline was added to the monovettes. Moreover, blood sampling and sample preparation were executed on ice and in a chilled centrifuge (0 °C) to avoid degradation of the fragile peptides as observed when processing the samples at room temperature. As a strong and reversible binding of Substance P to plasma proteins was found previously [28], Substance P could possibly be lost during sample preparation by  $\mu$ -SPE. Thus, 5% FA was added to the plasma samples before the  $\mu$ -SPE protocol to avoid loss of bound peptides, as higher levels of

unbound Substance P were described after plasma acidification (blood pH < 6.5) [29]. Assuming that Substance P and human Hemokinin-1 were not bound to plasma proteins and were stable in the plasma samples, the presence of Substance P and human Hemokinin-1 in plasma could not be verified by LC-MS analysis. The plasma sample from one individual was also assessed using a commercially available immunoassay, which reported Substance P concentrations of about 50 pg/mL, which should be detectable by the here-developed highly sensitive LC-MS assay. As the previously reported levels of Substance P were exclusively measured by immunoassays, cross-reactivity of the antibodies to metabolites or analogs of Substance P could explain why the immunoassays show Substance P concentrations that were not detected by the LC-MS assay. This hypothesis is consistent with previously published LC-MS assays, which were also not able to detect distinct endogenous peptides (e.g. apelin) [30]. These findings raise the question about possible cross-reactive Substance P species measured by immunoassays, which should be further investigated and elucidated.

## 4.5 Conclusion

By using the here-presented Design of Experiments concept, a highly sensitive LC-MS assay for the quantification of Substance P and human Hemokinin-1 in plasma was comprehensively developed, enabling LLOQs that were suitable for the determination of endogenous plasma concentrations. The successful method validation according to FDA bioanalytical guidelines concerning linearity, accuracy, precision, sensitivity, and carry-over emphasizes the usefulness of implementing a Design of Experiments concept to develop robust and reliable LC-MS assays in a limited number of experiments. This proof-of-concept study enabled the development of the first validated LC-MS method for the simultaneous and reliable quantification of Substance P and human Hemokinin-1 utilizing a 120  $\mu$ L sample of human plasma.

## 4.6 Disclosure

*Parts of this chapter were previously published as an original publication in the Journal of Pharmaceutical and Biomedical Analysis (doi: 10.1016/j.jpba.2020.113542). The author of this thesis was responsible for the conceptualization, the methodology, the formal analysis, the investigation, the validation, the data curation and visualization and the writing of the original draft of this publication.*

## **5. Mass spectrometric studies on the peptide integrity of Substance P and related human tachykinins in human biofluids**

### **5.1 Background and Aim**

The amino acid structure of Substance P, the first tachykinin described (in 1931), is highly conserved in all mammals [1]. First identified as a vasodilatory substance in horse tissue [147], subsequent attention was given to the physiological and pathological roles of Substance P in humans. Over the years, Substance P has been found in various human tissues (e.g., brain [148]) and biofluids (e.g. plasma, saliva, seminal fluid, and tears [4,104,149,150]), indicating its widespread presence in the human organism. Its biological effects are predominantly mediated by the G protein-coupled neurokinin-1 receptor, through which it activates and modulates inflammatory and immune processes [8]. The amidated C-terminal sequence of Substance P plays a critical role in receptor binding and activation. By substituting the amide with a carboxylic acid, the receptor affinity and biological activity of Substance P were almost completely extinguished [151]. In 2002, human Hemokinin-1 was discovered as an endogenously present tachykinin in human tissues that possesses an amidated C-terminal structure identical to that of Substance P [152]. Consequently, human Hemokinin-1 binds to the NK-1 receptor with a similar affinity as Substance P, resulting in analogous inflammatory and immunomodulatory effects [30]. In the recent years, human Hemokinin-1 was found to be involved in various nociceptive and inflammatory pathways as e.g. endotoxin-induced airway inflammation [153] and the activation of lung mast cells [154]. Similar to Substance P, human Hemokinin-1 upregulated various interleukins and the tumor necrose factor- $\alpha$  from monocytes [31]. Furthermore, elevated blood levels of both Substance P and human Hemokinin-1 were found in subjects with fibromyalgia syndrome, indicating its role in pain modulation [34]. Although Substance P and human Hemokinin-1 were associated with similar inflammatory reactions, a differentiation of both peptides is mandatory due to additional other signaling pathways of Hemokinin-1, also leading to opposite effects compared to Substance P as e.g. the promotion of B-cell precursors or dose-dependent analgesic effects of human Hemokinin-1 [30].

Consequently, the discovery of human Hemokinin-1 led to discussions about the proportional roles of these tachykinins in NK-1 receptor activation [131,155]. Additionally, the co-presence

of human Hemokinin-1 complicated the bioanalysis of Substance P in human biosamples, as levels of Substance P in humans were exclusively measured by immunoassays. Due to the cross-reactivity of the antibodies to the C-terminal portion of human Hemokinin-1, most of the manufacturers of these assays could no longer recommend their use for the determination of Substance P concentrations in human biosamples. The alternative bioanalytical method, LC-MS/MS, has the potential to overcome the issues of immunoassay cross-reactivity and enables the selective determination of both peptides, although the mass spectrometric detection of endogenous levels is quite challenging due to the low concentration of Substance P in, for example, blood plasma (as low as 12.3 pg/mL) [87]. By utilizing a recently developed and highly sensitive mass spectrometric assay, neither endogenous Substance P nor human Hemokinin-1 could be detected in the plasma of five human volunteers, raising questions about the peptide integrity in the plasma samples [156]. Instead, the biologically inactive carboxylic acid of Substance P was observed in the human plasma samples.

Several factors were shown to affect the peptide integrity and accurate quantification of Substance P in bioanalytical samples. The sample extraction process [157,158], metabolic degradation in bioanalytical samples [128], nonspecific adsorption to materials [159], peptide binding to plasma proteins [4], and the assay used [129] all demonstrated a substantial impact on the measured Substance P concentrations. Subsequently, a high variance in Substance P plasma levels measured in distinct studies with similar populations (e.g., healthy volunteers exhibiting Substance P plasma concentrations of 12.3–397.0 pg/mL) was attributed to selecting immunoassays based on the sample processing protocol used, complicating the accurate determination of plasma Substance P concentration [87].

To address these issues, the objectives of this study were (1) the comprehensive investigation and optimization of various sampling protocols for the recovery and integrity of Substance P and human Hemokinin-1 in human plasma samples for LC-MS/MS analysis; (2) the evaluation of the sample processing protocols developed using various biosources (human blood plasma, saliva, seminal fluid, and urine and porcine brain tissue) by LC-MS/MS; and (3) the identification of Substance P cross-reactors using an immunoaffinity–HR-MS/MS approach.

## 5.2 Materials and Methods

### 5.2.1 Chemicals and materials

Substance P, human Hemokinin-1, and (Sar9)-Substance P (internal standard) were purchased from Sigma-Aldrich (Darmstadt, Germany) as high-performance liquid chromatography (HPLC)-grade lyophilized acetic salts with a purity of 96% for Substance P, 99% for human Hemokinin-1, and 96% for (Sar9)-Substance P. The carboxylic acid of Substance P was supplied by VWR Chemicals (Hannover, Germany) in HPLC grade as a trifluoroacetic salt with a purity of >95%. Water (MS grade) was obtained from Honeywell (Offenbach, Germany); acetonitrile (HPLC grade) was acquired from VWR; acetonitrile for tryptic digestion (MS grade), dichloroacetic acid (DCA; analytical reagent grade), dimethyl sulfoxide (DMSO; analytical reagent grade), methanol (MeOH; MS grade), and isopropanol (HPLC grade) were provided by Fisher Chemicals (Langenfeld, Germany); phosphoric acid (PhA; analytical reagent grade) and trifluoroacetic acid (TFA; analytical reagent grade) were obtained from AppliChem (Darmstadt, Germany); ammonium bicarbonate, amino ethylene benzene sulfur fluoride (AEBSF), ethylene diamine tetraamine acetic acid (EDTA), formic acid (FA), guanidine hydrochloride, leupeptin, phenanthroline, sodium deoxycholate, and urea were purchased from Sigma-Aldrich; L-(tosylamido-2-phenyl) ethyl chloromethyl ketone (TCPK)-treated modified trypsin was obtained from Thermo Fisher Scientific (Rockford, IL, USA); low-protein-binding polypropylene tubes (1.5 mL) and 1.6 mg/mL EDTA monovettes and salivettes were obtained from Sarstedt (Nuembrecht, Germany); and the Substance P enzyme-linked immunosorbent assay (ELISA) kit (EIA 3120) was supplied by DRG Diagnostics (Marburg, Germany).

### 5.2.2 Preparation of peptide solutions

Stock solutions of 1 mg/mL Substance P, 1 mg/mL (Sar9)-Substance P, 4 mg/mL the carboxylic acid of Substance P, and 0.5 mg/mL human Hemokinin-1 were prepared in water fortified with 0.1% FA and stored in 100  $\mu$ L aliquots in low-protein-binding polypropylene tubes at -80°C. For analysis, freshly thawed stock solutions were diluted in a mixture of 10% FA added to equal parts DMSO and water (50:50 [v/v]) in low-protein-binding tubes to avoid unspecific peptide adsorption, as previously described [159].

## 5.2.3 Sample processing

### 5.2.3.1 Biosample handling

Porcine brain tissue was obtained from a freshly slaughtered animal, homogenized onsite for 10 sec, immediately frozen in a dry ice/MeOH bath, and stored at  $-80^{\circ}\text{C}$  within 20 min of slaughter. For analysis, the brain tissue was weighed and prepared according to the following protocol modified from Beaudry [103]. A 0.5% TFA solution was added to the brain homogenate at a ratio of 1:2 (w/v) and the samples were sonicated for 20 min at  $20^{\circ}\text{C}$ . Next, 500  $\mu\text{L}$  sonicated sample was mixed with 500  $\mu\text{L}$  ice-cold acetonitrile, vigorously vortexed for 5 min, and centrifuged at  $16,000 \times g$  for 10 min at  $0^{\circ}\text{C}$ . The supernatant was evaporated under nitrogen and  $60^{\circ}\text{C}$  to a residual volume of approximately 100  $\mu\text{L}$ . A 10% FA solution was added to the evaporated sample at a ratio of 1:4 (v/v) and further extracted via  $\mu$ -solid phase extraction ( $\mu$ -SPE; please refer to section 2.3.2).

Blood was collected by aspiration. Blood was drawn on ice and immediately centrifuged at  $1500 \times g$  for 15 min at  $0^{\circ}\text{C}$ . Distinct pre-extraction reagents were added to the plasma (section 2.5) and the plasma was stored on ice in low-protein-binding tubes until  $\mu$ -SPE. In contrast to the invasive blood sampling, which needs trained personal for blood collection, human saliva, seminal fluid and urine were furthermore investigated on the presence of the tachykinins but also to screen for potential non-invasive sampling alternatives. Human saliva was obtained using salivettes<sup>®</sup> with biocompatible synthetic swabs (Sarstedt, Nuembrecht, Germany). Following the saliva sampling, the salivettes were centrifuged at  $3200 \times g$  for 10 min at  $0^{\circ}\text{C}$ . The saliva supernatant was mixed with a 10% FA solution at a ratio of 1:1 (v/v), vortexed for 5 min, and stored on ice in low-protein-binding tubes until  $\mu$ -SPE. Fresh human urine was mixed with a 10% FA solution at a ratio of 1:1 (v/v), vortexed for 5 min, and stored on ice in low-protein-binding tubes until  $\mu$ -SPE. Fresh human seminal fluid was mixed with a 0.5% TFA solution at a ratio of 1:2 (w/v) and extracted as described for the porcine brain tissue.

### 5.2.3.2 Micro-solid phase extraction protocol

Before LC-MS/MS analysis, each porcine and human sample was extracted with a customized  $\mu$ -SPE protocol using a hydrophilic-lipophilic balance (HLB) exchanger (Oasis PRiME HLB  $\mu$ elution, Waters, Eschborn, Germany). The HLB sorbent material was conditioned with 300

$\mu\text{L}$  MeOH and equilibrated with 300  $\mu\text{L}$  water fortified with 0.1% FA. Next, 240  $\mu\text{L}$  of each sample was loaded onto the sorbent material, then washed with 300  $\mu\text{L}$  water fortified with 0.1% FA and 190  $\mu\text{L}$  of a water-MeOH mixture (87:13 [v/v]). The peptides were eluted in two steps utilizing 2 x 60  $\mu\text{L}$  of a water-MeOH-FA mixture (10:83:7 [v/v/v]), evaporated to dryness at 60°C and 650 RPM under nitrogen, and reconstituted in 60  $\mu\text{L}$  of the optimized injection solvent composition (45% DMSO, 45% water, 10% FA [v/v/v]) to avoid unspecific peptide adsorption to the deep well plates [159].

### 5.2.3.3 Ethics

Sample collection was conducted following the Declaration of Helsinki. The sampling has been approved by the authors' institutional review committee (ethics commission of the medical faculty, Heinrich Heine University, study number: 2019–705). Written informed consent was obtained from the human volunteer. The porcine brain tissue was acquired as a slaughterhouse byproduct from an animal intended for consumption as food to avoid unnecessary animal euthanization.

### 5.2.4 Plasma extraction recovery studies

Due to the strong and reversible binding of Substance P to plasma proteins [4], which was thought to contribute to low recoveries of Substance P [158], various MS-compatible pre-extraction reagents were added to the plasma before the  $\mu\text{-SPE}$  to cleave possible binding with plasma protein. As one option, the plasma was acidified through the addition of individual acids (FA, PhA, and DCA) at a ratio of 1:1 (v/v) to final concentrations of 5%. As a chaotropic reagent, guanidine (final concentration: 2.5 M) alone [1:3 (v/v)] and in combination with 2.5% sodium deoxycholate and 0.5 M urea [1:1:1:1 (v/v/v/v)] was added to the plasma sample. Each sample was vigorously vortexed for 5 min and stored on ice until  $\mu\text{-SPE}$ . Furthermore, organic extractors (MeOH, acetonitrile or isopropanol) were individually added to the plasma at a ratio of 1:1 (v/v) and vortexed for 5 min, followed by restriction of the organic fraction under nitrogen to avoid breakthroughs of the analytes during  $\mu\text{-SPE}$ . As a control, plasma samples were diluted with water at a ratio of 1:1 (v/v) and were treated identically. Pre-spiked plasma samples (1 ng/mL per peptide) were measured to quantify the impact of the pre-extraction reagents on the recovery of Substance P and human Hemokinin-1. Furthermore, the experiments were performed with non-spiked plasma samples for the determination of

endogenous tachykinins levels. Each experiment was run at least in triplicate. The time from sample preparation to  $\mu$ -SPE was less than one hour.

### 5.2.5 Sample processing studies

The addition of protease inhibitors to the plasma samples and their processing on ice was demonstrated to be essential for the preservation of the peptide integrity of Substance P [128]. Thus, diverse protease inhibitors were investigated for the simultaneous recovery of intact Substance P and human Hemokinin-1, since the metabolic degradational path for human Hemokinin-1 has not yet been described. Based on the most commonly used protease inhibitors for Substance P in biofluids, metalloprotease inhibitors (75 mM EDTA combined with 10 mM phenanthroline), a serine protease inhibitor (140  $\mu$ M AEBSF), and a serine and cysteine protease inhibitor (100  $\mu$ M leupeptin) were spiked alone and in combination into the blood collection devices before blood sampling. This approach ensured the fastest protease inhibition in freshly collected blood.

Unspecific peptide adsorption to the collection material may lead to reduced recoveries of the targeted peptides [159]. Therefore, regular blood sampling by aspiration into monovettes using a butterfly device was compared to a customized blood collection procedure involving passive blood dropping in low-protein-binding tubes utilizing a microneedle device to minimize the contact of the blood with the collection material (Figure 33). Each experiment was run in triplicate and was performed with non-spiked and pre-spiked samples (1 ng/mL per peptide) in the blood collection materials in order to quantify the recoveries of intact endogenous or exogenous Substance P and human Hemokinin-1. Each plasma sample was extracted with the most suitable pre-extractor from the previous experiments (section 5.2.4) and using a  $\mu$ -SPE. For the spiking approach, the best performing inhibitor cocktail was added to both the monovettes and the low-protein-binding tubes before the blood sampling.

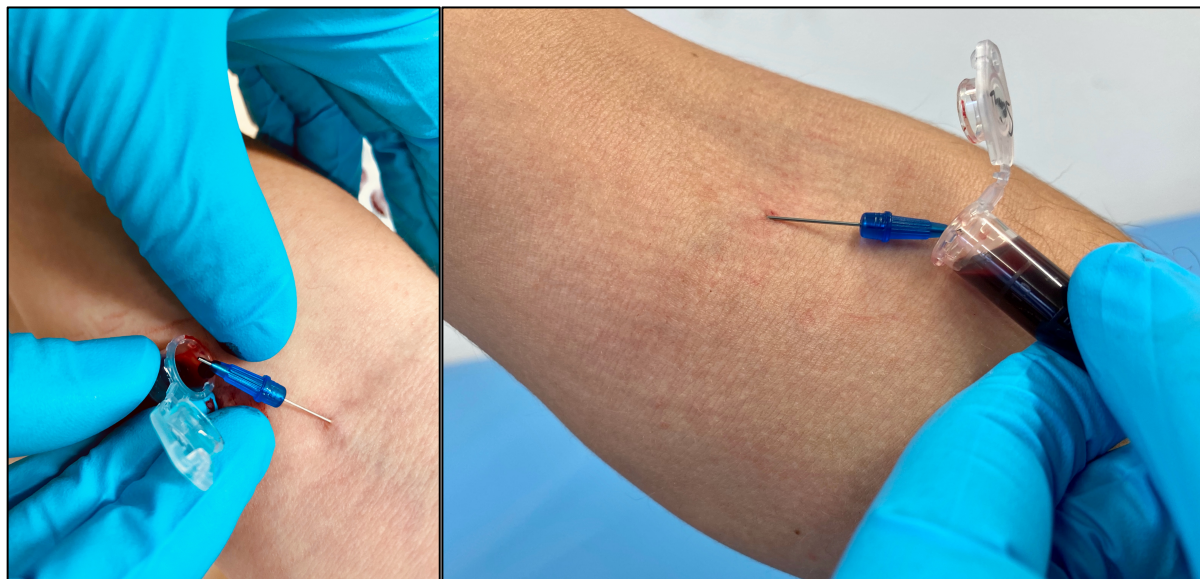


*Figure 33: Customized blood draw in protein low binding tubes using a microneedle to avoid unspecific peptide adsorption to the sampling material.*

### 5.2.6 Comparative immunoassay studies

For the evaluation of diverse sample processing protocols, human plasma samples and porcine brain tissue samples were analyzed in parallel by the LC-MS/MS assay and a commercially available ELISA (DRG Diagnostics; EIA 3120), which was conducted according to the manufacturer's protocol. The used immunoassay was randomly chosen from commercially available immunoassays, which did not have yet described cross-reactivity to human Hemokinin-1 in their data sheets (those, demonstrating cross-reactivity to human Hemokinin-1, were pre-excluded in the selection process). For a better comparison between both assays, Substance P levels measured by the immunoassay are hereafter referred to as “Substance P-like immunoreactivity” (Substance P-LI), as cross-reactivity of the antibody to Substance P analogs or metabolites might affect the results. Various extraction protocols utilizing (1) plasma inhibited with 140  $\mu\text{M}$  AEBSF or (2) plasma inhibited with 140  $\mu\text{M}$  AEBSF, 75 mM EDTA, and 10 mM phenanthroline, collected in both monovettes and low-protein-binding tubes, were evaluated by determining the concentrations of Substance P and human Hemokinin-1 by LC-MS/MS in parallel to the quantification of Substance P-LI by ELISA. All LC-MS/MS samples were extracted by  $\mu\text{-SPE}$ , as plasma extraction was mandatory for LC-MS/MS analysis. Moreover, as various pre-extraction reagents and protease inhibitors (EDTA, FA, phenanthroline, TFA) interfered with the immunoassay, these samples were also extracted utilizing the  $\mu\text{-SPE}$  protocol to remove interfering chemicals and to enable better comparison of the ELISA samples to the samples for LC-MS/MS analysis due to similar sample preparation.

Furthermore, immunoassays were performed with both unextracted and extracted plasma (using  $\mu$ -SPE) to compare the impact of extraction on the recovery of Substance P-LI. Additionally, porcine brain tissue samples and human plasma samples were extracted using the TFA protocol described (section 2.3) and quantified using both analytical assays. The experiments were performed at least in triplicate with non-spiked biosamples.

### 5.2.7 Cross-reactivity studies

As no cross-reactivity data for the investigated tachykinins were available for the immunoassay used, Substance P, its carboxylic acid and human Hemokinin-1 were analyzed by ELISA. Thus, 1 ng/mL solutions of Substance P, its carboxylic acid and human Hemokinin-1 were prepared in the assay buffer in low-protein-binding tubes and quantified by ELISA at least in triplicate according to the manufacturer's protocol.

### 5.2.8 Compound discovery by a hybrid immunoaffinity–LC-MS approach

For the compound discovery of Substance P-LI in human blood plasma, a hybrid immunoaffinity–high-resolution (HR)-MS approach was developed. Thus, 100  $\mu$ L fresh blood plasma inhibited with 140  $\mu$ M AEBSF was loaded into the ELISA wells, captured by the coated antibodies, and incubated at 500 rpm for 90 min at 20°C. After incubation, the wells were washed three times with 250  $\mu$ L phosphate-buffered saline–Tween 20 buffer (0.01% Tween 20). The samples for intact protein analysis were afterward reconstituted in 75  $\mu$ L of the injection solvent (45% DMSO/45% water/10% FA [v/v/v]), whereas the samples for tryptic digestion were reconstituted in 100  $\mu$ L 0.1% TFA solution, neutralized with 5  $\mu$ L ABC-buffer (800 mM), and transferred onto a plate with 1  $\mu$ g trypsin. Protein digestion was conducted through the addition of 100  $\mu$ L 62% acetonitrile and 38% ABC buffer [v/v] for 60 min at 37°C, as described by Burdman et al. [160]. Following evaporation of the solvent (60°C, 650 rpm, under nitrogen), the residue was reconstituted in 75  $\mu$ L of the injection solvent. As a control, 100  $\mu$ L fresh plasma without inhibitors that had been incubated for 20 min at 40°C to generate reference samples and 100  $\mu$ L assay buffer (blank) were treated analogously and measured by LC-HR-MS. Each sample was conducted in biological triplicate.

BiopharmaView® (version 3.0.2, SCIEX, Darmstadt, Germany) was used for the in-silico simulation of intact protein analysis and evaluation of the tryptic digestion. As the structure of Substance P-LI was unknown, but expected to be related to Substance P or human Hemokinin-

1, the simulation was conducted based on possible metabolites of the protachykinin-1 and protachykinin-4 amino acid sequences listed in the UniProt® database (entry numbers P20366 [TKN1\_HUMAN] and Q86UU9 [TKN4\_HUMAN]). The assay information was constructed in BiopharmaView, setting the digest agent as trypsin and allowing zero missed cleavages. By adjusting the processing setting to a mass-to-charge tolerance of 10 ppm, extracted ion chromatogram (XIC) was set to 0.025 ppm and MS/MS matching tolerance was adjusted to 0.05 Da, as recommended in the literature [98].

## 5.2.9 Instrumentation

### 5.2.9.1 Peptide quantification by LC-MS/MS analysis

Recovery studies and peptide quantification were performed on an ultra-high-performance liquid chromatography system (Agilent 1200 SL series binary pump system, Waldbronn, Germany) coupled to a tandem mass spectrometer (SCIEX API 4000). Peptide separation was achieved using a Waters XSelect Peptide CSH column (130 Å, 3.5 µm, 2.1 x 150 mm). Sample handling and injection were executed by a CTC Analytics HTC PAL system (Zwingen, Switzerland). A validated LC-MS/MS method was used for the quantification of Substance P, its carboxylic acid and human Hemokinin-1, as previously published [156]. Using the sensitive and validated method, limits of detection of 5.8 pg/mL for Substance P, 6.2 pg/mL for its carboxylic acid and 5.3 pg/mL for human Hemokinin-1 were achieved, which were principally suitable for the quantification of reported tachykinin levels in human plasma, which were quantified by immunoassays. Matrix effects due to plasma proteins were investigated and minimized during method development. Workflows for the used MS assays are presented in Figure 34.

### 5.2.9.2 Compound elucidation by LC-HR-MS/MS analysis

Compound elucidation and analyte identification were achieved on an ultra-high-performance liquid chromatography system (Shimadzu Nexera, Duisburg, Germany) coupled to a quadrupole time of flight high-resolution mass spectrometer (HR-MS; SCIEX TripleTOF 6600). Samples were injected in full loop mode (40-µL injection volume). Peptide separation was executed on a Phenomenex Kinetex C18 (100 Å, 1.7 µm, 2.1 x 100 mm) at an oven

temperature of 60°C using a gradient of mobile phase A (water:DMSO:FA, 98.9:1:0.1, v/v/v) and mobile phase B (MeOH:DMSO:FA, 98.9:1:0.1, v/v/v). The gradient started with 5% of mobile phase B for 3 min and was increased to 25% mobile phase B from 3 to 5.5 min. This was followed by a further change to 98% mobile phase B within the next 2 min. The gradient was kept at 98% mobile phase B for another 3 min before being reduced to 5% of mobile phase B again. The total runtime from injection to injection was 14 min. The flow rate was set to 300  $\mu$ L/min. Analyte detection was performed in positive mode, utilizing electro spray ionization. Nitrogen was used as the collision and curtain gas. Curtain gas was set to 40 psi, nebulizer gas to 40 psi, heater gas to 70 psi, and ion spray voltage to 5500 V. The temperature in the ion source was held at 425°C. The qualitative profiling of the compounds of interest was conducted using a sequential window acquisition of all theoretical fragment ion spectra MS (SWATH®). For the data-independent acquisition experiments, the scan range was set from 400 m/z to 1500 m/z for the digested peptides with 34 independent windows and from 300–20,000 m/z for intact protein analysis. Workflows for the used MS assays are presented in Figure 34.

### 5.2.9.3 Data analysis

Data acquisition and evaluation were accomplished using Analyst© (SCIEX, version 1.6.2 and TF 1.7.1) and Multiquant© (SCIEX, version 3.0.2). MS/MS spectra for structure identification were analyzed using the Bio Tool Kit of PeakView© (SCIEX, version 2.2).

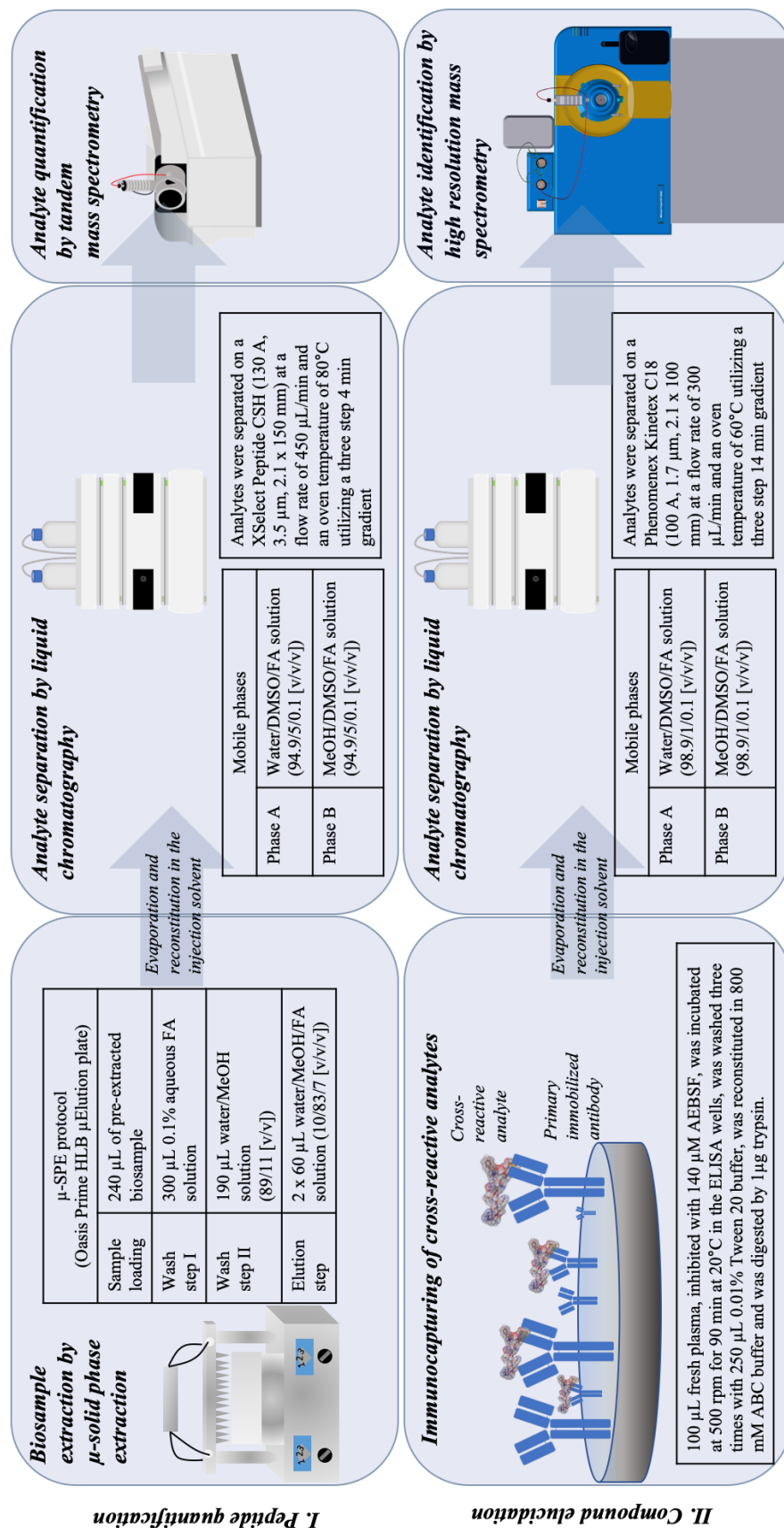


Figure 34: Workflow of the used mass spectrometry methods for peptide quantification applying triple quadrupole mass spectrometry and for compound elucidaion by using high-resolution mass spectrometry.

(ABC: ammonium bicarbonate; AEBSF: 4-(2-Aminoethyl)benzenesulfonyl fluoride; FA: formic acid; DMSO: dimethyl sulfoxide; MeOH: methanol)

## 5.3 Results

### 5.3.1 Plasma extraction recovery studies

Whereas full recoveries were observed in aqueous solutions spiked with the peptides, in the spiked plasma samples, low recoveries of both peptides (mean recovery  $\pm$  standard deviation [SD]: 30.2%  $\pm$  4.3% for Substance P; 29.6%  $\pm$  1.7% for human Hemokinin-1;  $n = 3$ ) were achieved without the addition of an acidic, organic, or chaotropic reagent prior to  $\mu$ -SPE (Figure 35), indicating the need for an appropriate pre-extractor. High recoveries of Substance P and human Hemokinin-1 were observed with plasma acidification with 5% PhA (mean  $\pm$  SD: 86.0%  $\pm$  14.3% for Substance P; 71.4%  $\pm$  8.9% for human Hemokinin-1) and 5% FA (mean  $\pm$  SD: 88.0%  $\pm$  8.3% for Substance P; 73.6%  $\pm$  3.2% for human Hemokinin-1;  $n = 3$ ). High recoveries for both peptides were also accomplished with the addition of the organic extractors' acetonitrile, MeOH, or isopropanol (mean recoveries: 77.1%–87.3% for Substance P; 73.1%–76.3% for human Hemokinin-1;  $n = 3$ ). In contrast, basic extraction utilizing 2.5 M guanidine or its combination with sodium deoxycholate and urea led to substantially lower recoveries (mean recoveries: 28.9%–58.1% for Substance P; 24.3%–38.0% for human Hemokinin-1;  $n = 3$ ). An optimal recovery for both peptides was achieved using either the acidic extraction with 5% FA or the organic extraction utilizing isopropanol (1:1 [v/v]), which yielded equivalent results. As nonspecific peptide adsorption of Substance P and human Hemokinin-1 complicated the sensitive determination of both peptides and sample evaporation could be associated with pronounced adsorption effects [159], further experiments were performed using FA-extracted samples to avoid the additional evaporation step before the  $\mu$ -SPE utilizing isopropanol. Despite high recoveries of spiked peptides utilizing acidic and organic modifiers, signals of endogenous Substance P nor human Hemokinin-1 were under the limits of detection in the non-spiked extracted plasma samples by LC-MS/MS.

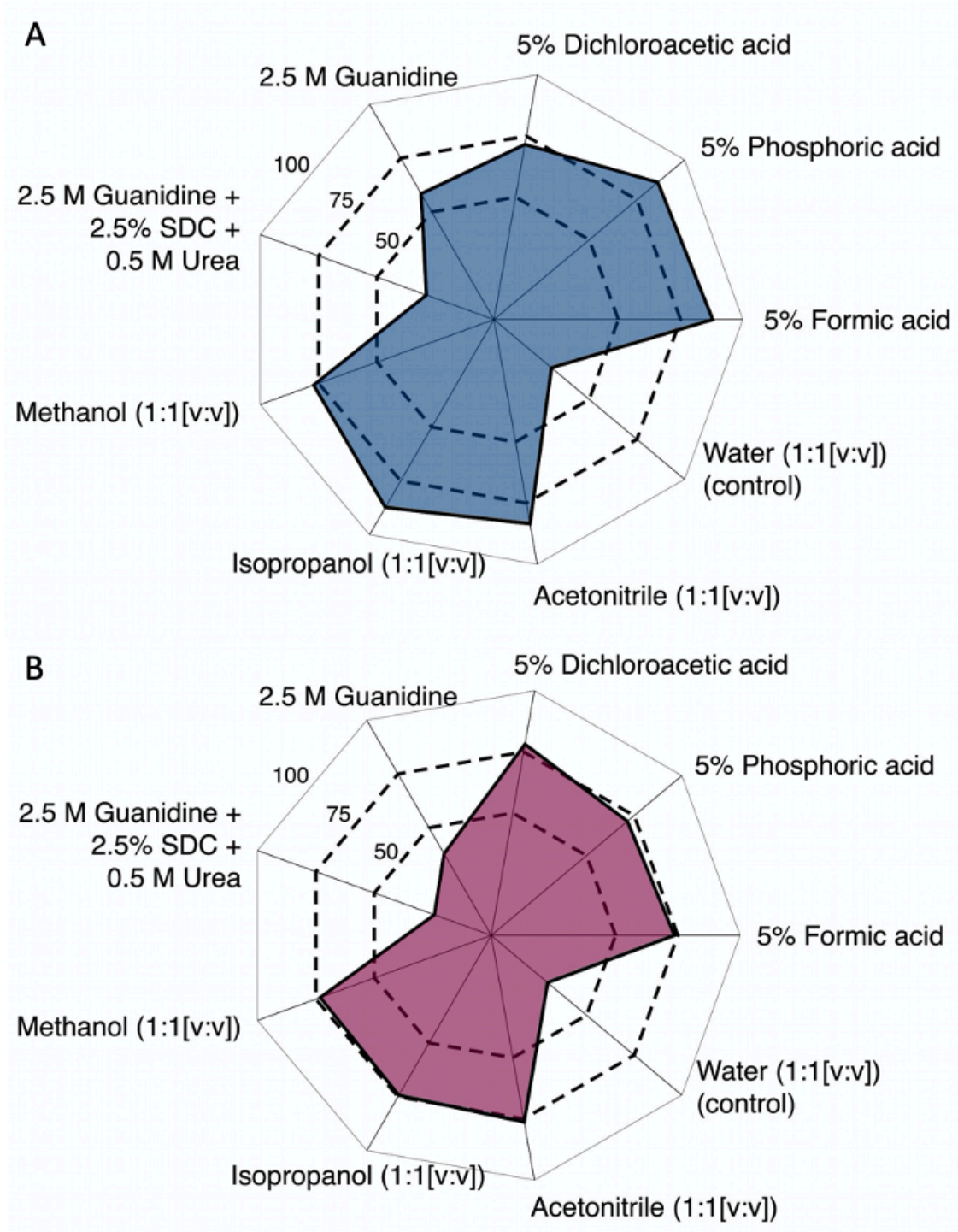


Figure 35: Polar charts indicating the mean plasma extraction recovery rates of spiked Substance P and human Hemokinin-1.

Distinct pre-extraction reagents were added to the plasma samples spiked with Substance P (blue) and human Hemokinin-1 (red) before the  $\mu$ -solid-phase extraction [mean recoveries;  $n = 3$ ].

### 5.3.2 Sample processing studies

As a fast metabolic degradation of Substance P was described in plasma samples (-50% recovery within one hour) [128] and assumed for human Hemokinin-1 due to their similar amino acid structures, different protease inhibitor classes were investigated (Figure 36). Without the addition of inhibitors to the sampling material, a substantially reduced recovery of intact Substance P and human Hemokinin-1 was observed within the analysis time of approximately 1 h (mean  $\pm$  SD: 37.4%  $\pm$  8.7% for Substance P; 25.5%  $\pm$  8.8% for human Hemokinin-1; n = 3). Hence, by adding a metalloprotease inhibitor cocktail (EDTA + phenanthroline) to the collection material, higher recoveries were achieved (mean  $\pm$  SD: 49.2%  $\pm$  2.7% for Substance P; 49.7%  $\pm$  4.3% for human Hemokinin-1; n = 3). The use of a serine protease inhibitor (AEBSF) was associated with higher recoveries of intact Substance P (mean  $\pm$  SD: 57.4%  $\pm$  11.2%; n = 3), but led to low recoveries for human Hemokinin-1 (mean  $\pm$  SD: 25.6%  $\pm$  4.1%; n = 3), similar to the absence of protease inhibitors. The addition of leupeptin as a cysteine and serine protease inhibitor resulted in profoundly low recoveries for intact Substance P and human Hemokinin-1 (mean  $\pm$  SD: 3.6%  $\pm$  1.8% for Substance P; 29.0%  $\pm$  11.6% for human Hemokinin-1; n = 3), which were even lower than obtained in the absence of protease inhibitors for Substance P. By combining the protease inhibitors investigated (AEBSF, EDTA, leupeptin, and phenanthroline), mean recoveries of 35.1%  $\pm$  2.2% for Substance P and 37.8%  $\pm$  2.4% for human Hemokinin-1 were observed (n = 3). As the addition of leupeptin led to unexpected losses of Substance P, the combination of AEBSF, EDTA, and phenanthroline was further tested, resulting in higher recoveries (mean  $\pm$  SD: 72.4%  $\pm$  5.0% for Substance P; 57.9%  $\pm$  8.0% for human Hemokinin-1; n = 3). The best performing inhibitor cocktail was added to protein low-protein-binding tubes, which were used to collect blood to minimize possible peptide adsorption effects. Subsequently, using AEBSF, EDTA, and phenanthroline as a protease inhibitor cocktail, suitable recoveries were realized (mean  $\pm$  SD: 102.8%  $\pm$  8.3% for Substance P; 100.9%  $\pm$  3.8% for human Hemokinin-1; n = 3).

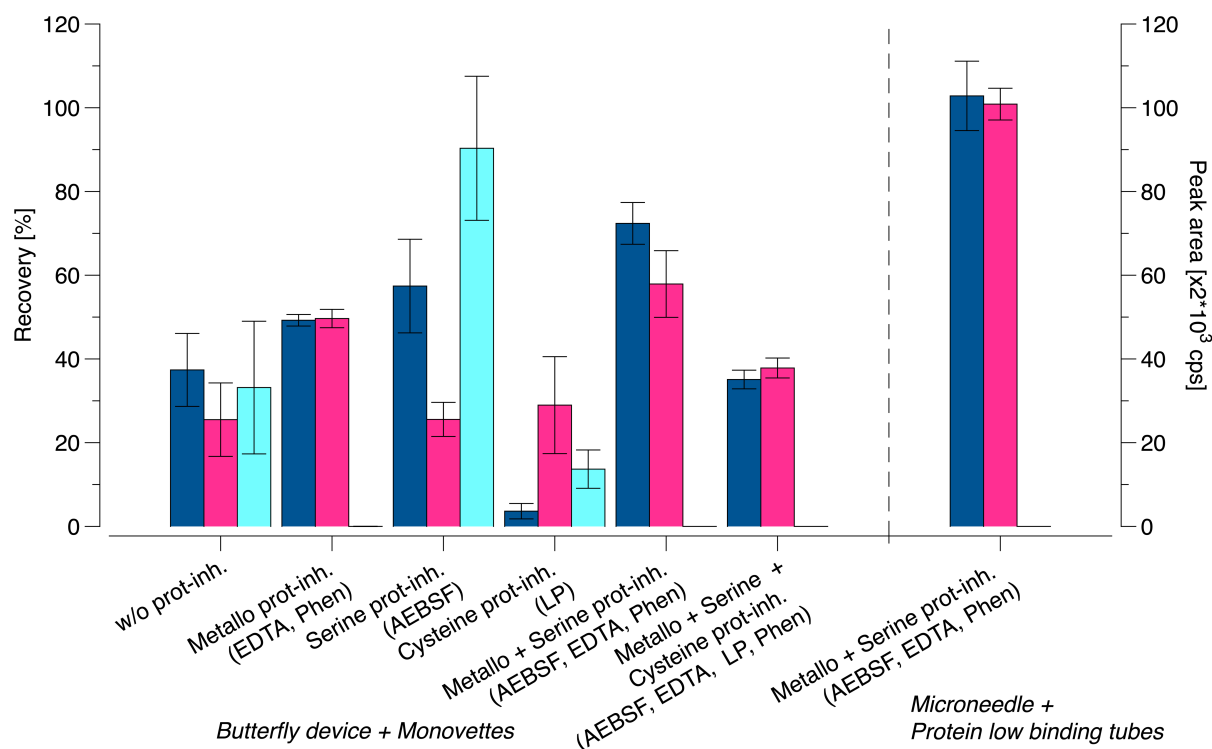


Figure 36: Impact of different protease inhibitor classes and sampling devices on the mean recovery rates of Substance P and human Hemokinin-1.

The recoveries of Substance P (blue) and human Hemokinin-1 (red), which were spiked to the blood collection material before blood sampling, were monitored. Without the addition of metalloprotease inhibitors, an interfering substance was observed (observed peak area (light blue)) [mean  $\pm$  SD;  $n = 3$ ]. (AEBSF: 4-(2-Aminoethyl)benzenesulfonyl fluoride; cps: counts per second; EDTA: ethylene diamine tera acetic acid; LP: leupeptin; Phen: phenanthroline; Prot-inh: Protease inhibitor; w/o: without)

### 5.3.3 Protocol evaluation in human biofluids and porcine brain tissue

The best performing sample processing protocol from previous experiments was evaluated for its use for human biofluids and porcine brain tissue. Utilizing an acidic extraction with FA before  $\mu$ -SPE and plasma inhibited with AEBSF, EDTA and phenanthroline, 125 pg/mL of Substance P, its carboxylic acid and human Hemokinin-1 spiked to the collection material could be accurately separated and quantified by LC-MS/MS analysis (Figure 37-A).

Next, endogenous levels were measured in human samples. The biologically active Substance P was measured in human acidified (5% FA) saliva (mean  $\pm$  SD: 153.1  $\pm$  90.5 pg/mL;  $n = 3$ ; Figure 37-C). No Substance P was observed in acidified (5% FA) urine samples (Figure 37-D)

using the same protocol, while, biologically active Substance P was measured in human seminal fluid (mean  $\pm$  SD:  $700.9 \pm 195.1$  pg/g;  $n = 3$ ; Figure 37-E). The extraction of the porcine brain tissue resulted in the quantification of  $6.07 \pm 0.71$  ng/g active Substance P by LC-MS/MS analysis (two independent experiments;  $n = 3$ ; Figure 37-F). However, no biologically active Substance P and human Hemokinin-1 were found in human acidified (5% FA) plasma by LC-MS/MS analysis by the given LOD of the LC-MS/MS analysis; instead, the biologically inactive carboxylic acid of Substance P was quantified (mean  $\pm$  SD:  $151.8 \pm 12.3$  pg/mL;  $n = 3$ ; Figure 37-B). Meanwhile, human Hemokinin-1 could not be detected in any of the investigated non-spiked samples.

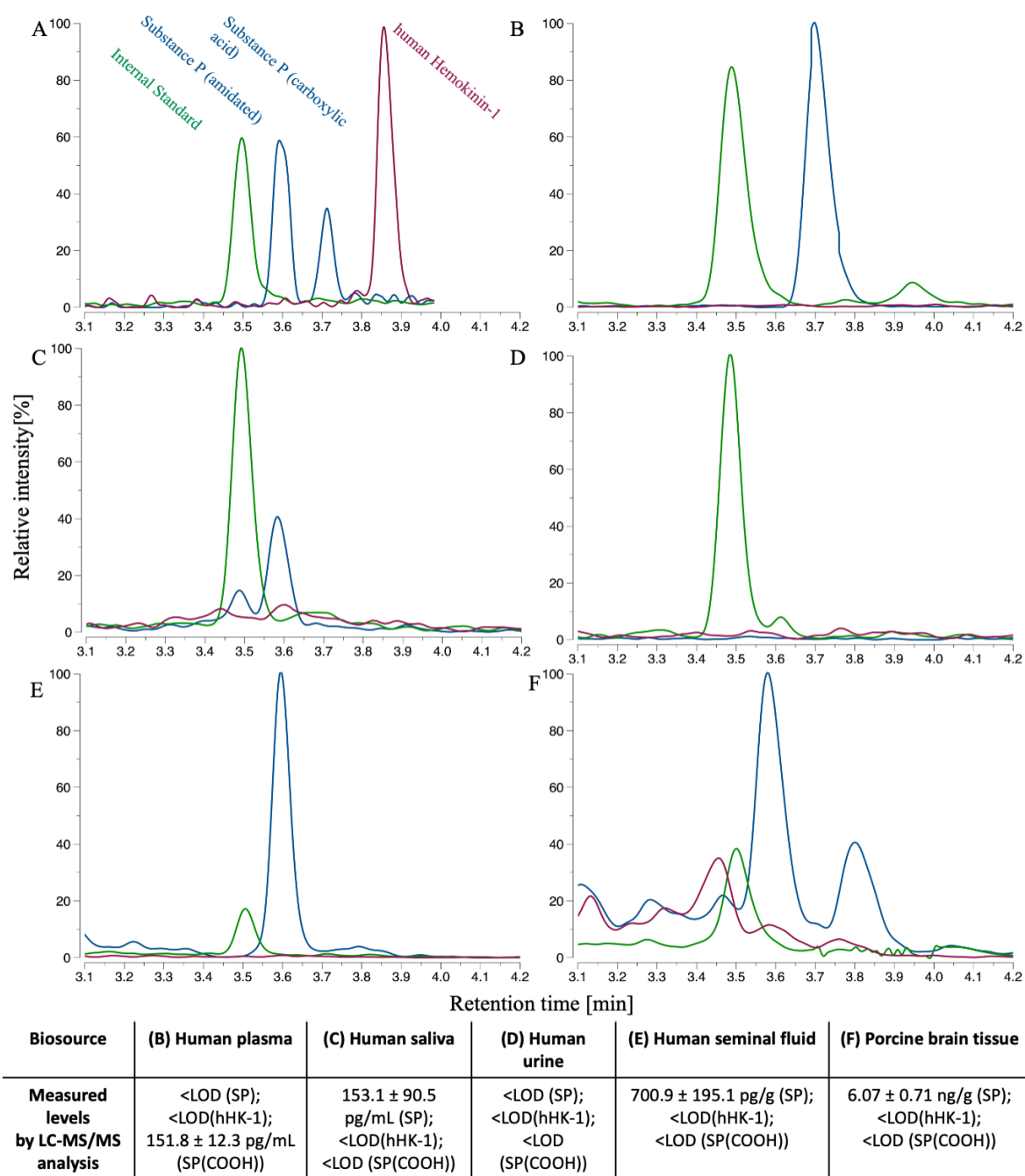


Figure 37: Representative chromatograms and measured levels of the neuropeptides in different biofluids and tissues.

Amidated (bioactive) Substance P (SP) (retention time: 3.6 min), the carboxylic acid of Substance P (SPCOOH) (retention time: 3.7 min) (both blue), human Hemokinin-1 (hHK-1) (red) and (Sar9)-Substance P as the internal standard (green) were analyzed in (A) human plasma spiked with 125 pg/mL of each peptide, (B) non-spiked human plasma, (C) human saliva, (D) human urine (E) human seminal fluid and (F) porcine brain tissue (LC-MS/MS: liquid chromatography coupled to tandem mass spectrometry; LOD: limit of detection [mean ± standard deviation, at least  $n = 3$ ])

### 5.3.4 Comparative immunoassay studies

For the further evaluation of the sample processing protocols, human plasma samples and porcine brain tissue were comparatively analyzed using both the MS assay and ELISA (Table 7). Using unextracted plasma inhibited with AEBSF, a Substance P-LI concentration of  $240.6 \pm 22.3$  pg/mL was measured by ELISA (mean  $\pm$  SD;  $n = 3$ ). The addition of AEBSF, EDTA, and phenanthroline to the monovettes resulted in a lack of enzyme reaction of the ELISA on unextracted plasma, likely due to a lack of activity of the alkaline phosphatase conjugate, which is dependent on the presence of  $Mg^{2+}$  and  $Zn^{2+}$  ions. The analysis of AEBSF-treated, acidified (5% FA), and extracted ( $\mu$ -SPE) plasma, revealed a mean concentration of  $50.2 \pm 29.4$  pg/mL Substance P-LI (mean  $\pm$  SD;  $n = 3$ ) by ELISA. In contrast, mean levels of  $95.4 \pm 17.4$  pg/mL of the carboxylic acid of Substance P and no signals for active Substance P and human Hemokinin-1 were detected by LC-MS/MS analysis when using monovettes for blood collection (mean  $\pm$  SD;  $n = 3$ ). With the identical inhibitors and extraction procedure, using low-protein-binding tubes as collection material instead, a  $51.2 \pm 10.5$  pg/mL concentration of Substance P-LI was quantified by ELISA and  $151.8 \pm 12.3$  pg/mL of the carboxylic acid of Substance P was measured by LC-MS/MS. Using FA-SPE-extracted plasma inhibited with AEBSF, EDTA, and phenanthroline,  $194.4 \pm 5.1$  pg/mL (monovettes) and  $175.3 \pm 40.0$  pg/mL (low-protein-binding tubes) Substance P-LI were measured (mean  $\pm$  SD;  $n = 3$ ), while no detectable signals were observed for Substance P, its carboxylic acid, or human Hemokinin-1 by LC-MS/MS analysis. Using the same protease inhibitor mix spiked into monovettes, by following the 0.5% TFA-extraction protocol instead, similar levels of Substance P-LI were quantified by ELISA (mean  $\pm$  SD:  $200.4 \pm 13.3$  pg/mL;  $n = 3$ ), whereas no MS signals were detected for Substance P, its carboxylic acid and human Hemokinin-1 in human plasma. By comparing TFA-extracted porcine brain tissue,  $6.81 \pm 0.87$  ng/g Substance P-LI (mean  $\pm$  SD;  $n = 3$ ) was quantified by ELISA, similar to the porcine brain tissue levels ( $6.07 \pm 0.71$  ng/g Substance P) determined by LC-MS/MS.

Table 7: Comparative studies between the enzyme-linked immunosorbent assay and the mass spectrometric assay using various sample processing protocols.

Utilized sample processing protocol	ELISA results	MS results
Unextracted human plasma inhibited with AEBSF	240.6 ± 22.3 pg/mL (SP-LI)	- <sup>1</sup>
Unextracted human plasma inhibited with AEBSF, EDTA, phenanthroline	no enzyme reaction	- <sup>1</sup>
FA-Extracted human plasma inhibited with AEBSF (monovettes)	50.2 ± 29.4 pg/mL (SP-LI)	< LOD (SP); < LOD (hHK-1); 95.4 ± 17.4 pg/mL (SP(COOH))
FA-Extracted human plasma inhibited with AEBSF (protein low binding tubes)	51.2 ± 10.5 pg/mL (SP-LI)	< LOD (SP); < LOD (hHK-1); 151.8 ± 12.3 pg/mL (SP(COOH))
FA-Extracted human plasma inhibited with AEBSF, EDTA, phenanthroline (monovettes)	194.4 ± 5.1 pg/mL (SP-LI)	< LOD (SP); < LOD (hHK-1); < LOD (SP(COOH))
FA-Extracted human plasma inhibited with AEBSF, EDTA, phenanthroline (protein low binding tubes)	175.3 ± 40.0 pg/mL (SP-LI)	< LOD (SP); < LOD (hHK-1); < LOD (SP(COOH))
TFA-Extracted human plasma inhibited with AEBSF, EDTA, phenanthroline	200.4 ± 13.3 pg/mL (SP-LI)	< LOD (SP); < LOD (hHK-1); < LOD (SP(COOH))
TFA-Extracted porcine brain tissue	6.81 ± 0.87 ng/g (SP-LI)	6.07 ± 0.71 ng/g (SP)

(AEBSF: 4-(2-Aminoethyl)benzenesulfonyl fluoride; EDTA: ethylene diamine tetraamine acetic acid; ELISA: enzyme-linked immunosorbent assay; FA: formic acid; hHK-1: human Hemokinin-1; LOD: limit of detection; MS: mass spectrometry; SP: Substance P; SP(COOH): Substance P (carboxylic acid); SP-LI: Substance P-like immunoreactivity; TFA: trifluoroacetic acid) [mean ± standard deviation; at least n = 3] <sup>1</sup>Plasma extraction was mandatory for MS analysis

### 5.3.5 Cross-reactivity studies

As the carboxylic acid of Substance P may have contributed to the observed discrepancy between the ELISA and LC-MS/MS analyses, the cross-reactivity with human Hemokinin-1

and the carboxylic acid of Substance P was tested for the ELISA kit used. The MS standard of Substance P (Sigma-Aldrich) was used as the positive control, resulting in an observed cross-reactivity of 99.2% (n = 3). As expected from results using kits by other ELISA manufacturers, a cross-reactivity of 104.4% was found for human Hemokinin-1 (n = 6). Despite the high structural similarity of the carboxylic acid of Substance P to its biologically active form, no cross-reactivity was observed for the carboxylic acid of Substance P (0%; n = 3), with the ELISA kit used in this study (EIA 3120).

### 5.3.6 Compound discovery by LC-HR-MS/MS analysis

#### 5.3.6.1 Confirmation of the carboxylic acid of Substance P

During the sample processing experiments (section 3.2), an interfering substance was observed. It had the same multiple reaction monitoring transitions as Substance P (674.3 m/z to 600.6 m/z and 674.3 m/z to 254.3 m/z) but appeared at a different chromatographic retention time (3.6 min for Substance P and 3.7 min for the interfering substance). Signals of the observed substance observed were more pronounced with the addition of AEBSF compared to the absence of protease inhibitors (mean peak areas: 180.633 counts per second [cps] vs. 66.330 cps; n = 3). When metalloprotease inhibitors (EDTA + phenanthroline) were added to the collection material, no interfering substance was detected (Figure 35 – light blue bars).

For the elucidation of the compound structure of the interfering substance, which was expected to be the carboxylic acid of Substance P, plasma samples with the protease-inhibitor mixes investigated were analyzed by HR-MS. In plasma samples spiked with AEBSF and without protease inhibitors, the precursor ion of the interfering substance was identified as a two-fold positively charged ion of 674.8567 m/z by a time of flight scan (Figure 38-B). Its peptide fragment pattern by MS/MS scan was similar to spiked Substance P but was distinguished by a distinct precursor ion of Substance P (674.3649 m/z; Figure 38-A). Due to its precursor mass-to-charge ratio and its fragmentation pattern, the interfering substance matched the MS/MS signal of the carboxylic acid of Substance P calculated by the Bio Tool Kit of PeakView (mass error: 0.0043 Da).

### 5.3.6.2 Compound discovery of immunoreactive Substance P in plasma

As the carboxylic acid did not show cross-reactivity, a hybrid immunoaffinity LC-HRMS approach involving a bottom-up and top-down approach was used for the identification of Substance P-LI. For the top-down approach, the total ion counts (TICs) of the protease-inhibited plasma samples were compared to the TICs of the incubated (blank) plasma sample to reveal any differences in the intact protein analysis. The TICs of the protease-inhibited samples demonstrated one additional signal at 8.17 min retention time, which was further investigated (Figure 39-A). The MS spectra of the peak revealed a 4-fold charged protein with an average precursor mass of 6243.42 Da (Figure 39-B). The MS/MS fragmentation of this protein by SWATH analysis showed three dominant signals of 464.2486 m/z, 614.2251 m/z, and 745.3363 m/z (Figure 39-C). The MS and subsequent MS/MS signals found were aligned to possible precursors and metabolites of Substance P and human Hemokinin-1, resulting in a possible match to an acetylated precursor of Substance P (20. – 70. amino acid of UniProtKB - P20366 [TKN1\_HUMAN]; Figure 39-D). For verification, the protease-inhibited samples were digested with trypsin in a bottom-up approach, which led to three fragmented peptides depicted by in silico digestion (Figure 39-E). Two of these were found in the HR-MS analysis, resulting in a coverage of 70.4%. The peptides identified were confirmed by MS/MS analysis, indicated by several  $b^+$  and  $y^+$  fragments (Figure 39-F).

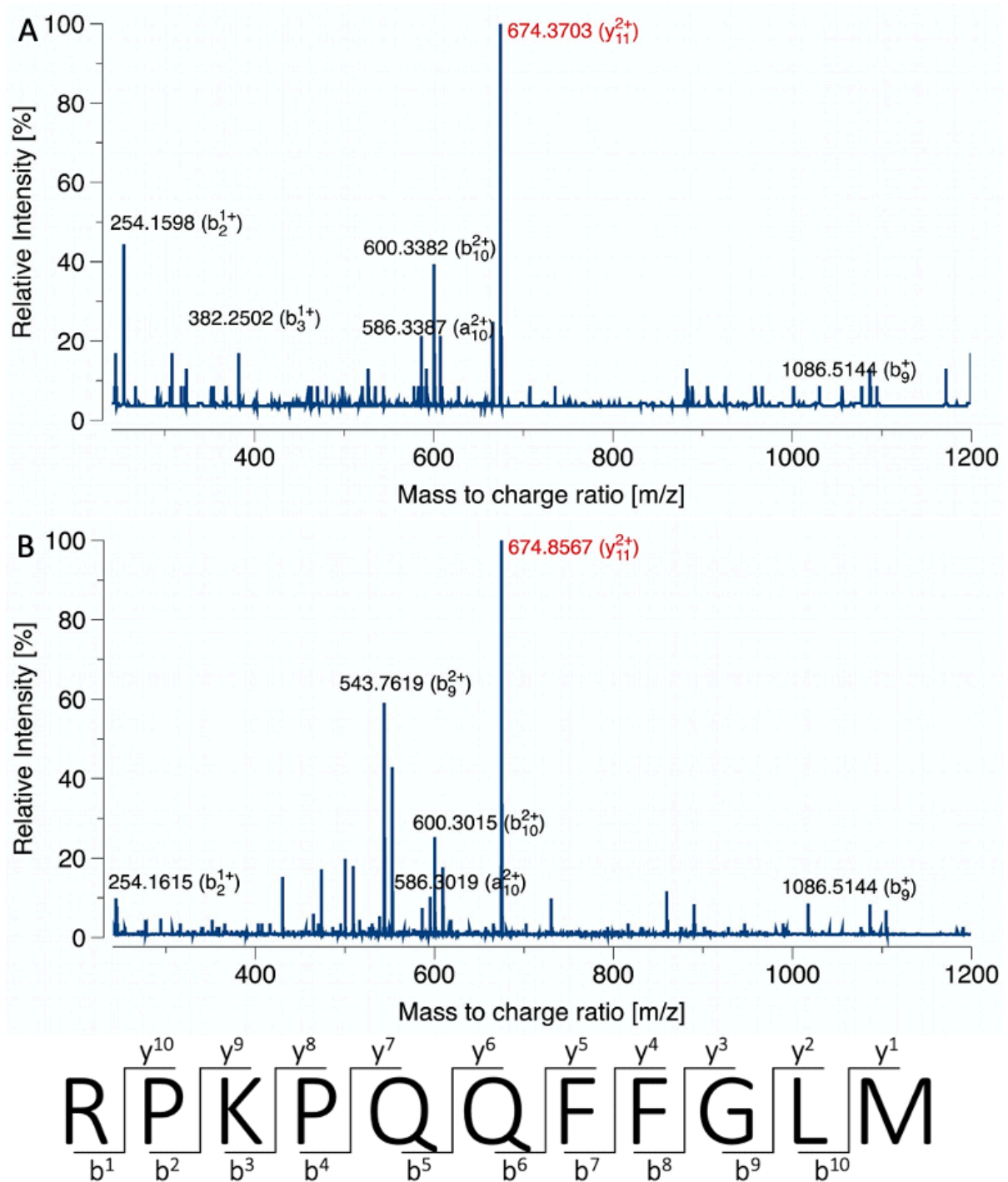


Figure 38: High-resolution MS/MS spectra of spiked Substance P in human plasma and the interfering substance.

(A) Precursor ion and fragmentation pattern of Substance P to plasma. (B) The interfering substance demonstrated a similar fragmentation pattern as Substance P, but the precursor ion was different to spiked Substance P (both shown in red). Using the Bio tool kit of PeakView® the interfering substance was identified as the carboxylic acid of Substance P in human plasma. The fragmentation pattern of Substance P is shown in the one-letter amino acid code.

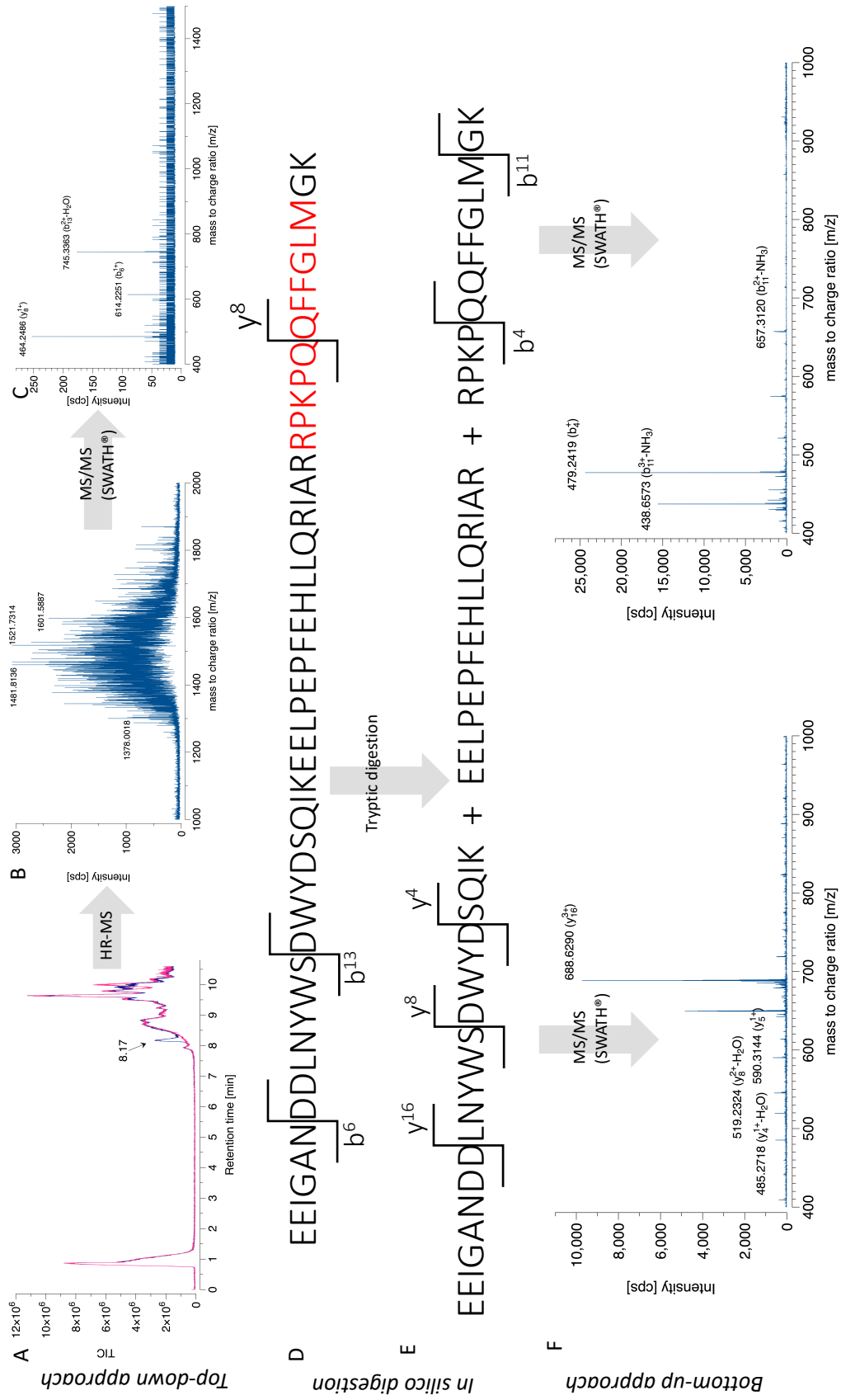


Figure 39: Workflow and results of the protein characterization by immunocapture-LC-HR-MS/MS approach

(see next page for further information)

*(A) Representative, overlaid total ion counts (TIC) of the protease-inhibited sample (blue) showing an additional peak at the retention time of 8.17 min compared to the blank sample incubated at 40°C (red); (B) HR-MS spectra of the found protein at the retention time of 8.17 min; (C) HR-MS/MS spectra of the CID-fragmented protein (SWATH® scan); (D) Amino acid structure of the precursor of Substance P in the one-letter code, which matched the MS/MS data of the found protein [Substance P is shown in red]; (E) In silico digestion by trypsin, (F) After tryptic digestion, two digested peptides were found in HR-MS/MS spectra; (cps: counts per second; CID: collision induced dissociation; LC-HR-MS/MS: liquid chromatography coupled to high-resolution tandem mass spectrometry)*

## 5.4 Discussion

As the former determinations of Substance P in human plasma were affected by the cross-reactivity of the applied immunoassays, a suitable sample processing protocol for the selective quantification of Substance P and its related human tachykinins by LC-MS/MS should be established in the here-presented studies. Using a recently developed validated LC-MS/MS assay, plasma sample processing was comprehensively investigated, covering the entire workflow from blood collection to final sample preparation for LC-MS/MS, thereby achieving the complete recovery of intact Substance P and human Hemokinin-1 in spiked human plasma. While endogenous Substance P concentrations were measured in human saliva and seminal fluid and porcine brain tissue, the active form was not detectable in endogenous human plasma. Instead, the inactive carboxylic acid of SP was previously reported and confirmed in human plasma samples by LC-MS/MS analysis. Remarkably, the evaluation of endogenous levels in plasma via ELISA found a high variance in Substance P-LI concentrations (50.2–240.6 pg/mL). These different results from the two methods used were followed by a compound discovery using a hybrid approach to identify the substance captured in the immunoassay.

Since metabolic degradation and plasma protein binding severely affect the integrity of tachykinins, leading to their loss during sample processing, a special focus was placed on developing a suitable sample processing protocol [4,128]. Both plasma acidification and precipitation by organic extractors were associated with high recoveries of spiked Substance P ( $\geq 72\%$ ) and human Hemokinin-1 ( $\geq 71\%$ ), leading to full recovery if unspecific absorption was further controlled by using low-protein-binding material. Furthermore, the main degradation path of Substance P described in the literature suggests the addition of a combination of metalloprotease and serine inhibitors, which was in line with the findings on Substance P

presented here [128]. Unlike Substance P, no degrading enzymes have yet been described for human Hemokinin-1 in biosamples. However, the results demonstrate that the addition of metalloproteases seemed to be more efficient than the addition of serine protease inhibitors in preserving the peptide integrity of the tachykinin human Hemokinin-1.

When endogenous biofluids and tissues were investigated, Substance P was successfully detected in porcine brain tissue by LC-MS/MS ( $6.07 \pm 0.71$  ng/g). The results obtained were confirmed by the commercial ELISA ( $6.81 \pm 0.87$  ng/g). Active Substance P was quantified in lower levels, as previously reported for Substance P in mouse brain tissue (185.1–348.2 ng/g) [161,162], likely due to degradation of the intact peptide during the slaughtering process (within 20 min). Substance P concentrations in human saliva and seminal fluid were determined by LC-MS/MS for the first time, and the levels obtained for saliva were in line with reported Substance P-LI concentrations determined by immunoassay ( $153 \pm 91$  pg/mL [LC-MS/MS] vs.  $235 \pm 137$  pg/mL [ELISA]) [150]. No Substance P levels were observed in urine, which could be based on a dilution effect with the need of an even more sensitive method.

Although Substance P-LI concentrations in human plasma were quantified by ELISA, this finding was not confirmed by LC-MS/MS. As only biased values of Substance P levels in human plasma were reported due to the possible cross-reactivity, the true concentrations of Substance P and human Hemokinin-1 might be present in femtomolar ranges and so might be even under the LOD of the here-presented highly optimized LC-MS/MS assay and consequently needs a more sensitive bioanalytical assay. Instead, the unknown compound detected in the chromatogram was identified as a carboxylic acid of Substance P via downstream HR-MS analysis. The results of the experiments conducted suggested the possible degradation of the carboxylic acid of Substance P by serine proteases. Moreover, no carboxylic acid of Substance P was quantified in samples spiked with EDTA and/or phenanthroline, suggesting that an artificial *ex vivo* generation of the carboxylic acid of Substance P by a metalloprotease may have occurred.

Remarkably, the carboxylic acid of Substance P did not show cross-reactivity in the immunoassay and did not contribute to the discrepancy in concentrations between ELISA and mass spectrometric analysis. As human Hemokinin-1 demonstrated a cross-reactivity of 100%, the antibodies of the immunoassay used seem to bind to the C-terminal portion of active Substance P. Binding to the carboxylic acid of Substance P was not observed, likely due to the

negative charge of the carboxylic acid in the neutral buffered ELISA protocol, which would impede the generation of hydrogen bonds. Concentrations of the carboxylic acid of Substance P in human plasma measured by LC-MS/MS were dependent on the collection material used, indicating that the use of low-protein-binding tubes was favorable for higher recoveries of the carboxylic acid of Substance P from blood plasma (151.8 pg/mL [low-protein-binding tubes] vs. 95.4 pg/mL [monovettes]). In contrast, Substance P-LI concentrations analyzed by the ELISA were not affected by the collection material used (51.2 pg/mL [low-protein-binding tubes] vs. 50.2 pg/mL [monovettes]). This different behavior in the context of nonspecific peptide absorption underlined that the compound captured in the ELISA was not the carboxylic acid of Substance P. This finding was further strengthened by experiments performed to elucidate the possible degradation pathway. The concentrations of Substance P-LI were dependent on the protease inhibitors used, with the highest concentrations observed when using AEBSF, EDTA, and phenanthroline as protease inhibitors, indicating that Substance P-LI seems also to be degraded by serine and metalloproteases. Moreover, substantially lower Substance P-LI concentrations were found in extracted plasma samples compared to unextracted plasma samples (50.2 pg/mL vs. 240.6 pg/mL), which is consistent with previous findings that reported substantial losses of Substance P-LI after plasma extraction [87]. Since the concentrations of Substance P-LI diminished in the absence of protease inhibitors and with plasma extraction, a protein-like structure of Substance P-LI seems to be very likely, as plasma protein precipitation and solid-phase extraction are among the methods indicated for the separation of undesired plasma proteins from the targeted analytes. Presuming a protein-like structure of Substance P-LI, both top-down and bottom-up approaches were used for elucidation of its structure, as recommended for proteomic research by MS [94]. By comparing HR-MS data of from stabilized (protease inhibited, on ice) and degraded (no protease inhibitors, 40°C) plasma samples, an antibody-captured proteomic analyte that cross-reacted with the ELISA used was found. This could be the propeptide of Substance P. This falsify detection is not unlikely as investigation with the amino acid sequence PQQFFGLM showed 85.9% cross-reactivity of this peptide hapten concerning its data sheet. Assuming the propeptide of Substance P is measured by the ELISA, the highest concentrations were found in plasma samples stabilized with a combination of AEBSF, EDTA, and phenanthroline, indicating its degradation by several proteases. Its present and stability in saliva and seminal fluid was not investigated within this study. The carboxylic acid of Substance P, which was not found in samples stabilized with EDTA and phenanthroline, seems to be an artificial degradation product of the pro-peptide in samples that were not sufficiently stabilized. This is more likely, as direct

conversion of active Substance P to its carboxylic acid was not observed for exogenous spiked Substance P in plasma samples.

This is not the first time that LC-MS analysis has revealed an unexpected structure of a tachykinin. Recently, the structure of the related mouse hemokinin-1 was found to be present as a decapeptide instead of the expected undecapeptide in murine brain tissue, as revealed by an immunoaffinity mass spectrometric assay [163]. Analogically, human Hemokinin-1, which was expected to be the main cross-reactor in human plasma, may also be present in another structural form, which was not detectable by the targeted LC-MS/MS analysis. Since human Hemokinin-1 was reported to be involved in the activation of immune cells in human blood as well as in the modulation of sperm motility, the absence of human Hemokinin-1 in plasma and seminal fluid samples was unexpected [30]. However, human Hemokinin-1 was merely quantified in only one study in human blood, utilizing an immunoassay, which is not available anymore [34]. To the best of the author's knowledge, currently there do not exist any commercially available immunoassay to quantify human Hemokinin-1 in biosamples and to assess cross-reactivity of these assays. So, based on distinct antibodies used in different ELISA kits, extended hemokinin forms as endokinin A/B or other tachykinins as endokinin C/D may also theoretically interact in these biosamples [131,164]. This requires further investigations on the selectivity of the antibodies and further elucidation on the presence of Substance P and related tachykinins in human plasma and other biofluids.

## 5.5 Conclusion

Utilizing a recently developed validated LC-MS/MS assay, plasma sample processing was comprehensively investigated in order to preserve the integrity of intact Substance P and human Hemokinin-1 from blood collection to final extraction. While endogenous concentrations of Substance P were measured in human saliva and seminal fluid and porcine brain tissue, the active form was not detectable in endogenous human plasma. Instead, the inactive carboxylic acid of Substance P was identified in human plasma samples. As the carboxylic acid of Substance P did not contribute to the cross-reactivity of the immunoassay used, the captured Substance P-LI was analyzed by LC-HR-MS/MS, revealing a precursor of Substance P as a possible cross-reactor. These findings raise the question about the presence of active Substance P in human plasma samples and should be more elucidated for its role in human plasma.

## **5.6 Disclosure**

*Parts of this chapter were previously accepted for publication in Peptides (18<sup>th</sup> November 2020). The author of this thesis was responsible for the conceptualization, the methodology, the formal analysis, the investigation, the data curation and visualization and the writing of the original draft of this publication.*

## 6. Overall conclusion and future prospects

Recent publications have underlined the emerging role of Substance P in the development and progress of inflammatory cardiovascular diseases [42,43,45,59,165], leading to its promising use as a biomarker in plasma samples. However, comprehensive investigations of the reported blood levels of Substance P in subjects with cardiovascular disease have demonstrated high variability owing to the bioanalytical assays used [132]. As human Hemokinin-1, also reported in human blood, interferes with most commercially available immunoassays, a reliable bioanalytical procedure is not available; therefore, a bioanalytical alternative to immunoassay is required. Selective quantification of Substance P is achievable with LC-MS/MS; moreover, its application allows simultaneous measurement of Substance P and human Hemokinin-1. For the latter, no LC-MS/MS assay has hitherto been published, and existing LC-MS/MS assays for Substance P lack the sensitivity to quantify endogenous plasma concentrations [166].

This thesis presents the first sensitive LC-MS/MS assay for simultaneous quantification of Substance P and human Hemokinin-1. It was validated according to international bioanalytical guidelines requiring a small volume of human blood plasma (120  $\mu$ L). Maximum sensitivity and robustness were achieved by a customized and innovative Design of Experiments concept for bioanalytical peptide quantification, addressing each critical aspect of the method. By applying the concept, nonspecific peptide adsorption was substantially minimized by concordantly optimizing the composition of the injection solvent and the container material used. Furthermore, the application of this assay led to primary description of Substance P concentrations in human saliva and seminal fluid by MS analysis. The author did not expect bioactive Substance P to be absent in human plasma because measured Substance P plasma levels are widely described in previous studies [88,100]. However, as immunoassays were used only for quantification of human Substance P plasma levels, these findings underline the issues of selectivity of immunoassays due to cross-reactivity and the enormous advantage of using MS analysis for selective bioanalytical questions. As only immunoassay-based, and, therefore, cross-reactivity-affected, human plasma Substance P levels have been reported in the literature, the true concentrations of Substance P may still be under the established limit of detection of the LC-MS/MS assay presented in this study; consequently, an even more sensitive bioanalytical assay may be necessary. With the LC-MS/MS components available to this thesis, maximum sensitivity was achieved using the described Design of Experiments concept. Each

aspect—from nonstandard blood sampling in low protein binding tubes, minimization of nonspecific peptide adsorption to optimal conditions in LC-MS/MS settings—was comprehensively investigated and optimized, resulting in a method of the highest sensitivity achievable with the available technique. By using MS systems with ion mobility cells and ultra-performance liquid chromatography (with feasible pressure up to 1200 bar), higher methodological sensitivity may be reached, which could eventually reveal the presence of bioactive Substance P at femtomolar concentrations. Successful detection of Substance P in porcine brain tissue, human saliva, and seminal fluid by LC-MS/MS analysis demonstrated that this technique is mainly suitable for bioanalysis of Substance P in biofluids and tissue.

Unexpectedly, neither Substance P nor human Hemokinin-1 was detected in any of the human plasma samples investigated, although the limits of detection were feasible according to the Substance P levels measured by the immunoassays. In contrast, the carboxylic acid of Substance P was identified in human plasma. However, it did not show cross-reactivity in the immunoassay and did not contribute to the observed divergence between the two bioanalytical assays. Therefore, immunoreactive Substance P bound by the immunoassay antibodies was analyzed by LC-HRMS to identify the structure of the captured substance. This approach uncovered the presence of a precursor of Substance P in human plasma as a possible cross-reactor of the immunoassay. This untargeted approach, which led to the identification of the precursor, underlines the possible future prospects of bioanalytical MS assay of Substance P. Using MS, it is possible to identify and quantify whole peptide systems rather than defined single analytes. Since most biomolecules are embedded in a complex bioregulatory system, the application of MS analysis to these biosystems would be a beneficial alternative to the traditional approach of analyzing single defined peptides or proteins. Moreover, precursors of bioactive analytes are often more stable and are present in higher concentrations compared to their bioactive metabolites (e.g. prorenin and renin [167]), which would make them more accessible biomarkers.

For Substance P in particular, it would be advantageous to additionally monitor its precursors and metabolites, since the complex tachykinin system in peripheral tissue, such as blood cells, is not yet fully understood. Based on the findings of this study, the previously described Substance P concentrations and its postulated role as a potential blood biomarker of inflammatory diseases have to be reevaluated. By using the chemometric tools developed in this thesis and adopting the approaches it has demonstrated to overcome critical issues in sample

preparation, such as nonspecific peptide adsorption and biosample instability, future studies may discover potential biomarkers within the tachykinin system, e.g., the precursor of Substance P identified in this study, which could be valuable and reliable clinical markers of cardiac inflammatory diseases.

## **7. Funding**

Partial research leading to these results has received funding from the European Union Seventh Framework Program (FP7/2007-2013) under grant agreement n°602295 (LENA).

Travel grants for the oral presentation “Design of experiments as a key element for enabling the endogenous mass spectrometric determination of substance P and related hemokinin-1”, presented at the Euroanalysis conference, Istanbul (Turkey) in September 2019, which is included in this thesis, were funded by the Heine Research Academies.

---

## 8. References

1. Harrison S, Geppetti P. Substance P. *Int J Biochem Cell Biol.* 2001;33(1):555–76.
2. Steinhoff MS, von Mentzer B, Geppetti P, Pothoulakis C, Bunnett NW. Tachykinins and Their Receptors: Contributions to Physiological Control and the Mechanisms of Disease. *Physiol Rev.* 2014;94(1):265–301.
3. Mistrova E, Kruzliak P, Chottova Dvorakova M. Role of substance P in the cardiovascular system. *Neuropeptides.* 2016;58(1):41–51.
4. Corbally N, Powell D, Trptont KF. The binding of endogenous and exogenous Substance P in human plasma. *Biochem Pharmacol.* 1990;39(7):1161–6.
5. Ducroc R, This S, Garzon B, Couraud J. Immunoreactive substance P and calcitonin-gene-related peptide (CGRP) in rat milk and in human milk and infant formulas. *Am J Clin Nutr.* 1995;62(3):554–8.
6. Parris W. Immunoreactive Substance P in Human Saliva. *Ann New York Acad Sci.* 1993;694(1):308–10.
7. Yoon YJ, Yoon J, Lee EJ, Kim JS. Substance P and calcitonin gene-related peptide in the glands of external auditory canal skin. *Clin Exp Otorhinolaryngol.* 2017;10(4):321–4.
8. Muñoz M, Coveñas R. Involvement of substance P and the NK-1 receptor in human pathology. *Amino Acids.* 2014;46(7):1727–50.
9. Eipper BA, Milgram SL, Jean Husten E, Yun H -Y, Mains RE. Peptidylglycine  $\alpha$ -amidating monooxygenase: A multifunctional protein with catalytic, processing, and routing domains. *Protein Sci.* 1993;2(4):489–97.
10. Corcho FJ, Salvatella X, Canto J, Giralt E, Perez JJ. Structural analysis of substance P using molecular dynamics and NMR spectroscopy. *J Pept Sci.* 2007;13(11):728–41.
11. Jurasekova Z, Garcia-Leis A, Sanchez-Cortes S, Tinti A, Torreggiani A. Structural analysis of the neuropeptide substance P by using vibrational spectroscopy. *Anal Bioanal Chem.* 2019;411(28):7419–30.
12. Saidi M, Kamali S, Beaudry F. Characterization of Substance P processing in mouse spinal cord S9 fractions using high-resolution Quadrupole-Orbitrap mass spectrometry. *Neuropeptides.* 2016;59(1):47–55.
13. Wang L, Sadoun E, Stephens RE, Ward PE. Metabolism of substance P and neurokinin A by human vascular endothelium and smooth muscle. *Peptides.* 1994;15(3):497–503.

14. Nausch I, Heymann E. Substance P in Human Plasma Is Degraded by Dipeptidyl Peptidase IV, Not by Cholinesterase. *J Neurochem.* 1985;44(5):1354–7.
15. Tomaki M, Ichinose M, Miura M, Hirayama Y, Kageyama N, Yamauchi H, et al. Angiotensin converting enzyme (ACE) inhibitor-induced cough and substance P. *Thorax.* 1996;51(2):199–201.
16. Vodovar N, Séronde MF, Laribi S, Gayat E, Lassus J, Januzzi JL, et al. Elevated Plasma B-Type Natriuretic Peptide Concentrations Directly Inhibit Circulating Nephilysin Activity in Heart Failure. *JACC Hear Fail.* 2015;3(8):629–36.
17. Hallberg M. Neuropeptides: Metabolism to Bioactive Fragments and the Pharmacology of Their Receptors. *Med Res Rev.* 2014;35(3):464–519.
18. Duarte FS, Testolin R, De Lima TCM. Further evidence on the anxiogenic-like effect of substance P evaluated in the elevated plus-maze in rats. *Behav Brain Res.* 2004;154(2):501–10.
19. Bury RW, Mashford ML. Biological Activity of C-Terminal Partial Sequences of Substance P. *J Med Chem.* 1976;19(6):854–6.
20. Satake H, Kawada T. Overview of the primary structure, tissue-distribution, and functions of tachykinins and their receptors. *Curr Drug Targets.* 2006;7(8):963–74.
21. Jensen DD, Lieu TM, Halls ML, Veldhuis NA, Imlach WL, Mai QN, et al. Neurokinin 1 receptor signaling in endosomes mediates sustained nociception and is a viable therapeutic target for prolonged pain relief. *Sci Transl Med.* 2017;9(392):1–16.
22. Nederpelt I, Bleeker D, Tuijt B, IJzerman AP, Heitman LH. Kinetic binding and activation profiles of endogenous tachykinins targeting the NK1 receptor. *Biochem Pharmacol.* 2016;118:88–95.
23. Kang HJ, Loftus S, DiCristina C, Green S, Pong A, Zwaan CM. Aprepitant for the prevention of chemotherapy-induced nausea and vomiting in paediatric subjects: An analysis by age group. *Pediatr Blood Cancer.* 2018;65(10):e27273.
24. Saito Y, Kumamoto T, Arima T, Shirakawa N, Ishimaru S, Sonoda T, et al. Evaluation of aprepitant and fosaprepitant in pediatric patients. *Pediatr Int.* 2019;61(3):235–9.
25. Warr DG, Hesketh PJ, Gralla RJ, Muss HB, Herrstedt J, Eisenberg PD, et al. Efficacy and tolerability of aprepitant for the prevention of chemotherapy-induced nausea and vomiting in patients with breast cancer after moderately emetogenic chemotherapy. *J Clin Oncol.* 2005;23(12):2822–30.
26. Choi MR, Jiles C, Seibel NL. Aprepitant use in children, adolescents, and young adults for the control of chemotherapy-induced nausea and vomiting (CINV). *J Pediatr*

- Hematol Oncol. 2010;32(7):268–71.
27. Gore L, Chawla S, Petrilli A, Hemenway M, Schissel D, Chua V, et al. Aprepitant in adolescent patients for prevention of chemotherapy-induced nausea and vomiting: a randomized, double-blind, placebo-controlled study of efficacy and tolerability. *Pediatr Blood Cancer*. 2009;52(2):242–7.
  28. Patel P, Leeder JS, Piquette-Miller M, Dupuis LL. Aprepitant and fosaprepitant drug interactions: a systematic review. *Br J Clin Pharmacol*. 2017;83(10):2148–62.
  29. Kang HJ, Loftus S, Taylor A, DiCristina C, Green S, Zwaan CM. Aprepitant for the prevention of chemotherapy-induced nausea and vomiting in children: a randomised, double-blind, phase 3 trial. *Lancet Oncol*. 2015;16(4):385–94.
  30. Borbély É, Helyes Z. Role of hemokinin-1 in health and disease. *Neuropeptides*. 2017;64(8):9–17.
  31. Cunin P, Caillon A, Corvaisier M, Garo E, Scotet M, Blanchard S, et al. The Tachykinins Substance P and Hemokinin-1 Favor the Generation of Human Memory Th17 Cells by Inducing IL-1, IL-23, and TNF-Like 1A Expression by Monocytes. *J Immunol*. 2011;186(7):4175–82.
  32. Morelli AE, Sumpter TL, Rojas-Canales DM, Bandyopadhyay M, Chen Z, Tkacheva O, et al. Neurokinin-1 Receptor Signaling Is Required for Efficient Ca<sup>2+</sup> Flux in T-Cell-Receptor-Activated T Cells. *Cell Rep*. 2020;30(10):3448–65.
  33. Martinez AN, Philipp MT. Substance P and Antagonists of the Neurokinin-1 Receptor in Neuroinflammation Associated with Infectious and Neurodegenerative Diseases of the Central Nervous System. *J Neurol neuromedicine*. 2016;1(2):29–36.
  34. Tsilioni I, Russell IJ, Stewart JM, Gleason RM, Theoharides TC. Neuropeptides CRH, SP, HK-1, and Inflammatory Cytokines IL-6 and TNF Are Increased in Serum of Patients with Fibromyalgia Syndrome, Implicating Mast Cells. *J Pharmacol Exp Ther*. 2016;356(3):664–72.
  35. Tavano F, di Mola FF, Latiano A, Palmieri O, Bossa F, Valvano MR, et al. Neuroimmune interactions in patients with inflammatory bowel diseases: Disease activity and clinical behavior based on Substance P serum levels. *J Crohn's Colitis*. 2012;6(5):563–70.
  36. Arnalich F, Sanchez JF, Martinez M, Jimenez M, Lopez J, Vazquez JJ, et al. Changes in plasma concentrations of vasoactive neuropeptides in patients with sepsis and septic shock. *Life Sci*. 1995;56(2):75–81.
  37. Li L, Gao X, Zhao J, Ji X, Wei H, Luo Y. Plasma and cerebrospinal fluid substance P

- in post-stroke patients with depression. *Psychiatry Clin Neurosci.* 2009;63(3):298–304.
38. Jang MU, Park JW, Kho HS, Chung SC, Chung JW. Plasma and saliva levels of nerve growth factor and neuropeptides in chronic migraine patients. *Oral Dis.* 2011;17(2):187–93.
39. Wang X, Douglas SD, Song L, Wang Y-J, Ho W-Z. Neurokinin-1 receptor antagonist (aprepitant) suppresses HIV-1 infection of microglia/macrophages. *J Neuroimmune Pharmacol.* 2008;3(4):257–64.
40. Barrett JS, Spitsin S, Moorthy G, Barrett K, Baker K, Lackner A, et al. Pharmacologic rationale for the NK1R antagonist, aprepitant as adjunctive therapy in HIV. *J Transl Med.* 2016;14(1):148–56.
41. Spitsin S, Tebas P, Barrett JS, Pappa V, Kim D, Taylor D, et al. Antiinflammatory effects of aprepitant coadministration with cART regimen containing ritonavir in HIV-infected adults. *JCI insight.* 2017;2(19):e95893.
42. Robinson P, Kasembeli M, Bharadwaj U, Engineer N, Eckols KT, Tweardy DJ. Substance P Receptor Signaling Mediates Doxorubicin-Induced Cardiomyocyte Apoptosis and Triple-Negative Breast Cancer Chemoresistance. *Biomed Res Int.* 2016;2016(2):e1959270.
43. Robinson P, Taffet GE, Engineer N, Khumbatta M, Firozgary B, Reynolds C, et al. Substance P receptor antagonism: A potential novel treatment option for viral-myocarditis. *Biomed Res Int.* 2015;2015(1):e645153.
44. Hoover DB, Chang Y, Hancock JC, Zhang L. Actions of tachykinins within the heart and their relevance to cardiovascular disease. *Jpn J Pharmacol.* 2000;84(4):367–73.
45. Dehlin HM, Levick SP. Substance P in heart failure: The good and the bad. *Int J Cardiol.* 2014;170(3):270–7.
46. Levick SP. Understanding the Complex Roles of Substance P in the Diseased Heart. *Hear Lung Circ.* 2018;27(12):1394–7.
47. Jubair S, Li J, Dehlin HM, Manteufel EJ, Goldspink PH, Levick SP, et al. Substance P induces cardioprotection in ischemia-reperfusion via activation of AKT. *Am J Physiol Heart Circ Physiol.* 2015;309(4):676–84.
48. Xu Y, Gu Q, Tang J, Qian Y, Tan X, Yu Z, et al. Substance P Attenuates Hypoxia/Reoxygenation-Induced Apoptosis Via the Akt Signalling Pathway and the NK1-Receptor in H9C2Cells. *Hear Lung Circ.* 2017;27(12):1–9.
49. Heymes C, Vanderheyden M, Bronzwaer JGF, Shah AM, Paulus WJ. Endomyocardial nitric oxide synthase and left ventricular preload reserve in dilated cardiomyopathy.

- Circulation. 1999;99(23):3009–16.
50. Janicki JS, Brower GL, Levick SP. The Emerging Prominence of the Cardiac Mast Cell as a Potent Mediator of Adverse Myocardial Remodeling. *Mol Biol Rep.* 2015;1220(5):121–39.
  51. Levick SP, Murray DB, Brower GL. Sympathetic Nervous System Modulation of Inflammation and Remodeling in the Hypertensive Heart. *Hypertension.* 2010;55(2):270–6.
  52. Meléndez GC, Li J, Law BA, Janicki JS, Supowit SC, Levick SP. Substance P induces adverse myocardial remodelling via a mechanism involving cardiac mast cells. *Cardiovasc Res.* 2011;92(3):420–9.
  53. Brower GL, Chancey AL, Thanigaraj S, Matsubara BB, Janicki JS. Cause and effect relationship between myocardial mast cell number and matrix metalloproteinase activity. *Am J Physiol Hear Circ Physiol.* 2002;283(2):518–25.
  54. Morrey C, Brazin J, Seyedi N, Corti F, Silver RB, Levi R. Interaction between Sensory C-fibers and Cardiac Mast Cells in Ischemia/Reperfusion: Activation of a Local Renin-Angiotensin System Culminating in Severe Arrhythmic Dysfunction. *J Pharmacol Exp Ther.* 2010;335(1):76–84.
  55. Levick SP, Murray DB, Brower GL. Sympathetic Nervous System Modulation of Inflammation and Remodeling in the Hypertensive Heart Experimental Protocol and Sympathectomy Surgery Substance P-mediated Production of Angiotensin II by Isolated Cardiac Inflammatory Cells Immunofluorescent Stain. *Hypertension.* 2010;55(2):270–6.
  56. Shaik-Dasthagirisaheb YB, Varvara G, Murmura G, Saggini A, Potalivo G, Caraffa A, et al. Vascular endothelial growth factor (VEGF), mast cells and inflammation. *Int J Immunopathol Pharmacol.* 2013;26(2):327–35.
  57. Dehlin HM, Manteufel EJ, Monroe AL, Reimer MH, Levick SP. Substance P acting via the neurokinin-1 receptor regulates adverse myocardial remodeling in a rat model of hypertension. *Int J Cardiol.* 2013;168(5):4643–51.
  58. Weglicki WB, Mak IT, Phillips TM. Blockade of cardiac inflammation in Mg<sup>2+</sup> deficiency by substance P receptor inhibition. *Circ Res.* 1994;74(5):1009–13.
  59. Robinson P, Garza A, Moore J, Eckols TK, Parti S, Balaji V, et al. Substance P is required for the pathogenesis of EMCV infection in mice. *Int J Clin Exp Med.* 2009;2(1):76–86.
  60. Wang Y, Shimada M, Xu Y, Hu D, Nishio R, Matsumori A. Role of substance P in

- viral myocarditis in mice. *Heart Vessels*. 2010;25(4):348–52.
61. Mashagi A. Neuropeptide Substance P and the Immune Response. *Cell Mol Life Sci*. 2016;73(22):4249–64.
62. Zimmer G, Rohn M, McGregor GP, Schemann M, Conzelmann KK, Herrler G. Virokinin, a Bioactive Peptide of the Tachykinin Family, Is Released from the Fusion Protein of Bovine Respiratory Syncytial Virus. *J Biol Chem*. 2003;278(47):46854–61.
63. Lipshultz SE, Lipsitz SR, Sallan SE, Simbre VC, Shaikh SL, Mone SM, et al. Long-term enalapril therapy for left ventricular dysfunction in doxorubicin-treated survivors of childhood cancer. *J Clin Oncol*. 2002;20(23):4517–22.
64. Levick SP, Soto-Pantoja DR, Bi J, Hundley WG, Widiapradja A, Manteufel EJ, et al. Doxorubicin-Induced Myocardial Fibrosis Involves the Neurokinin-1 Receptor and Direct Effects on Cardiac Fibroblasts. *Heart Lung Circ*. 2019;28(10):1598–605.
65. Mak IT, Kramer JH, Chmielinska JJ, Spurney CF, Weglicki WB. EGFR-TKI, erlotinib, causes hypomagnesemia, oxidative stress, and cardiac dysfunction: attenuation by NK-1 receptor blockade. *J Cardiovasc Pharmacol*. 2015;65(1):54–61.
66. Lipshultz SE, Rifai N, Dalton VM, Levy DE, Silverman LB, Lipsitz SR, et al. The Effect of Dexrazoxane on Myocardial Injury in Doxorubicin-Treated Children with Acute Lymphoblastic Leukemia. *N Engl J Med*. 2004;351(2):145–53.
67. Ponikowski P, Voors AA, Anker SD, Bueno H, Cleland JGF, Coats AJS, et al. 2016 ESC Guidelines for the diagnosis and treatment of acute and chronic heart failure. *Eur Heart J*. 2016;37(27):2129–200.
68. Redfield MM, Jacobsen SJ, Burnett Jr JC, Mahoney DW, Bailey KR, Rodeheffer RJ. Burden of Systolic and Diastolic Ventricular Dysfunction in the Community: Appreciating the Scope of the Heart Failure Epidemic. *JAMA*. 2003;289(2):194–202.
69. Mosterd A, Hoes AW. Clinical epidemiology of heart failure. *Heart*. 2007;93(9):1137–46.
70. Jacobs JP, Quintessenza JA, Karl TR, Asante-Korang A, Everett AD, Collins SB, et al. Summary of the 2015 international paediatric heart failure summit of Johns Hopkins All Children’s Heart Institute. *Cardiol Young*. 2015;25(2):8–30.
71. Lipshultz SE, Cochran TR, Briston DA, Brown SR, Peter J, Miller TL, et al. Pediatric cardiomyopathies: causes, epidemiology, clinical course, preventive strategies and therapies. *Futur Cardiol*. 2014;9(6):817–48.
72. Stout KK, Broberg CS, Book WM, Cecchin F, Chen JM, Dimopoulos K, et al. Chronic Heart Failure in Congenital Heart Disease: A Scientific Statement from the American

- 
- Heart Association. *Circulation*. 2016;133(8):770–801.
73. Lee TM, Hsu DT, Kantor P, Towbin JA, Ware SM, Colan SD, et al. Pediatric cardiomyopathies. *Circ Res*. 2017;121(7):855–73.
74. Tátrai E, Hartyánszky I, Lászik A, Acsády G, Sótonyi P, Hubay M. The Role of Viral Infections in the Development of Dilated Cardiomyopathy. *Pathol Oncol Res*. 2011;17(2):229–35.
75. Shauer A, Gotsman I, Keren A, Zwas DR, Hellman Y, Durst R, et al. Acute viral myocarditis: current concepts in diagnosis and treatment. *Isr Med Assoc J*. 2013;15(3):180–5.
76. Jiang X, Sucharov J, Stauffer BL, Miyamoto SD, Sucharov CC. Exosomes from pediatric dilated cardiomyopathy patients modulate a pathological response in cardiomyocytes. *Am J Physiol - Hear Circ Physiol*. 2017;312(4):818–26.
77. Lipshultz SE, Wilkinson JD. Beta-adrenergic adaptation in idiopathic dilated cardiomyopathy: Differences between children and adults. *Eur Heart J*. 2014;35(1):10–2.
78. Ratnasamy C, Kinnamon DD, Lipshultz SE, Rusconi P. Associations between neurohormonal and inflammatory activation and heart failure in children. *Am Heart J*. 2008;155(3):527–33.
79. Kianifar H-R, Akhondian J, Najafi-Sani M, Sadeghi R. Evidence based medicine in pediatric practice: brief review. *Iran J Pediatr*. 2010;20(3):261–8.
80. Schranz D, Voelkel NF. “Nihilism” of chronic heart failure therapy in children and why effective therapy is withheld. *Eur J Pediatr*. 2016;175(4):445–55.
81. Bajcetic M, de Wildt SN, Dalinghaus M, Breitzkreutz J, Klingmann I, Lagler FB, et al. Orodispersible minitabets of enalapril for use in children with heart failure (LENA): Rationale and protocol for a multicentre pharmacokinetic bridging study and follow-up safety study. *Contemp Clin Trials Commun*. 2019;15(6):e100393.
82. Schaefer J, Burckhardt BB, Tins J, Bartel A, Laeer S. Validated low-volume immunoassay for the reliable determination of direct renin especially valuable for pediatric investigations. *J Immunoass Immunochem*. 2017;38(6):579–94.
83. Feickert M, Burdman I, Makowski N, Ali M, Bartel A, Burckhardt BB. A continued method performance monitoring approach for the determination of pediatric renin samples - application within a European clinical trial. *Clin Chem Lab Med*. 2020;58(11):1847–55.
84. Burckhardt BB. Child - appropriate analytical technologies as key elements for

- pharmacokinetic and pharmacodynamic investigations of drugs acting on the renin - angiotensin - aldosterone system (Thesis, Institute of Clinical Pharmacy, Dusseldorf). 2014.
85. Ali M, Tins J, Burckhardt BB. Fit-for-Purpose Quality Control System in Continuous Bioanalysis During Long-Term Pediatric Studies. *AAPS J.* 2019;21(6):104–15.
  86. Valdemarsson S, Edvinsson L, Ekman R, Hedner P, Sjöholm A. Increased plasma level of substance P in patients with severe congestive heart failure treated with ACE inhibitors. *J Intern Med.* 1991;230(4):325–31.
  87. Campbell DE, Raftery N, Tustin R, Tustin NB, DeSilvio ML, Cnaan A, et al. Measurement of plasma-derived substance P: Biological, methodological, and statistical considerations. *Clin Vaccine Immunol.* 2006;13(11):1197–203.
  88. Weglicki WB, Mak IT, Phillips TM. Blockade of cardiac inflammation in Mg<sup>2+</sup> deficiency by substance P receptor inhibition. *Circ Res.* 1994;74(5):1009–13.
  89. Zhang Y, Lu L, Furlonger C, Wu GE, Paige CJ. Hemokinin is a hematopoietic-specific tachykinin that regulates B lymphopoiesis. *Nat Immunol.* 2000;1(5):392–7.
  90. Ganjiwale A, Cowsik SM. Membrane-induced structure of novel human tachykinin hemokinin-1 (hHK1). *Biopolymers.* 2015;103(12):702–10.
  91. Mou L, Xing Y, Kong Z, Zhou Y, Chen Z, Wang R. The N-terminal domain of human hemokinin-1 influences functional selectivity property for tachykinin receptor neurokinin-1. *Biochem Pharmacol.* 2011;81(5):661–8.
  92. Levick SP, Brower GL, Janicki JS. Substance P-mediated cardiac mast cell activation: An in vitro study. *Neuropeptides.* 2019;74(4):52–9.
  93. Kong ZQ, Fu CY, Chen Q, Wang R. Cardiovascular responses to intravenous administration of human hemokinin-1 and its truncated form hemokinin-1(4-11) in anesthetized rats. *Eur J Pharmacol.* 2008;590(1–3):310–6.
  94. Han X, Aslanian A, Yates III JR. Mass spectrometry for Proteomics. *Proteomics.* 2008;12(5):483–90.
  95. van den Broek I, Sparidans RW, Schellens JHM, Beijnen JH. Quantitative bioanalysis of peptides by liquid chromatography coupled to (tandem) mass spectrometry. *J Chromatogr B Anal Technol Biomed Life Sci.* 2008;872(1):1–22.
  96. Costa E, Menschaert G, Luyten W. Peptide identification using tandem mass spectrometry data (Report, KU Leuven, Heverlee, Belgium). 2011.
  97. Yates JR, Ruse CI, Nakorchevsky A. Proteomics by Mass Spectrometry: Approaches, Advances, and Applications. *Annu Rev Biomed Eng.* 2009;11(1):49–79.

- 
98. Eng JK, Searle BC, Clauser KR, Tabb DL. A face in the crowd: Recognizing peptides through database search. *Mol Cell Proteomics*. 2011;10(11):1–9.
  99. Fernández-Rodríguez CM, Prieto J, Quiroga J, Zozoya J, Andrade A, Nunez M, et al. Plasma levels of substance p in liver cirrhosis: Relationship to the activation of vasopressor systems and urinary sodium excretion. *Hepatology*. 1995;21(1):35–40.
  100. Fehder WP, Ho WZ, Campbell DE, Tourtellotte WW, Michaels L, Cutilli JR, et al. Development and evaluation of a chromatographic procedure for partial purification of substance P with quantitation by an enzyme immunoassay. *Clin Diagn Lab Immunol*. 1998;5(3):303–7.
  101. Sobhi HR, Vatansever B, Wortmann A, Grouzmann E, Rochat B. Generic approach for the sensitive absolute quantification of large undigested peptides in plasma using a particular liquid chromatography-mass spectrometry setup. *J Chromatogr A*. 2011;1218(47):8536–43.
  102. Beaudry F, Vachon P. Determination of substance P in rat spinal cord by high-performance liquid chromatography electrospray quadrupole ion trap mass spectrometry. *Biomed Chromatogr*. 2006;20(2):1344–50.
  103. Beaudry F. Stability comparison between sample preparation procedures for mass spectrometry-based targeted or shotgun peptidomic analysis. *Anal Biochem*. 2010;407(2):290–2.
  104. Varnell RJ, Freeman JY, Maitchouk D, Beuerman RW, Gebhardt BM. Detection of substance P in human tears by laser desorption mass spectrometry and immunoassay. *Curr Eye Res*. 1997;16(9):960–3.
  105. Beaudry F, Ferland CE, Vachon P. Identification, characterization and quantification of specific neuropeptides in rat spinal cord by liquid chromatography electrospray quadrupole ion trap mass spectrometry. *Biomed Chromatogr*. 2009;23(9):940–50.
  106. Saidi M, Kamali S, Beaudry F. Characterization of Substance P processing in mouse spinal cord S9 fractions using high-resolution Quadrupole-Orbitrap mass spectrometry. *Neuropeptides*. 2016;59(1):47–55.
  107. Pailleux F, Beaudry F. Evaluation of multiple reaction monitoring cubed for the analysis of tachykinin related peptides in rat spinal cord using a hybrid triple quadrupole-linear ion trap mass spectrometer. *J Chromatogr B Anal Technol Biomed Life Sci*. 2014;947(1):164–7.
  108. Hecht ES, Oberg AL, Muddiman DC. Optimizing Mass Spectrometry Analyses: A Tailored Review on the Utility of Design of Experiments. *J Am Soc Mass Spectrom*.

- 2016;27(5):767–85.
109. Debrus B, Guillarme D, Rudaz S. Improved quality-by-design compliant methodology for method development in reversed-phase liquid chromatography. *J Pharm Biomed Anal.* 2013;84(10):215–23.
  110. Oliva A, Llabres Martinez M. Application of capability indices and control charts in the analytical method control strategy. *J Sep Sci.* 2017;40(15):3046–53.
  111. Martin GP, Barnett KL, Burgess C, Curry PD, Ermer J, Gratzl GS, et al. Lifecycle management of analytical procedures: Method development, procedure performance qualification, and procedure performance verification (Stimuli article of the USP Validation and Verification Expert Panel, Rockville, USA). Vol. 39, *Pharmacopeial Forum.* 2013.
  112. Parr MK, Schmidt AH. Life cycle management of analytical methods. *J Pharm Biomed Anal.* 2018;147(1):506–17.
  113. Maes K, Van Liefferinge J, Viaene J, Van Schoors J, Van Wanseele Y, Béchade G, et al. Improved sensitivity of the nano ultra-high performance liquid chromatography-tandem mass spectrometric analysis of low-concentrated neuropeptides by reducing aspecific adsorption and optimizing the injection solvent. *J Chromatogr A.* 2014;1360(9):217–28.
  114. Van Wanseele Y, Viaene J, Van den Borre L, Dewachter K, Vander Heyden Y, Smolders I, et al. LC-method development for the quantification of neuromedin-like peptides. Emphasis on column choice and mobile phase composition. *J Pharm Biomed Anal.* 2017;137(4):104–12.
  115. Walsh DA, F McWilliams D, McWilliams D, F McWilliams D. Tachykinins and the cardiovascular system. *Curr Drug Targets.* 2006;7(8):1031–42.
  116. Ejaz A, Lo Gerfo FW, Pradhan L. Diabetic neuropathy and heart failure: role of neuropeptides. *Expert Rev Mol Med.* 2011;13(8):26–45.
  117. Dvorakova MC, Kruzliak P, Rabkin SW. Role of neuropeptides in cardiomyopathies. *Peptides.* 2014;61(11):1–6.
  118. Wang LH, Zhou SX, Li RC, Zheng LR, Zhu JH, Hu SJS, et al. Serum levels of calcitonin gene-related peptide and substance P are decreased in patients with diabetes mellitus and coronary artery disease. *J Int Med Res.* 2012;40(1):134–40.
  119. Han H, Seo HS, Jung BH, Woo K, Yoo YS, Kang MJ. Substance P and neuropeptide y as potential biomarkers for diagnosis of acute myocardial infarction in korean patients. *Bull Korean Chem Soc.* 2014;35(1):158–64.

120. Noug e H, Pezel T, Picard F, Sadoune M, Arrigo M, Beauvais F, et al. Effects of sacubitril/valsartan on neprilysin targets and the metabolism of natriuretic peptides in chronic heart failure: a mechanistic clinical study. *Eur J Heart Fail.* 2019;21(5):598–605.
121. Howie SRC. Blood sample volumes in child health research: review of safe limits. *Bull World Health Organ.* 2011;89(1):46–53.
122. Butler MG, Nelson TA, Driscoll DJ, Manzardo AM. Evaluation of Plasma Substance P and Beta- Endorphin Levels in children with Prader-Willi Syndrome. *J Rare Disord.* 2015;3(2):1–14.
123. O’Dorisio MS, Hauger M, O’Dorisio TM. Age-dependent levels of plasma neuropeptides in normal children. *Regul Pept.* 2002;109(1):189–92.
124. Herberth G, Weber A, R der S, Elvers HD, Kr mer U, Schins RPF, et al. Relation between stressful life events, neuropeptides and cytokines: Results from the LISA birth cohort study. *Pediatr Allergy Immunol.* 2008;19(8):722–9.
125. Wong CM, Boyle EM, Stephen RI, Smith J, Stenson BJ, McIntosh N, et al. Normative values of substance P and neurokinin A in neonates. *Ann Clin Biochem.* 2010;47(4):331–5.
126. El-Raziky MS, Gohar N, El-Raziky M. Study of Substance P, Renin and Aldosterone in chronic liver disease in Egyptian children. *J Trop Pediatr.* 2005;51(5):320–3.
127. Brandow AM, Wandersee NJ, Dasgupta M, Raymond G, Hillery CA, Stucky CL, et al. Substance P is increased in patients with sickle cell disease and associated with haemolysis and hydroxycarbamide use. *Br J Haematol.* 2016;175(2):237–45.
128. Mosher RA, Coetzee JF, Allen PS, Havel JA, Griffith GR, Wang C. Effects of sample handling methods on substance P concentrations and immunoreactivity in bovine blood samples. *Am J Vet Res.* 2014;75(2):109–16.
129. Han H, Pyun J-C, Yoo H, Seo HS, Jung BH, Yoo YS, et al. Highly Sensitive Immunoassay for the Diagnosis of Acute Myocardial Infarction Using Silica Spheres Encapsulating a Quantum Dot Layer. *Anal Chem.* 2014;86(20):10157–63.
130. Sato Y, Itoh H, Suzuki Y, Tatsuta R, Takeyama M. Effect of pilocarpine on substance P and calcitonin gene-related peptide releases correlate with salivary secretion in human saliva and plasma. *J Clin Pharm Ther.* 2013;38(1):19–23.
131. Page NM. Hemokinins and endokinins. *Cell Mol Life Sci.* 2004;61(13):1652–63.
132. Feickert M, Burckhardt BB. Substance P in cardiovascular diseases – A bioanalytical review. *Clin Chim Acta.* 2019;495(8):501–6.

- 
133. Maes K, Smolders I, Michotte Y, Van Eeckhaut A. Strategies to reduce aspecific adsorption of peptides and proteins in liquid chromatography-mass spectrometry based bioanalyses: An overview. *J Chromatogr A*. 2014;1358(9):1–13.
  134. Rakow T, El Deeb S, Hahne T, El-Hady DA, AlBishri HM, Wätzig H. Investigating effects of sample pretreatment on protein stability using size-exclusion chromatography and high-resolution continuum source atomic absorption spectrometry. *J Sep Sci*. 2014;37(18):2583–90.
  135. Chico DE, Given RL, Miller BT. Binding of cationic cell-permeable peptides to plastic and glass. *Peptides*. 2003;24(1):3–9.
  136. Kristensen K, Henriksen JR, Andresen TL. Adsorption of cationic peptides to solid surfaces of glass and plastic. *PLoS One*. 2015;10(5):e0122419.
  137. Vatansever B, Lahrichi SL, Thiocone A, Salluce N, Mathieu M, Grouzmann E, et al. Comparison between a linear ion trap and a triple quadrupole MS in the sensitive detection of large peptides at femtomole amounts on column. *J Sep Sci*. 2010;33(16):2478–88.
  138. Goebel-Stengel M, Stengel A, Taché Y, Reeve JR. The importance of using the optimal plasticware and glassware in studies involving peptides. *Anal Biochem*. 2011;414(1):38–46.
  139. Pont L, Benavente F, Barbosa J, Sanz-Nebot V. An update for human blood plasma pretreatment for optimized recovery of low-molecular-mass peptides prior to CE-MS and SPE-CE-MS. *J Sep Sci*. 2013;36(24):3896–902.
  140. Hoofnagle AN, Whiteaker JR, Carr SA, Kuhn E, Liu T, Massoni SA, et al. Recommendations for the generation, quantification, storage, and handling of peptides used for mass spectrometry-based assays. *Clin Chem*. 2016;62(1):48–69.
  141. John RCS, Draper NR. D-Optimality for regression designs: A review. *Technometrics*. 1975;17(1):15–23.
  142. Golub GH, Heath M, Wahba G. Generalized cross-validation as a method for choosing a good ridge parameter. *Technometrics*. 1979;21(2):215–23.
  143. Van Midwoud PM, Rieux L, Bischoff R, Verpoorte E, Niederländer HAG. Improvement of recovery and repeatability in liquid chromatography-mass spectrometry analysis of peptides. *J Proteome Res*. 2007;6(2):781–91.
  144. EMA Committee for Medicinal Products for Human Use. Guideline on bioanalytical method validation. EMEA/CHMP/EWP/192217/2009 Rev. 1 Corr. 2\*\*. 2012.
  145. Ogedengbe JO, Adelaiye AB, Mohammed A, Ayo JO, Odili AN, Adeyemi OM, et al.

- Evaluation of physiologic pain in relation to pain substances in healthy subjects. *Pathophysiology*. 2015;22(4):183–7.
146. García MC. The effect of the mobile phase additives on sensitivity in the analysis of peptides and proteins by high-performance liquid chromatography-electrospray mass spectrometry. *J Chromatogr B Anal Technol Biomed Life Sci*. 2005;825(2):111–23.
147. von Euler U, Gaddum J. An unidentified depressor substance in certain tissue extracts. *J Physiol*. 1948;72(1):74–87.
148. Mai JK, Stephens PH, Hopf A, Cuello AC. Substance P in the human brain. *Neuroscience*. 1986;17(3):709–39.
149. Sastry BVR, Janson VE. Substance P in Human Spermatozoa and Modulation of Sperm Motility by Substance P and Its Antagonists. presented at: Substance P and Neurokinins (Conference Abstract). 1987.
150. Jasim H, Carlsson A, Hedenberg-Magnusson B, Ghafouri B, Ernberg M. Saliva as a medium to detect and measure biomarkers related to pain. *Sci Rep*. 2018;8(1):3220–9.
151. Liang T, Cascieri MA. Substance P receptor on parotid cell membranes. *J Neurosci*. 1981;1(10):1133–41.
152. Kurtz MM, Wang R, Clements MK, Cascieri MA, Austin CP, Cunningham BR, et al. Identification, localization and receptor characterization of novel mammalian substance P-like peptides. *Gene*. 2002;296(1):205–12.
153. Hajna Z, Borbély É, Kemény Á, Botz B, Kereskai L, Szolcsányi J, et al. Hemokinin-1 is an important mediator of endotoxin-induced acute airway inflammation in the mouse. *Peptides*. 2015;64(2):1–7.
154. Manorak W, Idahosa C, Gupta K, Roy S, Panettieri R, Ali H. Upregulation of Mas-related G Protein coupled receptor X2 in asthmatic lung mast cells and its activation by the novel neuropeptide hemokinin-1. *Respir Res*. 2018;19(1):1–5.
155. Patacchini R, Lecci A, Holzer P, Maggi CA. Newly discovered tachykinins raise new questions about their peripheral roles and the tachykinin nomenclature. *Trends Pharmacol Sci*. 2004;25(1):1–3.
156. Feickert M, Burckhardt BB. Validated Mass Spectrometric Assay for the Quantification of Substance P and human Hemokinin-1 in Plasma Samples: A Design of Experiments concept for comprehensive Method Development. *J Pharm Biomed Anal*. 2020;191(11):113542–51.
157. Liu Z, Welin M, Bragee B, Nyberg F. A high-recovery extraction procedure for quantitative analysis of substance P and opioid peptides in human cerebrospinal fluid.

- Peptides. 2000;21(6):853–60.
158. Campbell DE, Bruckner P, Tustin NB, Tustin R, Douglas SD. Novel method for determination of substance P levels in unextracted human plasma by using acidification. *Clin Vaccine Immunol.* 2009;16(4):594–6.
159. Feickert M, Burckhardt BB. A design of experiments concept for the minimization of nonspecific peptide adsorption in the mass spectrometric determination of substance P and related hemokinin-1. *J Sep Sci.* 2020;43(4):818–28.
160. Burdman I, Burckhardt BB. Human prorenin determination by hybrid immunocapture LC-MS: A mixed-solvent-triggered digestion utilizing D-optimal design. *Rapid Commun Mass Spectrom.* 2020;34(24):e8932.
161. Pailleux F, Lemoine J, Beaudry F. Quantitative mass spectrometry analysis reveals that deletion of the TRPV1 receptor in mice alters substance P and neurokinin a expression in the central nervous system. *Neurochem Res.* 2012;37(12):2678–85.
162. Alasağ N, Şener E, Doğrukol-Ak D. Simultaneous Determination of Substance P and CGRP in Rat Brainstem Tissue Using LC-ESI-MS/MS Method. *Curr Anal Chem.* 2018;14(6):583–90.
163. Deliconstantinos G, Barton S, Soloviev M, Page N. Mouse hemokinin-1 decapeptide subjected to a brain-specific post-translational modification. *In Vivo (Brooklyn).* 2017;31(5):991–8.
164. Page NM, Bell NJ, Gardiner SM, Manyonda IT, Brayley KJ, Strange PG, et al. Characterization of the endokinins: human tachykinins with cardiovascular activity. *Proc Natl Acad Sci U S A.* 2003;100(10):6245–50.
165. D'Souza M, Garza MA, Xie M, Weinstock J, Xiang Q, Robinson P, et al. Substance P is associated with heart enlargement and apoptosis in murine dilated cardiomyopathy induced by taenia crassiceps infection. *J Parasitol.* 2007;93(5):1121–7.
166. Sobhi HR, Vatansever B, Wortmann A, Grouzmann E, Rochat B. Generic approach for the sensitive absolute quantification of large undigested peptides in plasma using a particular liquid chromatography-mass spectrometry setup. *J Chromatogr A.* 2011;1218(47):8536–43.
167. Schrotten NF, Gaillard CAJM, Van Veldhuisen DJ, Szymanski MK, Hillege HL, De Boer RA. New roles for renin and prorenin in heart failure and cardiorenal crosstalk. *Heart Fail Rev.* 2012;17(2):191–201.

---

## 9. Appendix

### 9.1 Table of Supplementary

SUPPLEMENTARY TABLE 1: SUMMARY OF SUBSTANCE P BLOOD LEVELS IN CARDIOVASCULAR-DISEASED ADULTS. ....	146
SUPPLEMENTARY TABLE 2: OVERVIEW OF SUBSTANCE P BLOOD LEVELS IN HEALTHY CHILDREN. ....	148
SUPPLEMENTARY TABLE 3: CALCULATED MASS SPECTROMETRIC PEPTIDE FRAGMENT PATTERN OF SUBSTANCE P AND HUMAN HEMOKININ-1 .....	149
SUPPLEMENTARY TABLE 4: WORKSHEET FOR THE OPTIMIZATION OF THE INJECTION SOLVENT COMPOSITION WITHIN THE DESIGN OF EXPERIMENTS CONCEPT.....	150
SUPPLEMENTARY TABLE 5: WORKSHEET FOR THE SELECTION OF THE MOST APPROPRIATE DEEP-WELL PLATES WITHIN THE DESIGN OF EXPERIMENTS CONCEPT. ....	154
SUPPLEMENTARY TABLE 6: WORKSHEET FOR THE SELECTION OF THE MOST APPROPRIATE TIPS WITHIN THE DESIGN OF EXPERIMENTS CONCEPT. ....	157
SUPPLEMENTARY TABLE 7: WORKSHEET FOR THE SOLID PHASE EXTRACTION PROTOCOL WITHIN THE DESIGN OF EXPERIMENTS CONCEPT.....	160
SUPPLEMENTARY TABLE 8: WORKSHEET FOR THE CHROMATOGRAPHIC GRADIENT WITHIN THE DESIGN OF EXPERIMENTS CONCEPT.....	163
SUPPLEMENTARY TABLE 9: WORKSHEET FOR THE ION SOURCE PARAMETERS WITHIN THE DESIGN OF EXPERIMENTS CONCEPT.....	166
SUPPLEMENTARY TABLE 10: MULTIQUANT DATA OF THE 1. RUN TO DETERMINE THE ACCURACY AND PRECISION OF THE METHOD.....	169
SUPPLEMENTARY TABLE 11: MULTIQUANT DATA OF THE 2. RUN TO DETERMINE THE ACCURACY AND PRECISION OF THE METHOD.....	173
SUPPLEMENTARY TABLE 12: MULTIQUANT DATA OF THE 3. RUN TO DETERMINE THE ACCURACY AND PRECISION OF THE METHOD.....	177
SUPPLEMENTARY TABLE 13: LINEARITY AND SENSITIVITY OF THE THREE VALIDATION RUNS FOR EACH ANALYTE.....	180
SUPPLEMENTARY TABLE 14: INTRA-RUN ACCURACY OF THREE VALIDATION RUNS WITHIN TWO DAYS OF FOUR CONCENTRATION LEVELS OF SUBSTANCE P, ITS CARBOXYLIC ACID AND HUMAN HEMOKININ-1 IN HUMAN PLASMA SAMPLES. ....	181

SUPPLEMENTARY TABLE 15: INTER-RUN ACCURACY AND PRECISION OF THREE VALIDATION RUNS WITHIN TWO DAYS OF FOUR CONCENTRATION LEVELS OF SUBSTANCE P, ITS CARBOXYLIC ACID AND HUMAN HEMOKININ-1 IN HUMAN PLASMA SAMPLES..... 182

SUPPLEMENTARY TABLE 16: RECOVERY, ABSOLUTE MATRIX EFFECTS AND STABILITY DATA FOR SUBSTANCE P, ITS CARBOXYLIC ACID AND HUMAN HEMOKININ-1 IN HUMAN PLASMA SAMPLES AT THREE QUALITY CONTROL LEVELS. .... 183

SUPPLEMENTARY TABLE 17: FREEZE-THAW STABILITY DATA FOR SUBSTANCE P, ITS CARBOXYLIC ACID AND HUMAN HEMOKININ-1 IN HUMAN PLASMA SAMPLES AT THREE QUALITY CONTROL LEVELS..... 184

*Supplementary Table 1: Summary of Substance P blood levels in cardiovascular-diseased adults.*

Author (year)	Cardiovascular disease [subject number]	SP mean value* ( $\pm$ SD or IQR) [pg/mL]	Analytical assay	Matrix + Sampling additives
Valdemarsson et al. (1991) [86]	Severe CHF under ACEI [n = 15] Severe CHF without ACEI [n = 17] Mild CHF without ACEI [n = 10] Controls [n = 31]	5.5 ( $\pm$ 1.1) 3.1 ( $\pm$ 0.4) 4.1 ( $\pm$ 0.4) <sup>a</sup> 1.7 ( $\pm$ 0.2) <sup>a</sup>	RIA	Plasma + EDTA (1 mg/mL)
Wang et al. (2012) [118]	Diabetes [n = 46] CAD [n = 44] Controls [n = 44] Diabetes + CAD [n = 50]	35 ( $\pm$ 5) <sup>a</sup> 37.5 ( $\pm$ 6) <sup>a</sup> 65 ( $\pm$ 15) <sup>a</sup> 15 ( $\pm$ 5) <sup>a</sup>	RIA	Serum without additives
Han et al. (2014) [119]	Cardiac infarction [n = 30] Unstable angina [n = 21] Angina pectoris [n = 30] Controls [n = 29]	191 ( $\pm$ 141) 103 ( $\pm$ 111) 31 ( $\pm$ 80) 70 ( $\pm$ 131)	ELISA	Serum + Aprotinin (0.6 TIU/mL)
Han et al. (2014) [129]	Cardiac infarction [n = 16]  Controls [n = 30]	215 (median) (100 - 400) <sup>a</sup>  99 (median) (75-125) <sup>a</sup>	ELISA	Serum + Aprotinin (0.6 TIU/mL)
	Cardiac infarction [n = 16]  Controls [n = 30]	367 (median) (250 – 475) <sup>a</sup>  95 (median) (50 – 100) <sup>a</sup>	SQSLISA	Serum + Aprotinin (0.6 TIU/mL)
Vodovar et al. (2015) [16]	ADHF/CHF: With irBNP < 916 pg/mL [n = 440] With irBNP > 916 pg/mL [n = 224]	43 (median) (37 - 49) 59 (median) (57 - 64)	RIA	EDTA Plasma
Nougué et al. (2018) [120]	CHF Baseline [n = 73] Under low dose of Sacubitril/Valsartan (49/51 mg) [n = 86] Under high dose of Sacubitril/Valsartan (97/103 mg) [n = 56] After 30 days of treatment [n = 30] After 90 days of treatment [n = 30]	36 (median) (27 - 44) 75 (median) (25 - 275) <sup>a</sup>  100 (median) (50 - 300) <sup>a</sup>  75 (median) (50 - 100) <sup>a</sup> 175 (median) (75 - 400) <sup>a</sup>	RIA	EDTA Plasma

*(ACEI: Angiotensin converting enzyme inhibition, ADHF: acute decompensated heart failure, CAD: coronary arterial disease, CHF: chronic heart failure, EDTA: ethylene diamine tetra acetic acid, ELISA: enzyme-linked-immunosorbent assay, IQR: interquartile range, irBNP: immunoreactive B-type natriuretic peptide, RIA: radioimmunoassay, SD: standard deviation, SP: Substance P, SQSLISA: silica spheres encapsulating a quantum dot layer-linked immunosorbent assay, TIU: thrombin-inhibition unit; \*unless otherwise mentioned; <sup>a</sup>estimated values) [16,86,118–120,129]*

*Supplementary Table 2: Overview of Substance P blood levels in healthy children.*

<b>Author (year)</b>	<b>Children's age [subject number]</b>	<b>Mean value (<math>\pm</math> SD or IQR) [pg/mL]</b>	<b>Analytical assay</b>	<b>Matrix + Additives</b>
O'Dorisio et al. (2002) [123]	0 - 11 months [n = 2] 12 - 35 months [n = 3] 3 - 5 years [n = 10] 6 - 11 years [n = 15] 12 - 21 years [n = 11]	81 ( $\pm$ 7 [range]) 94 ( $\pm$ 49) 108 ( $\pm$ 50) 110 ( $\pm$ 65) 55 ( $\pm$ 38)	RIA	EDTA Plasma
El-Raziky et al. (2005) [126]	6.3 $\pm$ 2.5 years (mean $\pm$ SD) [n = 10]	16.2 ( $\pm$ 4.6)	RIA	Blood (not specified)
Herberth et al. (2008) [124]	6 years - without stressful life events [n = 80] - with stressful life events [n = 187]	217.8 (median) (141.4 - 260.6) 201.7 – 214.5 (medians)	ELISA	Heparin Plasma
Wong et al. (2010) [125]	Neonates [n = 142] thereof on Day 1 [n = 70] Day 2 [n = 76] Day 3 [n = 142] Day 7 [n = 115] Day 14 [n = 82]	2.3 (median) (1.3 - 15.1) 1.5 (median) 2.1 (median) 2.7 (median) 2.4 (median) 1.8 (median)	RIA	Plasma + Aprotinin + EDTA
Butler et al. (2015) [122]	5 - 11 years [n = 18]	35 ( $\pm$ 20)	MSIA	EDTA Plasma
Brandow et al. (2016) [127]	7 - 19 years [n = 21]	21 ( $\pm$ 7.1)	ELISA	Citrate Plasma

(EDTA: ethylene diamine tetra acetic acid, ELISA: enzyme-linked immunosorbent assay, IQR: interquartile range; IQR: interquartile range; MSIA: magnetic beads supported immunoassay, RIA: radioimmunoassay; SD: standard deviation) [122–127]

Supplementary Table 3: Calculated mass spectrometric peptide fragment pattern of Substance P and human Hemokinin-1

(A)

<b>b</b> Fragment [m/z]	<b>b<sup>+2</sup></b> Fragment [m/z]	<b>AA</b> Position	<b>AA</b>	<b>AA</b> Position	<b>y</b> Fragment [m/z]	<b>y<sup>+2</sup></b> Fragment [m/z]
---	---	1	<b>R</b>	11	---	---
254.1612	127.5842	2	<b>P</b>	10	1191.6343	596.3208
382.2561	191.6317	3	<b>K</b>	9	1094.5815	547.7944
479.3089	240.1581	4	<b>P</b>	8	966.4866	---
607.3675	304.1874	5	<b>Q</b>	7	869.4338	---
735.4260	368.2167	6	<b>Q</b>	6	741.3752	---
882.4944	441.7509	7	<b>F</b>	5	613.3167	---
1029.5629	515.2851	8	<b>F</b>	4	466.2483	---
1086.5843	543.7958	9	<b>G</b>	3	319.1798	---
1199.6684	600.3378	10	<b>L</b>	2	262.1584	---
---	---	11	<b>M</b>	1	149.0743	---
			<b>Amidated</b>			

(B)

<b>b</b> Fragment [m/z]	<b>b<sup>+2</sup></b> Fragment [m/z]	<b>AA</b> Position	<b>AA</b>	<b>AA</b> Position	<b>y</b> Fragment [m/z]	<b>y<sup>+2</sup></b> Fragment [m/z]
---	---	1	<b>T</b>	11	---	---
<b>159.0764</b>	---	2	<b>G</b>	10	1084.5608	542.7840
<b>287.1714</b>	144.0893	3	<b>K</b>	9	1027.5393	514.2733
<b>358.2085</b>	179.6079	4	<b>A</b>	8	899.4444	---
<b>445.2405</b>	223.1239	5	<b>S</b>	7	828.4073	---
<b>573.2991</b>	287.1532	6	<b>Q</b>	6	741.3752	---
<b>720.3675</b>	360.6874	7	<b>F</b>	5	613.3167	---
<b>867.4359</b>	434.2216	8	<b>F</b>	4	466.2483	---
<b>924.4574</b>	462.7323	9	<b>G</b>	3	319.1798	---
<b>1037.5415</b>	519.2744	10	<b>L</b>	2	262.1584	---
---	---	11	<b>M</b>	1	149.0743	---
			<b>Amidated</b>			

The amino acid sequences of (A) Substance P and (B) human Hemokinin-1 are shown in the one-letter code. Source: Protein Prospector (ExPaSy, SIB Swiss Institute of Bioinformatics) (AA: Amino acid; m/z: mass to charge ratio)

*Supplementary Table 4: Worksheet for the optimization of the injection solvent composition within the Design of Experiments concept.*

<b>Experiment</b>	<b>Run Order</b>	<b>Material</b>	<b>Type of Organic</b>	<b>DMSO fraction</b>	<b>Water fraction</b>	<b>Formic acid fraction</b>	<b>Organic fraction</b>
1	45	LB Eppendorf	MeOH	0	1	0	0
2	23	LB Eppendorf	MeOH	0.25	0.25	0	0.5
3	38	LB Eppendorf	MeOH	0	0.4	0.1	0.5
4	32	LB Eppendorf	MeOH	0.7	0.25	0.05	0
5	114	LB Eppendorf	MeOH	0.325	0.575	0.1	0
6	100	LB Sarstedt	MeOH	0	1	0	0
7	133	LB Sarstedt	MeOH	0.65	0.25	0.1	0
8	132	LB Sarstedt	MeOH	0.25	0.25	0	0.5
9	36	LB Sarstedt	MeOH	0	0.4	0.1	0.5
10	31	Eppendorf	MeOH	0	0.9	0.1	0
11	76	Eppendorf	MeOH	0.65	0.25	0.1	0
12	125	Eppendorf	MeOH	0.375	0.625	0	0
13	1	Eppendorf	MeOH	0.2	0.25	0.05	0.5
14	104	Sarstedt	MeOH	0.75	0.25	0	0
15	106	Sarstedt	MeOH	0	0.9	0.1	0
16	81	Sarstedt	MeOH	0	0.5	0	0.5
17	98	Sarstedt	MeOH	0.4	0.25	0.1	0.25
18	124	Glass vial	MeOH	0.75	0.25	0	0
19	119	Glass vial	MeOH	0	0.9	0.1	0
20	29	Glass vial	MeOH	0.15	0.25	0.1	0.5
21	78	Glass vial	MeOH	0	0.75	0	0.25
22	34	LB Eppendorf	ACN	0	0.9	0.1	0
23	107	LB Eppendorf	ACN	0.65	0.25	0.1	0
24	41	LB Eppendorf	ACN	0	0.45	0.05	0.5
25	4	LB Eppendorf	ACN	0.375	0.625	0	0
26	112	LB Sarstedt	ACN	0.75	0.25	0	0
27	123	LB Sarstedt	ACN	0	0.9	0.1	0
28	87	LB Sarstedt	ACN	0	0.5	0	0.5
29	99	LB Sarstedt	ACN	0.15	0.25	0.1	0.5
30	90	Eppendorf	ACN	0	1	0	0
31	27	Eppendorf	ACN	0.75	0.25	0	0
32	28	Eppendorf	ACN	0	0.5	0	0.5
33	26	Eppendorf	ACN	0.15	0.25	0.1	0.5
34	64	Eppendorf	ACN	0.35	0.6	0.05	0
35	135	Sarstedt	ACN	0	1	0	0

## 9. Appendix

36	113	Sarstedt	ACN	0.65	0.25	0.1	0
37	105	Sarstedt	ACN	0	0.4	0.1	0.5
38	129	Sarstedt	ACN	0.5	0.25	0	0.25
39	70	Glass vial	ACN	0	1	0	0
40	93	Glass vial	ACN	0.65	0.25	0.1	0
41	6	Glass vial	ACN	0.25	0.25	0	0.5
42	71	Glass vial	ACN	0	0.65	0.1	0.25
43	60	Glass vial	ACN	0.225	0.475	0.05	0.25
44	80	Glass vial	ACN	0.225	0.475	0.05	0.25
45	127	Glass vial	ACN	0.225	0.475	0.05	0.25
46	94	LB Eppendorf	MeOH	0	1	0	0
47	21	LB Eppendorf	MeOH	0.25	0.25	0	0.5
48	11	LB Eppendorf	MeOH	0	0.4	0.1	0.5
49	79	LB Eppendorf	MeOH	0.7	0.25	0.05	0
50	97	LB Eppendorf	MeOH	0.325	0.575	0.1	0
51	96	LB Sarstedt	MeOH	0	1	0	0
52	48	LB Sarstedt	MeOH	0.65	0.25	0.1	0
53	12	LB Sarstedt	MeOH	0.25	0.25	0	0.5
54	68	LB Sarstedt	MeOH	0	0.4	0.1	0.5
55	89	Eppendorf	MeOH	0	0.9	0.1	0
56	128	Eppendorf	MeOH	0.65	0.25	0.1	0
57	30	Eppendorf	MeOH	0.375	0.625	0	0
58	53	Eppendorf	MeOH	0.2	0.25	0.05	0.5
59	35	Sarstedt	MeOH	0.75	0.25	0	0
60	95	Sarstedt	MeOH	0	0.9	0.1	0
61	13	Sarstedt	MeOH	0	0.5	0	0.5
62	25	Sarstedt	MeOH	0.4	0.25	0.1	0.25
63	115	Glass vial	MeOH	0.75	0.25	0	0
64	67	Glass vial	MeOH	0	0.9	0.1	0
65	88	Glass vial	MeOH	0.15	0.25	0.1	0.5
66	102	Glass vial	MeOH	0	0.75	0	0.25
67	16	LB Eppendorf	ACN	0	0.9	0.1	0
68	116	LB Eppendorf	ACN	0.65	0.25	0.1	0
69	77	LB Eppendorf	ACN	0	0.45	0.05	0.5
70	91	LB Eppendorf	ACN	0.375	0.625	0	0
71	131	LB Sarstedt	ACN	0.75	0.25	0	0
72	37	LB Sarstedt	ACN	0	0.9	0.1	0
73	2	LB Sarstedt	ACN	0	0.5	0	0.5
74	14	LB Sarstedt	ACN	0.15	0.25	0.1	0.5
75	82	Eppendorf	ACN	0	1	0	0

## 9. Appendix

76	74	Eppendorf	ACN	0.75	0.25	0	0
77	51	Eppendorf	ACN	0	0.5	0	0.5
78	92	Eppendorf	ACN	0.15	0.25	0.1	0.5
79	56	Eppendorf	ACN	0.35	0.6	0.05	0
80	61	Sarstedt	ACN	0	1	0	0
81	57	Sarstedt	ACN	0.65	0.25	0.1	0
82	130	Sarstedt	ACN	0	0.4	0.1	0.5
83	86	Sarstedt	ACN	0.5	0.25	0	0.25
84	49	Glass vial	ACN	0	1	0	0
85	8	Glass vial	ACN	0.65	0.25	0.1	0
86	55	Glass vial	ACN	0.25	0.25	0	0.5
87	108	Glass vial	ACN	0	0.65	0.1	0.25
88	83	Glass vial	ACN	0.225	0.475	0.05	0.25
89	54	Glass vial	ACN	0.225	0.475	0.05	0.25
90	121	Glass vial	ACN	0.225	0.475	0.05	0.25
91	66	LB Eppendorf	MeOH	0	1	0	0
92	122	LB Eppendorf	MeOH	0.25	0.25	0	0.5
93	10	LB Eppendorf	MeOH	0	0.4	0.1	0.5
94	126	LB Eppendorf	MeOH	0.7	0.25	0.05	0
95	19	LB Eppendorf	MeOH	0.325	0.575	0.1	0
96	46	LB Sarstedt	MeOH	0	1	0	0
97	42	LB Sarstedt	MeOH	0.65	0.25	0.1	0
98	120	LB Sarstedt	MeOH	0.25	0.25	0	0.5
99	39	LB Sarstedt	MeOH	0	0.4	0.1	0.5
100	117	Eppendorf	MeOH	0	0.9	0.1	0
101	44	Eppendorf	MeOH	0.65	0.25	0.1	0
102	85	Eppendorf	MeOH	0.375	0.625	0	0
103	111	Eppendorf	MeOH	0.2	0.25	0.05	0.5
104	59	Sarstedt	MeOH	0.75	0.25	0	0
105	33	Sarstedt	MeOH	0	0.9	0.1	0
106	69	Sarstedt	MeOH	0	0.5	0	0.5
107	109	Sarstedt	MeOH	0.4	0.25	0.1	0.25
108	9	Glass vial	MeOH	0.75	0.25	0	0
109	15	Glass vial	MeOH	0	0.9	0.1	0
110	5	Glass vial	MeOH	0.15	0.25	0.1	0.5
111	17	Glass vial	MeOH	0	0.75	0	0.25
112	101	LB Eppendorf	ACN	0	0.9	0.1	0
113	43	LB Eppendorf	ACN	0.65	0.25	0.1	0
114	52	LB Eppendorf	ACN	0	0.45	0.05	0.5
115	58	LB Eppendorf	ACN	0.375	0.625	0	0

## 9. Appendix

<b>116</b>	50	LB Sarstedt	ACN	0.75	0.25	0	0
<b>117</b>	63	LB Sarstedt	ACN	0	0.9	0.1	0
<b>118</b>	72	LB Sarstedt	ACN	0	0.5	0	0.5
<b>119</b>	18	LB Sarstedt	ACN	0.15	0.25	0.1	0.5
<b>120</b>	65	Eppendorf	ACN	0	1	0	0
<b>121</b>	75	Eppendorf	ACN	0.75	0.25	0	0
<b>122</b>	103	Eppendorf	ACN	0	0.5	0	0.5
<b>123</b>	7	Eppendorf	ACN	0.15	0.25	0.1	0.5
<b>124</b>	22	Eppendorf	ACN	0.35	0.6	0.05	0
<b>125</b>	134	Sarstedt	ACN	0	1	0	0
<b>126</b>	24	Sarstedt	ACN	0.65	0.25	0.1	0
<b>127</b>	62	Sarstedt	ACN	0	0.4	0.1	0.5
<b>128</b>	84	Sarstedt	ACN	0.5	0.25	0	0.25
<b>129</b>	20	Glass vial	ACN	0	1	0	0
<b>130</b>	40	Glass vial	ACN	0.65	0.25	0.1	0
<b>131</b>	3	Glass vial	ACN	0.25	0.25	0	0.5
<b>132</b>	118	Glass vial	ACN	0	0.65	0.1	0.25
<b>133</b>	73	Glass vial	ACN	0.225	0.475	0.05	0.25
<b>134</b>	47	Glass vial	ACN	0.225	0.475	0.05	0.25
<b>135</b>	110	Glass vial	ACN	0.225	0.475	0.05	0.25

(ACN: acetonitrile, DMSO: dimethyl sulfoxide, LB: protein low binding; MeOH: methanol)

*Supplementary Table 5: Worksheet for the selection of the most appropriate deep-well plates within the Design of Experiments concept.*

<b>Experiment</b>	<b>Run Order</b>	<b>Material</b>	<b>Solution</b>
1	1	Eppendorf LB-PP	aqueous
2	45	Sarstedt PP	aqueous
3	48	Sarstedt PS	aqueous
4	11	Brand PP	aqueous
5	66	Brand PS	aqueous
6	41	Corning PP	aqueous
7	7	Waters PP	aqueous
22	22	Eppendorf LB-PP	aqueous
23	16	Eppendorf LB-PP	aqueous
24	68	Eppendorf LB-PP	aqueous
25	72	Eppendorf LB-PP	aqueous
26	17	Sarstedt PP	aqueous
27	37	Sarstedt PS	aqueous
28	46	Brand PP	aqueous
29	34	Brand PS	aqueous
30	14	Corning PP	aqueous
31	63	Waters PP	aqueous
46	27	Eppendorf LB-PP	aqueous
47	50	Eppendorf LB-PP	aqueous
48	13	Eppendorf LB-PP	aqueous
49	9	Eppendorf LB-PP	aqueous
50	10	Sarstedt PP	aqueous
51	5	Sarstedt PS	aqueous
52	67	Brand PP	aqueous
53	35	Brand PS	aqueous
54	51	Corning PP	aqueous
55	29	Waters PP	aqueous
70	70	Eppendorf LB-PP	aqueous
71	20	Eppendorf LB-PP	aqueous
72	56	Eppendorf LB-PP	aqueous
8	39	Eppendorf LB-PP	sweet spot LowBind
9	54	Sarstedt PP	sweet spot LowBind
10	53	Sarstedt PS	sweet spot LowBind
11	26	Brand PP	sweet spot LowBind
12	8	Brand PS	sweet spot LowBind

## 9. Appendix

13	58	Corning PP	sweet spot LowBind
14	65	Waters PP	sweet spot LowBind
32	59	Eppendorf LB-PP	sweet spot LowBind
33	60	Sarstedt PP	sweet spot LowBind
34	57	Sarstedt PS	sweet spot LowBind
35	32	Brand PP	sweet spot LowBind
36	12	Brand PS	sweet spot LowBind
37	71	Corning PP	sweet spot LowBind
38	44	Waters PP	sweet spot LowBind
56	55	Eppendorf LB-PP	sweet spot LowBind
57	62	Sarstedt PP	sweet spot LowBind
58	47	Sarstedt PS	sweet spot LowBind
59	23	Brand PP	sweet spot LowBind
60	19	Brand PS	sweet spot LowBind
61	64	Corning PP	sweet spot LowBind
62	3	Waters PP	sweet spot LowBind
15	31	Eppendorf LB-PP	sweet spot regular
16	4	Sarstedt PP	sweet spot regular
17	40	Sarstedt PS	sweet spot regular
18	61	Brand PP	sweet spot regular
19	33	Brand PS	sweet spot regular
20	43	Corning PP	sweet spot regular
21	49	Waters PP	sweet spot regular
39	25	Eppendorf LB-PP	sweet spot regular
40	21	Sarstedt PP	sweet spot regular
41	38	Sarstedt PS	sweet spot regular
42	69	Brand PP	sweet spot regular
43	36	Brand PS	sweet spot regular
44	15	Corning PP	sweet spot regular
45	2	Waters PP	sweet spot regular
63	28	Eppendorf LB-PP	sweet spot regular
64	18	Sarstedt PP	sweet spot regular
65	30	Sarstedt PS	sweet spot regular
66	24	Brand PP	sweet spot regular
67	52	Brand PS	sweet spot regular
68	42	Corning PP	sweet spot regular
69	6	Waters PP	sweet spot regular

*The compositions of the solutions were as follows: aqueous (water:formic acid (90/10 [v/v])), sweet spot LowBind (water:dimethyl sulfoxide:formic acid (45/45/10 [v/v/v])), sweet spot*

*regular (water:methanol:dimethyl sulfoxide:formic acid (25/50/15/10 [v/v/v/v])). (LB: low binding, PP: polypropylene, PS: polystyrene)*

*Supplementary Table 6: Worksheet for the selection of the most appropriate tips within the Design of Experiments concept.*

<b>Experiment</b>	<b>Run Order</b>	<b>Plates</b>	<b>Solution</b>	<b>Pipette tips</b>
1	61	LowBind PP	aqueous	LowBind tips
2	31	regular PP	aqueous	LowBind tips
3	69	regular PP	sweet spot LowBind	LowBind tips
4	54	LowBind PP	sweet spot regular	LowBind tips
5	80	LowBind PP	aqueous	Low Retention tips
6	48	LowBind PP	sweet spot LowBind	Low Retention tips
7	30	regular PP	sweet spot LowBind	Low Retention tips
8	27	regular PP	sweet spot regular	Low Retention tips
9	28	regular PP	aqueous	regular tips
10	25	LowBind PP	sweet spot LowBind	regular tips
11	9	LowBind PP	sweet spot regular	regular tips
12	72	regular PP	sweet spot regular	regular tips
13	12	LowBind PP	aqueous	LowBind tips
14	3	regular PP	aqueous	LowBind tips
15	26	LowBind PP	sweet spot LowBind	LowBind tips
16	65	regular PP	sweet spot regular	LowBind tips
17	11	regular PP	aqueous	Low Retention tips
18	35	LowBind PP	sweet spot LowBind	Low Retention tips
19	50	regular PP	sweet spot LowBind	Low Retention tips
20	42	LowBind PP	sweet spot regular	Low Retention tips
21	53	LowBind PP	aqueous	regular tips
22	36	regular PP	sweet spot LowBind	regular tips
23	57	LowBind PP	sweet spot regular	regular tips
24	62	regular PP	sweet spot regular	regular tips
25	66	regular PP	sweet spot regular	regular tips
26	24	regular PP	sweet spot regular	regular tips
27	55	regular PP	sweet spot regular	regular tips
28	67	LowBind PP	aqueous	LowBind tips
29	70	regular PP	aqueous	LowBind tips
30	46	regular PP	sweet spot LowBind	LowBind tips
31	7	LowBind PP	sweet spot regular	LowBind tips
32	59	LowBind PP	aqueous	Low Retention tips
33	76	LowBind PP	sweet spot LowBind	Low Retention tips
34	73	regular PP	sweet spot LowBind	Low Retention tips
35	71	regular PP	sweet spot regular	Low Retention tips
36	75	regular PP	aqueous	regular tips

37	43	LowBind PP	sweet spot LowBind	regular tips
38	52	LowBind PP	sweet spot regular	regular tips
39	51	regular PP	sweet spot regular	regular tips
40	56	LowBind PP	aqueous	LowBind tips
41	10	regular PP	aqueous	LowBind tips
42	18	LowBind PP	sweet spot LowBind	LowBind tips
43	78	regular PP	sweet spot regular	LowBind tips
44	19	regular PP	aqueous	Low Retention tips
45	40	LowBind PP	sweet spot LowBind	Low Retention tips
46	16	regular PP	sweet spot LowBind	Low Retention tips
47	2	LowBind Eppendorf PP	sweet spot regular	Low Retention tips
48	45	LowBind PP	aqueous	regular tips
49	79	regular PP	sweet spot LowBind	regular tips
50	44	LowBind PP	sweet spot regular	regular tips
51	34	regular PP	sweet spot regular	regular tips
52	29	regular PP	sweet spot regular	regular tips
53	8	regular PP	sweet spot regular	regular tips
54	21	regular PP	sweet spot regular	regular tips
55	22	LowBind PP	aqueous	LowBind tips
56	14	regular PP	aqueous	LowBind tips
57	41	regular PP	sweet spot LowBind	LowBind tips
58	64	LowBind PP	sweet spot regular	LowBind tips
59	63	LowBind PP	aqueous	Low Retention tips
60	58	LowBind PP	sweet spot LowBind	Low Retention tips
61	47	regular PP	sweet spot LowBind	Low Retention tips
62	77	regular PP	sweet spot regular	Low Retention tips
63	32	regular PP	aqueous	regular tips
64	1	LowBind PP	sweet spot LowBind	regular tips
65	49	LowBind PP	sweet spot regular	regular tips
66	20	regular PP	sweet spot regular	regular tips
67	39	LowBind PP	aqueous	LowBind tips
68	4	regular PP	aqueous	LowBind tips
69	38	LowBind PP	sweet spot LowBind	LowBind tips
70	37	regular PP	sweet spot regular	LowBind tips
71	6	regular PP	aqueous	Low Retention tips
72	68	LowBind PP	sweet spot LowBind	Low Retention tips
73	60	regular PP	sweet spot LowBind	Low Retention tips
74	81	LowBind PP	sweet spot regular	Low Retention tips
75	15	LowBind PP	aqueous	regular tips
76	74	regular PP	sweet spot LowBind	regular tips

---

<b>77</b>	33	LowBind PP	sweet spot regular	regular tips
<b>78</b>	23	regular PP	sweet spot regular	regular tips
<b>79</b>	5	regular PP	sweet spot regular	regular tips
<b>80</b>	17	regular PP	sweet spot regular	regular tips
<b>81</b>	13	regular PP	sweet spot regular	regular tips

*The compositions of the solutions were as follows: aqueous (water:formic acid (90/10 [v/v])), sweet spot LowBind (water:dimethyl sulfoxide:formic acid (45/45/10 [v/v/v])), sweet spot regular (water:methanol:dimethyl sulfoxide:formic acid (25/50/15/10 [v/v/v/v])); PP: polypropylene*

*Supplementary Table 7: Worksheet for the solid phase extraction protocol within the Design of Experiments concept.*

<b>Experiment</b>	<b>Run Order</b>	<b>Organic elution fraction [%]</b>	<b>Elution volume [μL]</b>	<b>Formic acid fraction [%]</b>	<b>Organic wash fraction [%]</b>	<b>Wash volume [μL]</b>	<b>Block</b>
1	15	50	400	0	0	150	B1
2	44	50	50	0	40	150	B1
3	10	50	400	10	40	150	B1
4	12	50	50	0	0	450	B1
5	45	100	400	0	0	450	B1
6	34	50	400	10	0	450	B1
7	25	100	50	0	40	450	B1
8	40	50	400	0	40	450	B1
9	27	50	50	10	40	450	B1
10	4	90	166.667	10	0	150	B1
11	3	72.5	50	5	20	300	B1
12	20	75	225	0	20	300	B1
13	21	72.5	225	5	40	300	B1
14	13	72.5	225	5	20	450	B1
15	18	72.5	225	5	20	300	B1
16	17	72.5	225	5	20	300	B1
17	1	72.5	225	5	20	300	B1
18	43	50	400	0	0	150	B1
19	16	50	50	0	40	150	B1
20	49	50	400	10	40	150	B1
21	6	50	50	0	0	450	B1
22	29	100	400	0	0	450	B1
23	14	50	400	10	0	450	B1
24	38	100	50	0	40	450	B1
25	9	50	400	0	40	450	B1
26	33	50	50	10	40	450	B1
27	37	90	166.667	10	0	150	B1
28	47	72.5	50	5	20	300	B1
29	8	75	225	0	20	300	B1
30	28	72.5	225	5	40	300	B1
31	30	72.5	225	5	20	450	B1
32	7	72.5	225	5	20	300	B1
33	48	72.5	225	5	20	300	B1
34	2	72.5	225	5	20	300	B1

## 9. Appendix

35	32	50	400	0	0	150	B1
36	24	50	50	0	40	150	B1
37	46	50	400	10	40	150	B1
38	26	50	50	0	0	450	B1
39	42	100	400	0	0	450	B1
40	19	50	400	10	0	450	B1
41	5	100	50	0	40	450	B1
42	22	50	400	0	40	450	B1
43	11	50	50	10	40	450	B1
44	23	90	166.667	10	0	150	B1
45	41	72.5	50	5	20	300	B1
46	39	75	225	0	20	300	B1
47	35	72.5	225	5	40	300	B1
48	51	72.5	225	5	20	450	B1
49	36	72.5	225	5	20	300	B1
50	31	72.5	225	5	20	300	B1
51	50	72.5	225	5	20	300	B1
52	69	100	50	0	0	150	B2
53	59	50	50	10	0	150	B2
54	72	100	400	0	40	150	B2
55	84	90	400	10	0	150	B2
56	77	90	50	10	40	150	B2
57	78	90	50	10	0	450	B2
58	55	90	400	10	40	450	B2
59	74	66.6667	50	0	40	450	B2
60	60	66.6667	400	0	0	450	B2
61	56	50	225	5	20	300	B2
62	86	72.5	225	5	20	300	B2
63	80	72.5	225	5	20	300	B2
64	70	72.5	225	5	20	300	B2
65	88	100	50	0	0	150	B2
66	79	50	50	10	0	150	B2
67	81	100	400	0	40	150	B2
68	57	90	400	10	0	150	B2
69	52	90	50	10	40	150	B2
70	76	90	50	10	0	450	B2
71	87	90	400	10	40	450	B2
72	89	66.6667	50	0	40	450	B2
73	66	66.6667	400	0	0	450	B2
74	62	50	225	5	20	300	B2

## 9. Appendix

---

<b>75</b>	85	72.5	225	5	20	300	B2
<b>76</b>	73	72.5	225	5	20	300	B2
<b>77</b>	54	72.5	225	5	20	300	B2
<b>78</b>	90	100	50	0	0	150	B2
<b>79</b>	64	50	50	10	0	150	B2
<b>80</b>	75	100	400	0	40	150	B2
<b>81</b>	83	90	400	10	0	150	B2
<b>82</b>	63	90	50	10	40	150	B2
<b>83</b>	53	90	50	10	0	450	B2
<b>84</b>	68	90	400	10	40	450	B2
<b>85</b>	82	66.6667	50	0	40	450	B2
<b>86</b>	65	66.6667	400	0	0	450	B2
<b>87</b>	61	50	225	5	20	300	B2
<b>88</b>	58	72.5	225	5	20	300	B2
<b>89</b>	71	72.5	225	5	20	300	B2
<b>90</b>	67	72.5	225	5	20	300	B2

*Supplementary Table 8: Worksheet for the chromatographic gradient within the Design of Experiments concept.*

<b>Experiment</b>	<b>Run Order</b>	<b>Oven temperature [°C]</b>	<b>Organic elution fraction [%]</b>	<b>Gradient phase 1 [min]</b>	<b>Gradient phase 2 [min]</b>	<b>Gradient phase 3 [min]</b>
1	12	45	50	5	0.1	0.1
4	67	45	100	5	3	0.1
5	90	45	100	0	3	3
6	31	45	50	5	3	3
7	6	45	50	0	0.1	2.03333
8	97	45	50	0	3	1.06667
9	19	45	50	0	1.06667	3
10	62	45	50	3.33333	3	0.1
11	1	45	100	0	2.03333	0.1
12	75	45	100	5	0.1	1.06667
13	101	45	100	1.66667	0.1	3
14	22	45	83.3333	0	0.1	0.1
15	37	45	83.3333	5	0.1	3
38	68	45	50	5	0.1	0.1
41	30	45	100	5	3	0.1
42	33	45	100	0	3	3
43	21	45	50	5	3	3
44	9	45	50	0	0.1	2.03333
45	48	45	50	0	3	1.06667
46	26	45	50	0	1.06667	3
47	23	45	50	3.33333	3	0.1
48	29	45	100	0	2.03333	0.1
49	83	45	100	5	0.1	1.06667
50	80	45	100	1.66667	0.1	3
51	58	45	83.3333	0	0.1	0.1
52	100	45	83.3333	5	0.1	3
75	45	45	50	5	0.1	0.1
78	63	45	100	5	3	0.1
79	25	45	100	0	3	3
80	56	45	50	5	3	3
81	66	45	50	0	0.1	2.03333
82	84	45	50	0	3	1.06667
83	34	45	50	0	1.06667	3
84	74	45	50	3.33333	3	0.1

## 9. Appendix

85	99	45	100	0	2.03333	0.1
86	89	45	100	5	0.1	1.06667
87	109	45	100	1.66667	0.1	3
88	57	45	83.3333	0	0.1	0.1
89	41	45	83.3333	5	0.1	3
29	53	56.6667	50	0	3	0.1
30	103	56.6667	50	5	0.1	3
66	73	56.6667	50	0	3	0.1
67	43	56.6667	50	5	0.1	3
103	50	56.6667	50	0	3	0.1
104	28	56.6667	50	5	0.1	3
34	106	62.5	75	2.5	1.55	1.55
35	10	62.5	75	2.5	1.55	1.55
36	51	62.5	75	2.5	1.55	1.55
37	64	62.5	75	2.5	1.55	1.55
71	36	62.5	75	2.5	1.55	1.55
72	54	62.5	75	2.5	1.55	1.55
73	17	62.5	75	2.5	1.55	1.55
74	85	62.5	75	2.5	1.55	1.55
108	70	62.5	75	2.5	1.55	1.55
109	20	62.5	75	2.5	1.55	1.55
110	76	62.5	75	2.5	1.55	1.55
111	110	62.5	75	2.5	1.55	1.55
31	24	68.3333	100	0	0.1	3
32	61	68.3333	100	5	0.1	0.1
33	46	68.3333	100	5	3	3
68	59	68.3333	100	0	0.1	3
69	38	68.3333	100	5	0.1	0.1
70	5	68.3333	100	5	3	3
105	77	68.3333	100	0	0.1	3
106	2	68.3333	100	5	0.1	0.1
107	13	68.3333	100	5	3	3
2	94	80	100	0	3	0.1
3	40	80	50	5	3	0.1
16	86	80	50	0	1.06667	0.1
17	7	80	50	0	2.03333	3
18	8	80	50	5	0.1	1.06667
19	104	80	50	1.66667	0.1	3
20	71	80	50	3.33333	3	3
21	18	80	100	0	0.1	2.03333

9. Appendix

22	107	80	100	5	1.06667	3
23	96	80	100	3.33333	0.1	0.1
24	32	80	100	1.66667	3	3
25	39	80	66.6667	0	0.1	0.1
26	14	80	66.6667	0	3	3
27	91	80	66.6667	5	0.1	3
28	98	80	83.3333	5	3	0.1
39	60	80	100	0	3	0.1
40	42	80	50	5	3	0.1
53	69	80	50	0	1.06667	0.1
54	88	80	50	0	2.03333	3
55	82	80	50	5	0.1	1.06667
56	52	80	50	1.66667	0.1	3
57	111	80	50	3.33333	3	3
58	78	80	100	0	0.1	2.03333
59	108	80	100	5	1.06667	3
60	102	80	100	3.33333	0.1	0.1
61	4	80	100	1.66667	3	3
62	15	80	66.6667	0	0.1	0.1
63	87	80	66.6667	0	3	3
64	55	80	66.6667	5	0.1	3
65	72	80	83.3333	5	3	0.1
76	79	80	100	0	3	0.1
77	11	80	50	5	3	0.1
90	105	80	50	0	1.06667	0.1
91	16	80	50	0	2.03333	3
92	81	80	50	5	0.1	1.06667
93	92	80	50	1.66667	0.1	3
94	47	80	50	3.33333	3	3
95	3	80	100	0	0.1	2.03333
96	49	80	100	5	1.06667	3
97	35	80	100	3.33333	0.1	0.1
98	95	80	100	1.66667	3	3
99	93	80	66.6667	0	0.1	0.1
100	27	80	66.6667	0	3	3
101	44	80	66.6667	5	0.1	3
102	65	80	83.3333	5	3	0.1

*Supplementary Table 9: Worksheet for the ion source parameters within the Design of Experiments concept.*

<b>Experiment</b>	<b>Run Order</b>	<b>Curtain gas [psi]</b>	<b>Nebulizer gas [psi]</b>	<b>Heater gas [psi]</b>	<b>Ion spray voltage [eV]</b>	<b>Ion source temperature [°C]</b>
1	3	31.25	50	50	4000	425
2	80	43.75	70	70	5000	425
3	33	43.75	70	70	4000	575
4	46	43.75	70	50	5000	575
5	68	43.75	50	70	5000	575
6	96	31.25	70	70	5000	575
7	34	31.25	50	50	4000	425
8	22	43.75	70	70	5000	425
9	84	43.75	70	70	4000	575
10	92	43.75	70	50	5000	575
11	89	43.75	50	70	5000	575
12	82	31.25	70	70	5000	575
13	50	31.25	50	50	4000	425
14	31	43.75	70	70	5000	425
15	7	43.75	70	70	4000	575
16	12	43.75	70	50	5000	575
17	23	43.75	50	70	5000	575
18	25	31.25	70	70	5000	575
19	91	25	40	80	3500	350
20	20	50	80	80	3500	350
21	45	25	40	40	5500	350
22	17	50	80	40	5500	350
23	15	50	40	80	5500	350
24	19	25	80	80	5500	350
25	5	25	40	40	3500	650
26	6	50	40	80	3500	650
27	8	50	40	40	5500	650
28	10	25	80	40	5500	650
29	24	25	40	80	5500	650
30	62	50	80	80	5500	650
31	21	25	80	40	4166.67	350
32	69	25	80	66.6667	3500	650
33	42	25	53.3333	40	3500	350
34	52	25	66.6667	80	3500	650

## 9. Appendix

35	86	50	40	40	4166.67	350
36	55	50	80	40	3500	550
37	79	50	80	40	4833.33	650
38	74	50	66.6667	40	3500	650
39	28	41.6667	40	40	3500	350
40	4	50	60	60	4500	500
41	14	37.5	60	80	4500	500
42	59	37.5	60	60	4500	650
43	11	37.5	60	60	4500	500
44	58	37.5	60	60	4500	500
45	36	37.5	60	60	4500	500
46	76	25	40	80	3500	350
47	26	50	80	80	3500	350
48	67	25	40	40	5500	350
49	71	50	80	40	5500	350
50	38	50	40	80	5500	350
51	66	25	80	80	5500	350
52	44	25	40	40	3500	650
53	78	50	40	80	3500	650
54	70	50	40	40	5500	650
55	85	25	80	40	5500	650
56	61	25	40	80	5500	650
57	47	50	80	80	5500	650
58	73	25	80	40	4166.67	350
59	32	25	80	66.6667	3500	650
60	51	25	53.3333	40	3500	350
61	77	25	66.6667	80	3500	650
62	53	50	40	40	4166.67	350
63	27	50	80	40	3500	550
64	95	50	80	40	4833.33	650
65	88	50	66.6667	40	3500	650
66	83	41.6667	40	40	3500	350
67	2	50	60	60	4500	500
68	57	37.5	60	80	4500	500
69	90	37.5	60	60	4500	650
70	97	37.5	60	60	4500	500
71	35	37.5	60	60	4500	500
72	1	37.5	60	60	4500	500
73	16	25	40	80	3500	350
74	39	50	80	80	3500	350

9. Appendix

75	64	25	40	40	5500	350
76	18	50	80	40	5500	350
77	41	50	40	80	5500	350
78	40	25	80	80	5500	350
79	81	25	40	40	3500	650
80	37	50	40	80	3500	650
81	87	50	40	40	5500	650
82	43	25	80	40	5500	650
83	65	25	40	80	5500	650
84	60	50	80	80	5500	650
85	29	25	80	40	4166.67	350
86	56	25	80	66.6667	3500	650
87	72	25	53.3333	40	3500	350
88	63	25	66.6667	80	3500	650
89	48	50	40	40	4166.67	350
90	93	50	80	40	3500	550
91	94	50	80	40	4833.33	650
92	49	50	66.6667	40	3500	650
93	54	41.6667	40	40	3500	350
94	30	50	60	60	4500	500
95	98	37.5	60	80	4500	500
96	75	37.5	60	60	4500	650
97	99	37.5	60	60	4500	500
98	13	37.5	60	60	4500	500
99	9	37.5	60	60	4500	500

*Supplementary Table 10: Multiquant Data of the 1. run to determine the accuracy and precision of the method.*

<b>Sample Name</b>	<b>Sample Type</b>	<b>Analyte</b>	<b>Actual Conc.</b>	<b>Area Ratio</b>	<b>Used</b>	<b>Calculated Conc.</b>	<b>Accuracy</b>
<b>K9</b>	Standard	SP	7.8	0.15	True	7.67	98.28
<b>K8</b>	Standard	SP	15.6	0.35	True	16.88	108.21
<b>K7</b>	Standard	SP	31.25	0.60	True	28.30	90.56
<b>K6</b>	Standard	SP	62.5	0.97	False	45.14	72.22
<b>K5</b>	Standard	SP	125	2.68	True	123.10	98.47
<b>K4</b>	Standard	SP	250	3.69	False	169.00	67.61
<b>K3</b>	Standard	SP	500	11.30	True	515.70	103.13
<b>K2</b>	Standard	SP	1000	22.27	True	1015.00	101.48
<b>K1</b>	Standard	SP	2000	43.85	True	1997.00	99.85
<b>Blank</b>	Double Blank	SP	N/A	2.77	True	N/A	N/A
<b>Zero</b>	Blank	SP	N/A	0.03	True	2.49	N/A
<b>QC4_1</b>	Quality Control	SP	7.8	0.17	True	8.85	113.43
<b>QC4_2</b>	Quality Control	SP	7.8	0.16	True	8.29	106.3
<b>QC4_3</b>	Quality Control	SP	7.8	0.14	True	7.28	93.34
<b>QC4_4</b>	Quality Control	SP	7.8	0.14	True	7.59	97.33
<b>QC4_5</b>	Quality Control	SP	7.8	0.17	True	8.93	114.46
<b>QC3_1</b>	Quality Control	SP	15.6	0.37	True	17.94	114.98
<b>QC3_2</b>	Quality Control	SP	15.6	0.34	True	16.56	106.14
<b>QC3_3</b>	Quality Control	SP	15.6	0.35	True	17.18	110.11
<b>QC3_4</b>	Quality Control	SP	15.6	0.29	True	14.40	92.3
<b>QC3_5</b>	Quality Control	SP	15.6	0.35	True	17.11	109.7
<b>QC2_1</b>	Quality Control	SP	1000	23.42	True	1067.00	106.71
<b>QC2_2</b>	Quality Control	SP	1000	24.56	True	1119.00	111.91
<b>QC2_3</b>	Quality Control	SP	1000	24.76	True	1128.00	112.8
<b>QC2_4</b>	Quality Control	SP	1000	24.97	True	1138.00	113.75

## 9. Appendix

<b>QC2_5</b>	Quality Control	SP	1000	23.33	True	1063.00	106.29
<b>QC1_1</b>	Quality Control	SP	2000	49.96	True	2275.00	113.76
<b>QC1_2</b>	Quality Control	SP	2000	49.59	True	2258.00	112.92
<b>QC1_3</b>	Quality Control	SP	2000	52.45	True	2389.00	119.43
<b>QC1_4</b>	Quality Control	SP	2000	48.26	True	2198.00	109.89
<b>QC1_5</b>	Quality Control	SP	2000	49.64	True	2261.00	113.04
<b>Sample Name</b>	<b>Sample Type</b>	<b>Analyte</b>	<b>Actual Conc.</b>	<b>Area Ratio</b>	<b>Used</b>	<b>Calculated Conc.</b>	<b>Accuracy</b>
<b>K9</b>	Standard	hHK1	7.8	0.35	True	7.64	97.96
<b>K8</b>	Standard	hHK1	15.6	0.80	False	20.55	131.75
<b>K7</b>	Standard	hHK1	31.25	1.29	True	34.62	110.78
<b>K6</b>	Standard	hHK1	62.5	2.10	True	57.85	92.56
<b>K5</b>	Standard	hHK1	125	4.69	True	131.90	105.49
<b>K4</b>	Standard	hHK1	250	6.32	False	178.50	71.39
<b>K3</b>	Standard	hHK1	500	17.30	True	492.50	98.5
<b>K2</b>	Standard	hHK1	1000	33.54	True	957.00	95.7
<b>K1</b>	Standard	hHK1	2000	69.32	True	1980.00	99.01
<b>Blank</b>	Double Blank	hHK1	N/A	5.53	True	N/A	N/A
<b>Zero</b>	Blank	hHK1	N/A	0.49	True	11.72	N/A
<b>QC4_1</b>	Quality Control	hHK1	7.8	0.35	True	7.70	98.73
<b>QC4_2</b>	Quality Control	hHK1	7.8	0.37	True	8.34	106.95
<b>QC4_3</b>	Quality Control	hHK1	7.8	0.31	True	6.69	85.76
<b>QC4_4</b>	Quality Control	hHK1	7.8	0.38	True	8.45	108.26
<b>QC4_5</b>	Quality Control	hHK1	7.8	0.39	True	8.88	113.84
<b>QC3_1</b>	Quality Control	hHK1	15.6	0.56	True	13.65	87.49
<b>QC3_2</b>	Quality Control	hHK1	15.6	0.67	True	17.00	108.96
<b>QC3_3</b>	Quality Control	hHK1	15.6	0.71	True	17.89	114.7
<b>QC3_4</b>	Quality Control	hHK1	15.6	0.56	True	13.62	87.33
<b>QC3_5</b>	Quality Control	hHK1	15.6	0.61	True	15.17	97.27

## 9. Appendix

<b>QC2_1</b>	Quality Control	hHK1	1000	30.19	True	861.00	86.1
<b>QC2_2</b>	Quality Control	hHK1	1000	31.20	True	889.90	88.99
<b>QC2_3</b>	Quality Control	hHK1	1000	33.11	True	944.60	94.46
<b>QC2_4</b>	Quality Control	hHK1	1000	32.07	True	914.80	91.48
<b>QC2_5</b>	Quality Control	hHK1	1000	30.50	True	869.90	86.99
<b>QC1_1</b>	Quality Control	hHK1	2000	77.43	True	2212.00	110.6
<b>QC1_2</b>	Quality Control	hHK1	2000	74.66	True	2133.00	106.64
<b>QC1_3</b>	Quality Control	hHK1	2000	82.27	True	2350.00	117.52
<b>QC1_4</b>	Quality Control	hHK1	2000	66.40	True	1897.00	94.83
<b>QC1_5</b>	Quality Control	hHK1	2000	66.91	True	1911.00	95.55
<b>Sample Name</b>	Sample Type	Analyte	Actual conc.	Area Ratio	Used	Calculated conc.	Accuracy
<b>K9</b>	Standard	<i>caSP</i>	7.8	0.23	True	7.90	101.26
<b>K8</b>	Standard	<i>caSP</i>	15.6	0.56	False	21.00	134.6
<b>K7</b>	Standard	<i>caSP</i>	31.25	0.79	True	30.37	97.2
<b>K6</b>	Standard	<i>caSP</i>	62.5	1.49	True	58.20	93.13
<b>K5</b>	Standard	<i>caSP</i>	125	3.31	True	130.40	104.35
<b>K4</b>	Standard	<i>caSP</i>	250	4.27	False	168.60	67.44
<b>K3</b>	Standard	<i>caSP</i>	500	12.58	True	499.10	99.81
<b>K2</b>	Standard	<i>caSP</i>	1000	26.19	True	1040.00	104.01
<b>K1</b>	Standard	<i>caSP</i>	2000	50.45	True	2005.00	100.25
<b>Blank</b>	Double Blank	<i>caSP</i>	N/A	0.79	True	N/A	N/A
<b>Zero</b>	Blank	<i>caSP</i>	N/A	0.06	True	1.42	N/A
<b>QC4_1</b>	Quality Control	<i>caSP</i>	7.8	0.28	True	9.90	126.93
<b>QC4_2</b>	Quality Control	<i>caSP</i>	7.8	0.23	True	8.18	104.83
<b>QC4_3</b>	Quality Control	<i>caSP</i>	7.8	0.24	True	8.43	108.1
<b>QC4_4</b>	Quality Control	<i>caSP</i>	7.8	0.24	True	8.57	109.88
<b>QC4_5</b>	Quality Control	<i>caSP</i>	7.8	0.24	True	8.26	105.91
<b>QC3_1</b>	Quality Control	<i>caSP</i>	15.6	0.39	True	14.40	92.32

## 9. Appendix

<b>QC3_2</b>	Quality Control	<i>caSP</i>	15.6	0.40	True	14.65	93.94
<b>QC3_3</b>	Quality Control	<i>caSP</i>	15.6	0.48	True	17.85	114.39
<b>QC3_4</b>	Quality Control	<i>caSP</i>	15.6	0.44	True	16.29	104.41
<b>QC3_5</b>	Quality Control	<i>caSP</i>	15.6	0.37	True	13.56	86.93
<b>QC2_1</b>	Quality Control	<i>caSP</i>	1000	24.97	True	991.60	99.16
<b>QC2_2</b>	Quality Control	<i>caSP</i>	1000	23.97	True	951.80	95.18
<b>QC2_3</b>	Quality Control	<i>caSP</i>	1000	25.98	True	1032.00	103.19
<b>QC2_4</b>	Quality Control	<i>caSP</i>	1000	26.08	True	1036.00	103.6
<b>QC2_5</b>	Quality Control	<i>caSP</i>	1000	25.05	True	994.80	99.48
<b>QC1_1</b>	Quality Control	<i>caSP</i>	2000	56.69	True	2253.00	112.65
<b>QC1_2</b>	Quality Control	<i>caSP</i>	2000	54.50	True	2166.00	108.3
<b>QC1_3</b>	Quality Control	<i>caSP</i>	2000	61.31	True	2437.00	121.84
<b>QC1_4</b>	Quality Control	<i>caSP</i>	2000	54.43	True	2163.00	108.15
<b>QC1_5</b>	Quality Control	<i>caSP</i>	2000	51.48	True	2046.00	102.29

Concentration is expressed in pg/mL and the accuracy in %. (*caSP*: Carboxylic acid of Substance P, *conc*: concentration; *hHK-1*: human Hemokinin-1; *N/A*: not available; *SP*: Substance P)

*Supplementary Table 11: Multiquant Data of the 2. run to determine the accuracy and precision of the method.*

Sample Name	Sample Type	Analyte	Actual Conc.	Area Ratio	Used	Calculated Conc.	Accuracy
<b>K9</b>	Standard	SP	7.8	0.21	True	8.07	103.43
<b>K8</b>	Standard	SP	15.6	0.28	True	15.01	96.2
<b>K7</b>	Standard	SP	31.25	0.44	True	29.64	94.85
<b>K6</b>	Standard	SP	62.5	0.73	True	57.13	91.4
<b>K5</b>	Standard	SP	125	1.60	True	140.00	112.03
<b>K4</b>	Standard	SP	250	2.92	True	264.30	105.71
<b>K3</b>	Standard	SP	500	4.80	True	443.10	88.61
<b>K2</b>	Standard	SP	1000	11.88	True	1113.00	111.29
<b>K1</b>	Standard	SP	2000	20.50	True	1929.00	96.47
<b>Blank</b>	Double Blank	SP	N/A	0.29	True	N/A	N/A
<b>Zero</b>	Blank	SP	N/A	0.08	True	< 0	N/A
<b>QC4_1</b>	Quality Control	SP	7.8	0.19	True	6.38	81.73
<b>QC4_2</b>	Quality Control	SP	7.8	0.20	True	7.21	92.4
<b>QC4_3</b>	Quality Control	SP	7.8	0.21	True	8.37	107.32
<b>QC4_4</b>	Quality Control	SP	7.8	0.20	True	6.78	86.95
<b>QC4_5</b>	Quality Control	SP	7.8	0.20	True	7.53	96.59
<b>QC3_1</b>	Quality Control	SP	15.6	0.31	True	17.33	111.11
<b>QC3_2</b>	Quality Control	SP	15.6	0.29	True	15.67	100.45
<b>QC3_3</b>	Quality Control	SP	15.6	0.27	True	13.55	86.86
<b>QC3_4</b>	Quality Control	SP	15.6	0.31	True	17.22	110.42
<b>QC3_5</b>	Quality Control	SP	15.6	0.31	True	17.93	114.96
<b>QC2_1</b>	Quality Control	SP	1000	12.18	True	1142.00	114.15
<b>QC2_2</b>	Quality Control	SP	1000	11.09	True	1038.00	103.8
<b>QC2_3</b>	Quality Control	SP	1000	11.94	True	1119.00	111.9
<b>QC2_4</b>	Quality Control	SP	1000	11.95	True	1119.00	111.94

## 9. Appendix

<b>QC2_5</b>	Quality Control	SP	1000	12.47	True	1169.00	116.88
<b>QC1_1</b>	Quality Control	SP	2000	24.01	True	2262.00	113.09
<b>QC1_2</b>	Quality Control	SP	2000	21.07	True	1983.00	99.17
<b>QC1_3</b>	Quality Control	SP	2000	23.94	True	2255.00	112.75
<b>QC1_4</b>	Quality Control	SP	2000	24.84	True	2340.00	117
<b>QC1_5</b>	Quality Control	SP	2000	25.16	True	2371.00	118.53
<b>Sample Name</b>	<b>Sample Type</b>	<b>Analyte</b>	<b>Actual Conc.</b>	<b>Area Ratio</b>	<b>Used</b>	<b>Calculated Conc.</b>	<b>Accuracy</b>
<b>K9</b>	Standard	hHK1	7.8	0.20	True	8.18	104.9
<b>K8</b>	Standard	hHK1	15.6	0.28	True	13.84	88.69
<b>K7</b>	Standard	hHK1	31.25	0.42	False	24.32	77.82
<b>K6</b>	Standard	hHK1	62.5	0.94	True	62.80	100.47
<b>K5</b>	Standard	hHK1	125	1.94	True	136.10	108.88
<b>K4</b>	Standard	hHK1	250	3.73	True	267.80	107.11
<b>K3</b>	Standard	hHK1	500	6.39	True	463.60	92.72
<b>K2</b>	Standard	hHK1	1000	14.97	True	1095.00	109.52
<b>K1</b>	Standard	hHK1	2000	23.92	True	1754.00	87.69
<b>Blank</b>	Double Blank	hHK1	N/A	0.28	True	N/A	N/A
<b>Zero</b>	Blank	hHK1	N/A	0.02	True	< 0	N/A
<b>QC4_1</b>	Quality Control	hHK1	7.8	0.21	True	8.63	110.66
<b>QC4_2</b>	Quality Control	hHK1	7.8	0.19	True	7.57	97.01
<b>QC4_3</b>	Quality Control	hHK1	7.8	0.19	True	7.01	89.86
<b>QC4_4</b>	Quality Control	hHK1	7.8	0.19	True	7.21	92.45
<b>QC4_5</b>	Quality Control	hHK1	7.8	0.21	True	8.57	109.87
<b>QC3_1</b>	Quality Control	hHK1	15.6	0.30	True	15.26	97.83
<b>QC3_2</b>	Quality Control	hHK1	15.6	0.30	True	15.15	97.09
<b>QC3_3</b>	Quality Control	hHK1	15.6	0.33	True	17.25	110.57
<b>QC3_4</b>	Quality Control	hHK1	15.6	0.31	True	15.89	101.89
<b>QC3_5</b>	Quality Control	hHK1	15.6	0.33	True	17.64	113.09

## 9. Appendix

<b>QC2_1</b>	Quality Control	hHK1	1000	15.29	True	1118.00	111.83
<b>QC2_2</b>	Quality Control	hHK1	1000	13.26	True	969.20	96.92
<b>QC2_3</b>	Quality Control	hHK1	1000	14.57	True	1066.00	106.58
<b>QC2_4</b>	Quality Control	hHK1	1000	15.10	True	1105.00	110.5
<b>QC2_5</b>	Quality Control	hHK1	1000	15.31	True	1120.00	112.02
<b>QC1_1</b>	Quality Control	hHK1	2000	28.83	True	2115.00	105.77
<b>QC1_2</b>	Quality Control	hHK1	2000	25.44	True	1866.00	93.29
<b>QC1_3</b>	Quality Control	hHK1	2000	29.04	True	2131.00	106.54
<b>QC1_4</b>	Quality Control	hHK1	2000	29.10	True	2135.00	106.73
<b>QC1_5</b>	Quality Control	hHK1	2000	30.33	True	2226.00	111.28
<b>Sample Name</b>	Sample Type	Analyte	Actual Conc.	Area Ratio	Used	Calculated Conc.	Accuracy
<b>K9</b>	Standard	caSP	7.8	0.17	True	7.18	92.03
<b>K8</b>	Standard	caSP	15.6	0.29	True	17.46	111.94
<b>K7</b>	Standard	caSP	31.25	0.48	True	33.74	107.96
<b>K6</b>	Standard	caSP	62.5	0.81	True	61.49	98.38
<b>K5</b>	Standard	caSP	125	1.62	True	129.80	103.82
<b>K4</b>	Standard	caSP	250	3.15	True	260.10	104.04
<b>K3</b>	Standard	caSP	500	5.59	True	466.50	93.29
<b>K2</b>	Standard	caSP	1000	11.86	True	997.60	99.76
<b>K1</b>	Standard	caSP	2000	21.04	True	1776.00	88.78
<b>Blank</b>	Double Blank	caSP	N/A	N/A	True	N/A	N/A
<b>Zero</b>	Blank	caSP	N/A	0.01	True	< 0	N/A
<b>QC4_1</b>	Quality Control	caSP	7.8	0.17	True	7.49	96.02
<b>QC4_2</b>	Quality Control	caSP	7.8	0.18	True	8.38	107.47
<b>QC4_3</b>	Quality Control	caSP	7.8	0.17	True	7.20	92.29
<b>QC4_4</b>	Quality Control	caSP	7.8	0.17	True	7.24	92.76
<b>QC4_5</b>	Quality Control	caSP	7.8	0.18	True	8.12	104.07
<b>QC3_1</b>	Quality Control	caSP	15.6	0.28	True	16.80	107.72

## 9. Appendix

<b>QC3_2</b>	Quality Control	caSP	15.6	0.27	True	15.78	101.19
<b>QC3_3</b>	Quality Control	caSP	15.6	0.29	True	17.48	112.07
<b>QC3_4</b>	Quality Control	caSP	15.6	0.28	True	16.91	108.38
<b>QC3_5</b>	Quality Control	caSP	15.6	0.25	True	13.81	88.54
<b>QC2_1</b>	Quality Control	caSP	1000	12.99	True	1094.00	109.38
<b>QC2_2</b>	Quality Control	caSP	1000	11.48	True	965.60	96.56
<b>QC2_3</b>	Quality Control	caSP	1000	12.40	True	1044.00	104.36
<b>QC2_4</b>	Quality Control	caSP	1000	12.92	True	1088.00	108.78
<b>QC2_5</b>	Quality Control	caSP	1000	13.52	True	1138.00	113.82
<b>QC1_1</b>	Quality Control	caSP	2000	26.21	True	2214.00	110.68
<b>QC1_2</b>	Quality Control	caSP	2000	22.26	True	1879.00	93.95
<b>QC1_3</b>	Quality Control	caSP	2000	24.84	True	2097.00	104.87
<b>QC1_4</b>	Quality Control	caSP	2000	26.31	True	2223.00	111.13
<b>QC1_5</b>	Quality Control	caSP	2000	24.50	True	2069.00	103.43

*Concentration is expressed in pg/mL and the accuracy in %. (caSP: Carboxylic acid of Substance P, conc: concentration; hHK-1: human Hemokinin-1; N/A: not available; SP: Substance P)*

*Supplementary Table 12: Multiquant Data of the 3. Run to determine the accuracy and precision of the method.*

Sample Name	Sample Type	Analyte	Actual Conc.	Area Ratio	Used	Calculated Conc.	Accuracy
K9	Standard	SP	7.8	0.98	True	7.79	99.82
K8	Standard	SP	15.6	2.20	False	96.88	621
K7	Standard	SP	31.25	2.73	False	135.60	433.96
K6	Standard	SP	62.5	1.80	True	67.76	108.41
K5	Standard	SP	125	2.33	True	106.60	85.31
K4	Standard	SP	250	4.37	True	255.10	102.03
K3	Standard	SP	500	7.37	True	473.60	94.71
K2	Standard	SP	1000	15.77	True	1085.00	108.53
K1	Standard	SP	2000	28.65	True	2024.00	101.19
Blank	Double Blank	SP	N/A	519.90	True	N/A	N/A
Zero	Blank	SP	N/A	0.13	True	< 0	N/A
QC4_1	Quality Control	SP	7.8	0.98	True	7.97	102.23
QC4_2	Quality Control	SP	7.8	0.97	True	7.50	96.12
QC4_3	Quality Control	SP	7.8	0.97	True	7.55	96.79
QC4_4	Quality Control	SP	7.8	0.97	True	7.13	91.4
QC3_1	Quality Control	SP	15.6	1.08	True	15.53	99.58
QC3_2	Quality Control	SP	15.6	1.08	True	15.06	96.56
QC3_3	Quality Control	SP	15.6	1.06	True	13.84	88.72
QC3_4	Quality Control	SP	15.6	1.08	True	15.13	97
QC3_5	Quality Control	SP	15.6	1.09	True	16.11	103.26
QC2_1	Quality Control	SP	1000	15.35	True	1055.00	105.49
QC2_2	Quality Control	SP	1000	14.28	True	976.80	97.68
QC2_3	Quality Control	SP	1000	16.01	True	1103.00	110.32
QC2_4	Quality Control	SP	1000	15.74	True	1083.00	108.29
QC2_5	Quality Control	SP	1000	15.89	True	1094.00	109.44
QC1_1	Quality Control	SP	2000	26.45	True	1863.00	93.17
QC1_2	Quality Control	SP	2000	30.64	True	2169.00	108.43
QC1_3	Quality Control	SP	2000	30.97	True	2193.00	109.64
QC1_4	Quality Control	SP	2000	30.44	True	2154.00	107.71
QC1_5	Quality Control	SP	2000	26.57	True	1873.00	93.63
QC4_5	Quality Control	SP	7.8	0.97	True	7.21	92.47
Sample Name	Sample Type	Analyte	Actual Conc.	Area Ratio	Used	Calculated Conc.	Accuracy
K9	Standard	hHK1	7.8	0.11	True	7.32	93.83
K8	Standard	hHK1	15.6	0.30	True	17.71	113.54
K7	Standard	hHK1	31.25	0.51	True	28.98	92.74
K6	Standard	hHK1	62.5	1.20	True	65.99	105.58
K5	Standard	hHK1	125	2.53	True	137.50	110.03
K4	Standard	hHK1	250	4.68	True	253.20	101.3

## 9. Appendix

<b>K3</b>	Standard	hHK1	500	8.60	True	464.30	92.87
<b>K2</b>	Standard	hHK1	1000	18.74	True	1010.00	101.03
<b>K1</b>	Standard	hHK1	2000	33.08	True	1782.00	89.1
<b>Blank</b>	Double Blank	hHK1	N/A	103.30	True	N/A	N/A
<b>Zero</b>	Blank	hHK1	N/A	0.04	True	3.60	N/A
<b>QC4_1</b>	Quality Control	hHK1	7.8	0.12	True	8.02	102.86
<b>QC4_2</b>	Quality Control	hHK1	7.8	0.13	True	8.37	107.25
<b>QC4_3</b>	Quality Control	hHK1	7.8	0.12	True	7.97	102.11
<b>QC4_4</b>	Quality Control	hHK1	7.8	0.12	True	7.65	98.13
<b>QC3_1</b>	Quality Control	hHK1	15.6	0.29	True	17.16	109.98
<b>QC3_2</b>	Quality Control	hHK1	15.6	0.28	True	16.19	103.79
<b>QC3_3</b>	Quality Control	hHK1	15.6	0.23	True	13.67	87.6
<b>QC3_4</b>	Quality Control	hHK1	15.6	0.30	True	17.23	110.45
<b>QC3_5</b>	Quality Control	hHK1	15.6	0.31	True	18.17	116.46
<b>QC2_1</b>	Quality Control	hHK1	1000	17.89	True	964.40	96.44
<b>QC2_2</b>	Quality Control	hHK1	1000	17.87	True	963.40	96.34
<b>QC2_3</b>	Quality Control	hHK1	1000	18.18	True	980.10	98.01
<b>QC2_4</b>	Quality Control	hHK1	1000	18.37	True	990.10	99.01
<b>QC2_5</b>	Quality Control	hHK1	1000	19.29	True	1040.00	103.97
<b>QC1_1</b>	Quality Control	hHK1	2000	32.23	True	1736.00	86.81
<b>QC1_2</b>	Quality Control	hHK1	2000	35.93	True	1936.00	96.78
<b>QC1_3</b>	Quality Control	hHK1	2000	39.26	True	2115.00	105.75
<b>QC1_4</b>	Quality Control	hHK1	2000	36.02	True	1940.00	97
<b>QC1_5</b>	Quality Control	hHK1	2000	32.34	True	1742.00	87.1
<b>QC4_5</b>	Quality Control	hHK1	7.8	0.13	True	8.56	109.72
<b>Sample Name</b>	Sample Type	Analyte	Actual Conc.	Area Ratio	Used	Calculated Conc.	Accuracy
<b>K9</b>	Standard	caSP	7.8	0.13	True	7.65	98.01
<b>K8</b>	Standard	caSP	15.6	1.41	False	85.84	550.25
<b>K7</b>	Standard	caSP	31.25	1.46	False	88.82	284.22
<b>K6</b>	Standard	caSP	62.5	1.16	True	70.84	113.34
<b>K5</b>	Standard	caSP	125	2.17	True	132.90	106.28
<b>K4</b>	Standard	caSP	250	4.32	True	264.60	105.85
<b>K3</b>	Standard	caSP	500	7.05	True	432.20	86.44
<b>K2</b>	Standard	caSP	1000	16.39	True	1005.00	100.52
<b>K1</b>	Standard	caSP	2000	29.20	True	1791.00	89.57
<b>Blank</b>	Double Blank	caSP	N/A	125.80	True	N/A	N/A
<b>Zero</b>	Blank	caSP	N/A	0.02	True	0.95	N/A
<b>QC4_1</b>	Quality Control	caSP	7.8	0.13	True	7.67	98.33
<b>QC4_2</b>	Quality Control	caSP	7.8	0.13	True	7.28	93.37
<b>QC4_3</b>	Quality Control	caSP	7.8	0.15	True	8.95	114.77
<b>QC4_4</b>	Quality Control	caSP	7.8	0.13	True	7.79	99.86
<b>QC3_1</b>	Quality Control	caSP	15.6	0.31	True	18.53	118.77
<b>QC3_2</b>	Quality Control	caSP	15.6	0.28	True	16.80	107.71
<b>QC3_3</b>	Quality Control	caSP	15.6	0.30	True	17.73	113.64

## 9. Appendix

QC3_4	Quality Control	caSP	15.6	0.29	True	17.61	112.89
QC3_5	Quality Control	caSP	15.6	0.28	True	16.71	107.14
QC2_1	Quality Control	caSP	1000	16.84	True	1033.00	103.27
QC2_2	Quality Control	caSP	1000	15.09	True	925.10	92.51
QC2_3	Quality Control	caSP	1000	15.15	True	929.20	92.92
QC2_4	Quality Control	caSP	1000	15.93	True	976.70	97.67
QC2_5	Quality Control	caSP	1000	16.16	True	990.90	99.09
QC1_1	Quality Control	caSP	2000	27.55	True	1690.00	84.48
QC1_2	Quality Control	caSP	2000	31.34	True	1922.00	96.11
QC1_3	Quality Control	caSP	2000	33.61	True	2062.00	103.09
QC1_4	Quality Control	caSP	2000	30.25	True	1855.00	92.77
QC1_5	Quality Control	caSP	2000	27.61	True	1693.00	84.67
QC4_5	Quality Control	caSP	7.8	0.13	True	7.41	94.93

*Concentration is expressed in pg/mL and the accuracy in %. (caSP: Carboxylic acid of Substance P, conc: concentration; hHK-1: human Hemokinin-1; N/A: not available; SP: Substance P)*

*Supplementary Table 13: Linearity and sensitivity of the three validation runs for each analyte.*

<b>Analyte</b>	<b>Run</b>	<b>LLOQ/blank ratio</b>	<b>Regression (r)</b>
Substance P	1. run	6.89240506	0.99804
	2. run	5.13984298	0.99526
	3. run	7.34887218	0.99643
human Hemokinin-1	1. run	7.09005514	0.99774
	2. run	12.3020706	0.99489
	3. run	5.22796353	0.99523
Carboxylic acid of Substance P	1. run	5.35426858	0.99909
	2. run	14.4168096	0.99608
	3. run	5.8003518	0.99503

*The sensitivity is expressed as the LLOQ/blank ratio. The regression of the obtained calibration curves was used to determine the linearity of the defined calibration range (LLOQ: lower limit of quantification).*

*Supplementary Table 14: Intra-run accuracy of three validation runs within two days of four concentration levels of Substance P, its carboxylic acid and human Hemokinin-1 in human plasma samples.*

Analyte	Nominal conc. [pg/mL]	Intra-run accuracy (1. run) [n = 5]		Intra-run accuracy (2. run) [n = 5]		Intra-run accuracy (3. run) [n = 5]	
		Mean measured conc. [pg/mL]	ACC [%]	Mean measured conc. [pg/mL]	ACC [%]	Mean measured conc. [pg/mL]	ACC [%]
<b>SP</b>	7.8	8.2	104.97	7.3	93.00	7.5	95.80
	15.6	16.6	106.65	16.3	104.74	15.1	97.01
	1000	1103.0	110.30	1117.4	111.74	1062.4	106.23
	2000	2276.2	113.81	2242.2	112.11	2050.4	102.52
<b>hHK-1</b>	7.8	8.0	102.71	7.8	99.97	8.1	104.02
	15.6	15.5	99.14	16.2	104.09	16.5	105.67
	1000	896.0	89.60	1075.6	107.56	987.6	98.76
	2000	2100.6	105.03	2094.6	104.73	1893.8	94.69
<b>caSP</b>	7.8	8.7	111.13	7.7	98.52	7.8	100.25
	15.6	15.4	98.40	16.2	103.56	17.5	112.03
	1000	1001.2	100.12	1065.9	106.59	971.0	97.10
	2000	2213.0	110.65	2096.4	104.82	1844.4	92.22

*(LLOQ [7.8 pg/mL]; low QC [15.6 pg/mL]; middle QC [1000 pg/mL]; high QC [2000 pg/mL])  
(ACC: accuracy; caSP: The carboxylic acid of Substance P; conc: concentration; CV: coefficient of variation; hHK-1: human Hemokinin-1; SP: Substance P)*

*Supplementary Table 15: Inter-run accuracy and precision of three validation runs within two days of four concentration levels of Substance P, its carboxylic acid and human Hemokinin-1 in human plasma samples.*

Analyte	Nominal conc. [pg/mL]	Inter-run accuracy [n = 15]		Precision [n = 15]	
		Mean measured conc. [pg/mL]	ACC [%]	Repeatability [CV%]	Day-different intermediate precision [%]
<b>SP</b>	7.8	7.6	97.92	8.4	9.9
	15.6	16	102.8	8.5	9.1
	1000	1094.3	109.42	4.2	4.6
	2000	2189.6	109.48	6.3	7.9
<b>hHK-1</b>	7.8	8	102.23	8.7	8.7
	15.6	16	102.97	10.2	10.2
	1000	986.4	98.64	4.6	10
	2000	2029.7	101.48	8.1	9.3
<b>caSP</b>	7.8	8.1	103.3	7.9	9.7
	15.6	16.3	104.66	8.4	10
	1000	1012.7	101.27	4.9	6.5
	2000	2051.3	102.56	7.2	11.2

*(LLOQ [7.8 pg/mL]; low QC [15.6 pg/mL]; middle QC [1000 pg/mL]; high QC [2000 pg/mL])*  
*(ACC: accuracy; caSP: The carboxylic acid of Substance P; conc: concentration; CV: coefficient of variation; hHK-1: human Hemokinin-1; SP: Substance P)*

*Supplementary Table 16: Recovery, absolute matrix effects and stability data for Substance P, its carboxylic acid and human Hemokinin-1 in human plasma samples at three quality control levels.*

Analyte	QC level [pg/mL]	Recovery [%]	Matrix effects [%]	Benchtop stability (90 min) [%]		Autosampler stability (24 h; <15 °C) [%]
				4°C	20°C	
SP	20	90.4 ± 9.8	-15.6 ± 7.8	105.8 ± 2.1	59.2 ± 2.4	94.0 ± 10.6
	1000	106.2 ± 2.8	-14.1 ± 6.0	101.8 ± 3.8	66.7 ± 0.8	98.3 ± 5.7
	2000	103.3 ± 1.1	-9.3 ± 0.7	96.0 ± 10.3	74.2 ± 8.5	101.8 ± 6.9
hHK-1	20	110.8 ± 13.3	-9.8 ± 3.4	94.0 ± 8.3	50.5 ± 3.0	91.5 ± 4.9
	1000	97.5 ± 4.3	+9.8 ± 4.9	93.8 ± 1.0	49.7 ± 3.2	92.2 ± 1.7
	2000	95.0 ± 1.5	+5.5 ± 0.2	93.8 ± 9.7	56.2 ± 11.8	94.0 ± 1.9
caSP	20	103.9 ± 6.0	+6.3 ± 5.3	91.0 ± 2.9	44.5 ± 7.4	100.3 ± 2.1
	1000	95.1 ± 0.1	-19.7 ± 3.2	88.2 ± 2.1	50.9 ± 4.1	88.2 ± 5.0
	2000	95.4 ± 2.1	-12.9 ± 1.4	97.8 ± 11.2	57.8 ± 20.7	95.2 ± 1.4

*The stability is expressed in % by comparing the obtained results to reference values (immediately processed, spiked plasma samples). (caSP: Carboxylic acid of Substance P; hHK-1: human Hemokinin-1; QC: quality control; SP: Substance P) [mean ± standard deviation; each n = 3]*

*Supplementary Table 17: Freeze-thaw stability data for Substance P, its carboxylic acid and human Hemokinin-1 in human plasma samples at three quality control levels.*

Analyte	QC level [pg/mL]	Freeze-thaw stability [%]			
		1 <sup>st</sup> cycle (plasma)	2 <sup>nd</sup> cycle (plasma)	3 <sup>rd</sup> cycle (plasma)	3 <sup>rd</sup> cycle (stock solution)
SP	20	70.5 ± 2.3	64.5 ± 6.4	60.6 ± 5.6	85.8 ± 13.7
	1000	78.4 ± 10.1	63.4 ± 4.8	54.9 ± 4.2	82.1 ± 0.9
	2000	71.2 ± 3.0	55.6 ± 3.6	71.45 ± 23.0	92.9 ± 0.5
hHK-1	20	67.4 ± 2.9	44.7 ± 2.7	39.0 ± 3.3	89.3 ± 9.4
	1000	69.5 ± 4.6	48.9 ± 1.2	45.5 ± 3.4	79.9 ± 2.7
	2000	74.5 ± 2.6	44.7 ± 2.5	54.1 ± 12.1	94.5 ± 1.6
caSP	20	77.2 ± 2.6	62.8 ± 4.1	44.6 ± 8.5	94.9 ± 30.2
	1000	67.5 ± 0.8	55.0 ± 1.9	50.23 ± 3.0	81.6 ± 1.4
	2000	78.8 ± 2.4	51.2 ± 4.9	52.5 ± 2.1	91.8 ± 1.9

*The stability is expressed in % by comparing the obtained results to reference values (immediately processed, spiked plasma samples). (caSP: Carboxylic acid of Substance P; hHK-1: human Hemokinin-1; QC: quality control; SP: Substance P) [mean ± standard deviation; each n = 3]*

## 10. List of publications

Parts of this thesis were already published in international peer-reviewed journals and/or were presented at international congresses.

### 10.1 Publications in international peer-reviewed journals

- I. Feickert M, Burckhardt BB. Mass spectrometric studies on the peptide integrity of substance P and related human tachykinins in human biofluids. *Peptides*. *accepted for publication (18<sup>th</sup> November 2020)*.
- II. Feickert M, Burckhardt BB. Validated mass spectrometric assay for the quantification of substance P and human hemokinin-1 in plasma samples: A design of experiments concept for comprehensive method development. *Journal of Pharmaceutical and Biomedical Analysis*. 2020;191:113542.  
Available from: doi: 10.1016/j.jpba.2020.113542.
- III. Feickert M, Burdman I, Makowski N, Ali M, Bartel A, Burckhardt BB, *on behalf of the LENA consortium*. A continued method performance monitoring approach for the determination of pediatric renin samples – Application within a European clinical trial. *Clinical Chemistry and Laboratory Medicine*. 2020;58(11):1847-55.  
Available from: doi: 10.1515/cclm-2019-1162.
- IV. Suessenbach FK, Makowski N, Feickert M, Gangnus T, Tins J, Burckhardt BB, *on behalf of the LENA consortium*. A quality control system for ligand-binding assay of plasma renin activity: Proof-of-concept within a pharmacodynamic study. *Journal of Pharmaceutical and Biomedical Analysis*. 2020;181:113090.  
Available from: doi: 10.1016/j.jpba.2019.113090.
- V. Feickert M, Burckhardt BB. A design of experiments concept for the minimization of nonspecific peptide adsorption in the mass spectrometric determination of substance P and related hemokinin-1. *Journal of Separation Science*. 2020;43(4):818-28.  
Available from: doi: 10.1002/jssc.201901038.

- VI. Feickert M, Burckhardt BB. Substance P in cardiovascular diseases – A bioanalytical review. *Clinica Chimica Acta*. 2019;495:501-6.  
Available from: doi: 10.1016/j.cca.2019.05.014.

## 10.2 Oral presentations

- I. Feickert M, Burckhardt BB. Design of experiments as a key element for enabling the endogenous mass spectrometric determination of substance P and related hemokinin-1. Presented at: Euroanalysis XX conference; 2019 Sep 1-5; Istanbul, Turkey.  
Conference abstract available from:  
<http://euroanalysis2019.com/scientific-programme>  
[Accessed 19th November 2020]

## 10.3 Poster presentations

- I. Feickert M, Burckhardt BB. Exploring the role of substance P and hemokinin-1 in inflammatory diseases: Development of a mass spectrometric assay for clinical plasma samples. Online presented at: Mass spectrometry & Advances in the Clinical Lab 2020 US 12th Annual Conference & Exhibits; 2020 Mar 29 – Apr 2; Palm Springs, CA, USA.  
Conference abstract available from:  
[https://www.msaccl.org/view\\_abstract/view\\_abstract\\_in\\_program.php?id=1415&event=2020%20US](https://www.msaccl.org/view_abstract/view_abstract_in_program.php?id=1415&event=2020%20US)  
[Accessed 19th November 2020]
- II. Feickert M, Burckhardt BB. A quality-controlled and design of experiments-based approach for the optimization of the chromatographic solvent composition for the determination of substance P and hemokinin-1. Presented at: 48th International Symposium on High-Performance Liquid Phase Separations and Related Techniques; 2019 Jun 16-20; Milan, Italy  
Conference abstract available from:  
<https://www.hplc2019-milan.org/pages/programmeAtGlance/index.php#day6>  
[Accessed 19th November 2020]
- III. Feickert M, Burdman I, Makowski N, Ali M, Farahani S, Majid H, et al. Reliable results in continuous bioanalysis of pediatric renin samples - Comprehensive quality assessment within clinical studies in children. *Archives of Disease in*

- Childhood*. 2019;104:e31. Presented at: 17th European Society for Developmental Perinatal and Paediatric Pharmacology congress; 2019 May 28-30; Basel, Switzerland  
Conference abstract available from:  
<http://dx.doi.org/10.1136/archdischild-2019-esdppp.72>  
[Accessed 19th November 2020]
- IV. Feickert M, Burckhardt BB. Aprepitant in the prevention of cardiotoxic adverse effects of Doxorubicin in the pediatric population - A systematic literature investigation. *Archives of Disease in Childhood*. 2019;104:e31-e32. Presented at: 17th European Society for Developmental Perinatal and Paediatric Pharmacology congress; 2019 May 28-30; Basel, Switzerland  
Conference abstract available from:  
<http://dx.doi.org/10.1136/archdischild-2019-esdppp.73>  
[Accessed 19th November 2020]
- V. Suessenbach FK, Feickert M, Tins J, Burckhardt BB. Reliable acquisition of plasma renin activity in the maturing renin-angiotensin-aldosterone-system by a validated small-volume assay in context of the LENA project. *Archives of Disease in Childhood*. 2019;104:e56. Presented at: 17th European Society for Developmental Perinatal and Paediatric Pharmacology congress; 2019 May 28-30; Basel, Switzerland  
Conference abstract available from:  
<http://dx.doi.org/10.1136/archdischild-2019-esdppp.132>  
[Accessed 19th November 2020]
- VI. Farahani I, Laven A, Farahani S, Deters M, Feickert M, Suessenbach FK, et al. Effectiveness of OSCEs in training German pharmacy students in consultation on self-medication – a randomized controlled investigation. *Archives of Disease in Childhood*. 2019;104:e30-e31. Presented at: 17th European Society for Developmental Perinatal and Paediatric Pharmacology congress; 2019 May 28-30; Basel, Switzerland  
Conference abstract available from:  
<http://dx.doi.org/10.1136/archdischild-2019-esdppp.71>  
[Accessed 19th November 2020]